

Dissertation

Zur Erlangung des Doktorgrades
der Fakultät für Chemie und Pharmazie
der Ludwig-Maximilians-Universität München

**Degradation of lipid based drug delivery systems and
characterization of semi-synthetic spider silk proteins for
the application in pharmaceutical technology**

vorgelegt von

Martin Schwab

aus Ettenheim

2009

Erklärung

Diese Dissertation wurde im Sinne von § 13 Abs. 3 der Promotionsordnung vom 29. Januar 1998 von Herrn Prof. Dr. Gerhard Winter betreut.

Ehrenwörtliche Versicherung

Diese Dissertation wurde selbständig, ohne unerlaubte Hilfe erarbeitet.

München, am 03.03.2010

.....

Martin Schwab

Dissertation eingereicht am 08.07. 2009

1. Gutachter: Prof. G. Winter
2. Gutachter: Prof. W. Frieß

Mündliche Prüfung am 13.08.2009

Table of Contents

I. GENERAL INTRODUCTION.....	3
1. Proteins and the need for adequate delivery systems	3
2. Parenteral delivery and polymeric systems	5
3. Erosion of polymers.....	15
4. Polymer erosion and its influence on the entrapped drug.....	17
5. Lipids as alternative drug delivery systems.....	18
6. Lipid based drug carrier systems	20
7. Degradation and swelling behaviour of lipid particles	26
8. Silk proteins	28
9. Biomedical application of silk proteins.....	30
10. Silk as a material for the preparation of drug delivery systems.....	32
11. References	38
II. AIM OF THE THESIS.....	50
1. Chapter One: In vivo studies of rh- $\text{INF}\alpha$ releasing lipid implants.....	53
1.1. Introduction	53
1.2. Correlation of in vivo and in vitro release data for rh- $\text{INF}\alpha$ lipid implants.....	54
1.3. Discussion of the published correlation data.....	65
1.4. Short review on cellular activity at the implant tissue interface.....	66
2. Chapter Two: In vitro degradation studies of lipid based drug depot systems.....	73
2.1. Introduction	73
2.2. Studies on the lipase induced degradation of lipid based drug delivery systems	74
2.3. Discussion of the results of the in vitro degradation study.....	93
2.4. Lipase stability and lipid microparticle preparation.....	95
3. Chapter Three: Studies on the mechanisms of lipid matrix disintegration.....	101
3.1. Introduction	101
3.2. Studies on the lipase induced degradation of lipid based drug delivery systems. Part II – Investigations on the mechanisms leading to collapse of the lipid structure	102
3.3. Discussion of the results of the degradation experiments.....	122
3.4. Further studies on lipid drug depot degradation	123
4. Chapter Four: Investigations on spider silk proteins	130
4.1. Introduction	130
4.2. Processing conditions for the formation of spider silk microspheres.....	131
4.3. Discussion of the presented data.....	141
5. Chapter Five: In vitro release studies of spider silk microparticles.....	142
5.1. Introduction	142
5.2. Spider silk particles for controlled drug delivery	143
5.3. Discussion of the presented data.....	165
5.4. Characterization of eADF4(C ₁₆)-films for their application in drug release systems.....	166
III. FINAL SUMMARY & CONCLUSION	181
Acknowledgements.....	185

TABLE OF CONTENTS

Publications and presentations associated with this work	187
Curriculum Vitae	188

I. GENERAL INTRODUCTION

1. Proteins and the need for adequate delivery systems

Proteins, nucleic acids, polysaccharides and lipid assemblies are the four major biopolymers. Among them, because of their variety of important biological functions, proteins and nucleic acids have attracted much more attention from biological scientists than the other biopolymers. Proteins are an integral part of the body as they carry out all important physiological and biological processes like enzyme reactions, acting as receptors for hormones or antibodies in the immune system. Due to these facts, protein pharmaceuticals have gained significant importance in the treatment of many severe diseases e.g. hormonal disorders, cancer, autoimmune diseases [1]. Naturally occurring proteins all consist of only 21 kinds of α - and L-amino acids. Protein structure can principally be described at four different levels. The primary structure pertains to the linear arrangement of amino acids residues along a polypeptide chain or disulfide bonds between and within a chain. Secondary structure refers to the folding of parts of these chains into regular structures such as α -helices and β -sheets. The folding of regions between α -helices and β -sheets leads to the tertiary structure, which also includes all of the non-covalent interactions that ensure the proper folding of a single polypeptide chain, such as hydrogen bonds and hydrophobic, electrostatic and van der Waals interactions. The quaternary structure finally refers to the non-covalent interactions that bind several polypeptide chains into a single protein molecule, as seen in most proteins [2].

It is understood, that the specific function of proteins is reflected by its tertiary structure [3] which is a consequence of the mentioned substructures. This complex architecture of proteins, the tertiary structure with labile bonds and side chains with chemically reactive groups offers some serious limitation for their use as drug substances. They can undergo non-chemical changes i.e. physical instability e.g. unfolding (denaturation). This leads to loss of native structure resulting in interaction with surroundings by adsorbing to surfaces or aggregating with other protein molecules. Protein aggregation often leads to immunogenicity [4-6]

Chemical degradation e.g. oxidation, deamidation and disulfide exchange causes disruption of substructures or modification of side chains leading to loss activity. Above all, the most challenging task is their delivery. In contrast to conventional molecules, which are mostly stable with low molecular weight reasonable lipophilic properties and hence can be transported through cellular barriers and membranes, proteins require a sophisticated delivery system. Due to their hydrophilic nature and high molecular weight, proteins have poor intrinsic permeability across biological membranes.

GENERAL INTRODUCTION

Another barrier a protein has to overcome in the human body is the enzymatic equipment of the gastro intestinal tract: various enzymes (e.g. pepsin), intestinal pancreatic proteases (e.g. trypsin), elastases, brush border proteases (e.g. aminopeptidases) leading to degradation [2]. To avoid contact with these degrading enzymes, proteins can be delivered by several different ways:

- By parenteral injection: e.g. subcutaneous, intramuscular and i.v.
- Pulmonary: by inhalation
- Nasal: sprayed or inhaled
- Transdermal: via liposomes or patches

Nasal delivery: there are a few nasal products approved by the EMEA, e.g. nasal salmon calcitonin marketed by Novartis, nasal desmopressin marketed by Ferring and partners.

The major advantage of the nasal administration is the avoidance of protein degradation resulting from acidic, enzymatic and first pass metabolism. But there are also some serious disadvantages that limit the potential of the nasal drug delivery. First of all the volume that can be delivered is restricted to 25-200 μ l. The most important factor limiting the nasal absorption of large molecular weight drugs, such as proteins and peptides is the low membrane permeability. Only molecules with a molecular weight under 1000 Da can pass the membrane [7, 8].

Pulmonary delivery: Many proteins are absorbed from the deep lung surprisingly well. Protein bioavailabilities (relative to subcutaneous administration) of at least several percent and (in rare cases) up to almost 50% have been recorded [9]. An inhalable insulin preparation (ExuberaTM) invented by biotech startup Nektar Therapeutics and shepherded to market by Pfizer has been approved in January 2006 by the FDA. However in October 2007 Pfizer announced to take Exubera off the market and returned all rights to Nektar Therapeutics [10]. According to Pfizer Chief Executive Jeffrey Kindler Exubera has failed to gain acceptance of patients and physicians and therefore was not economically successful.

Transdermal delivery: Due to the anatomy of the skin, especially the horny layer, the so called stratum corneum, which prevents the entry of most pathogens and most chemicals when undamaged, bigger molecules like proteins, can hardly enter the deeper layers of the skin. The FDA has approved, throughout the past 22 years, more than 35 transdermal patch products, spanning 13 molecules, but none of them were proteins. This does not mean that there is no adequate method for transdermal protein delivery. There are a few promising techniques for protein delivery into the skin. These transdermal technologies are iontophoresis

(which uses low voltage electrical current to drive charged drugs through the skin) [11] and sonophoresis (which uses low frequency ultrasonic energy to disrupt the stratum corneum [12]. These systems can achieve significant skin permeation enhancement, enabling more effective delivery of proteins, such as insulin and calcitonin. A newer and potentially more promising technology for macromolecule delivery is microneedle-enhanced delivery [13]. These systems use an array of tiny needle-like structures to open pores in the stratum corneum and facilitate drug transport. Macroflux® from Alza or 3M's Microstructured Transdermal System (MTS).

2. Parenteral delivery and polymeric systems

Parenteral injection is the most often used route of drug administration. Since most pharmaceutical proteins, given by injection, must be administered in several doses to reach therapeutic useful concentrations in the blood plasma, resulting in low patient compliance and high hospital costs are resulting. To avoid the disadvantages of multi dose injections, the technology of retarded release was developed. The first controlled-release technology was developed in 1962 and was based upon diffusion of small molecules through the wall of silicone rubber tubing [14]. Although the molecular mass was not allowed to be bigger than 600 Daltons, to diffuse through the rubber, it was a first promising step into a new land. Only a few years later Langer showed that it is possible to release big molecules from polymers as described in the following part of this paper.

Controlled release of macromolecules from nondegradable polymers

As already mentioned earlier, most polymers, e.g. ethylene vinyl acetate copolymer (EVAc), are impermeable to molecules larger than 600 Daltons (e.g. polypeptides and proteins) since most of these macromolecules are too large to penetrate through the linked polymer chains, even after polymer swelling. In 1976, while working on tumor angiogenesis, Langer and Folkman discovered their need for a device that could provide steady diffusion of tumor angiogenesis factor (TAF) into rabbit cornea from a depot source. After failing to deliver the TAF with poly(acrylamide) pellets (they were often highly inflammatory), Langer and Folkman tried another polymer, ethylene vinyl acetate copolymer, which turned out to be very useful. They prepared the pellets by mixing the bioactive agents with a solution of EVAc in methylene chloride. The resulting dispersion was poured into a mold, allowing the solvent to evaporate under vacuum over night. Their pellets provided a zero order release between 20 and 100 days for several proteins e.g. lysozyme, catalase and soybean trypsin inhibitor. They

also used the ethylene vinyl acetate copolymer to release insulin, heparin and DNA. For periods up to 60 days nearly 1 μ g of each drug was released per day through these systems [15]. As explanation for the sustained release of macromolecules, Langer quoted the formation of a tortuous, interconnected pore network, through which the molecules can diffuse. These pores originated from dissolving embedded polypeptide powder within the polymer matrix. By varying the particle size and the loading of the matrix, rate of release can be controlled. If the matrix is low loaded, not all the polypeptide is released from the polymer. This can be easily explained: If the loading of the polymer matrix is low, the chance that 2 particles have contact or that they are embedded at the surface is low. These particles will be completely surrounded by the impermeable polymer matrix. They are trapped, since the water, dissolving the macromolecules and thus releasing them, isn't able to permeate through the polymer. Pores within the polymer matrix are the key for drug release. In contrast a highly loaded matrix is able to release almost all the embedded molecules, since more particles are embedded and the chance that they have contact with each other and the surface of the matrix is increased. Particles build clusters which can extend from the surface deep into the matrix. When dissolved by the releasing medium, these clusters leave a connected pore network behind, allowing the water to infiltrate through the pores deep into the matrix and dissolving all particles it contacts. There is also an increase of the released molecules if the polypeptide particle size is increased. This is because the larger the polypeptides are, the more they touch the surface and the bigger are the resulting pores when dissolved [16]

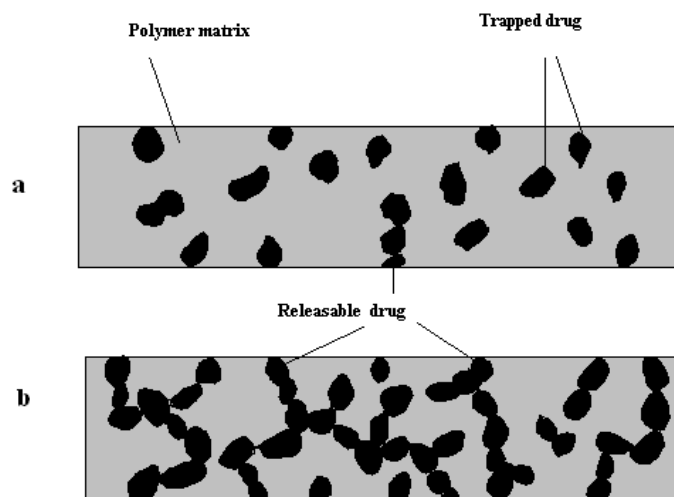


Figure 1: Schematic of EVAc-polypeptide matrices before release

a. Low loading – most drug is trapped by surrounding polymer

b. High loading – almost all drug is connected to surface via other drug particles, and is therefore releasable.[16]

Although the particles are dissolved in water and thus released through aqueous filled pores, the relevant diffusion coefficient isn't the diffusion coefficient of polypeptides in water. In this case the releasing times durations should be much shorter. Even assuming that the network within the matrix, containing pores (space evacuated by a drug particle) and channels (space connecting two pores), is highly tortuous, this would not explain a release continuing for months. It is also unlikely that retardation of release is due to absorption of polypeptides onto the pore walls. Assuming a monolayer of absorbed drug on the pore walls would only consist of an insignificant part (less than 1%) of the entire drug within the pores. Langer postulated that the sustained release is dependent to a geometrical feature of the pore structure within the polymer matrix. Scanning electron micrograph showed that pores are connected by channels whose radii are substantial smaller than the pore radii. Thus nature of sustained release is due to the random walk of drug molecules in the pores and due to the time a molecule takes until it exits the pore.

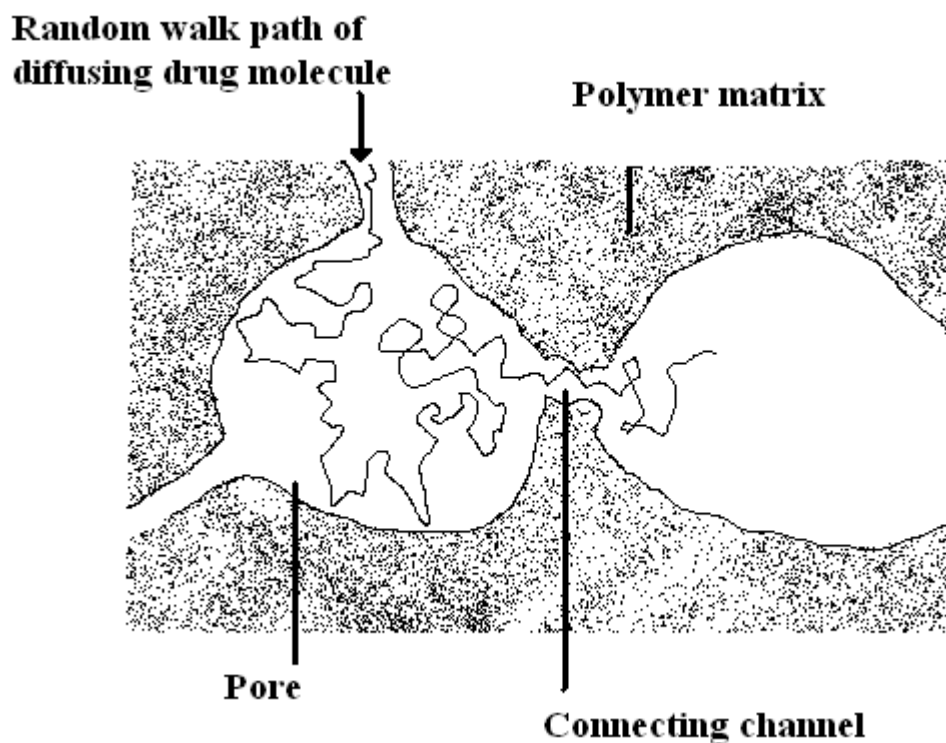


Figure 2: Schematic of pores through which a diffusing drug molecule must pass [16].

In addition to the already mentioned parameters influencing the sustained release there are a few more. Dissolution properties of polypeptides are variable. For instance native insulin, consisting of three dimers associated around two zinc ions, has a high solubility compared to Ultralente-insulin, one of the most protracted insulin analogs [17]. It is therefore understood that the resulting dissolution rate in the depot matrix leads to different releasing rates.

Concentrations of polypeptide and drug-excipient ratio are as well a parameter, influencing the releasing rate. If there is a high concentration of drug embedded within the matrix, resulting solution becomes very viscous, leading to a diffusion coefficient decrease, resulting in prolonged release [16]

Biodegradable polymers and their classification

After all the years of research associated with protein drug delivery with polymer devices, one major problem still persisted: The polymer systems were non-biodegradable and required surgical removal after drug delivery was complete, otherwise inflammation- and toxicity-problems could occur. Thus, there was a need for biodegradable polymers. Biodegradable polymers are synthetic or natural polymers which degrade in vivo, either enzymatically or non-enzymatically i.e. by hydrolysis or solubilization, to produce biocompatible or non toxic by-products along with the progressive release of dissolved/ dispersed drug. In general degradation is understood as the chain scission process by which polymer chains are cleaved into oligomers or monomers [18]. A variety of synthetic and naturally occurring polymers have been intensively studied over the last 30 years.

Table 1: Classification of biodegradable polymers/materials [19]:

Synthetic	Polyorthoesters
	Polyanhydrides
	Polyamides
	Polyalkylcyanoacrylates
	Polyesters: Lactides/Glycolides, Polycaprolactones
	Polyphosphazenes
	Pseudopolyaminoacids
Natural	Proteins
	Polysaccharides
	Starch
	Alginate
	Lipids

Biodegradable synthetic polymers and the preparation techniques used for the manufacturing of drug delivery systems

Synthetic polymers used for the preparation of drug delivery systems fulfil the following requirements: In general they are biologically inert, compared to natural occurring polymers they have more predictable properties and batch-to-batch uniformity in addition to that, they offer the advantage of having tailored property profiles for specific applications.. The successful application of the first synthetic polymer based biodegradable suture system in the late 1960s [19] was followed by a tremendous increase of design and development of a new series of biodegradable polymers used for the preparation of implants and related medical applications. Since then research has concentrated on the custom design of biodegradable polymer systems with predictable erosion kinetics as drug/gene delivery carriers or as materials scaffolding tissue and cells in several bio engineering applications.

PLGA

Out of all the synthetic polymers, in particular α polyesters prepared from polylactic acid and/or polyglycolic acid- i.e. poly(D,L-lactide) (**PLA**), polyglycolic acid (**PGA**) and copolymers of lactide and glycolide (**PLGA**) have found the most widespread use [20]. Poly(α -ester)s are thermoplastic polymers with hydrolytically labile aliphatic ester linkages in their backbone. Attractive features of these polymers are:

Largely abundant toxicological and chemical data, biocompatibility/histocompatibility, predictable biodegradation kinetics, ease of fabrication, versatility in properties, variety in copolymer ratio and molecular weights. However, the most important feature is the regulatory approval. Employing these polymers, a broad spectrum of performance characteristics can be obtained by manipulating four key variables: 1) monomer stereochemistry, 2) co-monomer ratio 3) polymer chain linearity and 4) polymer molecular weight. Varying co-polymer ratios results in different crystallinities, affects the glass transition temperature and the polymer hydrophilicity. A change in chain linearity influences as well the polymer hydrophilicity which directly influences the water influx into the polymer. This water influx has a great effect on the polymer degradation rate as highlighted later in the respective section of this introduction. Nowadays most PLGA drug release systems consist of drugs embedded in microparticles; however there are a few systems consisting of implants of various shapes and sizes. In the following section most PLGA drug release systems and their preparation techniques are presented.

PLGA-microparticles:

By definition microparticles are spherical devices with a size within the range of 1-1000 μm .

They can be divided into 2 categories: microcapsules and microspheres. Microcapsules contain a core in which the drug is embedded, surrounded by a polymeric membrane [21].

In microspheres the drug is embedded in the whole polymeric matrix. The ideal size of microparticles, for parenteral use is less than 125 μm . Several methods are suitable for producing microparticulate systems, all of them have to include following the requirements:

- stability and activity of the protein should not be adversely affected by the production method
- drug encapsulation efficiency should be high
- the drug release profile and the microsphere quality should be reproducible

Manufacturing techniques of PLGA Microparticles

There are two different types of methods to produce PLGA microparticles:

Chemical and **physical** preparation techniques. The former method deals with Polymerisation of the PLGA, complexation, emulsifying and altering the properties of the solvent. Physical methods involve working with a gas phase, which helps to congeal the polymer. Of course the author is aware that this nomenclature is somewhat confusing since all presented methods are based on physical processes and do not involve changes in the chemical structure of the polymers. However, this nomenclature has grown historically and therefore shall be still applied in this introduction:

So called **Chemical procedures** are:

Single emulsion method: This process involves oil-in-water-emulsification in which micronized protein powder is dispersed into the organic solvent phase containing dissolved polymer. The organic phase then is emulsified in an aqueous phase, leading to microcapsules [22]. **Double (multiple) emulsion process:** This is a water-in-oil-in-water (w/o/w) method and is best suited to encapsulate water-soluble drugs like peptides, proteins, and vaccines.

Disadvantages of the emulsion methods are the existence of diverse interfaces which are destabilize the fragile structure of the proteins. This adsorption step can induce protein unfolding, inactivation and aggregation. Morlock et al. showed that during the procedure of microencapsulation of rh-erythropoetin using PLGA, the first processing step namely the formation of W/O emulsion was mainly responsible for epo-aggregation. The following steps didn't seriously increase the total amount of aggregates [23, 24]

Phase separation (coacervation): This encapsulation process was discovered and developed by Barrett K Green of the National Cash Register Corporation (NCR) in the 1940's and 1950's. Coacervative encapsulation (or microencapsulation) is a three part process: particle or droplet formation; coacervative wall formation; and capsule isolation. In the field of drug microencapsulation into PLA/PLGA, the term coacervation is commonly used for polymer phase separation induced by the addition of a coacervating agent to the polymer solution. Typically, addition of poly(dimethylsiloxane) (PDMS, silicone oil) to PLA/PLGA dissolved in methylene chloride (DCM) yields the so-called coacervate droplets, which are solidified in a hardening agent, such as hexane or octamethylcyclotetrasiloxane (OMCTS), to produce the final microspheres. It is a non aqueous method and hence is suitable for encapsulating both water soluble and water insoluble proteins [25]

Physical Procedures:

Spray drying: The dissolved polymer (possible solvents are acetone, methylene chloride) therein the protein, suspended as solid or emulsified as aqueous solution, is atomized through a heated nozzle [26].

Varied spray drying techniques: A novel low-temperature spraying method for preparing PLA and PLGA microspheres has been reported by Herbert et al. PLGA solution with suspended or emulsified Protein was sprayed into a vessel containing liquid nitrogen overlaying a frozen extraction solvent like ethanol. The liquid nitrogen is subjected to evaporation causing the polymer solvent from the frozen droplets to be extracted then by liquid ethanol. The produced microspheres were then filtered and the residual solvents evaporated by filtration. Advantages of this spray freezing method include maintaining the proteins stability and activity as well as achieving very high encapsulation efficiency [27]

Techniques using supercritical fluids (SCF):

This method has the advantage of working without organic solvents since it replaces the solvents with carbon dioxide involving very low temperatures. Supercritical means the area above the critical point, which is defined as the point where the boundary layer between liquid and gas in a phase transition curve vanishes. Carbon dioxide is one of the most commonly used supercritical fluids for SCF processing of drug compounds, owing to the fact that it reaches super-criticality at a relatively mild temperature (~31°C). These fluids, the properties of which can be tuned by changing the fluid density between those of liquid and gases, have been adopted or are being explored as: alternative solvents for classical separation processes such as extraction, fractionation, adsorption, chromatography, and crystallization, as reaction

media as in polymerization or depolymerization, or simply as reprocessing fluid as in production of particles, fibers, or foams. Some of the extraction processes, such as decaffeination, and some polymerization and foaming processes, have become commercial. Because SCF processing conditions do not strictly necessitate temperature extremes, operational parameters may be developed that are more suitable for temperature-sensitive protein species besides lyophilization or spray-drying [28]. Presently several modified processes exist which use various mechanisms for precipitating particles:

Rapid expansion of supercritical solutions (RESS):

This process is based on the solubility difference of the polymer in SC in high and low pressures; it is used when the polymer has some degree of solubility in the SCF. The polymer is dissolved in the supercritical fluid. As this high-pressure solution is rapidly depressurizing through a nozzle, polymer is precipitating.

Gas antisolvent process (GAS):

The supercritical fluid is used as an antisolvent, due to the fact that many polymers aren't soluble in SCF. The polymer first is dissolved in a suitable solvent e.g. ethanol. For precipitating the polymer gas (not necessarily supercritical gas) is injected into the solution in a chamber. With increasing gas concentration in the solution, the polymer precipitates.

Supercritical antisolvent process (SAS):

In this technique a supercritical fluid acts as an antisolvent for polymer solutions like in the GAS process, but the contacting mechanism is different. Dissolved polymer is sprayed in a chamber in which a supercritical fluid, the antisolvent, already exists, causing rapid contact between the two media. Contact causes supersaturating leading to fast nucleation growth and hence smaller particles.

PLGA implants

Compared to the countless publications dealing with the manufacturing of PLGA microparticles there are only a few publications describing PLGA implants for protein delivery. There are several methods manufacturing PLGA implants:

Solvent casting method [29] Firstly an aqueous solution of the drug was poured into a Teflon mould and freeze-dried. A solution of the polymer was then poured on the cake. The solvent was allowed to evaporate at 4°C for 48h. The resulting drug-polymer cake was vacuum dried until all residual solvent was gone. This procedure leads to laminar implants with a thickness about half a millimetre.

Injection-molding method [30] A special adapted molding machine was used. Melted polymer-drug dispersion (100°C) was injected into the mold with a pressure of about 130 bar, then it was cooled at 14°. One of the implant ends was round shaped for injection for facilitation under the skin. The rods had a diameter of 4,6mm. Surely, due to the high temperatures and the pressure, this method isn't suitable for temperature-sensitive protein drugs.

Extrusion-techniques [31]: Using a ram extruder, implants were gained by extruding mixtures of polymer and drug. Extrusion temperatures range between 80°C and 175°C. Extrusion techniques are the most convenient ways of producing PLGA implants for protein delivery. Apart from the ram extruder, the screw extruder's also suitable for manufacturing implants. The goserilin acetate implant Zoladex© is produced with an extrusion technique: A lyophilisation cake containing the polymer and the drug is formed into implants by extruding this mixture. The obtained implant are sterilised with γ -radiation [32].

Polyanhydrides

In 1980, Langer was the first who exploited the hydrolytically unstable nature of the Polyanhydrides for sustained release of drug in controlled drug release applications, using poly[bis(*p*-carboxyphenoxy)methane], as a bioerodible matrix for controlled drug delivery [33]. Matrices fabricated from this material and containing cholic acid showed a period of nearly zero-order erosion kinetics during which this steroid was released at nearly the same constant rate. Five years later, Langer and his group developed Poly[bis(*p*-carboxyphenoxy)propane (P(CPP)) anhydrides with copolymers of sebacic acid (SA), (P(CPP:SA)) [34]. This biodegradable compound, which breaks down to dicarboxylic acids by spontaneous reaction with water, exhibits several important properties [35]:

- The macroscopic breakdown of the polymer is limited to its surface.
Zero order kinetic releasing rates can thus be achieved.
- The rate of breakdown of PCPP:SA polymers can be varied by altering the ratio of the monomers CPP and SA.
- The matrix is completely degradable.
- The degradation products of these polymers are nonmutagenic, noncytotoxic, and have a low teratogenic potential [34].

In 1996 Gliadel[®], a PCPP:SA wafer carrier containing carmustine for the treatment of brain tumour, entered the U.S. market [35]. In the last few years, investigations have expanded to newer polymers and other drugs such as 4-hydroperoxy cyclophosphamide (4 HC), cisplatin,

carboplatin, paclitaxel and several alkaloid drugs in an effort to develop a better system for treating brain tumors incorporated into poly(FAD-SA), prepared by mixing the drug in the melted polymer, has been evaluated for the treatment of brain tumors in laboratory animals [36]. Disadvantages of the Poly(anhydrides) may be the need for special fabrication techniques for controlled release devices. The temperature required for the fabrication of poly(anhydride) matrices is too high for sensitive molecules like proteins, thus a solvent extraction technique derived from the standard W/O/W emulsion method for PLGA microspheres had to be used [37].

Poly(ortho esters)

Over the last 30 years, poly(ortho esters) have evolved through four families, designated as POE I, POE II, POE III and POE IV. Of these, only POE IV has been shown to have all the necessary attributes to allow commercialization [38]. Therefore, only the POE IV will be outlined in this short review.

POE IV is a modification of POE II (as shown in Fig.3)

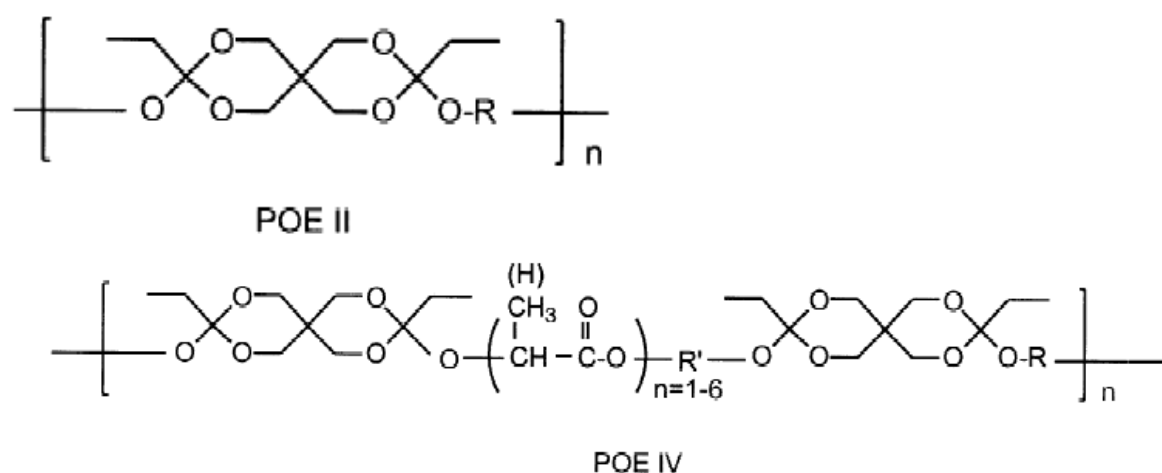


Figure 3: [38]

POE IV was created by incorporating short segments based on lactic acid or glycolic acid into the polymer backbone of POEII. These segments act as latent acids, because they readily hydrolyze to glycolic or lactic acids, which then catalyze hydrolysis of ortho ester linkages in the polymer backbone. By controlling the concentration of such segments in the polymer, rate of erosion can be accurately controlled. POE IV possesses 3 major features of protein release kinetics: First, there is either no drug burst or only a minimal burst, even when very hydrophilic drugs are incorporated in the polymer matrix. Second, a significant lag time was monitored. Finally, polymer weight loss and drug release occur concomitantly, due to the

surface erosion controlled protein release [30] [39]. The lag time can be reduced by admixing the monomethyl- polyethylene-glycol-ether to the polymer-protein mixture. Obtained extrudates liberated the protein for a 2 months period following zero order kinetics [30] in summary, poly(ortho esters) for protein and peptide delivery are very promising, but due to the fact that bulk degradation cannot be completely inhibited some questions about erosion properties have to be answered [38]

3. Erosion of polymers

Polymer erosion can be defined as a process of material loss of the polymer from the initial bulk weight [18]. This process usually is driven by degradation processes. Degradable polymers are classified in surface-eroding and bulk-eroding polymers. In addition to that, polymers can be defined as hydrolytically degradable polymers and enzymatically degradable polymers.

Hydrolytically degradable polymers are materials with hydrolytically labile chemical bonds in their back bone. The functional groups susceptible to hydrolysis include esters, orthoesters, anhydrides, carbonates, amides, urethanes, ureas [40]. Although all polyesters are theoretically degradable as esterification is a chemically reversible process, only aliphatic polyesters with reasonably short aliphatic chains between ester bonds can degrade over the time frame required for most of the biomedical applications. Hydrolytically degradable polymers can undergo both surface- and bulk-eroding processes. In general the basic composition of the polymer determines the erosion behaviour to some degree. Reactive groups such as anhydrides tend to fast degradation and therefore show surface erosion whereas polymers containing less reactive groups i.e., esters tend to bulk erosion [18]. In the case of surface eroding polymers, erosion proceeds at constant velocity. For bulk eroding polymers such as poly(d,l-lactic acid) (PLA) and poly(d,l-lactic-co-glycolic acid) (PLGA), however, things are more complicated as they have no constant erosion velocity [41]. Usually they do not erode for a long period of time. This time of constant mass is followed by a spontaneous loss of mass during a short period of time. When polymer areas within the polymer bulk degrade, they cannot erode if they have no connection to the erosion medium via pores. When the polymer is degraded to a critical degree, these degraded areas form a continuous cluster that stretches to the surface of the matrices and cause their spontaneous erosion. How a polymer matrix erodes depends on the size of the matrix, the diffusion coefficient of water inside the matrix and on the degradation rate of the polymer's functional groups. If the degradation rate of the polymer backbone is faster than the diffusion of water

into the polymer matrix, erosion will primarily occur at the surface. In contrary, a polymer matrix system undergoes bulk erosion, if water diffuses faster into the matrix than the degradation rate of the polymer backbone [41].

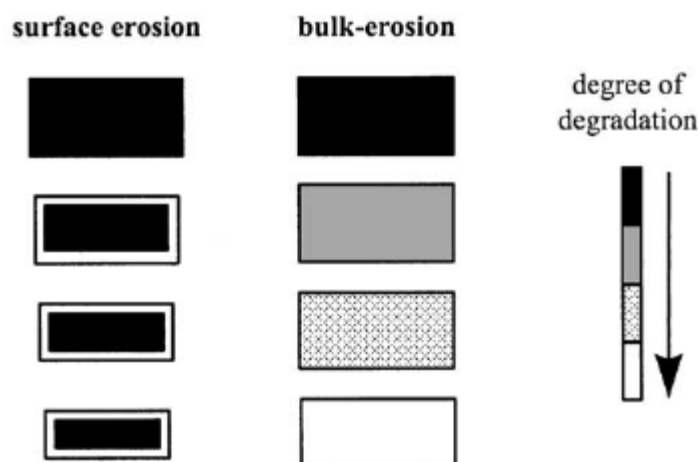


Figure 4: Schematic illustration of the changes a polymer matrix undergoes during surface erosion and bulk erosion [42]

Enzymatically degradable polymers comprise natural or synthetic materials like proteins, polysaccharides and lipids. These materials can undergo degradation in the presence of enzymes. The enzymes e.g. lipases exhibit an amino acid sequence consisting of serine, histidine and aspartad called the catalytic triad. This functional centre of the enzyme is buried under a short helical segment, termed the lid [39, 40]. When the enzyme adsorbs on a hydrophobic surface a conformational change opens the lid, activating this structure and enabling its enzymatic function [43, 44]. Due to this activation mechanism enzymatic degradation of polymers is a strict surface erosion process. The degradation velocity is mainly based on the enzyme activity therefore the rate of in vivo degradation can vary significantly with the site of implantation [19]. In addition to that degradation rate exhibits great differences when compared between different species. Enzyme activity and erosion velocity can be controlled to some degree by the addition of non-degradable polymers. Blending enzymatically degradable polymers with materials such as polystyrene alters the properties of the polymer surface i.e., the surface free energy. In that way the material life-time of such blended materials can be controlled in a reproducible manner [45]. In contrary to the above mentioned method non-degradable polymers can be processed into materials susceptible to enzymatic degradation by blending with biomaterials easily degraded by enzymes [46].

4. Polymer erosion and its influence on the entrapped drug

As a consequence of the erosion process the interior of polymer drug delivery systems can change dramatically involving changes in pH, osmotic pressure, polymer crystallinity and hydration [24]. Especially bulk eroding polymers show distinct pH-shifts in the release medium dropping down to pH-values of about 3 [47]. This acidification of the release medium has its origin in the inner part of the polymer material where the hydrolytic degradation of the polymer chains leads to a tremendous pH shift creating a micro environment with pH-values between 1.5 and 4.7 [21, 46-49]. Polymer cleavage and the accumulation of soluble oligomers and monomers lead to an increase of the osmotic pressure within the particles. This change in osmotic pressure and the pH shift can strongly affect the stability of the entrapped drug. Especially proteins – due to their biochemical structure – are susceptible to these changes in the microenvironment. Many publications [19,20,48-50] report on the negative effects of polymer bulk erosion on the stability of the entrapped peptides and proteins. Potential pathways leading to protein inactivation or incomplete protein release due to polymer bulk erosion are as followed:

Protein adsorption on polymer interfaces: Due to ionic interaction and non-covalent binding incomplete protein molecules adsorb on polymer interfaces leading to incomplete protein release and protein aggregation [19, 20].

Protein degradation induced by pH-shift and high osmotic pressure: As described above polymer erosion changes the microenvironment in the drug delivery systems and lead to low pH-values and high osmotic pressure. Since proteins are susceptible to changes in pH protein unfolding and aggregation are consequences of these changes [48]. But not only physical instability but also chemical degradation can result from the acidic environment in the polymer [49]. Deamidation and acid catalyzed hydrolysis of the amino acid chain has been reported to be one major chemical reason for protein instability within PLGA drug delivery systems [50].

5. Lipids as alternative drug delivery systems

In comparison to the vast number of papers about polymer-based drug delivery systems for sustained release of bioactives, especially PLGA-polymers, there are only a few publications which deal with lipid carriers for parenteral controlled drug delivery. Since the late 70s lipids i.e. fatty acids, triglycerides, cholesterol and lecithin have been used as excipients for the preparation drug delivery systems designed for the sustained release of drugs like steroids and morphine derivatives [51, 52]. In the past 30 years there have been many advances in the field of drug delivery systems based on lipids. Nowadays we know more than 10 different lipid based drug delivery systems resulting in numerous methods for the preparation thereof. These methods exhibit different approaches answering the complex questions one is faced with when dealing with the need for controlled release of bioactive substances. The term lipid comprises a diverse range of molecules and to some extent is a catchall for relatively water-insoluble or nonpolar compounds of biological origin, including waxes, fatty acids, fatty-acid derived phospholipids, sphingolipids, glycolipids and terpenoids, such as retinoids and steroids. They all show a good solubility in organic solvents such as acetone or methylene chloride. In our case, lipids are defined as esters made of glycerol and certain fatty acids like stearic acid, oleic acid, myristic acid. They are physiological, cheap and can be purchased in bulk. On the following pages the author attempts to highlight the unique properties of lipid materials in terms of drug delivery systems preparation and outlines the most important techniques for their production.

Polymorphic behavior of lipids

Lipids, like almost all other substances especially long-chain components can exhibit different three dimensional molecular arrangements resulting in different unit cells as modules in the higher order crystalline structures. This phenomenon of different long range order and crystalline structure of a single and pure component is called polymorphism. In fat polymorphism, the triglyceride molecules can be packed in solid state in three different ways so that each crystal form has a different melting point. The main polymorphic forms in triglycerides are the α , β , and the β' form [53, 54]. This property is explained by the Ostwald step rule [55]: A crystallizing system first will form a sequence of available metastable phases before finally forming the stable phase. Such behaviour is observed in crystallization sequences in systems as diverse as aqueous solutions and silicate melts.

The hydrocarbon chains in all the forms are arranged as “chairs” with the chains in the 1 and 3 position opposite to the chain in the 2 position. The hydrocarbon chains of the least stable α form have a loosely packed hexagonal sub cell structure. By quickly cooling a melt, the form with the lowest melting point, the α form can be obtained. This α form has the tendency to transform in the more stable β' having better chain packing. In the β' form the hydrocarbon chains are arranged according to the orthorhombic sub cell structure. Its transition to the most stable β is associated with the swelling or blooming of the triglycerides. As a result of the β' transition the obtained β form has an extended chain conformation with a triclinic sub cell structure [56]. These transformations may also occur during the production of releasing dosage forms such as microparticles or nanoparticles made of lipids. This surely can influence the structure; i.e. the stability [59, 60] and the property of the dosage form and hence the release of the embedded drugs. It has been shown that it is possible to conserve the state of modification of lipids used for producing sustained releasing forms by avoiding melting as workstep during the manufacturing. The melting points of tristearin implants loaded with 10% IFN/HP-h-CD lyophilisate obtained by compression, showed no differences when compared to the melting points of unprocessed tristearin bulk [57]. In contrast, tristearin implants obtained by melting which showed different thermodynamic behaviour. For instance lipid microparticles produced by melt dispersion method showed typical α modification behavior in contrast to microparticles produced by the solvent evaporation method, which had the same modification as the bulk material [58].

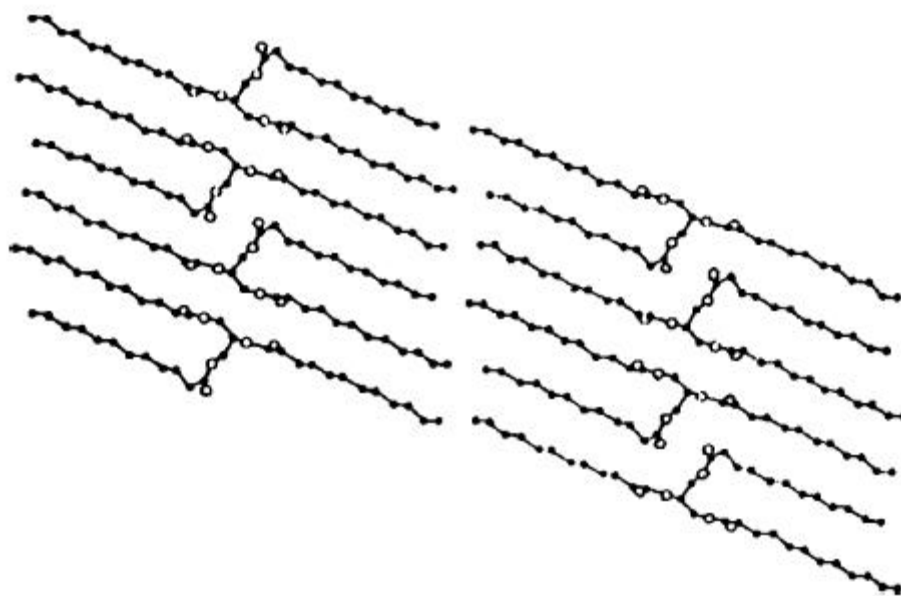


Figure 5: The molecular arrangement of a monoacid triglyceride trilaurin in the β -state as seen along the short unit cell axis [59].

Today there are several lipid drug carrier systems for the controlled release of bioactive substances: Solid lipid nanoparticles (SLN) and nanostructured lipid carriers (NLC), lipid Microparticles (MP), lipid drug conjugates (LDC), liposomes and liposomal gels, oil suspensions, lipid depot foams, lipid-based microbubbles, lipid extrudates and lipid implants.

6. Lipid based drug carrier systems

Solid lipid nanoparticles

In the middle of the 1990s, the attention of different research groups has focussed on alternative nanoparticles for intravenous injection made from solid lipids, the so-called solid lipid nanoparticles (SLNs, also called lipospheres or nanospheres). SLNs are particles with a solid lipid matrix with an average diameter in the nanometre range, they are made of solid lipids in contrary to mikroemulsion. SLNs formulations for various application routes (parenteral, oral, dermal, ocular, pulmonar, rectal) have been developed and thoroughly characterised in vitro and in vivo. The first product has recently been introduced to the Polish market (Nanobase, Yamanouchi) [60] as a topically applied moisturiser. The main characteristics of SLN with regards to parenteral application are the physical stability, good tolerability, controlled drug release and their ability to protect sensitive drugs of degradation. Disadvantages are their low drug loading capacity (normally up to 25 %), their affinity to polymorphic transition leading to drug expulsion, and the high water content of the SLN dispersion (70-99%)[61].

Preparation of SLN

Preparation by High Pressure Homogenisation (HPH).

This preparation method can be divided into the cold HMP and the hot HPH: The cold HPH is suitable for all temperature sensitive drugs. Lipid and drug are melted together and then rapidly ground under liquid nitrogen forming solid lipid microparticles. A pre-suspension is formed by high speed stirring of the particles in a cold aqueous surfactant solution. This pre-suspension is then homogenised (3 cycles at 500 bar) at or below room temperature forming SLNs. Hot HPH: Lipid and drug are melted together (approx. 5 C° over the melting point of the lipid). The melt is then combined with an aqueous surfactant solution having the same temperature. After high speed stirring for instance with an Ultra Turrax[®] machine, a hot pre-emulsion is obtained. This pre emulsion is processed in a heated homogeniser, generally a maximum of 3 cycles at 500 bar are sufficient [62].

Preparation via microemulsion

Gasco et al developed a method of producing SLNs via microemulsion. In the first step a microemulsion is prepared. This heated microemulsion is continuously injected through a needle which is placed a few centimetres beneath the surface of an ice cooled water bath, and stirred until the SLNs solidify [63].

Preparation by w/o/w double emulsion method

This method consists in the solubilization of the drug to be encapsulated in the internal aqueous phase of a w/o/w double emulsion, along with a stabiliser able to prevent loss of drug to the external phase during solvent evaporation. The aqueous drug solution is emulsified in the melted lipid using an Ultra Turrax[®]. This primary emulsion is stabilized by adding Poloxamer (polyoxyethylene–polyoxypropylene block copolymer). This primary emulsion is then dispersed into a heated aqueous solution containing PVA. The resulting double emulsion is stirred at 300 rpm by a four-blade turbine impeller. After 3–5 h, SLNs can be isolated by filtration [64].

Preparation by high speed stirring

Microparticles, produced by spray congealing, are high speed stirred or sonicated to obtain SLN. Generally high speed stirring and sonication should be combined to avoid producing SLNs with a diameter within the micrometer range. This broad particle distribution can lead to particle growth upon storage [61].

Lipid Microparticles

To avoid problems such as lack of biocompatibility, residual solvents and detrimental effects on incorporated drugs when handling polymers for drug carriers, micro particles made of natural occurring lipids can be a promising alternative. Lipid microparticles are solid particles with a size residing in the micrometer range. Like SLN they can be produced without solvents, but also their production includes the possibility of polymorphic transition during storage time. Using a model peptide during the melt dispersion method, Reithmeier et al showed that the encapsulation efficiency was higher than 80%, leading to a drug content of about 16.4% [58]. Different methods for the production of microparticles shall be introduced:

Melt dispersion method

After dispersion of the protein drug (as solid or as solution) into the melted lipid (temperatures should be 5°C higher than the melting point of the lipid) by vortex-mixing, the

resulting mixture is emulsified into a small amount of heated water containing a surfactant. This emulsion is poured into a bigger volume of ice cooled water, allowing the lipid particles to solidify. The hardened microparticles are filtrated, rinsed with water and vacuum dried over night. Microparticles produced with the melt dispersion method showed a medium diameter of 92.8 μm [58].

Solvent evaporation method

When preparing somatostatin loaded lipid microparticles, Reithmeier et al used a modified solvent evaporation method, widely used for the preparation of polymeric microparticles.

The lipid was dissolved in a suitable solvent (for instance methylene chloride), the drug was incorporated into the lipid by vigorous vortex-mixing (whether as a solid or as solution). Due to the surface ability of somatostatin acting as a surfactant, no stabilizer was added to this emulsion. The resulting preparation was further emulsified into a small volume of an aqueous phase containing stabilizer. After this workstep, the emulsion was poured into a bigger volume of ice cooled water and stirred, to allow the organic solvent to evaporize. Microparticles produced with the solvent evaporation method showed a medium diameter of 56.9 μm [58].

Spray congealing

Spray congealing is a technique of making microparticles by atomizing a solution or suspension of a drug in a melted carrier. The carrier can be a lipid as well as a polymer. The atomization or prilling process leads to the formation of melted droplets, which then solidify when in contact with cold air [65].

As there is no possibility for the drug to diffuse into an aqueous phase during preparation high encapsulation efficiencies can be achieved with this method. Maschke et al reported encapsulation efficiency for somatostatin and insulin of up to 100% [66].

Lipid microparticles formation with supercritical carbon dioxide

In 2000, a novel supercritical-fluid based process for the coating of proteins particles with lipids (e.g. trimyristate or glyceride esters of PEG, Gelucire©) was invented by the group of Benoit. This process has been applied to serum albumin as well as to sugar granules. In contrary to the Gas antisolvent method (GAS) and the Supercritical antisolvent Process (SAS), this method completely avoids the use of organic solvents. The method consists of dissolving the coating material in supercritical CO₂ in an autoclave and then adjusting the conditions of temperature and pressure so that the coating material becomes insoluble in the

carbon dioxide. This insolubilization step causes a coating to deposit on the surface of suspended particles. Scanning electron microscopy revealed that trimyristate precipitates as micro-needles of very large sizes. It was difficult to obtain uniform coating on the surface of the proteins since it mainly generates large non film-forming flakes. In contrast Gelucire, due to its multi component nature (Gelucire50-02 is a solid material composed of a complex mixture of mono-, di- and tri-glycerides, mono- and di-glyceride esters of poly(ethylene glycol) (PEG)) can form a smooth coating on BSA particles. The release of BSA from these coated microcapsules was sustained over 5 hours for crystals coated with trimyristate and over 24 hours coated with Gelucire [67-69].

Lipid microparticles preparation by cryonic micronization

In 2002, Del Curto described a novel method for manufacturing lipid microparticles as an alternative to the standard methods previously mentioned. He produced antide-(gonadotropin release hormone (GnRH) antagonist) loaded microparticles. The drug was either added to the lipid melt and stirred until a clear solution appeared (co-melting) or the antide and the lipid (glycerol monostearate, or glycerol monobehenat) were dissolved in a benzyl alcohol-ethanol mixture (solvent stripping) before being poured into a Petri dish for solvent evaporation. Resulting lipid matrices were micronized in a milling apparatus with liquid nitrogen. The obtained powders were sieved through a 125 μ m sieve in an automatic sieving apparatus [70].

Liposomes and liposome gel preparations

Liposomes are vesicular concentric bilayered structures with an aqueous core, usually 0.05-5.0 μ m in diameter which form spontaneously when certain lipids – i.e. amphiphilic substances like lecithin - are hydrated in aqueous media [71]. Liposomes may also contain other bilayer constituents such as cholesterol and hydrophilic polymer conjugated lipids. The drug can be encapsulated in the aqueous core or in the lipophilic shell during the preparation or after preparation by certain means like freeze drying in an aqueous drug solution [72]. Liposomes can control the delivery of drugs by targeting the drug to the site of action or by prolonged circulation of drugs [73]. The physicochemical properties of the lipids used for the liposome preparation can control the properties of the liposomes, such as membrane fluidity, charge density, steric hindrance, and permeability. All these factors can determine the interactions of these drug carriers with blood components and other tissues after systemic administration. The method commonly used for the preparation of liposomes is the thin-film hydration procedure in which a thin film of lipids is hydrated with an aqueous media at temperatures above the transition temperature of lipids. After the spontaneous formation of

the liposomes extrusion or sonication is necessary to reduce and unitize the particle size. Beside the film-method the injection method is the method used most often for the preparation of liposomes [74]. Derived from liposomes, liposomal gel or vesicular gel preparations have gained great interest in the last years. Based on phospholipids dispersed in water by high pressure homogenization or other suitable methods these systems form semisolid pastes with vesicular microstructure [75]. With this gels prolonged therapeutic drug levels at the site of action is achievable with almost no systemic side effects. Upon contact with the release medium the entrapped drug is slowly released by two different release mechanism: (1) erosion of the matrix with burst open of drug filled liposomes and (2) diffusion of dissolved drug out of the swollen phospholipid matrix [76].

Lipid microbubbles

Lipid microbubbles (LMB) are gas-filled spherical carriers derived from conventional ultrasound contrast agents and were initially used for improving image quality in sonography [77]. In this system the gas core – a physiological inert gas is used – is surrounded and stabilized by phospholipids. The drug is usually distributed in the material surrounding the core. LMB respond to the ultra sound field of their resonance frequency by oscillation. High ultra sound energies can cause high amplitude oscillations leading to MBs' destruction. Drug loaded LMBs can be used as ultra sound targeted carriers to locally deliver and release the bioactive substance [78]. LMB can be loaded during bubble preparation or after preparation by simple incubation with the desired bioactive substance. Due to electrostatic or weak non covalent binding the substance can be attached to the microbubble shell [79]. LMB can be produced by several methods: (1) the emulsification method uses an inner emulsion phase typically composed of a lyophilizable hydrophobic organic solvent, such as p-xylene or toluene, a volatile solid compound, such as camphor, and the lipid shell material. After freeze drying and evaporation of the organic phase the emulsion matrix can be treated with the MB core gas – immediately filling the free space. After reconstitution, the MBs instantly form in the injection medium [80]. The spray drying method is another approach to prepare LMB. During this preparation process the liquid droplet- consisting of phospholipids and volatile organic solvents - shrinks during solvent evaporation. Subsequently the dissolved shell-material accumulates at the air–water interface which leads to the formation of an elastic film. Finally, the lipid material solidifies to form the shell and the solvent inside evaporates leaving pores [81].

Lipid implants and extrudates

Implants, in our case, are small monolithic devices developed for parenteral delivering of bioactive substances into the human body in a controlled manner for a prolonged period of time. To avoid problems with their application (should be injectable with current canula) they should feature an average diameter of about one millimetre and an average length of about 10 millimetres [82]. In 1984, Kent et al described a technique of manufacturing a cholesterol-based implant matrix for the controlled release of macromolecules[83]. Matrix systems have therefore proven incapable of delivering large molecules at useful rates, due to the extremely low diffusivity of these molecules in known matrix materials. Exceptions to these theses are the polymeric matrix delivery systems disclosed in U.S. Pat. No. 4,164,560 to Folkman and Langer [84]. They function by simple diffusion through a flexuous pore network. Three years later Wang et al dispersed Insulin in a pellet disk by compressing it in mixture with cholesterol. It was found to reduce hyperglycemia in streptozocin-induced diabetic Wistar rats, by releasing the hormone for 24 days [85]. Opdebeek et al manufactured an implant by compressing bovine serum albumin into cholesterol. These pellets, injected in mice, delivered the albumin for 77 days[86]. Pure cholesterol implants showed no erosion, but cholesterol mixed with lecithin in different ratios showed characteristic erosion behaviour. Increasing the concentration of lecithin enhanced the rate of release of the incorporated drug and lead to a higher grade of erosion. The lecithin provided the formation of aqueous pores due to its amphiphilic properties [87]. In 2004 Mohl et al prepared tristearin implants for the controlled release of rh-INF by compressing the powdered components using a hydraulic press. The resulting tablet-shaped implants released rh-INF for more than 4 weeks with a distinct linear release phase of 2 weeks. In addition to that, these implants showed remarkable stabilizing effect on the encapsulated protein [57, 88]. A few years later Herrmann et al could show that the addition of PEG within the lipid matrix leads to a reversible precipitation of the embedded therapeutic protein thus the equilibrium of dissolution and precipitation drives the unique release mechanism [89, 90]. Sustained release of rh-INF for more than 60 days from extrudated implants was reported by Herrmann et al in 2007. Implants were prepared using a twin screw extrusion device and consisted of two lipid components: a low melting lipid component which was partially melted during the extrusion process and a high melting lipid component which melting temperature was above the extrusion temperature [91].

7. Degradation and swelling behaviour of lipid particles

As biodegradation of drug release systems is highly desirable, investigations on the degradation behaviour of lipid based drug delivery systems has come into focus of many research teams. In 2003 Vogelhuber et al investigated matrix swelling and erosion behaviour of glyceryl trimyristate matrices as a function of the cholesterol content. Their matrices (height was about 2 mm) were eroded at 37°C in 10 ml 0.08 M phosphate buffer solution (pH 7.4) containing 0.02% sodium azide to suppress the growth of bacteria and fungi. Matrices made of triglycerides alone showed no significant water uptake for more than 6 months. These matrices took up less than 3 % water and showed no erosion, proved by the constant mass of the matrices after drying. This was not surprising because triglycerides are known to be very stable in the absence of lipases – enzymes which would allow cleavage of the triglycerides into fatty acids and more water soluble degradation products such as mono- or diglycerides. When different glyceryl trimyristate/cholesterol mixtures were investigated there was again no significant mass loss noticeable, but the swelling behaviour changed significantly. The biggest mass gain of approx. 30% was recorded for matrices with equal amounts of triglyceride and cholesterol, whereas matrices containing 80-100% cholesterol showed only moderate water uptake i.e. less than 10%. This behaviour can be explained by the melting point depression of the triglyceride/cholesterol mixture, leading to a more soften structure with an increased possibility of water diffusing into the matrices [92]. In contrary to the lack of erosion of these matrices in vitro, Reithmeier et al showed a degradation of somatostatin triplamitate microparticles dispersed in the release medium [PBS-buffer pH 7.4, 0.05% w/v Pluronic F 68, 0.05% (w/v) NaN₃] and incubated at 37°C in a horizontal shaker water bath. The morphology of the microparticles changed significantly compared to the morphology of the microparticles shortly after the preparation, they were partly degraded and showed an eroded surface. Reithmeier et al also found a vanishing of tripalmitate microparticles 7 days after implantation in the subcutaneous tissue of mice a phenomenon which may give evidence to degradation processes at the implantation site [58]. In numerous papers, the group of Müller dealt with the effect of the particle size, lipid matrix, surfactants and crystallinity on the degradation behaviour of SLNs. They incubated their SLNs in a pancreatic lipase/colipase solution and measured the content of generated free fatty acids (as a result of the enzymatic saponification) using the NEFA (non-esterified-fatty-acid) C testkit [93-95].

Effect of surfactant on the degradation velocity:

It has been shown, that the degradation velocity is substantially affected by the stabilizer used for the preparation of SLNs. Some stabilizers such as cholic acid sodium salt (bile salt) have degradation accelerating effects, while others such as Poloxamer 407, distinctly slow down the degradation velocity. Degradation velocity can be modulated by changing the surfactant ratio. Phospholipids for instance are known to inhibit the activity of lipase. Since lipase needs contact with water-lipid interfaces to work properly, preventing their adsorption on the lipid-water interface leads to reversible enzyme inactivity. In vivo, hydrolysis products (i.e. fatty acids and monoglycerides), which could stop the enzyme reaction by accumulation in the interface, are removed by bile salts. It is presumed, that bile salts, used as stabilizers, facilitate the lipase-induced degradation of SLNs in the same way as they support the lipase in vivo. Furthermore, due to their amphiphilic properties as ionic surfactants, bile salts increase the exposed surface area of SLNs, through erosion, when they migrate from the particle into the aqueous phase. In contrast to the bile salt's promoting influence on the degradation ability of SLNs, Brokman explains the inhibiting effect on degradation of Poloxamer with surface effects such as steric-hindrance [94] [96] [97].

Effect of particle size

Size is expected to have a pronounced effect because lipid particles are degraded by surface erosion (lipase/colipase complex anchors on particle surface). By varying the homogenization parameters (pressure and number of cycles) Dynasan 114 (glyceryl trimyristate) SLNs with different size distributions were produced by Müller et al. One formulation had a distinct PCS diameter of about 800 nm. The other formulations had a diameter size range of 180-300 nm. Müller et al could not observe a difference in rate of degradation within the size range of 180-300 nm but a distinctly slower degradation rate of 800 nm SLNs could be detected. All of the SLNs (180-300nm) prepared with sodium cholate as surfactant degraded within 2 hours, whereas the microparticles prepared by Reithmeier (with a diameter size range of 57-95 μ m), using poly vinyl alcohol instead of sodium cholate, took more than 7 days to degrade [93].

Effect of crystallinity on the degradation velocity

To study the effect of crystallinity on the degradation velocity, Müller et al produced SLNs with different degrees of crystallinity. These SLN were produced by using glycerides with different length of fatty acid chains and known differences in crystallisation velocity (Dynasan 114, i.e. glyceryl trimyristate and 116, i.e. glyceryl palmitate), and using stabilisers

interfering differently with the crystallisation process of the lipid matrix (cholic acid sodium salt (NaCh), Poloxamer 407 (Plx 407)). After production, SLN with a lower crystallinity matrix (Dynasan 114 and 116, NaCh) degraded faster than higher crystalline particles (all SLN with Plx 407), and showed a decrease in degradation velocity with increasing crystallinity during storage [93-95]. Studies from Herrmann et al showed that the lipid modification has strong effect on the protein release kinetics from lipid implants. Lipid devices comprising the instable α -polymorph exhibited a high burst and a significant faster release compared to the same device composition formulated with the stable β -form lipid material. It is presumed that the poor packing of the lipid crystals in the α modification, leads to a more soften structure of the implant with a larger surface area. This increased surface area influences the growing possibility of pore formation, through which the protein can be liberated quicker. It further can be hypothesized, that this polymorphic modification has a big influence on the degradation velocity. Due to the increased exposed surface area, lipids containing mostly the α -modification should degrade faster than lipids containing the more stable β -modification [98].

8. Silk proteins

Since early times people have been fascinated by spiders and by the material produced by these arthropods for web construction and numerous other purposes. Already the publications from ancient scientist like Pliny the Elder convey the fascination for this material praising the extraordinary strength of this fiber [99]. But not only the physical properties but also the medical use was described by this early roman scientist. According to Pliny the placement of a spider web in open wounds and ulcers would promote healing [100]. This use as wound dressing has been conserved from roman times to modern era: In the wars of the 16th century packages of spider silk have been the constant companion of surgeons carried for the treatment of battle injuries [101]. This application has been immortalized by Shakespear's romantic comedy *A Midsummer Night's Dream* (Act II, 1) where the use of cobwebs is described as bandage material [102]. With the rise of modern medicine in the 19th century spider silk has fallen into therapeutic disregard. In the original Wood's dispensatory of the USA from 1870 only a few lines are devoted to its discussion, narrating about the use and success as filling material for a socket of an extracted tooth [103] but overall in those days the use of spider silk was declining and eventually terminated. Now, after so many years of disregard modern science is, once again, dealing with this fascinating material.

Today there are many hundred publications available investigating on silk protein properties for their application in material science and for medicinal use. In the last few years an understanding has emerged the reasons for the unique mechanical properties that silk possesses. In 1907 the protein nature of the silk fibres could be demonstrated [104] Since then it is known that all the different kinds of silks are composed principally of proteins (fibroin in silkworm silk, spidroin in spider silk) [105] but it took until the late 1980s that scientists concentrated on the structural properties of the different fibres [106] and the processes during the fibre spinning which are responsible for the unique combination of high strength, high elongation and extreme fineness. The process of spinning the fiber is surely one of nature's most exciting phenomena. Orb weaver spiders normally exhibit up to seven different specialized silk glands – evolutionary derived from limb glands [107] - each producing silk with a different amino acid composition. The silk protein is spun at ambient temperature and pressure from an aqueous solution to form a fiber. The state of the protein in the lumen of the gland is believed to be a liquid crystal [108], thus preventing fiber aggregation until passage down the duct. This is probably accomplished by a combination of protein structure and concentration that prevents formation of silk proteins into large protein arrays. The shear alignment during spinning induces the final assembly of the β -sheets rich structure into crystalline blocks [109]. Once formed, silk fibers are insoluble in most solvents such as water, ethanol, dilute acids and bases. Suitable solvents for silk materials, converting the β -sheet into a water soluble random coil conformation are highly concentrated sulphuric acid, formic acid, hexafluoroisopropanol (HFIP), calcium nitrate, guanidinium thiocyanate or LiBr. After dialysation from concentrated salt solutions silk proteins exhibit the water-soluble α -helical rich structure which can be converted into the water-insoluble β -sheet rich structure by addition of methanol or - in case of certain spider silk proteins- with phosphate solution [110-113]. Due to the numerous amounts of spider species spider silks are only partly characterized, but it is generally agreed that the secondary spidroin protein folding arrangement is similar to that of fibroin in *Bombyx. mori* – the common silk worm-silk. There are four different motifs: (a) elastic β -spirals; (b) crystalline β -sheets rich in alanine; (c) tight amino acid repeats forming helical structures; and (d) spacer regions [114-116]. While their structure is similar to *B. mori* silkworm silk, spider silks do not have an immunogenic sericin coating. Sericin which serves as glue, holding together the fibres to form the cocoons of silk worms was identified as a source of immunogenic reactions in vivo [117].

There are two main areas of interest for the application of silk – derived from spiders or other organisms like *Bombyx. mori* - in the modern human medicine:

Biomedical applications, i.e. tissue repair and tissue engineering and the use of spider silk proteins for the preparation of drug delivery systems.

9. Biomedical application of silk proteins

Since more than 20 years the application of silk and isolated silk proteins for application in tissue engineering i.e., the regeneration and restoration of various tissue types like bone and cartilaginous tissue with scaffolds and other appliances can be reported. Already 1989 Sakabe et al. tested silk fibroin proteins for their blood biocompatibility and thrombogenic behaviour. They implanted silk fibroin into a jugular and femoral vein of a dog. According to their in vivo studies, there was no thrombogenic activity of the silk proteins detectable [118]. In the same year Minoura et al prepared silk fibroin membranes and treated them with methanol for different amounts of time. Methanol treatment leads to a conversion into the water insoluble β -sheet conformation thus stabilizing the silk film. This methanol treated silk fibroin membranes had high oxygen permeability, high water vapour permeability, high transparency, good mechanical property and biodegradability [119]. All these properties make silk derived scaffolds ideal for the application in tissue engineering. In 1995 Minoura et al. conducted fibroblast cell studies on silk fibroin gained from silk worms. As a result they could conclude that the presence and the properties of silk proteins are ideal for the viability, growth and function of the used cells [120, 121]. In 2000 Yeo et al. prepared different dressings from polyvinylalcohol (P), chitosan (C) and fibroin (F) or used blends thereof, in order to test the resulting spongy sheets as wound dressing in an in vivo experiment. From all different wound dressing prepared a blend consisting of polyvinyl alcohol, chitosan and fibroin (PCF) promoted the best wound healing conditions by facilitating collagenization [122]. Petrini et al investigated in 2001 the interactions between silk fibroin coated polyurethane membranes and foams, and four different strains of normal human adult fibroblasts (HAF). Their results indicate that silk fibroin coated PU substrates promote cell adhesion and growth compared to unprocessed PU substrates [123]. In 2002 Cai et al. published that - when combined with poly(d,l-lactic acid) (PDLLA) - silk proteins like fibroin can improve the interaction between osteoblasts and the PDLLA films [124]. In the same year Vollrath et al. tested the biocompatibility of spider silk. In their study they used four types of spider silks: 1) dragline silk – also known as major ampullate silk - from *Nephila clavipes*, 2) native (unsterilised) silk reeled from a *Brachypelma* spider, 3) native silk taken from this spider's web and 4) its web silk thermally treated at 80 degrees C°. They compared these silk materials with fibrous silk analogue protein polymers and four already marketed wound dressings (polyurethane film,

collagen dressings, gauze pads) all these materials were implanted in epicutaneous split wounds. After 14 days the implanted silk wound stuffing were analyzed macroscopically and histological tests were conducted. Overall all sites healed rapidly. Nevertheless, marked inflammatory reactions in all sites with lympho-plasmacellular infiltrations could be detected, thus giving evidence to phagocytosis and granuloma formation but there were no distinct differences between all wound dressings [125]. In 2003 Chiarini et al tested silk coated membrane materials for their use in cell culture. Cell adsorption of adult fibroblasts was 2.2 fold higher than on uncoated polymer membranes. In addition to that, the seeded cells didn't release any major inflammatory cytokines in the culture media compared to cells seeded on normal uncoated polymer membranes [126]. It could be shown that the use of silk scaffolds resulted in advanced mineralization, with an increase of newly formed bone material, compared to collagen scaffolds which couldn't generate a similar outcome because of the rapid degradation rate [127]. Similar results could be achieved in experiments dealing with the production of cartilage-like tissue derived from human mesenchymal stem cells (hMSC) on silk scaffolds. The scaffolds – prepared from silk worm cocoons – allowed a continuous cartilage-like tissue formation applicable in clinical cartilage-repair [128]. In 2006 Jokuszies et al. published data dealing with the use and biocompatibility of spider silk fibres as a new material in nerve tissue engineering. In this study Schwann cells were cultivated on reconstituted spider silk fibres. These cells formed distinct columns along the spider fibre scaffold. These columns indicate that nerve cell reconstruction is possible with the application of this superior fibre serving as endoneural graft construction [129]. The results of this *in vitro* experiments based study was verified by a consequent *in vivo* study in rats with sciatic nerve defects. Once again, using spider silk fibres as nerve graft newly produced axons were aligned regularly and had a healthy appearance. In addition to that, a good histological evaluation and a diminishing degeneration of the gastrocnemius muscle proved the extraordinary applicability of spider silk fibres as material enabling Schwann cell migration for nerve regeneration [130]. Overall it can be concluded that silks are materials with superior mechanical and physico-chemical properties such as high oxygen permeability, high water vapour permeability and biodegradability. In contrast to native silk from *Bombyx mori* spider silk exhibit no immunogenic potential. All these properties make spider silk proteins ideal for the preparation of drug delivery systems.

10. Silk as a material for the preparation of drug delivery systems

The extraordinary properties of silk allow the use of a broad spectrum of preparation techniques resulting in several drug delivery systems for parenteral as well as for oral administration. In the following pages the authors concentrate only on drug delivery systems for parenteral application. Silk proteins can be processed resulting in: Silk hydrogels, silk based micro and nanoparticles, silk films processed as coatings and implantable matrices.

Silk films and matrices for the controlled delivery of drugs

One of the first silk based drug delivery system was developed by Tsukada et al. in 1994. This research team prepared porous silk matrices suitable for the preparation of matrix-controlled drug delivery systems. The matrices were produced either by freeze drying of aqueous silk solutions at different temperatures, by freeze drying of coagulated silk solutions at different temperatures or by mixing the silk solution with methanol-water solutions with different ratio resulting in coagulated silk solutions followed by a freeze-drying step. The results of this study showed that the addition of methanol is the most effective method to control the pore size of the resulting porous systems. By rendering the concentration of the used silk solutions and the temperature of freeze drying packing and the density of the matrices is controllable. In vitro release studies of acetylsalicylic acid entrapped in porous silk fibroin matrices showed a drug burst for the first 2 hours followed by a constant drug release for almost 3 days [131]. The need for methanol treatment inducing structure conversion can possibly endanger the stability of the entrapped drug. To investigate on the effect of this alcohol treatment Hofmann et al. conducted studies with respect to the bioactivity of the entrapped drugs. Interestingly they found out, that when using lysozyme as model drug methanol stabilization of the films resulted in significant loss of lysozyme activity whereas using horseradish peroxidase wasn't affected negatively by the methanol treatment but by the treatment with water vapours [132, 133]. Another aim of this study was the evaluation of the drug size/molecular weight impact on release patterns therefore dextrans with increasing sizes and molecular weights were used. The authors could show that the higher the molecular weight of the drug the higher was the retention in the matrix. Changes in the crystallinity of the silk in consequence of the methanol treatment and a decrease of the water solubility of the films are the explanation for that phenomenon. Nevertheless, horseradish peroxidase – a 44 kD molecule - was released in a linear manner for more than 22 days.

In 2007 Uebersax et al. published the results of their studies dealing with the preparation of silk fibroin matrices for the controlled delivery of Nerve Growth Factor (NGF). With this system Uebersax et al. could achieve a sustained release of NGF for more than 22 days. To prepare the silk films aqueous silk solutions were cast into Teflon moulds and – after water evaporation – stabilized with methanol to induce structure conversion. The obtained silk matrices had a pore free surface morphology. Bioactivity of NGF was assessed using an in vitro assay system. Uebersax et al. could show that although the total fraction of NGF released from the silk-based system was rather low – ranging from 0.3% to 13.0% - NGF activity was unaltered. In addition to that SEC-HPLC couldn't detect any NGF aggregation induced by methanol treatment or silk-NGF interaction [134].

Silk film coatings

Coatings of silk materials provide the possibility of enabling and controlling the release of bioactive substances from drug carrier systems or medicinal devices. Nanoscaled silk fibroin coatings on quartz slides produced by an all-aqueous stepwise deposition process were prepared for the controlled delivery of model compounds rhodamine B, Evan's blue and azoalbumin representing small molecules drugs and therapeutically relevant proteins. In these experiments Wang and co-workers could show a cumulative release of azoalbumin for more than 32 days from six layers of silk fibroin [135]. In other studies metallic stents used in angioplasty were coated with drug-loaded silk fibroin. Heparin, paclitaxel and clopidogrel were used as pharmacologic components and their antiproliferative effects on smooth muscle cell proliferation and endothelial cells was evaluated in this system. Human aortic endothelial cells (HAECs) and human coronary artery smooth muscle cells (HCASMCs) were used as an in vitro control system to evaluate the cellular responses to the drug-incorporated silk coatings. The conducted in vitro experiments could prove the capability of silk proteins in terms of controlling the adhesion, viability and growth of HAECs. Results from the in vivo experiments showed that the silk coatings promote the viability of the endothelial cells and reduce the platelet adhesion on the stent surface [136]. Another application of silk proteins was the coating of theophylline tablets using an aqueous coating process. As coating materials heat treated silk fibroin, fibroin-PEG mixtures and cross linked silk fibroin were applied. A sustained release for over 5h with zero order release kinetics was obtained using crosslinked silk fibroin and PEG-fibroin mixtures, whereas the heat treated possessed a brittle structure resulting in a rapid release of the drug from the tablet [137].

Silk hydrogels

Hydrogels prepared from *bombyx mori* fibroin were demonstrated to control the release of entrapped model drugs e.g., fluorescein isothiocyanate (FITC), buprenorphine and dextran conjugated with FITC with an average molecular weight of 4.4 kD. By rendering the fibroin concentration during gel preparation mechanical properties and drug release could be varied. Gels showed linear drug release for several hours indicating that silk fibroin hydrogels can serve as a rate-controlling barrier and may be used as a drug carrier system for the controlled delivery of drugs like buprenorphine [138]. Silk hydrogels prepared from genetically engineered proteins based on the sequence of *b. mori* fibroin were used to control the in vitro release of model drugs with molecular weights ranging from ca. 400 D to 500 kD. Release kinetics could be described as first order, high molecular drugs showed a constant release for over 10 days. In vivo biocompatibility was tested by implanting the hydrogels in guinea pig. After sacrifice of the animals no clinical signs of tissue reactions due to toxicity, allergy or irritancy were observed [139]. Hydrogels consisting of silk-like elastin-like polymers (SELP) were produced by the group around Ghandehari. By combining silk-like and elastin-like protein blocks in various ratios and sequences, it is possible to produce biomaterials with excellent material properties. In their publications they could show that hydrogels consisting of SELP can form injectable in situ forming depot systems for the release of bioactive substances such as DNA for gene delivery. Over 28 days almost 80% of the entrapped plasmid DNA was released by the prepared hydrogels [140]. Using the gel as a depot system for adenoviral release in vivo bioactive viruses could be delivered over a period of 4 weeks leading to a prolonged and localized expression of the viruses [141].

Preparation of silk protein microparticles by spray drying

The water solubility of the α -sheet rich structure and the possibility of stabilizing silk proteins by converting their secondary structure into the water insoluble β -sheet rich structure allow the use of organic-solvent-free preparation techniques such as spray drying. Silk microspheres generated by spray drying of aqueous silk solutions were prepared by Nakai, Shimabayashi and Kim. Whereas Nakai et al. and Shimabayashi [132] produced silk microparticles which maintained their helical structure after the drying treatment [142] the particles produced by the group around Kim changed their structure towards the water insoluble β -sheet structure during the drying [143]. Shimabayashi reported a structural conversion of their microparticles after spray drying upon an exposition to an atmosphere of 89% RH. These results indicate that it is possible to control the speed of structure conversion by means of the spray drying

parameters. Stabilized secondary structure is a prerequisite for the application of spider silk as a parenteral dosage form.

Recombinant spider silk proteins

Since all sorts of natural silk need to be harvested either from *b. mori* cocoons or from spider silk filaments followed by several processing steps involving the removal of the sericin coating on the bombyx. mori fibres [117], several research teams have been concentrating on facilitating the process of silk harvesting. The collection of silk from spiders is a time consuming and expensive procedure since spiders don't produce any cocoons with larger amounts of silk. Instead the desired drag line has to be harvested from living and fixed animals which have been refrigerated for a few minutes in order to tranquillize them. Then, after manual stimulation of the major ampullate gland the silk can be collected on spools using a winding machine. This procedure allows the collection of approx. 150 m an hour resulting in a few milligrams of silk protein [130]. A recombinant production of silk proteins overcomes disadvantages typical for natural materials such as differences in quality, variations of material structure due to genetic reasons and a limitation of the total amount of polymer harvested. Today in the era of recombinant proteins and genetic engineering there are many approaches to produce recombinant spider silk proteins but until today no dragline silk gene has been cloned in its entirety [144, 145]. In most cases there is only some sequence data available [110]. As a consequence of this, all recent studies used partial cDNA constructs of dragline silk genes to produce recombinant silk proteins in *E. coli* [146] in bovine and hamster cells [147] or in insect cells using the baculovirus expression system [148]. In 2004 the research group around Scheibel recombinantly produced synthetic spider silk proteins based on two major dragline silk proteins of *Araneus diadematus* called ADF-3 and ADF-4. The amino acid sequences of these proteins were back translated into nucleotide sequences. The modules were connected resulting in controlled assembly of synthetic genes. In this way the repetitive part C of the natural occurring silk protein ADF-4 comprising the sequence GSSAAAAAAAASGPGGYGPENQGPGSGPGGYGPGGP was multimerized and finally expressed in *escherichia coli* bacteria to obtain the repetitive synthetic 48 kD spider silk protein C₁₆.

Properties of recombinant spider silk protein C₁₆

The genetically engineered C₁₆ protein can be processed into nanofibers, nano- and microparticles, hydrogels and films using several techniques. Perhaps one of the biggest advantages of this synthetic silk material is the possibility to use both, aqueous and non-aqueous solvents for the preparations of all these different systems. A simple preparation technique for the production of spider silk films uses a casting method. Films can be cast from aqueous C₁₆-solution or from HFIP respectively formic acid solutions. Using aqueous or HFIP solutions leads to the generation of water soluble films – a conversion of the protein structure is necessary to stabilize the film and avoid dissolution. These structural conversions can be achieved by treating the films with methanol or potassium phosphate solutions. This treatment induces the conversion of the α -helical rich structure into the semi-crystalline β -sheet structure – a process similar to the proceedings occurring in the spider silk duct during spinning [109]. Films prepared from formic acid solutions self-assemble into the water insoluble β -sheet structure during solvent evaporation. The change in secondary protein structure can be monitored using circular dichroism (CD) and FT-IR-spectroscopy. Processed films show remarkable chemical stability after stabilization with methanol or potassium phosphate. Most known solvents are incapable of dissolving stabilized C₁₆ films, only guanidinium thiocyanate solutions with high molarity can lead to a complete disintegration of the film [149]. If a special functionality is necessary the C₁₆ film surface can be modified with respect to the desired feature. For instance enzymes like β -galactosidase and other macromolecules can be coupled to surface exposed carboxyl groups of the C₁₆. In 2007 Scheibel et al could show that the conversion of water soluble C₁₆ can be triggered by the interfacial adsorption of the protein. When emulsifying C₁₆ solution with toluene insoluble silk microcapsules form around the toluene droplets. These silk microcapsules were mechanically stable and permeable for smaller molecules possessing a molecular weight cut off of approx. 70kD molecules [150] [151]. Admixing aqueous solutions of C₁₆ with potassium phosphate solution initiates the change in secondary protein structure leading to the generation of water insoluble silk microparticles. The formation of C₁₆ microparticles involves a phase separation into a hydrophobic protein-rich phase and an aqueous phase. This process allows an encapsulation of hydrophobic substances participating in this phase separation and thus accumulating in the hydrophobic protein-rich phase. In 2008 Liebman et al could show β -carotene was encapsulated successfully in spider protein particles during the microparticle formation yielding in an encapsulation of 5% (m/m) [152].

GENERAL INTRODUCTION

Similar to fibroin proteins spider silk proteins can spontaneously form hydrogels which are physically stable for several weeks. The self assembling process leading to the gel structure can be disrupted by agitation or shearing and chemical cross-linking of the hydrogels yielded in elastic hydrogels probably applicable in medical applications [144, 149, 150].

In summary spider silk proteins especially genetically engineered C₁₆-proteins are very versatile. Due to their unique physicochemical properties they enable the use of a great variety of preparation techniques resulting in a diverse set of systems with a great potential for various medical and technical applications.

11. References

1. Reichert, J.M., *Trends in US approvals: new biopharmaceuticals and vaccines*. Trends in Biotechnology, 2006. 24(7): p. 293-298.
2. Banga, A.K., *Therapeutic Peptides and Proteins*. ISBN: 0-8493-1630-8, 2006.
3. Cleland, J.L.P.M.F.S., S. J., *The development of stable protein formulations: a close look at protein aggregation, deamidation, and oxidation*. Critical reviews in therapeutic drug carrier systems, 1993. 10(4)(307-77).
4. Chi, E.Y., et al., *Physical Stability of Proteins in Aqueous Solution: Mechanism and Driving Forces in Nonnative Protein Aggregation*. Pharmaceutical Research, 2003. 20(9): p. 1325-1336.
5. Nosoh, Y. and T. Sekiguchi, *Protein engineering for thermostability*. Trends in Biotechnology, 1990. 8: p. 16-20.
6. Theodore W. Randolph, J.F.C., *Engineering challenges of protein formulations*. AIChE Journal, 2007. 53(8): p. 1902-1907.
7. Arora, P., S. Sharma, and S. Garg, *Permeability issues in nasal drug delivery*. Drug Discovery Today, 2002. 7(18): p. 967-975.
8. Illum, L., *Nasal drug delivery--possibilities, problems and solutions*. Journal of Controlled Release, 2003. 87(1-3): p. 187-198.
9. Shoyele, S.A., *Controlling the Release of Proteins/Peptides via the Pulmonary Route*, in *Drug Delivery Systems*. 2008. p. 141-148.
10. Mack, G.S., *Pfizer dumps Exubera*. Nat Biotech, 2007. 25(12): p. 1331-1332.
11. Banga, A.K., *New Technologies to Allow Transdermal Delivery of Therapeutic Proteins and Small Water-Soluble Drugs*. American Journal of Drug Delivery, 2006. 4(4): p. 221-230.
12. Ogura, M., S. Paliwal, and S. Mitragotri, *Low-frequency sonophoresis: Current status and future prospects*. Advanced Drug Delivery Reviews, 2008. 60(10): p. 1218-1223.
13. Cormier, M., et al., *Transdermal delivery of desmopressin using a coated microneedle array patch system*. Journal of Controlled Release, 2004. 97(3): p. 503-511.
14. Folkman, J., *How the field of controlled-release technology began, and its central role in the development of angiogenesis research*. Biomaterials, 1990. 11(9): p. 615-618.
15. Langer, R.F., Judah., *Polymers for the sustained release of proteins and other macromolecules*. Nature (London, United Kingdom), 1976. 263(5580),: p. 797-800.

16. Siegel, R.A. and R. Langer, *Controlled Release of Polypeptides and Other Macromolecules*. Pharmaceutical Research, 1984. 1(1): p. 2-10.
17. Brange, J. and A. Vølund, *Insulin analogs with improved pharmacokinetic profiles*. Advanced Drug Delivery Reviews, 1999. 35(2-3): p. 307-335.
18. Siepmann, J. and A. Göpferich, *Mathematical modeling of bioerodible, polymeric drug delivery systems*. Advanced Drug Delivery Reviews, 2001. 48(2-3): p. 229-247.
19. Nair, L.S. and C.T. Laurencin, *Biodegradable polymers as biomaterials*. Progress in Polymer Science, 2007. 32(8-9): p. 762-798.
20. Whittlesey, K.J. and L.D. Shea, *Delivery systems for small molecule drugs, proteins, and DNA: the neuroscience/biomaterial interface*. Experimental Neurology, 2004. 190(1): p. 1-16.
21. Müller, R.H., Hildebrand, G. E., *Pharmazeutische Technology: moderne Arzneiformen*. Wissenschaftliche Verlagsgesellschaft mbH Stuttgart 1998: p. 243-256.
22. Park, T.G., H. Yong Lee, and Y. Sung Nam, *A new preparation method for protein loaded poly(,-lactic-co-glycolic acid) microspheres and protein release mechanism study*. Journal of Controlled Release, 1998. 55(2-3): p. 181-191.
23. Morlock, M., et al., *Microencapsulation of rh-erythropoietin, using biodegradable poly(,-lactide-co-glycolide): protein stability and the effects of stabilizing excipients*. European Journal of Pharmaceutics and Biopharmaceutics, 1997. 43(1): p. 29-36.
24. van de Weert, M., W.E. Hennink, and W. Jiskoot, *Protein Instability in Poly(Lactic-co-Glycolic Acid) Microparticles*. Pharmaceutical Research, 2000. 17(10): p. 1159-1167.
25. Claudio Thomasin, H.N.-T.H.P.M.B.G., *Drug microencapsulation by PLA/PLGA coacervation in the light of thermodynamics. I. Overview and theoretical considerations*. Journal of Pharmaceutical Sciences, 1998. 87(3): p. 259-268.
26. Jain, R.A., *The manufacturing techniques of various drug loaded biodegradable poly(lactide-co-glycolide) (PLGA) devices*. Biomaterials, 2000. 21(23): p. 2475-2490.
27. Herbert, P., et al., *A Large-Scale Process to Produce Microencapsulated Proteins*. Pharmaceutical Research, 1998. 15(2): p. 357-361.
28. Yeo, S.-D. and E. Kiran, *Formation of polymer particles with supercritical fluids: A review*. The Journal of Supercritical Fluids, 2005. 34(3): p. 287-308.
29. García, J.T., et al., *Biodegradable laminar implants for sustained release of recombinant human growth hormone*. Biomaterials, 2002. 23(24): p. 4759-4764.

30. Rothen-Weinhold, A.J.B.S.Y.N.H.-R.S.R.G.J.H., *Protein release from poly(ortho ester) extruded rods*. Macromolecular Symposia, 2001. 172(1): p. 67-72.
31. Rothen-Weinhold, A., et al., *Injection-molding versus extrusion as manufacturing technique for the preparation of biodegradable implants*. European Journal of Pharmaceutics and Biopharmaceutics, 1999. 48(2): p. 113-121.
32. Fildes, F.J.T.H., F. G.; Furr, B. J. A. , *The development of 'Zoladex'. A case history*. Polypept. Protein Drugs, 1991: p. 228-250.
33. Rosen, H.B., et al., *Bioerodible polyanhydrides for controlled drug delivery*. Biomaterials, 1983. 4(2): p. 131-133.
34. K. W. Leong, P.D.A.M.M.R.L., *Bioerodible polyanhydrides as drug-carrier matrices. II. Biocompatibility and chemical reactivity*. Journal of Biomedical Materials Research, 1986. 20(1): p. 51-64.
35. Wang, P.P., J. Frazier, and H. Brem, *Local drug delivery to the brain*. Advanced Drug Delivery Reviews, 2002. 54(7): p. 987-1013.
36. Brem, H.T., R. J.; Olivi, A.; Pinn, M.; Weingart, J. D.; Wharam, M; Epstein, J. I., *Biodegradable polymers for controlled delivery of chemotherapy with and without radiation therapy in the monkey brain*. Journal of Neurosurgery, 1994. 80(2).
37. Heller, J., et al., *Poly(ortho esters): synthesis, characterization, properties and uses*. Advanced Drug Delivery Reviews, 2002. 54(7): p. 1015-1039.
38. Heller, J., et al., *Development and applications of injectable poly(ortho esters) for pain control and periodontal treatment*. Biomaterials, 2002. 23(22): p. 4397-4404.
39. Chia, H.-H., et al., *Auto-catalyzed poly(ortho ester) microspheres: a study of their erosion and drug release mechanism*. Journal of Controlled Release, 2001. 75(1-2): p. 11-25.
40. Li, S., *Hydrolytic degradation characteristics of aliphatic polyesters derived from lactic and glycolic acids*. Journal of Biomedical Materials Research, 1999. 48 (2): p. 343-352.
41. Goepferich, A., *Polymer Bulk Erosion*. Macromolecules, 1997. 30 (9): p. 2508-2604.
42. Burkersroda, F.v., L. Schedl, and A. Göpferich, *Why degradable polymers undergo surface erosion or bulk erosion*. Biomaterials, 2002. 23(21): p. 4221-4231.
43. Agatha Bastida, P.S.P.A.R.F.-L.J.H.J.M.G., *A single step purification, immobilization, and hyperactivation of lipases via interfacial adsorption on strongly hydrophobic supports*. Biotechnology and Bioengineering, 1998. 58(5): p. 486-493.

44. Fernandez-Lafuente, R., et al., *Immobilization of lipases by selective adsorption on hydrophobic supports*. Chemistry and Physics of Lipids, 1998. 93(1-2): p. 185-197.
45. Lee, W.-K., J.-H. Ryou, and C.-S. Ha, *Retardation of enzymatic degradation of microbial polyesters using surface chemistry: effect of addition of non-degradable polymers*. Surface Science, 2003. 542(3): p. 235-243.
46. Yamada, M. and M. Amoo, *Enzymatic collapse of artificial polymer composite material containing double-stranded DNA*. International Journal of Biological Macromolecules, 2008. 42(5): p. 478-482.
47. Lu, W.P., Tae Gwan, *Protein release from poly(lactic-co-glycolic acid) microspheres: Protein stability problems*. Journal of Pharmaceutical Science and Technology, 1995. 49(1).
48. Tia Estey, J.K.S.P.S.J.F.C., *BSA degradation under acidic conditions: A model for protein instability during release from PLGA delivery systems*. Journal of Pharmaceutical Sciences, 2006. 95(7): p. 1626-1639.
49. M.L. Houchin, E.M.T., *Chemical degradation of peptides and proteins in PLGA: A review of reactions and mechanisms*. Journal of Pharmaceutical Sciences, 2008. 97(7): p. 2395-2404.
50. Houchin, M.L., K. Heppert, and E.M. Topp, *Deamidation, acylation and proteolysis of a model peptide in PLGA films*. Journal of Controlled Release, 2006. 112(1): p. 111-119.
51. Sullivan, M.F., P.S. Ruemmler, and D.R. Kalkwarf, *Sustained administration of cyclazocine for antagonism of morphine*. Drug and Alcohol Dependence, 1976. 1(6): p. 415-428.
52. Joseph, A.A., Hill J. L. J., Patel S., Kincl A., *Sustained-release hormonal preparations XV: Release of progesterone from cholesterol pellets <I>in vivo</I>*. Journal of Pharmaceutical Sciences, 1977. 66(4): p. 490-493.
53. Sato, K., *Crystallization behaviour of fats and lipids -- a review*. Chemical Engineering Science, 2001. 56(7): p. 2255-2265.
54. Tilcock, C.P.S., *Lipid polymorphism*. Chemistry and Physics of Lipids, 1986. 40(2-4): p. 109-125.
55. Van Santen, R.A., *The Ostwald step rule*. The Journal of Physical Chemistry, 1984. 88(24): p. 5768-5769.

56. Eldem, T., P. Speiser, and H. Altorfer, *Polymorphic Behavior of Sprayed Lipid Micropellets and Its Evaluation by Differential Scanning Calorimetry and Scanning Electron Microscopy*. *Pharmaceutical Research*, 1991. 8(2): p. 178-184.
57. Mohl, S. and G. Winter, *Continuous release of rh-interferon [alpha]-2a from triglyceride matrices*. *Journal of Controlled Release*, 2004. 97(1): p. 67-78.
58. Reithmeier, H., J. Herrmann, and A. Göpferich, *Lipid microparticles as a parenteral controlled release device for peptides*. *Journal of Controlled Release*, 2001. 73(2-3): p. 339-350.
59. Hongisto, V., V.-P. Lehto, and E. Laine, *X-ray diffraction and microcalorimetry study of the [alpha]->[beta] transformation of tripalmitin*. *Thermochimica Acta*, 1996. 276: p. 229-242.
60. Ales Prokop, J.M.D., *Nanovehicular intracellular delivery systems*. *Journal of Pharmaceutical Sciences*, 2008. 97(9): p. 3518-3590.
61. Wissing, S.A., O. Kayser, and R.H. Müller, *Solid lipid nanoparticles for parenteral drug delivery*. *Advanced Drug Delivery Reviews*, 2004. 56(9): p. 1257-1272.
62. Müller, R.H., K. Mäder, and S. Gohla, *Solid lipid nanoparticles (SLN) for controlled drug delivery - a review of the state of the art*. *European Journal of Pharmaceutics and Biopharmaceutics*, 2000. 50(1): p. 161-177.
63. Marengo, E., et al., *Scale-up of the preparation process of solid lipid nanospheres. Part I*. *International Journal of Pharmaceutics*, 2000. 205: p. 3-13.
64. Cortesi, R., et al., *Production of lipospheres as carriers for bioactive compounds*. *Biomaterials*, 2002. 23: p. 2283-2294.
65. Nadia Passerini, B.P.M.M.D.V.B.A.C.C.L.R., *Characterization of carbamazepine-Gelucire 50/13 microparticles prepared by a spray-congealing process using ultrasounds*. *Journal of Pharmaceutical Sciences*, 2002. 91(3): p. 699-707.
66. Maschke, A., et al., *Development of a spray congealing process for the preparation of insulin-loaded lipid microparticles and characterization thereof*. *European Journal of Pharmaceutics and Biopharmaceutics*, 2007. 65(2): p. 175-187.
67. Santos, I.R.D., et al., *A supercritical fluid-based coating technology. 3: Preparation and characterization of bovine serum albumin particles coated with lipids*. *Journal of Microencapsulation*, 2003. 20(1): p. 110 - 128.
68. Santos, I.R.D., et al., *A supercritical fluid-based coating technology. 2: Solubility considerations*. *Journal of Microencapsulation*, 2003. 20(1): p. 97 - 109.

69. Thies, C., et al., *A supercritical fluid-based coating technology 1: Process considerations*. Journal of Microencapsulation, 2003. 20: p. 87-96.
70. Del Curto, M.D., et al., *Lipid microparticles as sustained release system for a GnRH antagonist (Antide)*. Journal of Controlled Release, 2003. 89(2): p. 297-310.
71. Bangham, A.D.H., R. W., *Negative staining of phospholipids and their structural modification by surfaceactive agents as observed in the electron microscope*. Journal of molecular biology, 1964. 8 660-8(PubMed ID 14187392 AN 1964145415 MEDLINE).
72. Ohsawa, T.M., H. ; Harada, K. , *A novel method for preparing liposome with a high capacity to encapsulate proteinous drugs: freeze-drying method*. . Chemical & pharmaceutical bulletin, 1984. 32 (6): p. 2442-2445.
73. Sharma, A. and U.S. Sharma, *Liposomes in drug delivery: Progress and limitations*. International Journal of Pharmaceutics, 1997. 154(2): p. 123-140.
74. Reza, M.M., *Liposomes: An overview of manufacturing techniques*. Cellular & Molecular Biology Letters, 2005. 10: p. 711-719.
75. Brandl, M., et al., *Preparation and characterization of semi-solid phospholipid dispersions and dilutions thereof*. International Journal of Pharmaceutics, 1998. 170(2): p. 187-199.
76. Tardi, C., M. Brandl, and R. Schubert, *Erosion and controlled release properties of semisolid vesicular phospholipid dispersions*. Journal of Controlled Release, 1998. 55(2-3): p. 261-270.
77. Steliyan Tinkov, R.B.G.W.C.C., *Microbubbles as ultrasound triggered drug carriers*. Journal of Pharmaceutical Sciences, 2008. 9999(9999): p. n/a.
78. Xie, F., et al., *Effectiveness of lipid microbubbles and ultrasound in de clotting thrombosis*. Ultrasound in Medicine & Biology, 2005. 31(7): p. 979-985.
79. Bekeredjian, R., H.A. Katus, and H.F. Kuecherer, *Therapeutic Use of Ultrasound Targeted Microbubble Destruction: A Review of Non-Cardiac Applications*. Therapeutische Anwendung der ultraschallgesteuerten Zerstörung von gasgefüllten Mikrosphären - Übersicht über extrakardiale Einsatzmöglichkeiten, 2006(02): p. 134-140.
80. Dalia M. El-Sherif, M.A.W., *Development of a novel method for synthesis of a polymeric ultrasound contrast agent*. Journal of Biomedical Materials Research Part A, 2003. 66A(2): p. 347-355.

81. Tsapis, N., et al., *Onset of Buckling in Drying Droplets of Colloidal Suspensions*. Physical Review Letters, 2005. 94(1): p. 018302.
82. Müller, R.H., Hildebrand, G. E., *Pharmazeutische Technologie: moderne Arzneiformen*. . Wissenschaftliche Verlagsgesellschaft mbH Stuttgart, 1998: p. 243-256.
83. Kent, J.S.S.U.S.A., Inc., USA). *Cholesterol matrix delivery system for sustained release of macromolecules*. . USXXAM US 4452775 A 19840605 Patent, 1984. US 82-446749 19821203.: p. 8.
84. Langer, R.F., Judah., *Systems for the controlled release of macromolecules*. US Patent 4164560 1979.
85. Wang, P.Y., *Prolonged release of insulin by cholesterol-matrix implant*. Diabetes, 1987. 36(9): p. 1068-1072.
86. Opdebeeck, J.P. and I.G. Tucker, *A cholesterol implant used as a delivery system to immunize mice with bovine serum albumin*. Journal of Controlled Release, 1993. 23(3): p. 271-279.
87. Khan, M.Z.I., I.G. Tucker, and J.P. Opdebeeck, *Cholesterol and lecithin implants for sustained release of antigen: release and erosion in vitro, and antibody response in mice*. International Journal of Pharmaceutics, 1991. 76(1-2): p. 161-170.
88. Mohl, S. and G. Winter, *Continuous Release of rh-Interferon $\hat{I}\pm$ -2a from Triglyceride Implants: Storage Stability of the Dosage Forms*. Pharmaceutical Development and Technology, 2006. 11(1): p. 103-110.
89. Herrmann, S., et al., *Mechanisms controlling protein release from lipidic implants: Effects of PEG addition*. Journal of Controlled Release, 2007. 118(2): p. 161-168.
90. Herrmann, S., et al., *New Insight into the Role of Polyethylene Glycol Acting as Protein Release Modifier in Lipidic Implants*. Pharmaceutical Research, 2007. 24(8): p. 1527-1537.
91. Herrmann, S., *Lipidic Implants for Pharmaceutical Proteins. Mechanisms of Release and Development of Extruded Devices*. Dissertation, 2007(CAN 149:315271).
92. Vogelhuber, W., et al., *Monolithic glyceryl trimyristate matrices for parenteral drug release applications*. European Journal of Pharmaceutics and Biopharmaceutics, 2003. 55: p. 133-138.
93. Olbrich, C., O. Kayser, and R.H. Müller, *Enzymatic Degradation of Dynasan 114 SLN – Effect of Surfactants and Particle Size*. Journal of Nanoparticle Research, 2002. 4(1): p. 121-129.

94. Olbrich, C. and R.H. Müller, *Enzymatic degradation of SLN--effect of surfactant and surfactant mixtures*. International Journal of Pharmaceutics, 1999. 180(1): p. 31-39.
95. Olbrich, C., O. Kayser, and R.H. Müller, *Lipase degradation of Dynasan 114 and 116 solid lipid nanoparticles (SLN)--effect of surfactants, storage time and crystallinity*. International Journal of Pharmaceutics, 2002. 237(1-2): p. 119-128.
96. Brockman, H.L., *Kinetic behavior of the pancreatic lipase-colipase-lipid system*. Biochimie, 2000. 82(11): p. 987-995.
97. Borgström, B.E.-A., C. ; Wieloch, T., *Pancreatic colipase: chemistry and physiology*. Journal of Lipid Research 1979. Volume 20: p. 805-816.
98. Herrmann, S.W., G. , *Influence of the lipid modification on the release behaviour of a cytokine from lipid implants*. Poster from Controlled Release Society German Chapter Annual Meeting 2005 - Marburg), 2005.
99. Plinius, *Naturalis historiae, Buch XI, Über die verschiedenen Insektenarten*. 79 A.D.
100. James Newman, C.N., *Oh what a tangled web: The medicinal use of spider silk*. International Journal of Dermatology, 1995. 34(4): p. 290-292.
101. Haeger, K., *The illustrated history of surgery*. Bell New York, 1988. ISBN: 0-517-66574-3(1st edition.).
102. Shakespeare, W., *A Midsummer Night's Dream Act 3, 1595. Scene 1*.
103. Wood, G.B.B., F. ;, *The dispensatory of the United States of America*. First edition, 1870. J. B. LIPPINCOTT AND CO.
104. Lewis, R.V., *Spider silk: the unraveling of a mystery*. Acc. Chem. Res., 1992. 25(9): p. 392-398.
105. Ana C. MacIntosh, V.R.K.A.C.P.V.H., *Skeletal tissue engineering using silk biomaterials*. Journal of Tissue Engineering and Regenerative Medicine, 2008. 2(2-3): p. 71-80.
106. Lewis, R.V., *Spider Silk: Ancient Ideas for New Biomaterials*. Chemical Reviews, 2006. 106(9): p. 3762-3774.
107. Jeffrey W, S., *The origin of the spinning apparatus in spiders*. Biological Reviews, 1987. 62(2): p. 89-113.
108. Vollrath, F. and D.P. Knight, *Liquid crystalline spinning of spider silk*. Nature, 2001. 410(6828): p. 541-548.
109. Jin, H.-J. and D.L. Kaplan, *Mechanism of silk processing in insects and spiders*. Nature, 2003. 424(6952): p. 1057-1061.

110. Scheibel, T., *Spider silks: recombinant synthesis, assembly, spinning, and engineering of synthetic proteins*. Microbial Cell Factories, 2004. 3(1): p. 14.
111. Slotta, U., et al., *Structural Analysis of Spider Silk Films*. Supramolecular Chemistry, 2006. 18(5): p. 465 - 471.
112. Ute K. Slotta, S.R.S.G.T.S., *An Engineered Spider Silk Protein Forms Microspheres* Angewandte Chemie International Edition, 2008. 47(24): p. 4592-4594.
113. Haider, M., Z. Megeed, and H. Ghandehari, *Genetically engineered polymers: status and prospects for controlled release*. Journal of Controlled Release, 2004. 95(1): p. 1-26.
114. Gosline, J.M., et al., *The mechanical design of spider silks: from fibroin sequence to mechanical function*. J Exp Biol, 1999. 202(23): p. 3295-3303.
115. Sheu, H.-S., et al., *Lattice deformation and thermal stability of crystals in spider silk*. International Journal of Biological Macromolecules, 2004. 34(5): p. 267-273.
116. Sirichaisit, J., et al., *Analysis of Structure/Property Relationships in Silkworm (*Bombyx mori*) and Spider Dragline (*Nephila edulis*) Silks Using Raman Spectroscopy*. Biomacromolecules, 2003. 4(2): p. 387-394.
117. Panilaitis, B., et al., *Macrophage responses to silk*. Biomaterials, 2003. 24(18): p. 3079-3085.
118. Sakabe, H.I., Hiraku; Miyamoto, Takeaki; Noishiki, Yasuharu; Ha, Wan Shik., *In vivo blood compatibility of regenerated silk fibroin*. Sen'i Gakkaishi 1989. 45 (11): p. 487-490.
119. Minoura, N., M. Tsukada, and M. Nagura, *Physico-chemical properties of silk fibroin membrane as a biomaterial*. Biomaterials, 1990. 11(6): p. 430-434.
120. Norihiko Minoura, S.-I.A.Y.G.M.T.Y.I., *Attachment and growth of cultured fibroblast cells on silk protein matrices*. Journal of Biomedical Materials Research, 1995. 29(10): p. 1215-1221.
121. Minoura, N., et al., *Attachment and Growth of Fibroblast Cells on Silk Fibroin*. Biochemical and Biophysical Research Communications, 1995. 208(2): p. 511-516.
122. Yeo, J.H., et al., *The Effects of PVA/Chitosan/Fibroin (PCF)-Blended Spongy Sheets on Wound Healing in Rats*. Biological & pharmaceutical bulletin, 2000. 23(10): p. 1220-1223 %U <http://ci.nii.ac.jp/naid/110003639858/en/>.
123. Petrini, P., C. Parolari, and M.C. Tanzi, *Silk fibroin-polyurethane scaffolds for tissue engineering*. Journal of Materials Science: Materials in Medicine, 2001. 12: p. 849-853.

124. Cai, K., et al., *Poly(d,l-lactic acid) surfaces modified by silk fibroin: effects on the culture of osteoblast in vitro*. *Biomaterials*, 2002. 23: p. 1153-1160.
125. Vollrath, F.B., P.; Basedow, A.; Engstrom, W.; List, H, *Local tolerance to spider silks and protein polymers in vivo*. *In Vivo*, 2002. 16 (4)(229-234).
126. Chiarini, A., et al., *Silk fibroin/poly(carbonate)-urethane as a substrate for cell growth: in vitro interactions with human cells*. *Biomaterials*, 2003. 24: p. 789-799.
127. Meinel, L., Vassilis Karageorgiou Sandra Hofmann Robert Fajardo Brian Snyder Chunmei Li Ludwig Zichner Robert Langer Gordana Vunjak-Novakovic David L. Kaplan, *Engineering bone-like tissue in vitro using human bone marrow stem cells and silk scaffolds*. *Journal of Biomedical Materials Research Part A*, 2004. 71A(1): p. 25-34.
128. Lorenz Meinel, S.H.V.K.L.Z.R.L.D.K.G.V.-N., *Engineering cartilage-like tissue using human mesenchymal stem cells and silk protein scaffolds*. *Biotechnology and Bioengineering*, 2004. 88(3): p. 379-391.
129. Jokuszies, A., et al., *In vitro Herstellung biokompatibler Nervenimplantate durch die Verwendung von Spinnseide und azellularisierten Venolen*, in *Chirurgisches Forum 2006*. 2006. p. 375-376.
130. Allmeling, C.J., A.; Reimers, K.S.; Kall, C. Y; Choi, G.; Brandes, C. ; Kasper T.; Scheper, M.; Guggenheim, M.; Vogt, P. M. , *Spider silk fibres in artificial nerve constructs promote peripheral nerve regeneration*. *Cell Proliferation*, 2008. 41(3): p. 408-420.
131. Masuhiro Tsukada, G.F.N.M.G.A., *Preparation and application of porous silk fibroin materials*. *Journal of Applied Polymer Science*, 1994. 54(4): p. 507-514.
132. Hino, T., M. Tanimoto, and S. Shimabayashi, *Change in secondary structure of silk fibroin during preparation of its microspheres by spray-drying and exposure to humid atmosphere*. *Journal of Colloid and Interface Science*, 2003. 266(1): p. 68-73.
133. Hofmann, S., et al., *Silk fibroin as an organic polymer for controlled drug delivery*. *Journal of Controlled Release*, 2006. 111(1-2): p. 219-227.
134. Uebersax, L., et al., *Silk fibroin matrices for the controlled release of nerve growth factor (NGF)*. *Biomaterials*, 2007. 28(30): p. 4449-4460.
135. Wang, X., et al., *Nanolayer biomaterial coatings of silk fibroin for controlled release*. *Journal of Controlled Release*, 2007. 121(3): p. 190-199.
136. Wang, X., et al., *Controlled release from multilayer silk biomaterial coatings to modulate vascular cell responses*. *Biomaterials*, 2008. 29(7): p. 894-903.

137. Bayraktar, O., et al., *Silk fibroin as a novel coating material for controlled release of theophylline*. European Journal of Pharmaceutics and Biopharmaceutics, 2005. 60(3): p. 373-381.
138. Fang, J.-Y., et al., *Characterization and Evaluation of Silk Protein Hydrogels for Drug Delivery*. Chemical & pharmaceutical bulletin, 2006. 54(2): p. 156-162.
139. Cappello, J., et al., *In-situ self-assembling protein polymer gel systems for administration, delivery, and release of drugs*. Journal of Controlled Release, 1998. 53(1-3): p. 105-117.
140. Megeed, Z., J. Cappello, and H. Ghandehari, *Controlled Release of Plasmid DNA from a Genetically Engineered Silk-Elastinlike Hydrogel*. Pharmaceutical Research, 2002. 19(7): p. 954-959.
141. Hatefi, A., J. Cappello, and H. Ghandehari, *Adenoviral Gene Delivery to Solid Tumors by Recombinant Silk-Elastinlike Protein Polymers*. Pharmaceutical Research, 2007. 24(4): p. 773-779.
142. Hino, T., S. Shimabayashi, and A. Nakai, *Silk Microspheres Prepared by Spray-drying of an Aqueous System*. Pharmacy and Pharmacology Communications, 2000. 6: p. 335-339.
143. Yeo, J.-H., et al., *Simple preparation and characteristics of silk fibroin microsphere*. European Polymer Journal, 2003. 39(6): p. 1195-1199.
144. Hinman, M.B. and R.V. Lewis, *Isolation of a clone encoding a second dragline silk fibroin. Nephila clavipes dragline silk is a two-protein fiber*. J. Biol. Chem., 1992. 267(27): p. 19320-19324.
145. Guerette, P.A., et al., *Silk Properties Determined by Gland-Specific Expression of a Spider Fibroin Gene Family*. Science, 1996. 272(5258): p. 112-115.
146. Arcidiacono, S., et al., *Purification and characterization of recombinant spider silk expressed in Escherichia coli*. Applied Microbiology and Biotechnology, 1998. 49(1): p. 31-38.
147. Lazaris, A., et al., *Spider Silk Fibers Spun from Soluble Recombinant Silk Produced in Mammalian Cells*. Science, 2002. 295(5554): p. 472-476.
148. Huemmerich, D., et al., *Novel Assembly Properties of Recombinant Spider Dragline Silk Proteins*. 2004. 14(22): p. 2070-2074.
149. Huemmerich, D., U. Slotta, and T. Scheibel, *Processing and modification of films made from recombinant spider silk proteins*. Applied Physics A: Materials Science & Processing, 2006. 82(2): p. 219-222.

150. K. D. Hermanson, D.H.T.S.A.R.B., *Engineered Microcapsules Fabricated from Reconstituted Spider Silk*. *Advanced Materials*, 2007. 19(14): p. 1810-1815.
151. K. D. Hermanson, M.B.H., Thomas Scheibel and Andreas R. Bausch, *Permeability of silk microcapsules made by the interfacial adsorption of protein*. *Phys. Chem. Chem. Phys.*, , 2007. 9: p. 6442-6446.
152. Liebmann, B., et al., *Formulation of poorly water-soluble substances using self-assembling spider silk protein*. *Colloids and Surfaces A: Physicochemical and Engineering Aspects*, 2008. 331(1-2): p. 126-132.
153. Guse, C., et al., *Biocompatibility and erosion behavior of implants made of triglycerides and blends with cholesterol and phospholipids*. *International Journal of Pharmaceutics*, 2006. 314(2): p. 153-160.
154. Kreye, F., F. Siepmann, and J. Siepmann, *Lipid implants as drug delivery systems*. *Expert Opinion on Drug Delivery*, 2008. 5(3): p. 291-307.
155. Appel, B., et al., *Lipidic implants for controlled release of bioactive insulin: Effects on cartilage engineered in vitro*. *Int.J.Pharm.*, 2006. 314(2): p. 170-178.
156. Wang, P.Y., *Lipids as excipient in sustained release insulin implants*. *International Journal of Pharmaceutics*, 1989. 54(3): p. 223-230.
157. Maschke, A., et al., *Lipids: An alternative material for protein and peptide release*, in *ACS Symposium Series 879*, S.n. Svenson, Editor. 2004. p. 176-196.
158. Wang, P.Y., *Palmitic acid as an excipient in implants for sustained release of insulin*. *Biomaterials*, 1991. 12(1): p. 57-62.
159. Blumenthal, P.D.G.-D., Kristina; Marintcheva-Petrova, Maya., *Tolerability and clinical safety of Implanon*. *European Journal of Contraception & Reproductive Health Care* 2008. 13(1).
160. Shard, A.G. and P.E. Tomlins, *Biocompatibility and the efficacy of medical implants*. *Regenerative Medicine*, 2006. 1(6): p. 789-800.
161. M. Schlosser, L.W.G.U.B.Z.M.Z.R.Z., *Immunogenicity of polymeric implants: Long-term antibody response against polyester (Dacron) following the implantation of vascular prostheses into rats*. *Journal of Biomedical Materials Research*, 2002. 61(3): p. 450-457.

II. AIM OF THE THESIS

When the area of controlled release was starting in the early 70ties of the last century no one would have assumed that the development and research associated with this field of science would have such major influence on the therapeutic medicine. Today we know that the employment of controlled release devices crucially enhances the therapeutic success of treatments requiring multi dose injections or infusions of bioactives. Starting with rather simple materials such silicone rubber tubing the primary substance used to develop and manufacture controlled release devices such as implants and microparticles have traversed a remarkable pathway of scientific evolution. Today there are numerous materials applicable reaching from natural materials over semi-synthetic to fully synthetic substances. The application of these materials depends on their featured properties as well as on the bioactive drug to be released from the final depot system. Despite of the vast numbers of materials used for the preparation of drug depot systems there are only a few materials which are approved by regulatory agencies for this application in human medicine. Today these approved systems based on polymeric materials such as PLGA are state of the art. However, as it has been detailedly reviewed in the previous pages, these polymeric systems can interact with the encapsulated bioactive substance and – especially in case of therapeutic proteins – can lead to inactivation of these active agents. The aim of the work presented in this publication was to concentrate on lipid substances used for the preparation of drug depot systems. Controlled release from lipid based drug delivery systems is a very promising way to overcome obstacles associated with the use of approved polymeric systems, i.e. PLGA such as protein instability during encapsulation and release. Lipid based drug delivery systems have proofed their capability in terms of biocompatibility, release properties and stabilization of the encapsulated bioactive substances upon preparation and storage [57, 58, 70, 85, 88, 92, 153-158]. However, the question whether parenteral lipid drug delivery devices – especially implants - are biodegradable is still unanswered as there is no data available from application in humans. Despite the capabilities of some currently existing products based on non degradable polymers such as Implanon® [159], which can remain in the body and continuously deliver drugs for up to 3 years, it is highly impractical because these implants carry the risk of intoxication [160, 161] when left in the body thus surgical removal is required. In addition to that drug depot systems which remain in the body for years will lead to poor patient compliance especially in case of palpable implants since these systems are psychologically perceived as foreign body.

It was therefore an **aim of this thesis** to investigate on the biodegradation of lipid based drug delivery systems. Especially implants systems consisting of naturally derived triglycerides such as glyceryl stearate and other simple or mixed triglycerides consisting of glycerol esterified with fatty acids (C_{12} to C_{18}) are in the focus of this research work. Special interest lies on lipid based depot systems prepared by simple compression of the lipid matrix and extruded implants. Micro-particular systems such as microparticles are also within the scope of this thesis. In this presented work the author wanted to investigate on the behaviour of lipid based drug carrier systems in vivo. Especially the influence of physiological enzymes on the physical properties of the employed implant systems is of great interest. It was therefore a further aim of this thesis to develop an in vitro model for the simulation of biodegradation processes. Such a system would allow to be more independent of animal experiments and to fully characterize degradation and erosion processes. It was a further goal to analyze lipid degradation and erosion processes occurring in vivo and in vitro in a profound manner using different analysis techniques such as chromatographic and spectrometric techniques.

Summarizing, the major aim of the thesis associated with lipid depot system degradation was to arrive at a conclusion about the composition, the preparation technique, the dimensions and the time frame of degradable lipid-based drug depot systems.

In addition to the project of lipid based drug depot degradation this publication deals with the application of **spider silk proteins in pharmaceutical technology**.

Spider silk and silk derived from other arthropods such as the silk worm has gained a lot of attraction in recent years not only due to their outstanding physical properties exhibiting a tensile strength exceeding that of steel or Kevlar but also for its remarkable qualities in the application of biomedical tissue engineering. Although the application of spider silk in medicine goes back to ancient times, today there are only few modern publications describing the use of silk material for the preparation of drug depot systems. This may be contributed to the fact that silk is mostly collected as it was hundreds of years ago: by harvesting the cocoons of the silk worm and carefully and tedious reeling its precious and sensitive fibre. In case of spider silk the filament has to be collected from the living animal, a fact making its quarrying even more time consuming and expensive. Since silkworm silk is always coated with special proteins causing immunogenic reactions when brought into the human body, isolation of the pure silk proteins is necessary. Spider silk proteins don't exhibit such detrimental coating. Nevertheless, in general the harvesting and isolation of this natural polymer and the existence of natural occurring dissimilarities in silk compositions leading to

different protein properties is a major obstacle thus impeding the thorough investigation and development of drug depot systems based on these fascinating proteins. Only when genetically engineered spider silk proteins were producible in lab scale resulting in reproducible silk qualities of high purity, efficient investigation and production of silk-based sustained release devices was possible.

It was therefore the second **major aim of the presented work** to develop and thoroughly characterize micro particulate carriers consisting of genetically engineered spider silk proteins using preparation techniques which allow a controlled and reproducible upgrade towards batch sizes greater than lab-scale. Consequently, it was an aim to analyze the prepared silk particles with respect to their release behaviour of drug substances with different charges and properties. As already described, biodegradation of implanted drug depot devices is highly desired thus the biodegradation properties of the employed silk based systems should be evaluated towards their degradation behaviour.

1. Chapter One: In vivo studies of rh- $\text{INF}\alpha$ releasing lipid implants

1.1. Introduction

The following chapter deals with the investigation on the release of a therapeutic protein from compressed triglyceride discs which was implanted into rabbits. As already highlighted in the introduction of this dissertation, the potential of lipid implants for parenteral delivery of bioactives - although first investigations started already in the late 70ies – is still not exhausted. It is therefore not surprising that in vivo data of drug release from lipid based implants and even more data dealing with the physical changes of lipid implants upon in-vivo incubation are very few. . The release mechanism of the employed implant-drug systems was clarified previously in several in vitro experiments: the release of the protein out of the prepared triglyceride implant is controlled via proceedings comprising precipitation, and dissolution of the encapsulated protein followed by subsequent diffusion processes occurring within an interconnected pore network. However, it was not clear if this highly sophisticated mechanism would be possible under different conditions such as in vivo conditions. It was therefore of special interest if this mechanism may be influenced by potential immunogenic foreign-body reactions or by degradation processes occurring around or within the implant. Simultaneously this animal experiment offered the opportunity to examine the influence of the animal organism on the employed lipid implant. Accordingly, this chapter is organized with respect to the emphasis of the results of the conducted work. Some results of the above described animal experiment are already published whereas other results may be understood as impulses leading to subsequent experiments. In the following sections of this first chapter the published data is reprinted, followed by a little discussion about the content of the article. Finally, further studies related with this work are closing this chapter.

1.2. Correlation of in vivo and in vitro release data for rh- $\text{INF}\alpha$ lipid implants

M. Schwab¹, B. Kessler², E. Wolf², G. Jordan³, S. Mohl³, G Winter¹

¹Department of Pharmacy, Pharmaceutical Technology and Biopharmaceutics,
Ludwig-Maximilians-University, D-81377 Munich, Germany

²Institute of Molecular Animal Breeding and Biotechnology,
Ludwig-Maximilians-University, D-85764 Oberschleißheim

³Roche Pharma Research R&D Protein Analytics, Nonnenwald 2, 82377 Penzberg, Germany

Published in: European Journal of Pharmaceutics and Biopharmaceutics, Volume 70, Issue 2,
October 2008,

Abstract

Previous in vitro experiments had shown that rh- $\text{INF}\alpha$ releasing tristearin implants feature promising properties making them an excellent tool for the delivery of therapeutic proteins. Sustained release for periods up to one month could be achieved, associated with high protein stabilization. The objective of this study was to investigate for the first time the in vivo release properties of these implants in rabbits and to establish an in vivo-in vitro correlation. Computer modeling was used to simulate rh- $\text{INF}\alpha$ serum levels based on pharmacokinetic data. Protein serum concentrations on therapeutically relevant nearly constant levels could be detected for 9 days. Modeling revealed that in vivo release correlated closely with the release monitored in vitro.

Keywords: Protein release; Lipid implants; Computer modelling; In vivo-in vitro correlation;

Introduction

Since pharmaceutical proteins given by injection must be repeatedly administered in short intervals to reach and maintain therapeutic useful concentrations in the blood plasma, low patient compliance and high hospital costs are resulting. To overcome these problems polymer based delivery systems for therapeutic proteins have been developed. Although application of these new delivery devices is very promising most of the used polymer systems such as poly(lactic-co-glycolic acid) (PLGA) (1) show some major drawbacks i.e. interference with the protein stability like protein-polymer interaction, pH-shift and interface formation during formulation (2). Recently a new model depot system for the controlled delivery of rh- $\text{INF}\alpha$ has been developed in our working group (3). This implant consists of a lipid component, rh- $\text{INF}\alpha$, hydroxypropyl- β -cyclodextrin (HP- β -CD) or trehalose as a stabilizer and PEG 6000 as release modifier. The use of lipids known as matrix materials with a high biocompatibility (4,5,6) allows to generate implants capable of a sustained protein release. The application of solvent-free processing techniques like compressing the lipid mass satisfies the necessity for both a high biocompatibility and high protein stabilization. For long-time storage especially HP- β -CD can provide a high stability of the embedded therapeutic protein within the matrix (7). In vitro release experiments have shown a continuous release over 30 days with a close to linear release phase for the first 2 weeks. Overall protein liberation up to 95% can be achieved within 4 weeks. This controlled release is a consequence of the interaction of PEG with the incorporated rh- $\text{INF}\alpha$, leading to a reversible precipitation of the protein within the matrix, hence the resulting retardation of dissolution of the $\text{INF}\alpha$ strongly contributes to the controlled release (8). The aim of this work was to elucidate whether the release profile of the implants in vitro can be verified in vivo, i.e. in rabbits. We wanted to confirm whether the release mechanism was under total physiochemical control, independent of enzymes, and other components of body fluids and mechanical stress. Further we wanted to proof the expected excellent biocompatibility of the lipid implants.

Materials and Methods

Rh-interferon α -2a-(rh-IFN α , Roche Diagnostics, Penzberg, Germany; protein conc. 1.7 mg/ml in a 25 mM acetate buffer of pH 5.0, 120 mM sodium chloride) was lyophilized in a 1:3 ratio with hydroxypropyl- β -cyclodextrin (HP- β -CD, Merck, Darmstadt, Germany).

Tristearin (Dynasan 118) was purchased from Condea Chemie, Witten, Germany and polyethylene glycol 6000 (PEG 6000) is a product from Clariant, Gendorf, Germany.

All other materials (from Merck) were of high purity grade.

Implant manufacturing:

Implants were prepared by using a 5 ton hydraulic press (Maassen, Eningen, Germany).

The implant components- tristearin powder 80%, PEG 6000 10% and IFN α -lyophilisate 10%- were ground in an agate mortar. The resulting mixture was compressed with a pressure of 2 tons for 30 seconds. The obtained implants had an average weight of 50 mg and an average height of approximately 2.3 mm. The drug load of the implant was 2.5% of the implant weight, accounted for the rh-IFN α dose.

Animal experiment setup

In order to investigate the rh-IFN α release rate of the delivery device, lipid implants were administered to a group of 5 young female rabbits. Rabbits were chosen as experimental animals, because in contrast to rats or mice rabbits show a distinctive subcutaneous fat tissue which is quite similar to the human one. Under ketamin/xylazin anaesthesia one implant per animal was placed subcutaneously between the omoplates and the insertion site was sewn up. Samples of approx. 0.5-1ml blood-gained from the ear vein-were taken daily for the first week, afterwards every three days. Blank values were taken before the implantation. To gain basic pharmacokinetic data, another group of 3 rabbits received an injection of unretarded rh-IFN α solution (10^7 I.U. i.e. 37 μ g rh-IFN α per kg bodyweight). Samples were taken every hour for at least 9 hours and after 12 and 24 hours.

In vivo release studies:

Blood samples were centrifuged and the resulting serum frozen at -80 $^{\circ}$ until analysis.

Analysis was performed with a 96 well IFN α -ELISA (Bender MedSystems, Vienna, Austria). Rh-IFN α in rabbit blank serum solutions of known concentrations (8.0-1600.0 pg/mL) were used to generate calibration curves. Analysis was conducted according to the ELISA test

protocol. The absorbance of the colored product was measured using a CS-930-1PC platereader (Shimadzu, Kyoto, Japan). The detection limit of the rh- $\text{INF}\alpha$ -ELISA was 4pg/ml.

Rabbit anti-rh- $\text{INF}\alpha$ -antibody determination

Repeatedly administered injections of rh- $\text{INF}\alpha$, were reported to cause antibody generation in rabbits (9). As no rabbit anti-rh- $\text{INF}\alpha$ -antibody-ELISA was available spiking experiments with serum samples were conducted in order to investigate whether rabbit antibodies against rh- $\text{INF}\alpha$ were present in the serum. Aliquots of the samples drawn at day nine or later were analyzed by $\text{INF}\alpha$ -ELISA and showed no detectable amount of rh- $\text{INF}\alpha$. An exact amount (1.600 or 3.200 ng/mL) of rh- $\text{INF}\alpha$ solution was now added to this rabbit serum samples and the mixture was incubated for one hour at 40 rpm in a horizontal shaker. After such spiking the recovery of the added rh- $\text{INF}\alpha$ was determined via the rh- $\text{INF}\alpha$ ELISA kit from Bender.

It was expected that the antibodies generated in the rabbits against the recombinant human protein can also capture the added rh- $\text{INF}\alpha$ and analysis would therefore lead to low recovery of the added rh- $\text{INF}\alpha$.

Histological studies

At the end of the animal experiment (after 28 days) the implants were surgically removed. Slices of the implant and surrounding tissue were stained with a hematoxylin and eosin (H&E) stain. Image data were collected through a Leica DFC 320 camera (Leica Microsystems, Wetzlar, Germany) mounted on an Orthoplan microscope (Leica, Wetzlar, Germany).

In vitro release studies

Studies were conducted by incubating the implants (n=3) at 37°C in TopPac® vials containing 2.0 ml isotonic 0.01 M phosphate buffer pH 7.4. The samples were shaken at 40 rpm (Certomat® IS, Braun Biotech International, Melsungen, Germany). Samples were taken daily the first 7 days afterwards every 3 days. Sample volumes were replaced with fresh buffer. Analysis was conducted using a Thermo Separation Products HPLC system equipped with a Tosoh TSK-Gel G3000 SWxl column. 120 mM disodium hydrogen phosphate dehydrate, 20 mM sodium dihydrogen phosphate and 4 g/L sodium chloride, adjusted with hydrochloric acid to a pH of 5.0 was used as mobile phase. The flow rate was set to 0.6 mL/min, UV detection was performed at 210 nm wavelength.

Computer modeling

Basic pharmacokinetic data and data gained by the in vitro release studies were collected to calculate virtual rh- $\text{INF}\alpha$ blood levels by using the release curve as input function and the basic PK data for modeling distribution and elimination. Calculations were conducted with a self-programmed program and obtained data transferred into Microsoft Excel® for diagram generation. The pharmacokinetic analysis program WinNonlin® was used to determine half-life and elimination rate of rh- $\text{INF}\alpha$.

Results and Discussion

Pharmacokinetic data:

The reference group with non retarded rh- $\text{INF}\alpha$ -solution applied as s.c. injection provided basic pharmacokinetic data. The C_{max} was reached after 2.5 hours. Rh- $\text{INF}\alpha$ in serum was eliminated with an average terminal elimination half life of 3.4 hours. After 12 hours no rh- $\text{INF}\alpha$ was detectable any longer. The rh- $\text{INF}\alpha$ serum curve gained from the reference group is shown in Fig. 1. The modeled curve covering the rh- $\text{INF}\alpha$ serum curve consists of 2 functions: an inverted Gaussian function describing the inflow and a first order kinetics curve describing the elimination of rh- $\text{INF}\alpha$ used for PK data determination. This pharmacokinetic data revealed high similarity to data gained in human clinical trials with rh- $\text{INF}\alpha$ containing releasing systems. The human half life of rh- $\text{INF}\alpha$ was reported to be about 5 hours and therefore the chosen model is considered as appropriate and plausible.

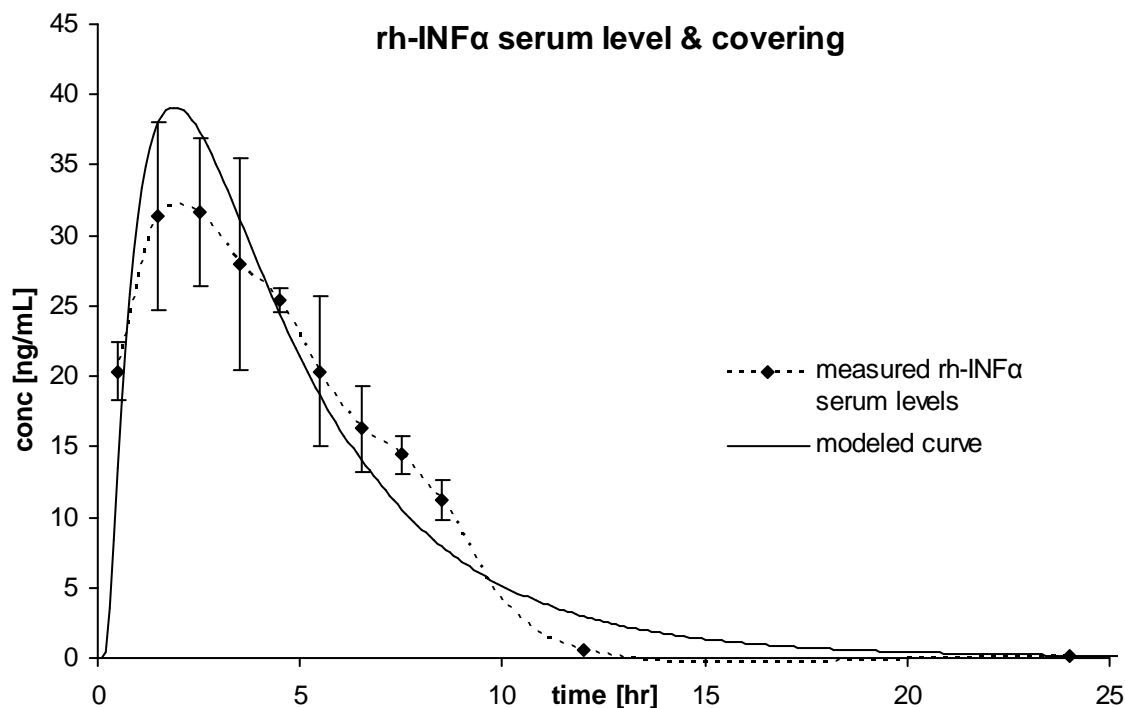


Figure 1: rh- $\text{INF}\alpha$ -serum levels after injection of $37\mu\text{g}$ rh- $\text{INF}\alpha$ per kg body mass to a collective of 3 female rabbits. The obtained curve was covered with a modeled curve providing necessary PK-data.

In vitro release studies and modeling

As shown in Fig. 2 the implants revealed continuous sustained protein release for 4 weeks.

The initial drug release was below 25% of the incorporated protein for the first 24 h.

Over 14 days the protein release was almost linear and overall protein liberation from the implant was higher than 90%. An inverted Gauss function was generated covering the in vitro release curve. This function served as an input function for the calculation of virtual rh- $\text{INF}\alpha$ serum levels.

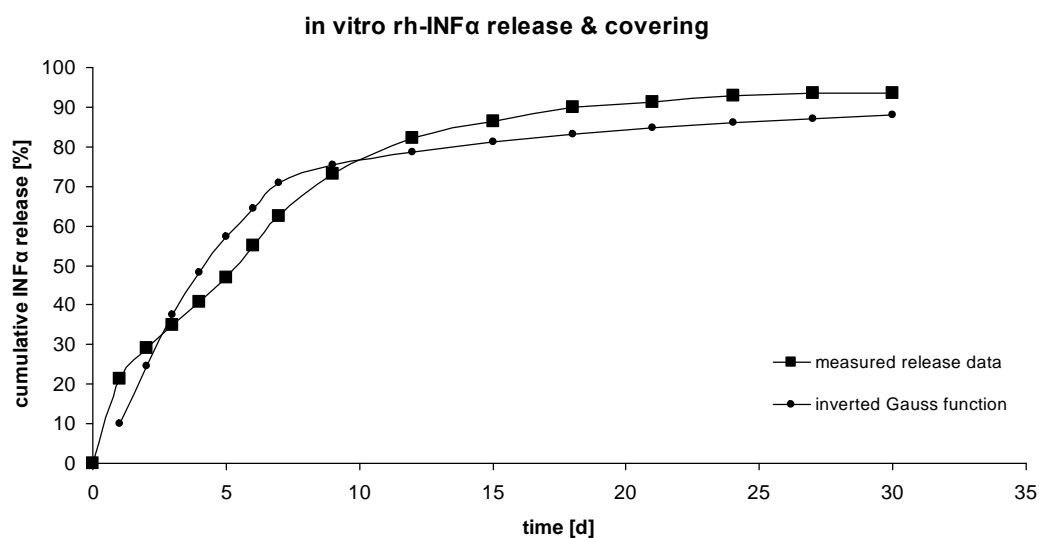


Figure 2: Cumulative rh- $\text{INF}\alpha$ in vitro release from tristearin implants. The release curve was covered with an inverted Gauss function serving as input function for computer modeling.

In vivo release studies and modeling

Serum samples revealed high rh- $\text{INF}\alpha$ -contents on an almost constant level over 9 days after insertion of the implant. Fig. 3 shows the obtained protein serum curves. High and therapeutic rh- $\text{INF}\alpha$ levels were still detectable at day 9, protein levels abruptly wear off from day 10 on. This phenomenon is most likely attributed to antibodies generated in rabbits against human recombinant $\text{INF}\alpha$ because neither in vitro data nor the in vivo serum level curve or the histology data allows any other explanation. In order to corroborate this hypothesis spiking experiments with serum samples after day 9 were conducted in a way that has already been described in the methods section. These experiments clearly revealed that serum components i.e. antibodies captured large amounts of the spiked rh- $\text{INF}\alpha$. From data shown in Fig. 4 it can be concluded that a massive production of antibodies against the rh- $\text{INF}\alpha$ had taken place. Presumably these antibodies were capable of masking all protein released from the implants. This leads to the presumption that rh- $\text{INF}\alpha$ is still continuously liberated from the implant after 9 days but released rh- $\text{INF}\alpha$ in the serum was quantitatively captured by the rabbit antibodies. In order to calculate virtual rh- $\text{INF}\alpha$ serum levels a simulated animal model was developed. This model consists of a serum compartment with an inflow function described as an inverted Gauss distribution and first order kinetics for the outflow. The values necessary for the inflow function were provided by the in vitro release experiments. First order kinetic data i.e. the elimination rate was obtained by the analysis of the rh- $\text{INF}\alpha$ -injection experiment of the control group.

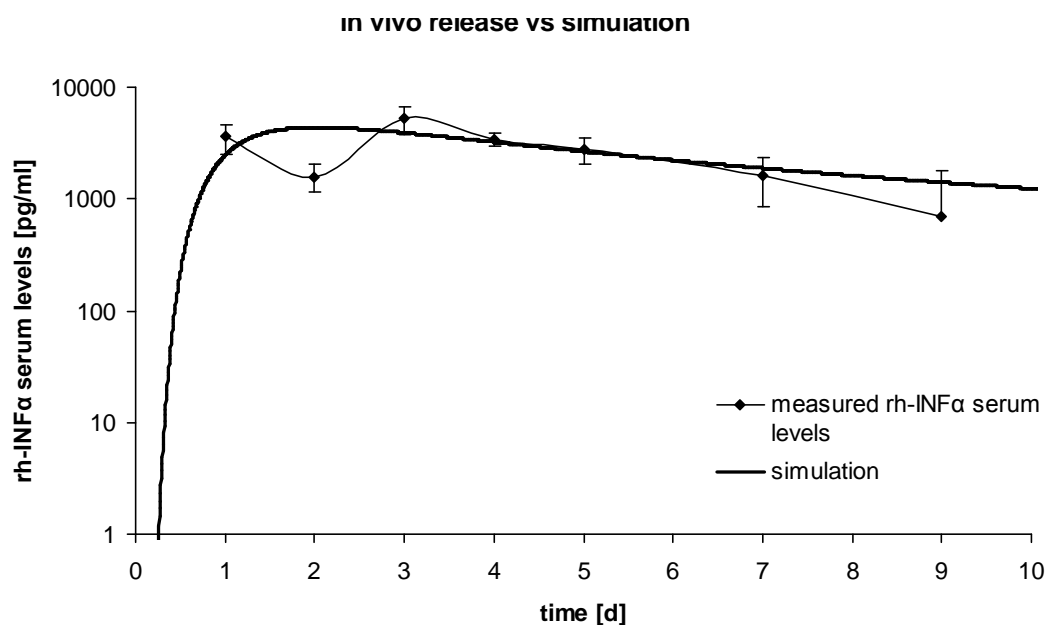


Figure 3: In vivo rh- $\text{INF}\alpha$ curve obtained by a collective of 5 young rabbits. Curve was covered with the simulated rh- $\text{INF}\alpha$ curve obtained by computer modeling.

The modeling of the rh- $\text{INF}\alpha$ rabbit serum levels revealed that the theoretical rh- $\text{INF}\alpha$ serum levels were in accordance with the experimentally obtained serum levels. Both the curve progression and the quantity of the modeled rh- $\text{INF}\alpha$ levels correlated very closely with the experimentally obtained rh- $\text{INF}\alpha$ serum level curve and values (Fig. 3). Of course, the early outrun of the in vivo data after 9 days does not allow correlations after that time point but it can be presumed that without the interference of rabbit antibodies against the rh- $\text{INF}\alpha$, release of rh- $\text{INF}\alpha$ would have been still detectable for many days.

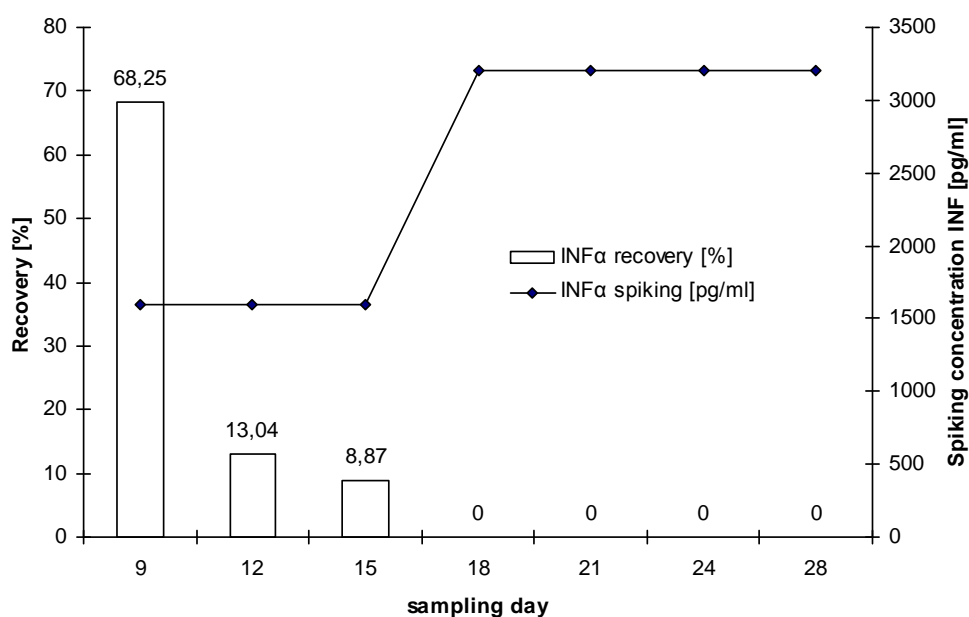


Figure 4: Spiking experiment data: analysis revealed an increasing rabbit-anti-rh $\text{INF}\alpha$ -antibody titer masking large amounts of rh- $\text{INF}\alpha$ in the rabbit serum.

Biocompatibility and degradation

After implantation of the device rabbit's body temperature, the behavior, as well as the eating habit was under steady observation. However, no fever or other signs of inflammation and illness like food repulsion could be noticed. Already after a few days the tissue at the incision site was healed and it was hardly visible that an implantation had taken place there (Fig. 5). At the end of the animal experiment the implants were surgically removed whereas no macroscopic encapsulation of the implant was noticeable (Fig 6). The surrounding tissue was unaffected by the implant and showed only low signs of inflammation. The implant maintained its structure and appeared to be intact and not eroded; migration of immune cells into the lipid matrix did not appear.



Figure 5: The implantation site before surgical removal of the implant for histological studies. The imprint of the implant is visible through the subcutaneous tissue.



Figure 6: Dissection of the implantation area: The implant maintained its structure and was located loosely beneath the sub cutis without any macroscopic noticeable encapsulation.

Microscopic investigations and tissue staining (Fig. 7) revealed that the implantation provoked only weak immune reactions leading to a migration of granulocytes into the surrounding tissue at the insertion site. Cicatrisation of the sub cutis was noticed indicating a quick healing rate and low irritation of the tissue.

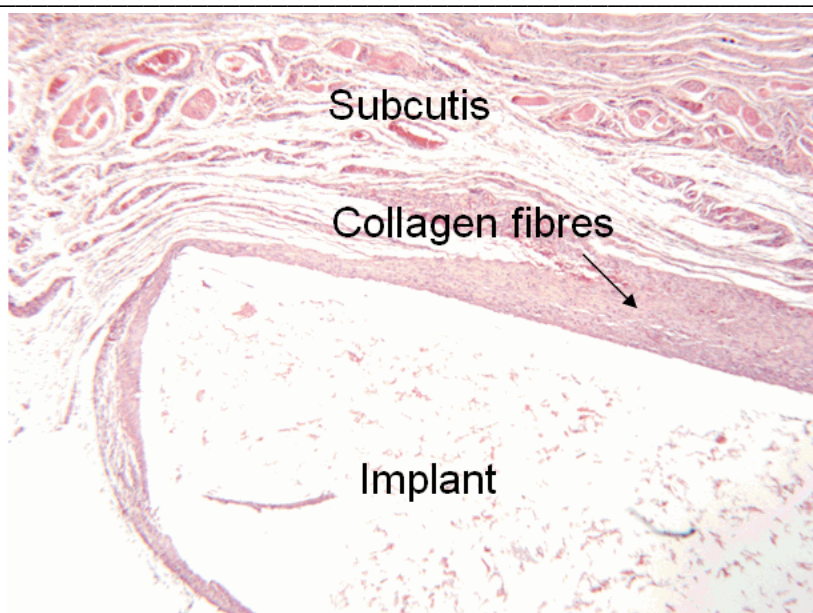


Figure 7: 25 times magnified immune-histological H&E staining of the subcutaneous tissue surrounding the implant: The tristearin implant is located on the lower half of the picture, surrounded by some collagen fibres.

Conclusion

The rh- $\text{INF}\alpha$ release in vitro from a sustained delivery system was compared to in vivo data in rabbits, a relevant model for the potential s.c. application in humans. It can be stated that during the first 9 days protein release in vivo is in surprisingly quantitative accordance with data gained by in vitro experiments. Computer modeling using PK data obtained in injection experiments revealed that the release properties observed in the animal experiment are in very close causal correlation to the simulated data. The modeled rh- $\text{INF}\alpha$ serum levels show the same curve progression for the first 9 days like the rh- $\text{INF}\alpha$ serum levels obtained in this animal experiment. Further on the quantity of the modeled rh- $\text{INF}\alpha$ levels are in accordance with the measured rh- $\text{INF}\alpha$ serum levels. This almost exact match of the curves concerning the quality and the quantities of the rh- $\text{INF}\alpha$ serum levels allows us to presume that without rabbit-rh- $\text{INF}\alpha$ -antibodies the rh- $\text{INF}\alpha$ release after day nine would be still ongoing on therapeutic relevant levels for several days. The virtual elimination half life of rh- $\text{INF}\alpha$ could be extended from approx. 4h up to more than 50hours by means of the depot system. Thus it can be stated that in terms of biocompatibility and controlled release the implant used in these experiment is a very suitable device for the delivery of rh- $\text{INF}\alpha$ and potentially for other pharmaceutically relevant drugs too. Studies to adjust the geometrical form of such devices towards convenient rod-like or micro particulate application forms are under way as well as studies for other protein drugs incorporated into depots of the presented type. Biodegradation studies are under way too. Based on the in vivo experience presented here the clinical use in animals and humans may be achievable in the near future.

References

1. V.R. Sinha and A. Trehan. Biodegradable microspheres for protein delivery. *J. Control. Release* 90:261-280 (2003).
2. M. Morlock, H. Koll, G. Winter and T. Kissel. Microencapsulation of rh-erythropoietin, using biodegradable poly(D, L-lactide-co-glycolide). Protein stability and the effects of stabilizing excipients. *Eur. J. Pharm. Biopharm.* 43:29-36 (1997).
3. S. Mohl and G. Winter. Continuous release of rh-interferon alpha-2a from triglyceride matrices. *J. Control. Release* 97:67-78 (2004).
4. H. Reithmeier, J. Herrmann and A. Göpferich. Lipid microparticles as a parenteral controlled release device for peptides. *J. Control. Release.* 73:339-350(2001).
5. W. Vogelhuber, E. Magni, M. Mouro, T. Spruss, C. Guse, A. Gazzaniga and A. Göpferich, Monolithic triglyceride matrices: a controlled-release system for proteins, *Pharm. Dev. Technol.* 8 (1) (2003) 71–79.
6. C. Guse, S. Koennings, A. Maschke, M. Hacker, C. Becker, S. Schreiner, T. Blunk, T. Spruss and A. Göpferich. Biocompatibility and erosion behaviour of implants made of triglycerides and blends with cholesterol and phospholipids. *International Journal of Pharmaceutics* (2006), 314(2), 153-160.
7. S. Mohl and G. Winter. Continuous release of rh-interferon (alpha-2a) from triglyceride implants: storage stability of the dosage forms, *Pharm. Dev. Technol.* 11 (2006) 103–110.
8. S. Herrmann, S. Mohl, F. Siepmann, J. Siepmann and G. Winter. New insight into the role of polyethylene glycol acting as protein release modifier in lipidic implants. *Pharmaceutical Research* (2007), 24(8), 1527-1537.
9. P.W. Trown, R.J. Wills and J.J. Kamm. The preclinical development of Roferon - A. Roche Res. Cent., Nutley, NJ, USA. *Cancer* (New York, NY, United States), (1986), 57(8, Suppl.), 1648-56.

1.3. Discussion of the published correlation data

The data presented in the preceding article proves that the release mechanisms featured by the employed implant was not negatively influenced by body fluids and immune reactions of the animals. Although the implant was surrounded by fibrous tissue, release wasn't affected by this sub acute response of the animal immunogenic system. Additionally, it was shown that there was macroscopically no hint for any degradation or erosion processes occurring at the implanted triglyceride disc. As light microscopy analysis didn't reveal any hints on implant erosion it was assumed that the employed triglycerides are not susceptible to any kind of agents secreted by immune cells or other protection mechanism of the animal body. At the first moment this outcome was rather disappointing, meaning that triglycerides can be used as stable drug release carriers but exhibiting properties comparable to that of many other substances known and already used for the preparation of drug depot systems. Eventually their disability of disintegration in vivo results in surgical removal. Of course, this explanation and conclusion is somewhat premature as we were observing only one sort of triglyceride incubated for a rather short period of time - 4 weeks – in one animal model. This set of data therefore may not be sufficient for consecutions regarding a broad spectrum of substances and circumstances which need to be taken into account. Therefore, it may be time to take a look at the literature and to spot the field of polymer degradation occurring when incubating these materials into a living organism. This short review is followed by a closer look at the surface of the implants excised from the rabbits in the animal experiment described in the article above. Maybe, after taking all these new facts into account this new set of unpublished data can change the view on this area of research.

1.4. Short review on cellular activity at the implant tissue interface

Within a few seconds to minutes after contact to living tissue or blood, surfaces of implanted biomaterials are covered with a strongly adherent proteinaceous layer [1]. Probably due to the properties of the hydrophobic surface of most applied biomaterials, the adsorbed proteins undergo structural changes; unfold themselves by exposing their hydrophobic core, usually buried inside the spherical protein structure [2]. This protein denaturation at the interface of implanted materials triggers procoagulant and inflammatory responses [3-5]. The most abundant adsorbed proteins on the surface of hydrophobic biomaterials comprise albumin, fibrinogen and immunoglobulin G (IgG) [6-8]. Especially fibrinogen adsorption seems to be a crucial factor in the genesis of inflammatory response [5]. Tang et al could show that the presence of fibrinogen at the implantation site is a major factor promoting the accumulation of phagocytes in the fibrous tissue surrounding the implant [9]. This accumulation of phagocytes leads to histamine associated morphology of the tissue, featuring hyperaemic and oedematous characteristics [4, 10, 11]. In order to fight against the alleged bacterial intruders, the accumulated monocytic macrophages release an abundance of enzymes from their lysosomes, mostly belonging to the families of hydrolases and oxidoreductases [12]. In particular, lysosomal hydrolases comprise acid and alkaline hydrolases and non-specific esterase as predominant enzymes. The family of oxidoreductases is represented by several hydrogenases and oxidases. Acid and alkaline phosphates - enzymes responsible for the hydrolysis of phosphate esters – are the most prominent hydrolases found in association with leucocytes such as monocytic macrophages and mast cells [13, 14]. Further effective weapons in the battle initiated by the implantation of the “foreign body” are highly active peroxide species, such as hydrogen peroxide, hydroxyl radical, hydroperoxyl radical and super oxide anion [15-17]. It is understood that this cocktail of different substances such as enzymes and peroxide species released from different leukocytes accumulated at the implant/tissue interface may influence the structure and the stability of the biomaterial. Thus, it is not surprising that even materials classified as stable and unsusceptible to hydrolysis undergo degradation in the living tissue [18]. Several papers report on the biodegradation of materials used for long term application in human tissue such as polyether polyurethanes (PEU). PEU has been used as insulation for cardiac pacemaker leads. However, in some cases, surface crazing has occurred, sometimes progressing to deeper cracks and breach of the insulation. It is hypothesized that biodegradation of these polymers might involve attack by chlorine- based and/or nitric oxide (NO)-derived oxidants, as major oxidative products of activated phagocytes [19-21]. For

implants prepared from polyesters and polycarbonates enzymatic surface degradation has been reported in many cases [22-24]. Implantation of copolymers of caprolactone and valerolactone implanted in rabbits, lead to a total biodegradation within 16 weeks due to enzymatic activity [25]. In additional studies it could be shown, that the breakdown of the polymeric material into particles in the μm -range leads to accelerated biodegradation due to phagosomal degradation [26]. Nowadays, after several decades of extensive clinical research on the medical application of polymeric materials, the development of polymeric biomaterials has resulted in the preparation of synthetic materials with controllable properties in terms of biodegradation. Rendering the surface properties and the hard segment chemistry of specific polyesters enables the control of cell adsorption and thus the control of biodegradation rate and velocity [3, 23, 27, 28]. Summarizing, it can be stated that materials implanted in living tissue have to face many attacks from different adversaries such as low pH level due to inflammation processes [29], enzymes and reactive peroxide species. Depending on the chemical and physical nature of the applied material complete biodegradation may take only several days or may take years. However, it seems that there is no material insusceptible to biodegradation processes, since even durable materials like stainless steel show signs of degradation after implantation [30]

Materials and methods

Implant manufacturing

Implants were prepared as described in chapter 1. The implants used in the animal experiments were surgically removed from the animals and washed 3 times with distilled water in order to remove loosely attached organic material. Reference implants were taken from the same batch of implants prepared for the animal experiment. The reference implants were incubated in PBS pH 7.4 at 37°C for 4 weeks with and without addition of lipases (100 U of Lipoprotein lipase and 100 U of lipase from rhizoma oryzae per 2ml PBS). After 3 days the buffer media was changed and new lipase-containing buffer was added.

Scanning electron microscopy

Surface morphology of all implants was analyzed using a Field Emission Scanning Electron Microscope Joel JSM-6500F (Joel Inc., Peabody, USA). Implants were fixed with adhesive carbon tape (BAL-TEC AG, Balzers, Principality of Liechtenstein) to a custom made brass stub, carbon-sputtered and analyzed.

Results and discussion

Tristearin implants (Fig. 1) incubated for 4 weeks in PBS without lipase addition showed a smooth surface morphology and exhibited pores with an average diameter of about 100 μ m. Pore generation was a result of rh-INF and PEG 6000 release. Higher magnifications of the implant revealed the flaky structure typical for crystalline lipids.

When incubated in lipase solution for 4 weeks implant structure was slightly changed. At lower magnifications surface morphology was almost comparable to the untreated tristearin tablets. However, due to triglyceride cleavage, crystalline microstructure was clearly visible at higher magnification. Presumably the detected rosette-like structure – somehow reminding at desert rose minerals – is resulting from the lipase affinity towards low ordered structures [31]. Regions with lower degrees of crystallinity are preferentially cleaved; regions with a higher degree of crystallinity remain - for the time being - untouched by the enzymatic hydrolysis.

The implant removed from the animal after 4 weeks certainly shows the most distinct change in morphology compared to the untreated reference implant. Already at low magnification rates it is visible that the former smooth surface is traversed by numerous rips and pores. Most prominent is the fact that the microcrystalline structure seems to be completely eradicated. At higher magnifications the surface morphology has changed dramatically: the flaky crystalline structure seems to be molten generating a scurf-like pattern.



Figure 1: Tristearin implant after incubation in PBS for 4 weeks. a) overview (25X magnification) b) pore in the implant structure due to drug release (150X magnification) c) microstructure of the lipid tablet (2700X magnification)

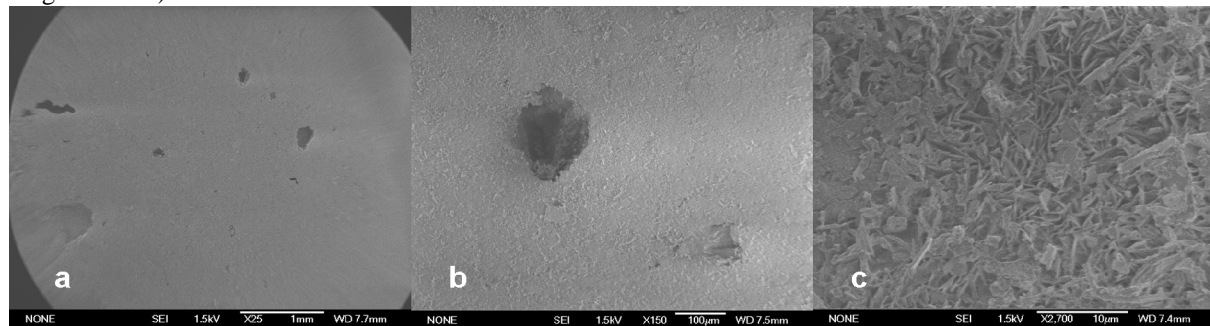


Figure 2: Tristearin implant incubated for 4 weeks in lipase containing buffer media. a) overview of the tablet (25X magnification) b) pore in the implant structure due to drug release (150X magnification) c) microstructure of the lipase incubated lipid tablet (2700X magnification)

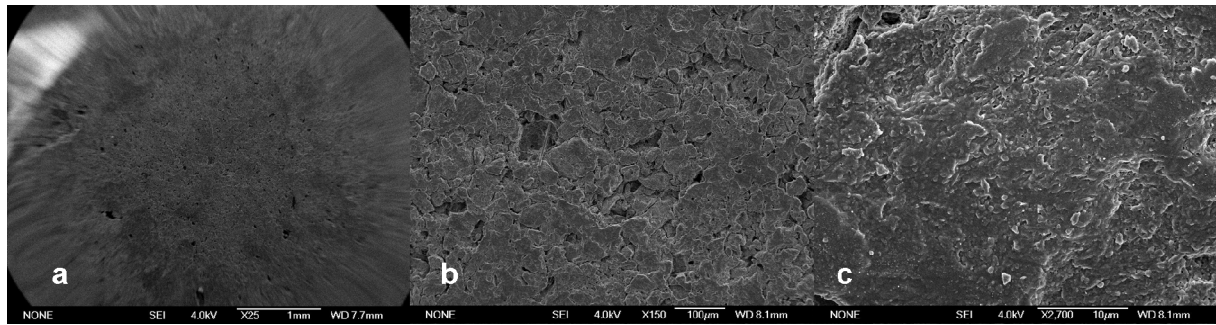


Figure 3: Tristearin implant after incubation in the animal body for 4 weeks. a) overview of the tablet (25X magnification) b) porous surface of the implant (150X magnification) c) change in microstructure (2700 X magnification)

Conclusion

Most biomaterials implanted in human or animal tissue have to face serious attacks from all sides such as physical stress and immunogenic attacks including contact with various enzymes and highly reactive peroxide species. These combined forces can lead to changes in the structure of the implanted biomaterials resulting in cleavage of hydrolytically or enzymatically sensitive bonds in the polymer. In our case tristearin implants were implanted for 4 weeks in rabbits, after excision the implants were analyzed with scanning electron microscopy for changes in the microstructure. These observations revealed that distinct changes in the structure of the implants had occurred. Especially the formation of numerous pores and rips in the surface of the implants can be assessed as a result of enzymatic or peroxide-derived degradation processes.

References

1. Robert E. Baier, R.C.D., *Initial events in interactions of blood with a foreign surface*. Journal of Biomedical Materials Research, 1969. 3(1): p. 191-206.
2. Banga, A.K., *Therapeutic Peptides and Proteins*. ISBN: 0-8493-1630-8, 2006.
3. Mingchao Shen, T.A.H., *The effects of surface chemistry and adsorbed proteins on monocyte/macrophage adhesion to chemically modified polystyrene surfaces*. Journal of Biomedical Materials Research, 2001. 57(3): p. 336-345.
4. T. L. Bonfield, E.C.J.M.A., *Protein adsorption of biomedical polymers influences activated monocytes to produce fibroblast stimulating factors*. Journal of Biomedical Materials Research, 1992. 26(4): p. 457-465.
5. [Tang, L.L., A. H.; Eataon, W., *Inflammatory responses to implanted polymeric biomaterials: Role of surface-adsorbed immunoglobulin G*
6. The Journal of Laboratory and Clinical Medicine 1993. Volume 122, Issue 3, Pages 292-300
7. James R. Keogh, F.F.V.J.W.E., *Albumin-binding surfaces for implantable devices*. Journal of Biomedical Materials Research, 1992. 26(4): p. 441-456.
8. Liping Tang, L.L.H.B.E., *Complement activation and inflammation triggered by model biomaterial surfaces*. Journal of Biomedical Materials Research, 1998. 41(2): p. 333-340.
9. Greisler, H., *Interactions at the blood/material interface*. Annals of Vascular Surgery, 1990. 4(1): p. 98-103.
10. Tang, L.E.J., *Natural responses to unnatural materials: A molecular mechanism for foreign body reactions*. Mol Med. 1999 1999. June; 5(6):p. 351–358. .
11. Tang, L.U., T.P.;Plow, E.F.;Eaton, J.W., *Molecular determinants of acute inflammatory responses to biomaterials*. J. Clin. Invest. , 1996. 92(5): 2360-2367 (1993).
12. Weidun Guo, R.W.X.L.R.O.B.C., *Splenic response to silicon drain material following intraperitoneal implantation*. Journal of Biomedical Materials Research, 1994. 28(12): p. 1433-1438.
13. Salthouse, T.N., *Cellular enzyme activity at the polymer-tissue interface: A review*. Journal of Biomedical Materials Research, 1976. 10(2): p. 197-229.

14. R. E. Marchant, K.M.M.J.M.A., *In vivo biocompatibility studies. V. In vivo leukocyte interactions with biomer.* Journal of Biomedical Materials Research, 1984. 18(9): p. 1169-1190.
15. R. E. Marchant, J.M.A.E.O.D., *In vivo biocompatibility studies. VII. Inflammatory response to polyethylene and to a cytotoxic polyvinylchloride.* Journal of Biomedical Materials Research, 1986. 20(1): p. 37-50.
16. Biggar, W.D. and J.M. Sturgess, *Hydrogen Peroxide Release by Rat Alveolar Macrophages: Comparison with Blood Neutrophils.* Infect. Immun., 1978. 19(2): p. 621-629.
17. Nathan, C.F. and R.K. Root, *Hydrogen peroxide release from mouse peritoneal macrophages: dependence on sequential activation and triggering.* J. Exp. Med., 1977. 146(6): p. 1648-1662.
18. Donaldson, K., et al., *Increased release of hydrogen peroxide and superoxide anion from asbestos-primed macrophages.* Inflammation, 1985. 9(2): p. 139-147.
19. Williams, D.F., *Biodegradation of surgical polymers.* Journal of Materials Science, 1982. 17(5): p. 1233-1246.
20. Sutherland, M.J.R., Coury, A. J. and Eaton J. , *Degradation of Biomaterials by Phagocyte-derived Oxidants.* J. Clin. Invest. 92(5): 2360-2367 (1993). doi:10.1172/JCII16841. , 1993. Volume 92, Issue 5.
21. Stokes, K.B., *Polyether Polyurethanes: Biostable or Not?* J Biomater Appl, 1988. 3(2): p. 228-259.
22. Chapanian, R., et al., *The role of oxidation and enzymatic hydrolysis on the in vivo degradation of trimethylene carbonate based photocrosslinkable elastomers.* Biomaterials, 2009. 30(3): p. 295-306.
23. Zaikov, G.E., *Quantitative Aspects of Polymer*
24. *Degradation in the Living Body.* MACROMOL . CHEM . PHYS., C25(4). , 1995: p. 551-597.
25. Tang, Y.W.L., R.S.; Santerre J. P., *Enzyme-induced biodegradation of polycarbonate-polyurethanes: Dependence on hard-segment chemistry.* Journal of Biomedical Materials Research, 2001. 57(4): p. 597-611.
26. Pulkkinen, M., et al., *Effects of block length on the enzymatic degradation and erosion of oxazoline linked poly-[var epsilon]-caprolactone.* European Journal of Pharmaceutical Sciences, 2007. 31(2): p. 119-128.

-
27. Pitt, C.G., et al., *The enzymatic surface erosion of aliphatic polyesters*. Journal of Controlled Release, 1984. 1(1): p. 3-14.
 28. S. C. Woodward, P.S.B.F.M.A.S.C.G.P., *The intracellular degradation of poly(ϵ -caprolactone)*. Journal of Biomedical Materials Research, 1985. 19(4): p. 437-444.
 29. Tang, Y.W., R.S. Labow, and J.P. Santerre, *Enzyme induced biodegradation of polycarbonate-polyurethanes: dose dependence effect of cholesterol esterase*. Biomaterials, 2003. 24(12): p. 2003-2011.
 30. Labow, R.S., et al., *Human macrophage-mediated biodegradation of polyurethanes: assessment of candidate enzyme activities*. Biomaterials, 2002. 23(19): p. 3969-3975.
 31. Steen, A.S., K.; Reeh, P., *A Dominant Role of Acid pH in Inflammatory Excitation and Sensitization of Nociceptors in Rat Skin, in vitro*. The Journal of Neuroscience, May 1995, 1~75): 3982-3989.
 32. Viegas, M.F.A., L.M. ;Lecoeur, J., *Metal materials biodegradation a chronoamperometric study*. Metal materials biodegradation: a chronoamperometric study 1989. Volume 1, Number 2 / Juli 1990.
 33. Olbrich, C., O. Kayser, and R.H. Müller, *Lipase degradation of Dynasan 114 and 116 solid lipid nanoparticles (SLN)--effect of surfactants, storage time and crystallinity*. International Journal of Pharmaceutics, 2002. 237(1-2): p. 119-128.

2. Chapter Two: In vitro degradation studies of lipid based drug depot systems

2.1. Introduction

In the first chapter which was divided in two major parts - a set of *in vivo*-release data already published, followed by results from subsequent SEM-analysis – we saw that triglycerides especially the employed glyceryl tristearate exhibit a great potential for the preparation of drug depot system controlling the release of sensitive bioactives such as therapeutic peptides and proteins. It was further shown that release mechanism based on a complex interaction of precipitation, diffusion and dissolution processes were unimpeded by the physiological system of the animal model. However, the hope that the used triglyceride implants would show distinct biodegradation behaviour i.e., by macroscopic visual disintegration wasn't fulfilled. Although SEM-analysis of the excised implant could proof that degradation processes had occurred on the surface of the compressed lipids, e.g. by changing the implants microstructure presumably resulting from attacks of reactive peroxide species, these humble signs were not suitable to undergird the allegation that triglyceride-based implants undergo complete degradation *in vivo*. One major argument for the biodegradation of parenteral applied lipids is their susceptibility towards lipases. However under normal condition the human body digests triglycerides in form of small oily droplets. Until today there was no data available concerning the lipase degradation of relatively large monolithic systems such as the implants applied in the described animal experiment. It was therefore necessary to go adrift from simple visual inspection of implanted triglycerides implants *in vivo* and concentrate on methods which bring out quantifiable results and thus enable statements on the degradation quantity of the employed lipid. The intended method development made it necessary to transfer the incubation and analysis of the lipid depot systems from *in vivo* systems towards *in vitro* incubation. It is understood that, if concentrating on the lipase-related degradation of lipid implants, these enzymes have to be included in the *in vitro* system.

Chapter two is dedicated on the implementation of this new method, simulating the *in vivo* incubation of triglyceride based drug depot systems within the presence of lipases. In the first part of this chapter the analytical method is detailedly described and first results of investigation on triglyceride degradation are presented. After a little discussion, additional data dealing with the development of the presented methods are displayed.

2.2. Studies on the lipase induced degradation of lipid based drug delivery systemsMartin Schwab^{1*}, Gerhard Sax¹, Sandra Schulze¹, Gerhard Winter¹¹Ludwig-Maximilians-University Munich, Butenandtstr.5, 81377 Munich, Germany.**Accepted for publication by:** Journal of Controlled Release**Abstract**

The question whether lipid based - especially triglyceride based - depot systems can undergo biodegradation is despite many in vivo studies still unanswered. In this paper we studied biodegradation processes in vitro by incubating these lipid based systems in buffer media containing lipases. The main degradation product the free fatty acids (FFA) were isolated from the drawn samples and after derivatization analyzed with RP-HPLC. Lipid microparticles showed a rapid biodegradation whereas the complete degradation of compressed implants would take several months or years. For these two systems surface degradation can be stated. Surprisingly lipid based extrudates changed their structure dramatically upon lipase incubation resulting in a breakdown of the lipid matrix and formation of small lipid particles in the μm -range. This sort of bulk-degradation may enable the use of lipid-based extrudates for the long term delivery of drugs. However additional in vivo experiments will be necessary to fully characterize these degradation processes.

Keywords: lipid based depot systems, biodegradation, erosion, extrudates, implants

Introduction

In recent years great efforts have been made in the development of lipid-based parenteral drug delivery devices. Although approved polymers like poly(D,L-lactide-co-glycolide-acid) (PLGA) are still state of the art for the preparation of parenteral drug delivery devices, depot systems based on lipid materials arouse much interest among protein formulators since biocompatibility, release and effect on the stability of the entrapped bioactive drug appear advantageous. Since the late 70s lipids i.e. fatty acids, triglycerides, cholesterol and lecithin have been used as excipients for the preparation of implants designed for the sustained delivery of drugs like steroids and morphine derivatives [1, 2]. In the late 80s Wang and coworkers prepared implants for the controlled delivery of insulin consisting of fatty acids or cholesterol. Implants made of fatty acids showed erosion in vivo; however it was reported that administration of fatty acids as matrix material lead to inflammation and formation of blisters in the animal tissue. Further on, the use of fatty acid-monoglycerides is limited due to the fast erosion of these systems [3-5]. In 2001 Reithmeier et al prepared glyceryltripalmitate microparticles and PLGA-based microparticles and compared their biocompatibility after implanting both formulations in mice. After 7 days the amount of PLGA-microparticles as well as lipid microparticles at the site of implantation was reduced most probably due to degradation in the subcutaneous tissue [3]. In 2003 Vogelhuber et al produced cylindrical matrices consisting of triglycerides or triglyceride/cholesterol mixtures which allowed a release of pyranine, a model compound, for more than 120 days. In vitro no erosion was detectable [4]. In 2006 Mohl et al developed a tristearin implant for the controlled delivery of rh-INF over 1 month. In further studies the stability of the entrapped protein in the lipid matrix could be verified [5, 6]. Stability and bioactivity of the encapsulated protein was also confirmed by Appel regarding release of insulin from tripalmitate cylinders in cell culture [7]. In 2006 Guse et al conducted an animal experiment with the aim to investigate on the biocompatibility of glyceryltripalmitate and on the effect of cholesterol and distearoyl-phosphatidyl-choline (DSPC) on the erosion behaviour of the lipid matrices. It could be shown that DSPC is quickly eroded leading to a residual porous lipid structure consisting of triglycerides [8]. In order to prove the biocompatibility and to investigate on the in vivo in vitro correlation of the rh-INF release from tristearin implants an experiment with rabbits as animal model was conducted by Schwab et al [9]. In this study, once again, triglyceride implants showed a good biocompatibility but signs of bioerosion couldn't be detected.

In summary, depot systems based on lipids – especially triglycerides – are a valuable alternative to already approved polymeric systems. Especially for long term drug delivery lipids seem to be superior to the commonly used polymers, due to their ability to maintain the stability of the entrapped proteins for a long period of time and due to their excellent biocompatibility. However, the question whether parenteral lipid drug delivery devices – especially implants - are biodegradable is still unanswered as there is no data available from application in humans. Biodegradation of lipid depot systems surely is one major parameter for the future success of these materials concerning an approval for their use in human medicine. Therefore we decided to systematically study the degradation of various lipid drug delivery devices incubated in lipase solution under physiological conditions. As lipases are present in human subcutaneous fat tissue [10-12] in muscle tissue [13] as well as in serum fluids [14] they therefore exhibit the possibility to hydrolyze lipid based drug delivery systems. Our aim was to investigate whether lipid based depot systems would undergo degradation in the presence of lipases. Further on, we wanted to elucidate the influence of the lipid composition, the size and the manufacturing process of the implants on the degradation kinetics. Little is known about the activity of lipases and their ability to degrade exogenous lipids brought in the body by injection or infusion [15] since research is mostly concentrating on the relationship of lipase activity - i.e. hormone sensitive lipase, lipoprotein lipase and serum hepatic lipase - and lipid metabolism in the context of obesity [10, 12, 14, 16-23]. In general one can state that the average lipase activity in the human serum and subcutaneous fat tissue has approximately an activity of 0.01 U/ ml. In these studies higher lipase activities were chosen with respect to the analytical sensitivity and time frame of the experiments. It is therefore understood that the results of the described experiments should be viewed with some caution as the employed lipase levels are 5000-15000 times higher than the activities present in human tissue.

Materials and Methods

Materials

All lipids (Glyceryl tristearate, -tripalmitate, -trimyristate –trilaurate, lipidmixture E85, lipidmixture H12) used in this study were purchased from Sasol GmbH, Witten, Germany. Lipases (Lipoproteinlipase from pseudomonas sp. and Lipase from Rh. Oryza) and all other chemicals were purchased from Sigma–Aldrich, Deisenhofen, Germany.

Methods

Preparation techniques

Preparation of microparticles

Placebo lipid microparticles either consisting of glyceryltripalmitate or glyceryl tristearate were produced resulting in 2 different particle sizes (10 μ m and 100 μ m mean particle size).

The production techniques are described as followed:

Lipid Microparticles preparation

Placebo Lipid Microparticles were produced using 2 different preparation techniques widely used for the preparation of polymeric or lipid based microparticles [3, 25]:

Solvent Evaporation method: 300 mg lipid powder was dissolved in 1.0 ml organic solvent (e.g. methylene chloride). The resulting solution was further emulsified at 40°C into a small volume (3.0 ml) of a 1% (w/v) aqueous PVA solution using an Ultra-Turrax[®] (IKA Werke GmbH & Co. KG Staufen, Germany). Particle size was controllable by adjusting the rotation speed of the emulsification tool. The emulsion was poured into a larger volume (150 ml) of an ice-cooled (5°C) aqueous phase (PVA 0.1% (w/v)) and stirred with a propeller stirrer to allow for the evaporation of the organic solvent. The hardened microparticles were separated from the aqueous phase by filtration, rinsed with 40 ml of water and vacuum dried overnight at room temperature.

Melt Dispersion method

With this preparation technique, a lipid melt was used instead of the solution of the lipid in an organic solvent. The lipid melt (300 mg lipid powder heated above its melting point) was poured into the PVA solution and emulsified as described for the solvent evaporation method. The following steps were the same as for the solvent evaporation method. The stirring time was reduced from 30 min to 5 min since this method is solvent free.

Implant manufacturing

Implants were prepared by using a 5 ton hydraulic press (Maassen, Eningen, Germany).

The implant component, i.e. tristearate-powder was ground either with or without pore builder and compressed with a pressure of 2 tons for 30 seconds. The obtained implants had an average weight of 50 mg a diameter of 5mm and an average height of approximately 2.3 mm.

Preparation of twin-screw extrudates (tsc-extrudates)

Lipid based tsc-extrudates were prepared using a MiniLab[®] Micro Rheology Compounder (Thermo Haake GmbH Karlsruhe, Germany). Extrusion temperature was set to 43°C to 48°C which was slightly above the melting temperature of the respective low melting triglyceride. As pore forming agent PEG 6000 was used either alone or in combination with hydroxypropyl- β -cyclodextrin lyophilisate (Iyo). After application of the lipid powder mixture into the extruder barrel and subsequent softening of the mixture, extrusion was performed through the extruder outlet die (diameter 2.0 mm). The rotation speed of the extruder screws was set to 40 rpm and the bypass channel was closed to inhibit material circulation within the extruder.

Degradation studies setup

In this study, solid lipid drug depot formulations i.e., microparticles, compressed implants, and extruded rods were incubated at 37°C in PBS (2.0 ml isotonic 0.01 M phosphate buffer pH 7.4) containing the lipases mentioned above in different activities (100, 200 and 300 U/2ml respectively). After 3 days of incubation the buffer media with the lipases was exchanged with fresh medium. FFA were isolated from the drawn samples and, after derivatization, analyzed. The amount of FFA released during the incubation was used to compare the different formulations in terms of biodegradation. Degradation of the lipid mass was calculated as percentage of the total amount of saponifiable lipid mass.

Microparticles

10mg of microparticles were incubated at 37°C in 2 ml PBS pH 7.4 containing 100 U of both lipases. After 3 days 100 μ l of the supernatant were drawn and the volume was replenished with fresh lipase solution. FFA were isolated from the drawn samples and, after derivatization, analyzed.

Compressed lipid implant study

In order to investigate on the degradation behaviour of compressed lipids tristearate implants were prepared from tristearate powder applying compression forces used for the preparation of the implants established in previous experiments [5, 9]. The relationship between lipase activity and FFA-rate was analyzed using 3 different lipase activities (100, 200 and 300 U /2ml respectively). To analyse the influence of pores in the lipid implants tristearate implants were produced with increasing amount of pore builder (PEG 6000). Amount of pore builder used was 0, 20, 30, 40 and 50%. Prior to the start of the degradation experiments the implants were incubated in PBS for 4 weeks to allow the pore building agent to dissolve.

Lipid extrudate degradation study

10 different formulations of lipid based extrudates have been produced for this study. The prepared lipid extrudates always consist of a low melting and a high melting lipid component. Glyceryltristearate (D118), glyceryltripalmitate (D116) and glyceryltrimyristate (D114) served as high melting lipid component, whereas glyceryltrilaurate (D112) and two triglyceride-mixtures (H12 and E85) served as low melting component. H12 and E85 are synthetically produced triglycerides consisting of different fatty acids (lauric-, myristic- and palmitic acid) esterified in different ratios with glycerol. Due to the specific composition H12 has a melting point of approx. 35 °C and E 85 melts at 41°C. In Table 1 the different formulations of the produced lipid extrudates are listed. Aim of this study was to investigate on the effect of the high melting lipid composition, the effect of the low melting lipid composition, the effect of the ratio of the lipid composition and the effect of different amounts of pore builder on the degradation behaviour. Results of preliminary experiments (data not shown) showed that the presence of PEG can interfere with the lipase induced lipolysis in an unpredictable manner therefore lipid extrudates have been incubated in 2ml PBS pH 7.4 for 4 weeks to allow the pore builder to dissolve. These extrudates were used for the lipase incubation. A second batch of extrudates has been incubated in PBS for 2 months without the addition of lipase solution to investigate on the stability under non lipolytic conditions

Batches	High melting lipid component (HMLC)	Low melting lipid component (LMLC)	Ratio of lipid components HMLC:LML	Amount/type of pore builder
E1	D118	H12	80:20	0% PEG
E2	D118	H12	80:20	20% PEG
E3	D118	H12	80:20	40% PEG
E4	D118	H12	90:20	10% lyo, 10%
E5	D118	H12	80:20	10% lyo, 10%
E6	D118	H12	70:30	10% lyo, 10%
E7	D118	E85	80:20	10% lyo, 10%
E8	D118	D112	80:20	10% lyo, 10%
E9	D116	H12	80:20	10% lyo, 10%
E10	D114	H12	80:20	10% lyo, 10%

Table 1: Formulation of lipid based extrudates: D118 (glyceryltristearate), D116 (glyceryltripalmitate), D114 glyceryltrimyristate), D112 (glyceryltrilaurate), H12 (lipid composition consisting of different fatty acids (lauric, myristic and palmitic acid) esterified in different ratios with glycerol; melting point 34°C), E85 (mixture of different fatty acids (lauric, myristic and palmitic acid) esterified in different ratios with glycerol; melting point 41°C)

Characterization Methods

FFA Extraction method

FFA were extracted from Lipase activity assays samples and samples drawn in the degradation experiments. Extraction provided quick analysis time and avoidance of derivatization interference with buffer components. The extraction method is based on the Dole and Meinertz extraction procedure [27]. The extraction solvent was prepared by mixing isopropanol–heptane–phosphoric acid (2 M) (40:10:1, v/v) and was thoroughly stirred before use. Extraction solvent (2.5 ml) was added and the tubes were thoroughly vortexed. The tubes were then immersed in a sonicator water bath (Branson Ultrasonic, Danbury, CT, USA) and the samples were sonicated in 30 s intervals for 2 min. Care was taken to avoid heating the samples during sonication. The samples were then vortexed vigorously and allowed to incubate at room temperature for 10 min. Heptane (1 ml) and water (1.5 ml) were added and the tubes were thoroughly vortexed and sonicated again for one min. Tubes were centrifuged at 1000 g for 10 min at 4°C. After centrifugation the top organic layer was seen to separate cleanly from the aqueous layer. A 1.5 ml aliquot (88% of the total organic layer of 1.7ml) of the top layer was transferred carefully using a pipette to 1.5 ml HPLC vials and dried under a stream of warm nitrogen. These samples were then used for derivatization.

Free fatty acid determination

As free fatty acids (FFA) are the major cleavage product of lipase induced triglyceride degradation, a quantifiable analysis was based on FFA-release upon lipid degradation. Phenacyl esters of fatty acids were prepared by the method described by Wood and Lee [26]. Briefly, samples were placed in HPLC-vials with closed silicone/PTFE screw caps (VWR international, Darmstadt, Germany), then 25 ml of a phenacyl bromide solution (10 mg/ml in acetone) and 25 ml of a triethylamine solution (10 mg/ml in acetone) were added, capped under N and heated in a boiling water-bath for 5 min. The excess of phenacyl bromide was reacted with acetic acid (40µl of a 2 mg/ml solution in acetone) and, after evaporation of solvents under a stream of N₂ at laboratory temperature, the derivatization products were reconstituted in methanol. FFA solutions of known concentrations (5-200.0 µg/ml) in methanol were used to generate calibration curves. Samples were analyzed using a Thermo Separation Products HPLC system (Thermo Fisher Scientific, Inc. Waltham, U.S.A.) equipped with a LiChrosphere RP C18 column (4.6 mm i.d. x 250 mm, 5 µm) (Merck, Darmstadt, Germany). Mobile phase was a mixture of MeOH-AcCN-water (80: 10: 10 (v/v)).

Elution of phenacyl esters was monitored by absorbance at 254 nm. The detection limit was about 5 μ g FFA per ml, accounted for stearic acid, i.e. approx. 20 nmol of fatty acid.

Lipase activity assay

In order to determine the activity and stability of the used lipases enzyme activity assays were carried out. For each assay a trioleate emulsion was prepared by mixing 4.5 ml polyvinyl alcohol solution (2% w/v) with 1.5 ml triolein. This mixture was then emulsified at 0°C with an Ultra Turrax® for 2 min at 15,000 rpm. 500 μ l of this emulsion and 400 μ l PBS buffer 0.01 M pH 7.4 then were incubated in a 2 ml Eppendorf cap for 10 min at 37°C in a water bath. 100 μ l of lipase solution was added and the mixture was incubated again at 37°C. After 10 min the reaction was stopped by adding 1 ml of a methanol:acetone:methylene chloride mixture (1:1:1 v/v). Before derivatization and HPLC analysis FFA produced in the triglyceride cleavage were extracted using the method described below. 1 U of enzyme activity was defined as the release of 1 μ mol FFA per min at 37°.

Scanning Electron Microscopy (SEM)

To investigate whether degradation of lipid drug delivery devices is visible SEM measurements were carried out. Samples were analyzed using a Field Emission Scanning Electron Microscope Joel JSM-6500F (Joel Inc., Peabody, USA). Therefore samples were put on adhesive carbon tape (BAL-TEC AG, Balzers, Principality of Liechtenstein) and attached to a custom made brass stub, carbon-sputtered and analyzed.

Particle size distribution

Particle size was determined using a Horiba LA 950 laser diffraction particle size distribution analyzer (Retsch Technology GmbH, Haan, Germany).

Determination of Lipase adsorption on lipid surface

In order to analyse the amount of lipase adsorbed on the surface of the lipid devices, i.e. the amount of lipase which is hydrolytically active at the lipid-water interface, adsorption studies were carried out using a modified method after Brockmann [28]. Briefly, after incubation of lipid implants in lipase solutions for a defined amount of time at 37°C, implants were washed in water and then incubated for 15 min in PBS pH 7.4 containing 0.15% Brij 35® to desorb bound lipase. Aliquots of the resulting solution were assayed for lipase concentration determination via fluorescence spectroscopy. A calibration curve of known lipase concentrations was prepared for each adsorption test.

Results and Discussion

Microparticles

Samples drawn from the incubated microparticles revealed steady generation of free fatty acids due to the lipase activity (Fig. 1). For D118 microparticles a distinctive differentiation can be made concerning the degradation velocity of microparticles produced with different preparation techniques: microparticles produced with the solvent evaporation technique show faster degradation than microparticles prepared with the melt dispersion technique. Regarding the influence of the particle size on the FFA-release from the microparticles it was found that it has a bigger influence for longer chain length triglycerides than for shorter chain lengths. For the particles made from D116 no such distinction can be made. All particle batches showed comparable degradation velocities. After 48 days degradation of the total lipid mass reached 80 % for D116 whereas D118 microparticles showed a degradation ranging from 45 to 65%. Over the time degradation velocity was decreasing in both studies probably due to the lipases inhibition by the cleavage products, i.e. by the accumulation of fatty acids in the incubation tubes as reported in literature [29]. To investigate whether degradation of lipid drug delivery devices was visible SEM measurements were carried out. SEM photographs revealed strong differences in the surface morphology prior and after the degradation period. As seen in Fig. 2a-b the surface of the microparticles before lipase incubation was smooth whereas microparticles incubated with lipase changed their morphology towards a rough and uneven surface. However cracks or pores couldn't be detected indicating that the degradation is only happening at the lipid water interface.

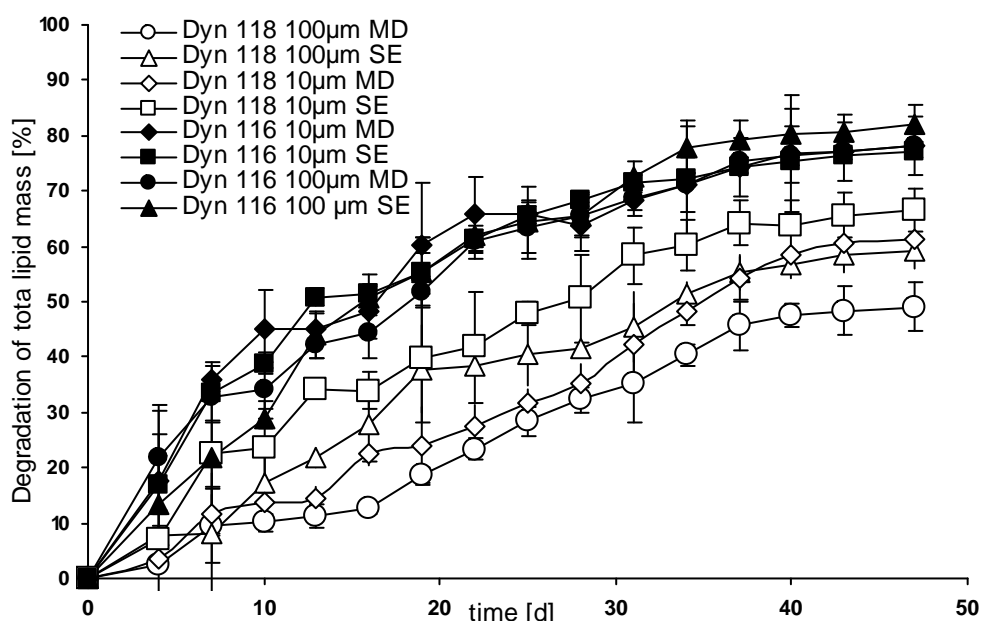


Figure 1: Degradation study of lipid microparticles over 48 days (Average + S.D., n = 3).

Implants degradation study

Compressed tristearate implants showed a constant and linear FFA release during lipase incubation. After 60 days of incubation only 0.7 % of the total lipid mass was degraded by the enzymes. Compared to the fatty acid release from the microparticles, degradation kinetics of the implants were very slow most probably due to the small surface area exhibited by the implants. When extrapolating the applied lipase activity to a level found in human tissue (approx. 0.01 U/ml) the total degradation of these systems would surely exceed the average life span of a human being (>100 years). Macroscopically analyzed implants showed no change in surface morphology. However, SEM photographs did show changes in surface morphology but revealed no cracks or holes in the lipid matrix (Fig. 2c-d). Typical lipid crystals were visible after lipase incubation in high magnification. As expected, these findings confirm the interfacial activity of the lipases [30-32] resulting in a strict surface degradation and erosion of the compressed lipid implants. In this study we can assume the substrate concentration, i.e. the lipid, to be very low and the enzyme being not saturated, thus resulting in linear fatty acid release over several days. To analyze whether an increase in surface area could increase lipid hydrolysis porous implants were prepared.

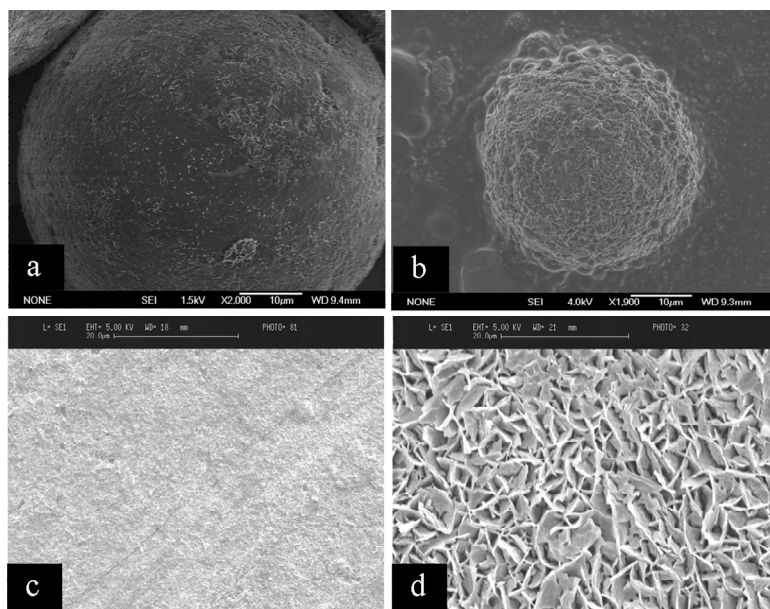


Figure 2: SEM-pictures of lipid microparticles and compressed implants: a) D116 Lipid microparticle prepared by melt dispersion (MD) method before incubation (magnification 2000X). b) D116 lipid microparticle (MD) after incubation with lipase (magnification 2000X). c) D118 implant surface before incubation (magnification 2000X). d) D118 implant surface after lipase incubation (magnification 2000X).

With increasing amount of pore builder fatty acid generation was increased in a linear manner. Implants with 50% of pore builder partially collapsed upon lipase incubation probably due to the physically instable porous structure. These fragments additionally increased the surface area presented to the lipase thus increasing the total degradation rate up to 1.8% after 30 days of incubation (Fig. 3a). The relationship between degradation rate and lipase activity was analyzed in another experiment. In this setup tristearate implants were incubated with 100, 200, 300 and 400 U /2ml lipase respectively. As seen in Fig. 3b the results indicate that, after an initial a plateau phase, a linear relationship between lipase activity and degradation velocity can be assumed over a wide range of the lipase activity. To investigate on the amount of lipase involved in the lipid cleavage lipase adsorption studies have been conducted as described above.

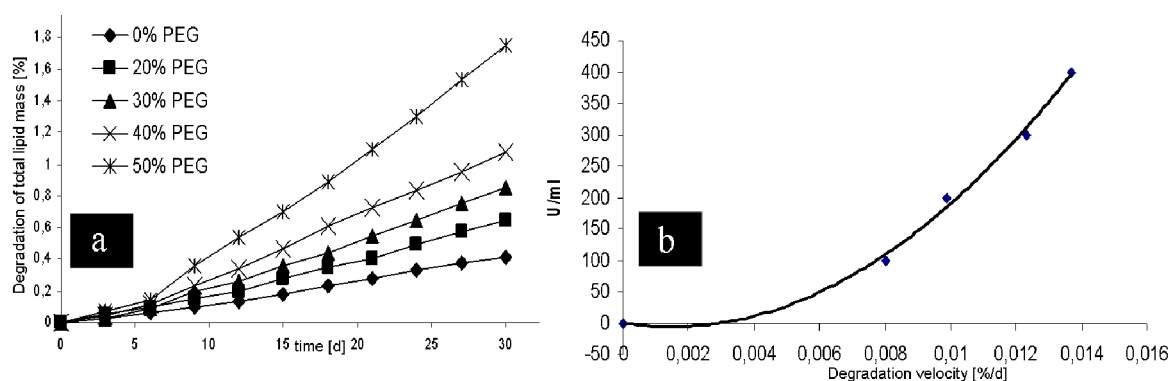


Figure 3: Results on porous implants: a) Studies on the effect of porosity on the degradation velocity (Average + S.D., n = 3). b) Degradation velocity [%/d] of compressed D118 implants versus the lipase activity.

Lipase adsorption studies

Results of these studies show that only a minor percentage of the total lipase used in these experiments is involved in the cleavage of the triglyceride. It can be presumed that less than 0.25 percent of the total lipase content is bound on the lipid surface of a compressed implant when applying a lipase activity of 100 U (Fig 4a). Another experiment confirmed the linear relationship between lipase adsorption and presented lipid surface (Fig. 4b).

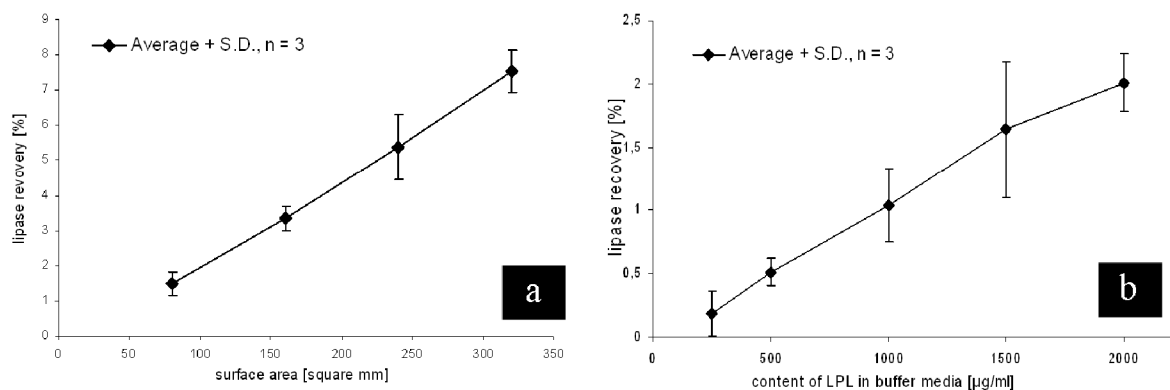


Figure 4: Lipase adsorption studies: a) Lipase recovery versus surface area. b) Lipase recovery plotted against lipase content in buffer media.

Extrudates degradation study

10 formulations of lipid based extrudates exhibited different degradation rates. Compared to the degradation rates of implants extrudate degradation was almost 10 times faster reaching up to 4% after 30 days of incubation. In our study we focussed on the influence of the low melting lipid component, the high melting lipid component, the effect of the ratio of the different lipid components and the effect of pore builder on the degradation behaviour.

Reference extrudates stored in lipase-free buffer media for 2 months remained stable and showed no signs of erosion.

Effect of the low melting component: as seen in Fig. 5 extrudates containing trilaurate or H12 showed the highest degradation rate, reaching over 3% of lipid mass degradation after 30 days of incubation, whereas extrudates comprising E85 showed a lipid mass degradation of about 1.5% .

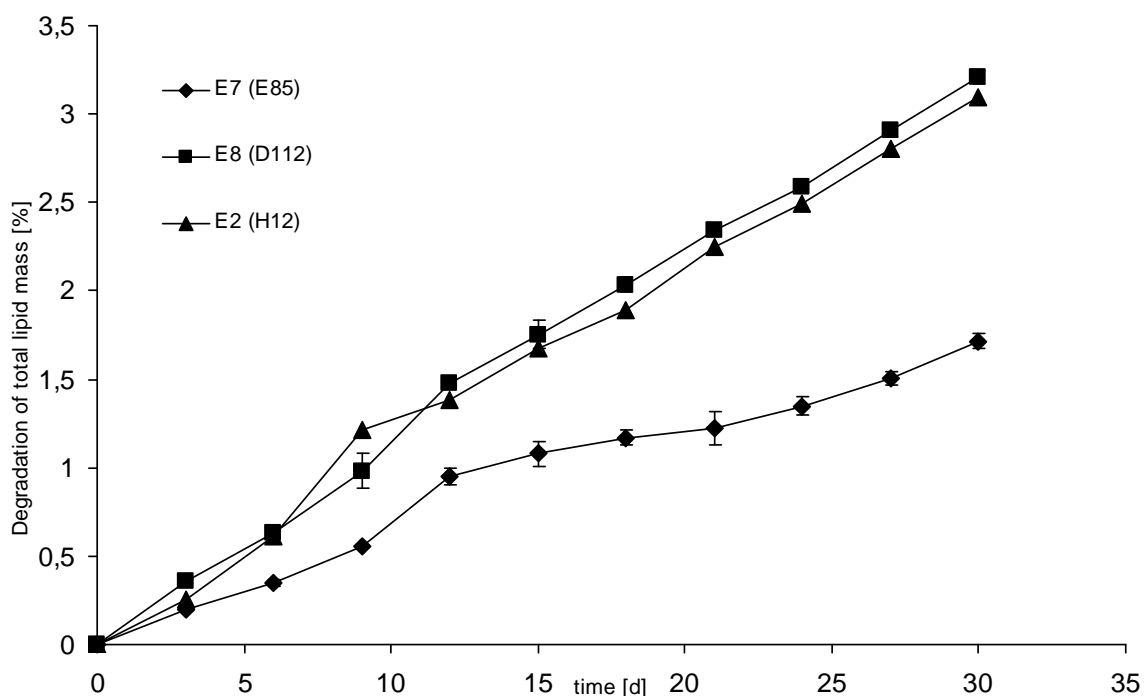


Figure 5: Extrudate degradation study: influence of the low melting lipid component on the degradation velocity (Average + S.D., n = 3).

Effect of the high melting lipid component: the use of D114 as high melting lipid component leads to the highest degradation rate (3.6%) compared with D116 or D118 based extruded implants (Fig. 6).

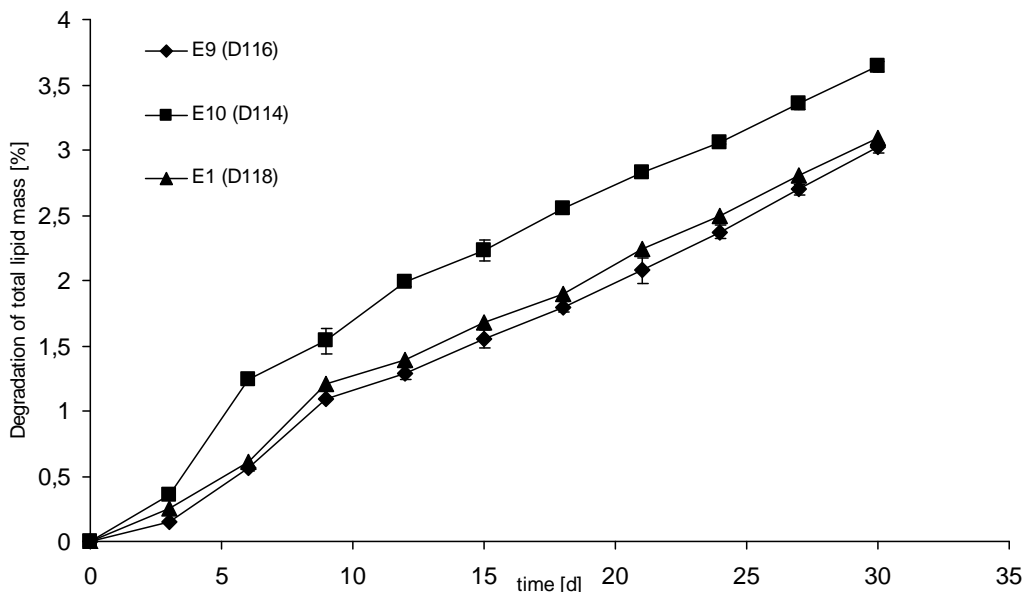


Figure 6: Extrudate degradation study: influence of the high melting lipid component on the degradation behaviour (Average + S.D., n = 3).

Effect of the mixing ratio of the lipid composition: Extruded lipid implants were always prepared from mixtures of high and low melting components. As seen in Fig. 7 the composition with a mixing ratio of 80:20 showed a degradation of 3.75% of the total lipid mass after 30 days and therefore seems superior to 70:30 (2.5%) or 90:10 (1.6%).

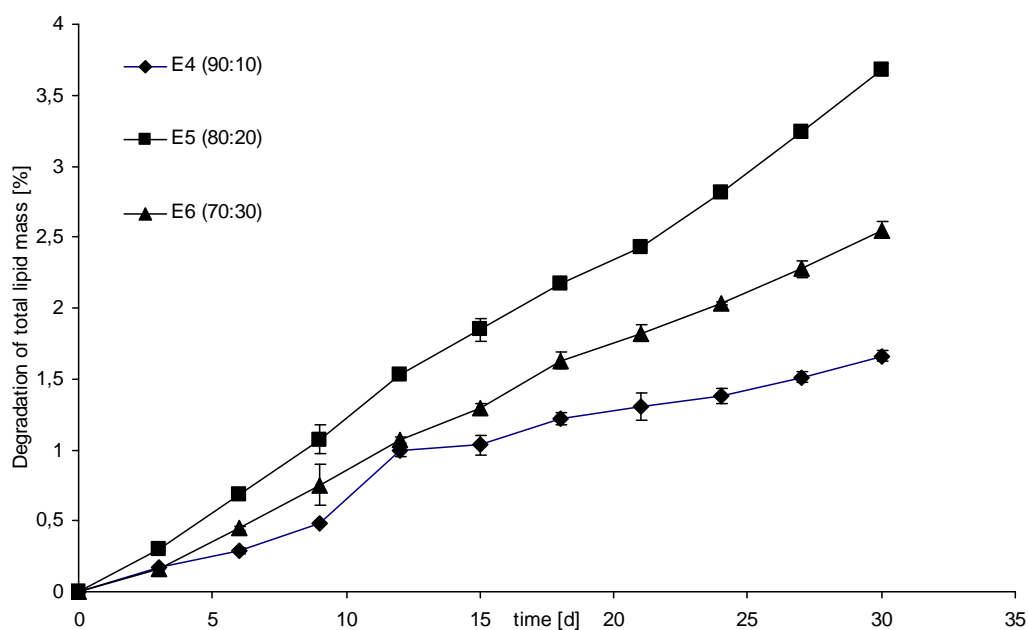


Figure 7: Extrudate degradation study: influence of the ratio of low and high melting component on the degradation behaviour (Average + S.D., n = 3).

Effect of the amount of pore builder: as already confirmed by the experiments with porous implants, extruded lipid rods containing the highest amount of pore builder exhibited the highest degradation rate (3.95%). Extrudates without any pre-built pores reached only 1.65% of total lipid degradation at the end of the degradation study (Fig. 8).

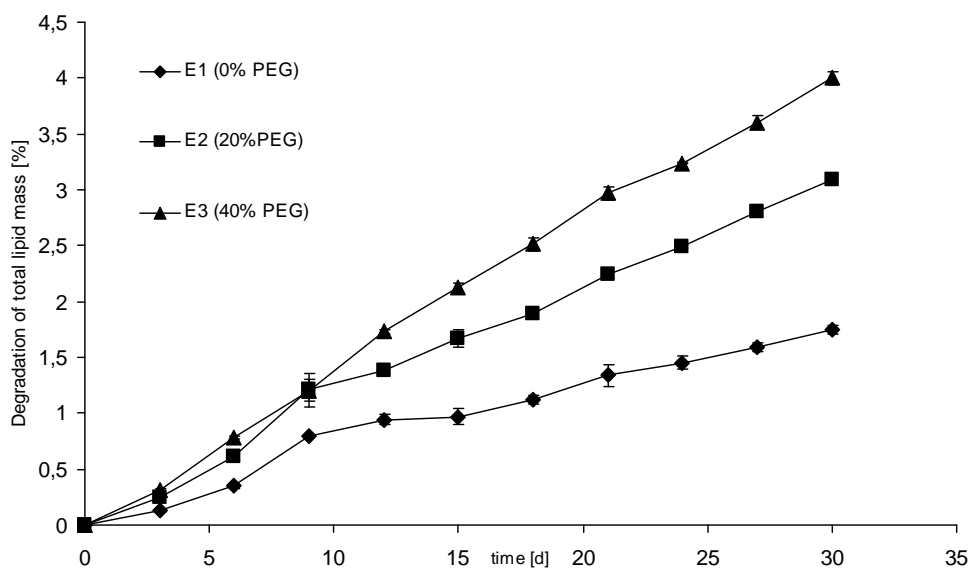


Figure 8: Extrudate degradation study: influence of the PEG content on the degradation behaviour (Average + S.D., n = 3).

Surprisingly almost all extrudates –except E1, E4 and E7- lost their physical integrity after a few days of lipase incubation resulting in small lipid particles suspended in the buffer media. The extrudates of the control group maintained their structure and morphology after incubation for more than 2 months in buffer media without lipase solution. Laser light diffraction measurements were carried out to analyze the size of the generated particles. As seen in Fig. 9 mean particle sizes of the collapsed lipid extrudates were in the μm size range.

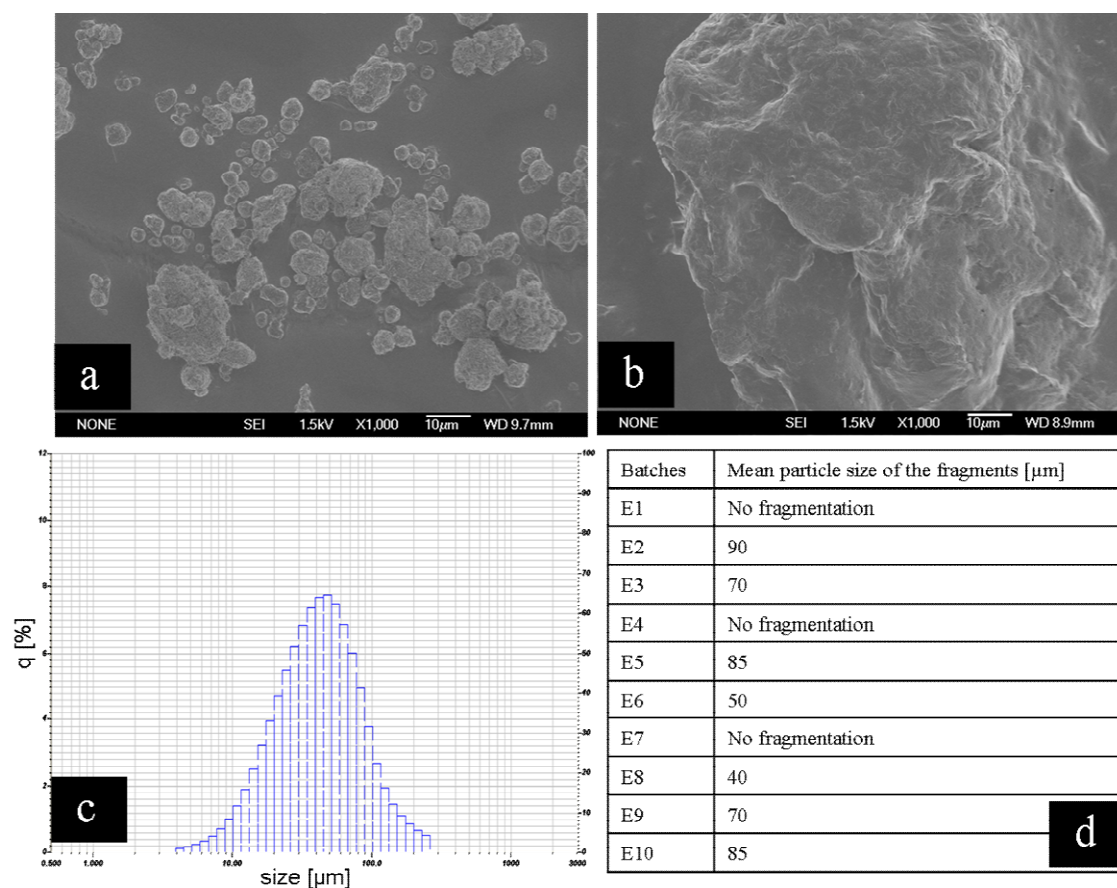


Figure 9: a) SEM photographs of particles generated during lipid matrix collapse of incubated extrudates (magnification 1000X). b) Surface morphology of particle generated by matrix collapse of lipid based extrudates (magnification 1000X). c) Typical particle size distribution of particles generated during lipase incubation of lipid based extrudates (size distribution of particles from extrudate formulation E6). d) Table of particle size distributions: mean particle size range (Average size [μm]).

This breakdown of the lipid matrix is rather unexpected and can be considered as a form of bulk erosion. Since polymers typically undergo surface erosion when they are enzymatically degraded [33-35] additional experiments have to be carried out in order to explain the reasons for the lipid extrudate erosion phenomenon and to analyze the mechanism of the lipid matrix breakdown. However, in vivo such degradation behaviour would be highly desirable as the generated small particles can be finally washed away by body fluids or can be eliminated by phagocytosis and therefore would lead to minimized irritation and foreign body reactions.

Conclusion

The presented results lead to the conclusion that depot systems based on single triglycerides and triglyceride-mixtures can be degraded by lipolytic enzymes under physiological conditions. Although lipid cleavage is a rather slow process, our studies clearly demonstrate that this process can be accelerated by using certain materials, implant geometries and preparation techniques. For particulate systems it can be stated that with decreasing particle sizes lipase degradation is increasing and finally capable to fully degrade such microparticles. This finding is consistent with the results of Reithmeier et al. who claimed a reduction of the number of implanted microparticles after 7 days of incubation [3]. Thus, if a short term drug delivery is necessary lipid microparticles may very well fulfil all the requirements for biodegradable controlled release devices. Compared to the microparticles compressed implants show only very slow degradation velocity. Presumably this is a result of the minor adsorption rate of the enzymes on the monolithic compressed lipid system: since microparticles exhibit a higher surface area due to their particulate nature these systems can be degraded quicker as monolithic systems with a relative small surface area. Our studies indicate that the lipid cleavage is strictly happening on the surface of the implants - a finding concordant with several other publications [32, 36]. This surface degradation and erosion process prevents interference with the drug release mechanism of such lipid drug delivery systems. Nevertheless a complete degradation of these compressed systems is extremely unlikely since – assuming a pure enzymatic based degradation – lipid cleavage would take more than hundred years. The results on extrudates studies show that it is possible to increase the degradation by changing the geometric form and the preparation technique of the depot system and thereby increasing the surface area. Using certain lipid components changes the degradation behaviour dramatically resulting in “collapsing” extrudates generating lipid particles in the μm range. This erosion process can be influenced by the amount of pore builder as well as by the sort and the ratio of the used lipid components. Dissolution of the pore builder or of the entrapped drugs promotes the generation of an interconnected pore network which seems to induce the observed collapse of the lipid structure. The generated particles exhibit a higher surface area thus resulting in the following to a faster biodegradation compared to an intact depot system based on the same components We can assume, that degradation of lipid based drug delivery systems will occur in the human body even if the lipase activity levels in vivo are lower than the levels used in these in vitro studies. Additionally, we conclude that the observed bulk erosion process may lead to the development of fully erodible drug delivery systems. With such systems, both long terms sustained release and eventual total biodegradation and bioerosion should be achievable.

References

1. Sullivan, M.F., P.S. Ruemmler, and D.R. Kalkwarf, *Sustained administration of cyclazocine for antagonism of morphine*. Drug and Alcohol Dependence, 1976. 1(6): p. 415-428.
2. Joseph, A.A., Hill J. L. J., Patel S., Kincl A., *Sustained-release hormonal preparations XV: Release of progesterone from cholesterol pellets <I>in vivo</I>*. Journal of Pharmaceutical Sciences, 1977. 66(4): p. 490-493.
3. Reithmeier, H., J. Herrmann, and A. Göpferich, *Lipid microparticles as a parenteral controlled release device for peptides*. Journal of Controlled Release, 2001. 73(2-3): p. 339-350.
4. Vogelhuber, W., et al., *Monolithic glyceryl trimyristate matrices for parenteral drug release applications*. European Journal of Pharmaceutics and Biopharmaceutics, 2003. 55: p. 133-138.
5. Mohl, S. and G. Winter, *Continuous release of rh-interferon [alpha]-2a from triglyceride matrices*. Journal of Controlled Release, 2004. 97(1): p. 67-78.
6. Mohl, S. and G. Winter, *Continuous Release of rh-Interferon $\hat{I}\pm$ -2a from Triglyceride Implants: Storage Stability of the Dosage Forms*. Pharmaceutical Development and Technology, 2006. 11(1): p. 103-110.
7. Appel, B., et al., *Lipidic implants for controlled release of bioactive insulin: Effects on cartilage engineered in vitro*. Int.J.Pharm., 2006. 314(2): p. 170-178.
8. Guse, C., et al., *Biocompatibility and erosion behavior of implants made of triglycerides and blends with cholesterol and phospholipids*. International Journal of Pharmaceutics, 2006. 314(2): p. 153-160.
9. Schwab, M., et al., *Correlation of in vivo and in vitro release data for rh-INF[alpha] lipid implants*. European Journal of Pharmaceutics and Biopharmaceutics, 2008. 70(2): p. 690-694.
10. Large, V., et al., *Hormone-sensitive lipase expression and activity in relation to lipolysis in human fat cells*. J. Lipid Res., 1998. 39(8): p. 1688-1695.
11. Frayn, K.N., et al., *Hormone-sensitive lipase: quantitation of enzyme activity and mRNA level in small biopsies of human adipose tissue*. Clinica Chimica Acta, 1993. 216(1-2): p. 183-189.
12. Ruge, T., et al., *Lipoprotein lipase activity/mass ratio is higher in omental than in subcutaneous adipose tissue*. European Journal of Clinical Investigation, 2006. 36(1): p. 16-21.

13. Richelsen, B., et al., *Regulation of lipoprotein lipase and hormone-sensitive lipase activity and gene expression in adipose and muscle tissue by growth hormone treatment during weight loss in obese patients*. *Metabolism*, 2000. 49(7): p. 906-911.
14. Kobayashi, J., et al., *Relationship of Lipoprotein Lipase and Hepatic Triacylglycerol Lipase Activity to Serum Adiponectin Levels in Japanese Hyperlipidemic Men*. *Hormone and Metabolic Research*, 2005(8): p. 505-509.
15. Thörne, A.Å., W ; Carneheim, C; Olivecrona, T ; Nordenström, J, *Influence of trauma on plasma elimination of exogenous fat and on lipoprotein lipase activity and mass*. *Clinical Nutrition*, 2005. 24(1): p. 66-74.
16. Persson, B. and B. Hood, *Characterization of lipoprotein lipase activity eluted from human adipose tissue*. *Atherosclerosis*, 1970. 12(2): p. 241-251.
17. Khoo, J.C., W.W. Fong, and D. Steinberg, *Activation of hormone-sensitive lipase from human adipose tissue by cyclic AMP-dependent protein kinase*. *Biochemical and Biophysical Research Communications*, 1972. 49(2): p. 407-413.
18. Fielding, P.E.S., V. G.; Fielding, C. J. *Cardiovasc., Lipoprotein lipase. Properties of the enzyme isolated from post-heparin plasma*. *Cardiovasc. Res. Inst., Univ. California, San Francisco, CA, USA. Biochemistry*, 1974. 13 (21).
19. Cheng, C.F., et al., *Purification and characterization of human lipoprotein lipase and hepatic triglyceride lipase. Reactivity with monoclonal antibodies to hepatic triglyceride lipase*. *J. Biol. Chem.*, 1985. 260(19): p. 10720-10727.
20. Iverius, P.H. and J.D. Brunzell, *Human adipose tissue lipoprotein lipase: changes with feeding and relation to postheparin plasma enzyme*. *Am J Physiol Endocrinol Metab*, 1985. 249(1): p. E107-114.
21. Hayashi, R., S. Tajima, and A. Yamamoto, *Purification and Characterization of Lipoprotein Lipase from Human Postheparin Plasma and Its Comparison with Purified Bovine Milk Lipoprotein Lipase*. *J Biochem*, 1986. 100(2): p. 319-331.
22. Chakrabarty, K., et al., *Lipogenic activity and brown fat content of human perirenal adipose tissue*. *Clinical Biochemistry*, 1988. 21(4): p. 249-254.
23. Yeaman, S.J., et al., *The multifunctional role of hormone-sensitive lipase in lipid metabolism*. *Advances in Enzyme Regulation*, 1994. 34: p. 355-370.
24. Olbrich, C., O. Kayser, and R.H. Müller, *Lipase degradation of Dynasan 114 and 116 solid lipid nanoparticles (SLN)--effect of surfactants, storage time and crystallinity*. *International Journal of Pharmaceutics*, 2002. 237(1-2): p. 119-128.

-
25. Bodmeier, R., J. Wang, and H. Bhagwatwar, *Process and formulation variables in the preparation of wax microparticles by a melt dispersion technique. II. W/O/W multiple emulsion technique for water-soluble drugs*. *Journal of Microencapsulation*, 1992. 9(1): p. 99 - 107.
 26. Wood, R. and T. Lee, *High-performance liquid chromatography of fatty acids: quantitative analysis of saturated, monoenoic, polyenoic and geometrical isomers*. *Journal of Chromatography A*, 1983. 254: p. 237-246.
 27. Dole, V.P.M., Hans., *Microdetermination of long-chain fatty acids in plasma and tissues*. *Journal of Biological Chemistry* 1960. 235: p. 2595-2599.
 28. Brockman, T.T.a.H.L., *Regulation of carboxylester lipase adsorption to surfaces. 2. Physical state specificity*. *Biochemistry*, 1987. 26((25)).
 29. Posner, I., ; DeSanctis, J., *Kinetics of product inhibition and mechanisms of lipoprotein lipase activation by apolipoprotein C-II*. *Biochemistry*, 1987. 26 (12): p. 3711-17.
 30. Reis, P., et al., *Competition between Lipases and Monoglycerides at Interfaces*. *Langmuir*, 2008. 24(14): p. 7400-7407.
 31. Dahim, M. and H. Brockman, *How Colipase−Fatty Acid Interactions Mediate Adsorption of Pancreatic Lipase to Interfaces†*. *Biochemistry*, 1998. 37(23): p. 8369-8377.
 32. Reis, P., et al., *Lipases at Interfaces: Unique Interfacial Properties as Globular Proteins*. *Langmuir*, 2008. 24(13): p. 6812-6819.
 33. Nair, L.S. and C.T. Laurencin, *Biodegradable polymers as biomaterials*. *Progress in Polymer Science*, 2007. 32(8-9): p. 762-798.
 34. Pitt, C.G., et al., *The enzymatic surface erosion of aliphatic polyesters*. *Journal of Controlled Release*, 1984. 1(1): p. 3-14.
 35. Zhang, Z., et al., *Enzymatic Surface Erosion of Poly(trimethylene carbonate) Films Studied by Atomic Force Microscopy*. *Biomacromolecules*, 2005. 6(6): p. 3404-3409.
 36. Brzozowski, A.M., et al., *A model for interfacial activation in lipases from the structure of a fungal lipase-inhibitor complex*. *Nature*, 1991. 351(6326): p. 491-494.

2.3. Discussion of the results of the in vitro degradation study

For the first time degradation of triglyceride based drug depot systems can be quantifiably investigated with the method described in the first part of this chapter. The applied method, consisting of lipid carrier incubation in lipase containing buffer media, isolation of the degradation products, i.e. fatty acids and the quantification of these substances allows the evaluation of lipid based drug release carriers with respect to their degradation velocity in the presence of lipases. Of course the results of this study have to be considered with some care, since the system contains some elements which should be discussed. At first the lipase levels applied in the in vitro system are worth some consideration: With respect to the detection limit and the time frame of the conducted incubation experiments lipase levels were approximately 10000 times higher than the activities known to be present in human tissue. On the one hand this extreme amplification of the main parameter in this system may jeopardize the plausibility of the generated results. On the other hand one can argue that an enzyme system consisting only of 3 different more or less purely isolated enzymes, totally separated from normally existing co-enzymes and other factors of biological relevance can hardly mimic a controlled and reactive physiological enzyme system. Secondly, one could criticize the setup of the applied incubation system. Incubating lipid implants and extrudates in free flowing buffer media exhibiting a total absence of physiological substances as albumin, collagen surfaces and last but not least a cellular and reactive immunogenic environment isn't a close depiction of the physiological environment an implanted drug depot system would face. Tissue fluids and collagenous encapsulation are parameter strongly influencing the degradation and erosion behaviour of the implanted systems. In addition to that, as described in the review in chapter 1, immunogenic reaction at the implant tissue interface can lead to remarkable physical and chemical changes which would surely influence a lipase-induced degradation. To avoid such strenuous argumentation one should consider the presented in vitro degradation system allows the direct and reproducible comparison of degradation processes of such different lipid carrier systems as microparticles and monolithic implants. Especially in the simplicity of the applied in vitro systems, in the understatement of its parameter lies the advantage. It is hardly imaginable to design an in vivo system capable of observing the lipase effects on lipid particles ranging in the micrometer area. When creating this system it wasn't aimed to fully mimic all physiological conditions and to get totally independent of animal experiments but it was aimed to concentrate one lipolytic systems of the human body and to thoroughly examine the effects of this system without any interference

from other biological factors. When dealing with the main points of criticism highlighted above, the author was also aware that some other factors in the applied incubation systems and incubated samples would need to be dealt with special attention in order to maintain a high degree of quality and reproducibility. In the following part additional experiments and preparation techniques employed during the development and execution of the lipase incubation studies are presented.

2.4. Lipase stability and lipid microparticle preparation

As described in the first part of this chapter, lipid microparticles and other lipid based drug depot systems were incubated in lipase solution, in order to determine lipid degradation rates of the applied systems. When working with enzymes such as lipase, it is crucial to thoroughly characterize these bio-catalysers in order to achieve a constant and reproducible activity. Since enzymes are generally proteins - with an amino acid range from only 62 [1] to several hundred or thousand amino acids [2] – these macromolecules comprise the risk of inactivation and activity loss. Enzyme activity and catalysis is a result of a complex process, involving structural changes thereby exposing the active site of this macromolecule comprising the amino acids serine, aspartate and histidine which form the catalytic triad [3-5]. Enzyme folding and interfacial activation can be impaired by several factors such as ion strength, heat or cold and mechanical forces [6]. Therefore, for long term experiments as described in 4.2 enzyme stability has to be evaluated. In the first part of this section the experiments of the conducted lipase stability test are outlined. The second part deals with the preparation of lipid microparticles featuring a defined particle size.

Materials and methods

Materials

All lipids (Dynasan 118 and Dynasan 116) used in these experiments were purchased from Sasol GmbH, Witten, Germany. All lipases and all other chemicals were purchased from Sigma–Aldrich, Deisenhofen, Germany.

Methods

Lipase activity assay

Lipase activity was tested with a trioleate emulsion. The emulsion was prepared freshly for each test by mixing 4.5 ml aqueous polyvinyl alcohol solution (2%) with 1.5 ml triolein. This mixture was then emulsified at 0°C with an Ultra Turrax® for 2 min at 15,000 rpm. 500µl of this emulsion and 400µl PBS buffer 0.01 M pH 7.4 then were incubated in a 2 ml Eppendorf cap for 10 min at 37°C in a water bath. 100µl of lipase solution was added and the mixture was incubated again at 37°C. After 10 min the reaction was stopped by adding 1 ml of a MeOH:acetone:methylene chloride mixture (1:1:1 v/v). Before derivatization and HPLC analysis free fatty acids produced in the triglyceride cleavage were extracted using the method already described in the first part of this chapter. In order to achieve a standardized quality of the used trioleate emulsion, oil droplet size was determined with static laser light scattering.

Stability study

In order to investigate on the stability of the lipases (Lipase amano M, lipoprotein lipase from *pseudomonas sp*, lipase from *candida rugosa* and lipase from *rhizoma oryzae*) used for the degradation studies lipase solutions of known concentrations were incubated in PBS pH 7.4 at 37° for 8 days in TopPac® vials. Every day a specified amount of the incubated solution was withdrawn and tested with the trioleate emulsion method described above. Preliminary to the start of this study the activity of all lipase was determined and the resulting level of activity was set to 100% as a starting point reference.

Lipid microparticle preparation

Lipid based microparticles were prepared as described in chapter 2. As 2 different particle sizes were required for the experiments (10µm and 100µm mean particle diameter) process conditions, i.e. the rotation speed of the Ultra Turrax® (TP 18/10, Stauffen, Germany) had to be adjusted in order to obtain the particle size needed for the experiments. Therefore in preliminary experiments the suitability of the applied method has been tested. Rotation speed of the Ultra Turrax® was controlled externally with a continuously variable 9-step TRIAC-controller (Messner, Dettenhausen, Germany). In order to validate the preparation of distinct particles sizes lipid microparticles were prepared using rotation speed settings from 1 to 9 on the TRIAC-controller. Preliminary to the mixing step the rotation tools were adjusted to the same temperature as the lipid melt in a temperature controlled water bath in order to avoid lipid solidification. Rotation time was set to 30 sec. After stabilizing the obtained particles in the ice cold aqueous phase the particles were collected and particle size was determined with static light scattering.

Particle size distribution

Size of lipid microparticles and oil droplets of prepared emulsions was determined using a Horiba LA 950 particle size distribution analyzer (Retsch Technology GmbH, Haan, Germany).

Results and discussion

Lipase stability

As expected lipase activity was decreasing with increasing time of storage at 37° in aqueous media. The tested enzymes exhibited different stabilities. Lipoprotein lipase from *pseudomonas sp.* (LPL) exhibited the highest stability in aqueous media (Fig. 1). After 3 days of incubation almost 80% of the initial activity was measured. However after 8 days activity level was decreased to 20%. Comparable to LPL was the obtained stability data for lipase from *rhizoma oryzae* (RO). After 3 days activity was decreased to 80% and after 8 days 20% of residual activity was measured.

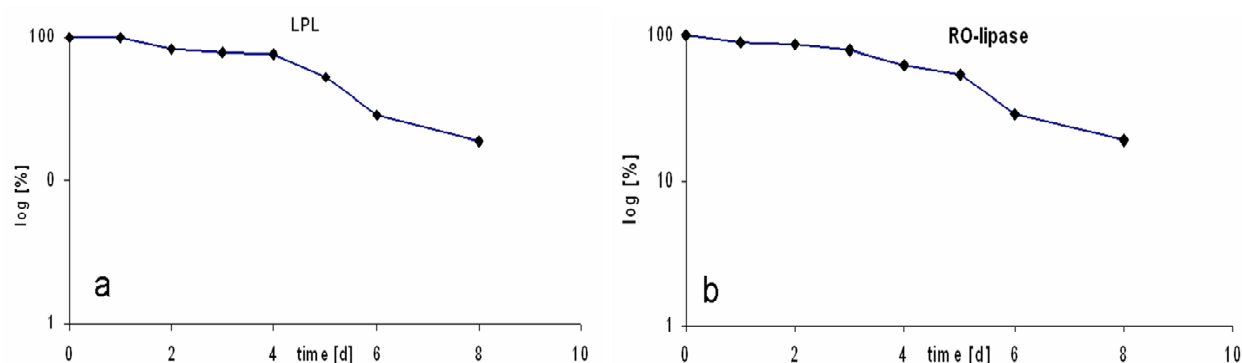


Figure 1: Stability data for lipase from *pseudomonas sp.* (a) and lipase from *rhizoma oryzae* (b)

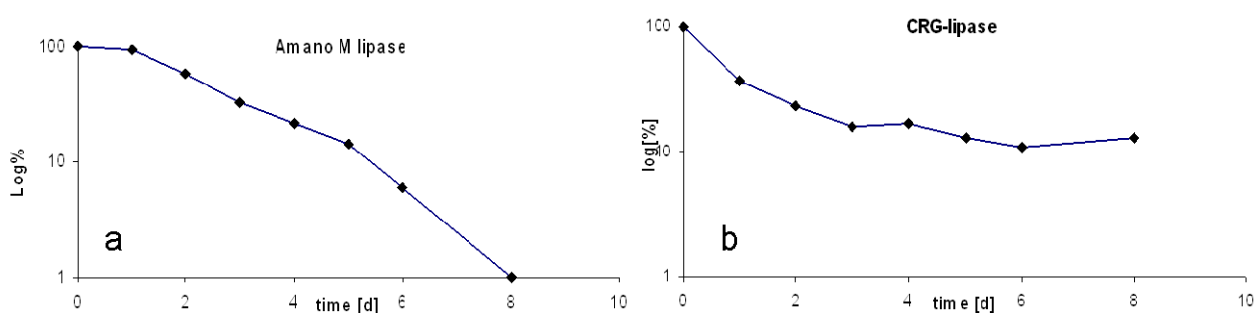


Figure 2: Stability data for lipase amano M (a) and lipase from *candida rugosa* (b)

Lipase amano M was shown to be very unstable under the tested conditions (Fig 2). After 3 days the activity levels was beneath 20% and after 8 days of incubation no activity was measurable anymore. Lipase from candida rugosa (CRG) was slightly better. After 3 days of incubation approximately 23% of the primordial activity was detected. After 8 days the activity level dropped to values of about 13%. According to the results generated in these stability tests, lipoprotein lipase from *pseudomonas sp.* and lipase from *rhizoma oryzae* were

selected for the long term degradation studies. Further on, as a consequence of these results, it was decided to change the lipase-containing buffer media every 3 days in order to maintain high lipase activity in the setup. According to these results the lipase activity level are almost kept constant for a 3 day cycle.

Trioleate emulsion

The oil droplet size of the obtained trioleate emulsions was in a narrow size range (0.5 μm to 25 μm) with an average droplet size of approximately 4 μm .

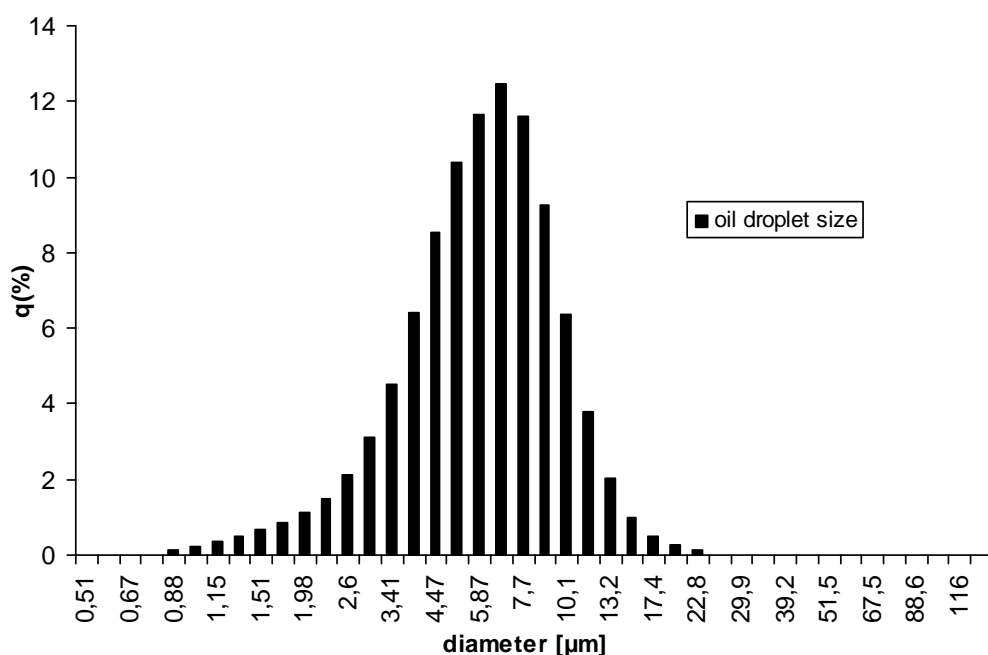


Figure 3: Typical size distribution of oil droplets generated during the preparation of a trioleate emulsion

Microparticle preparation

It was shown that the attached TRIAC-controller enabled the controlled preparation of microparticles. As seen in Fig. 4 the particles size and the rotation speed of the emulsification tool correlate closely in a certain range. As expected, with lower rotation velocity larger particles are obtained. It can be stated that this method it is not suitable to produce particles with a mean particle size smaller than 1-2 μm as the particle size didn't decrease significantly when using the settings 7 to 9. Unfortunately, it was not possible to obtain exact data concerning the number of revolutions with the TRIAC-controller attached. However it can be stated that level 9 corresponds to 20,000 rotations per minute.

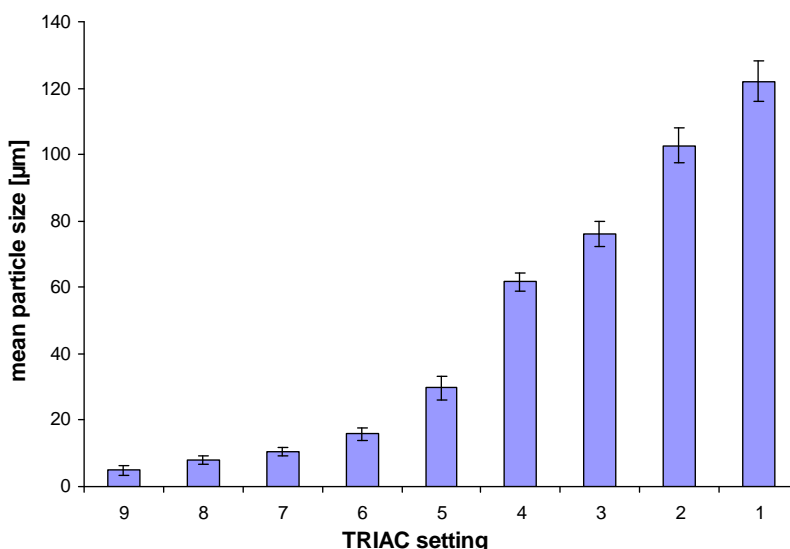


Figure 4: Size of microparticles correlated to settings of the TRIAC controller attached to the emulsification tool

Summary

It was shown that lipases designated for lipid depot system degradation studies exhibit different properties concerning their stability in aqueous environment. As a result of these experiments lipase from *pseudomonas sp* and lipase from *rhizoma oryzae* were employed in the degradation experiments described in chapter 1. Accordingly samples were drawn every three days in order to quantify the FFA amount and to refresh the lipase in the incubation set up. In addition to that a microparticle preparation method was presented which allows obtaining microparticles of a certain size range by controlling the rotation speed of the emulsification tool.

References

1. Chen, L.H., et al., 4-Oxalocrotonate tautomerase, an enzyme composed of 62 amino acid residues per monomer. *J. Biol. Chem.*, 1992. 267(25): p. 17716-17721.
2. Smith, S., The animal fatty acid synthase: one gene, one polypeptide, seven enzymes. *FASEB J.*, 1994. 8(15): p. 1248-1259.
3. Brady, L., et al., A serine protease triad forms the catalytic centre of a triacylglycerol lipase. *Nature*, 1990. 343(6260): p. 767-770.
4. Brumlik, M.J. and J.T. Buckley, Identification of the catalytic triad of the lipase/acyltransferase from *Aeromonas hydrophila*. *J. Bacteriol.*, 1996. 178(7): p. 2060-2064.
5. Emmerich, J., et al., Human lipoprotein lipase. Analysis of the catalytic triad by site-directed mutagenesis of Ser-132, Asp-156, and His-241. *J. Biol. Chem.*, 1992. 267(6): p. 4161-4165.
6. Iyer, P.V. and L. Ananthanarayan, Enzyme stability and stabilization--Aqueous and non-aqueous environment. *Process Biochemistry*, 2008. 43(10): p. 1019-1032.

3. Chapter Three: Studies on the mechanisms of lipid matrix disintegration

3.1. Introduction

In chapter 2 the development and preliminary results of a lipase incubation study conducted with several lipid based drug depot systems were presented. The results of this study were diverging. It was found that most examined simple triglycerides were rather resistant against the lipase incubation. Those implants and extrudates remained stable and didn't change their physical structure, a result consistent with the outcome of the animal experiment described in chapter 1. It still has to be analyzed whether this insensitivity of glyceryl tristearate, - tripalmitate, and - trimyristate towards the employed enzymes is a result of the observed minor accumulation of the lipases at the lipid water interface – a phenomenon which could be a consequence of the missing coenzymes and other factors present in physiological systems – or if these substances are per se to be considered as stable and inert. Concentrating on the results of the incubation experiments conducted with extruded implants, it seems that especially the triglycerides which feature a low melting point influence the behaviour of the implant upon lipase incubation. Extrudates consisting of low melting components disintegrated rapidly resulting in smaller lipid particles. Considering these results and aiming for lipid depot systems featuring such disintegration behaviour in vivo, one should concentrate on the analysis of the observed phenomenon. In the following third chapter subsequent experiments are described which were conducted in order to analyse the mechanism of lipid system disintegration. Looking back on the so far presented data dealing with lipid depot system degradation, no clear distinction has been made between degradation and erosion processes. However, regarding the phenomenon of extrudate disintegration observed in chapter 2 and considering that so far only chemical degradation processes were quantifiably analyzed with the employed RP-HPLC method, it may be time to differentiate more clearly between degradation and erosion. When speaking of degradation the cleavage of chemical bonds – in case of triesters such as the used lipids - the cleavage of the ester bond is understood. Erosion is defined as a loss of mass of the analyzed system. In the following these two connected processes are analyzed more distinctively. The data presented in the first part of this chapter highlights additional analytical methods applied for analyzing the erosion mechanism. Subsequently, the last part of this chapter deals with the aspects of preparation technique and lipid composition on the degradation of the discussed systems.

3.2. Studies on the lipase induced degradation of lipid based drug delivery systems.**Part II – Investigations on the mechanisms leading to collapse of the lipid structure**

Martin Schwab¹, Cushla McGoverin², Clare Strachan³, Keith Gordon², Thomas Rades³
Gerhard Winter¹

¹Ludwig-Maximilians-University Department of Pharmaceutical Technology, Munich, Germany.

²Department of Chemistry, University of Otago, Dunedin, New Zealand

³School of Pharmacy, University of Otago, Dunedin, New Zealand

Submitted to Journal of Controlled Release

Abstract

It has recently been found that lipid composition appears to have a major influence on the rate of lipase-induced degradation of lipid-based drug delivery systems (microparticles, compressed implants and extruded implants). During lipase incubation, most of the lipid extrudates produced for this study lost their physical strength and tended to collapse generating lipid particles in the μm -range. The aim of this study was to specify the processes leading to collapse of lipid based drug delivery systems during the *in vitro* lipase incubation. Compressed tablet-shaped lipid implants were used as model systems. A pre-column RP-HPLC derivatization method was used to characterize the degradation behavior of the single lipid component used for the preparation of lipidic extrudates. Raman spectroscopy, FT-IR spectroscopy and differential scanning calorimetry were used to investigate the physical and chemical changes in the tablets upon lipase incubation. This study revealed that the lipid component trilaurate plays a major role in the degradation and erosion processes occurring during lipase incubation. The production of trilaurate/lauric acid mixtures, with a melting point beneath human body temperature, leads to lipid matrices melting and losing their physical integrity.

Key words: lipid based depot systems, biodegradation, erosion, Raman spectroscopy

Introduction

Recently, there has been substantial interest in lipid-based drug delivery systems for the formulation of proteins due to their outstanding performance in stabilizing incorporated protein molecules. However, there is currently little known about the fate of lipid-based depot devices in the human body. In most of the publications dealing with triglyceride based drug delivery systems biodegradation and bioerosion *in vivo* was not reported [1, 2]. Nevertheless, biodegradation and -erosion would be necessary for human use of these drug delivery systems. As lipases play a crucial role in the metabolic system by hydrolyzing triglycerides to produce free fatty acids (FFA), which serve as a major source of energy, it is obvious that human lipase activity in the subcutaneous fat tissue and the serum could affect the structure and the stability of lipid based drug delivery systems. Therefore – in a recent study - we conducted *in vitro* lipase incubation studies with different lipidic delivery devices (microparticles, compressed implants and extruded implants) and investigated the chemical degradation rate of these systems. We could report that some of the investigated systems, mainly extrudates, tend to disintegrate during the lipase incubation resulting in suspended particles in the μm -range. In particular, extrudates containing glyceryltrilaurate as a low temperature melting component exhibited the lowest physical stability of the incubated extrudates and promoted lipid matrix disintegration. In this study, the chemical degradation and erosion behavior of the single lipid components used to produce the different lipidic drug depot systems have been analyzed. Raman and infrared spectroscopy, as well as differential scanning calorimetry have been used to analyze the process of lipid matrix breakdown.

Materials and Methods

Materials

All lipids (glyceryl tristearate (D118), -tripalmitate (D116), -trimyristate (D114) –trilaurate (D112), lipidmixture E85, lipidmixture H12) used in matrix preparation were purchased from Sasol GmbH, Witten, Germany. Lipases (lipoprotein lipase (LPL) from *Pseudomonas* sp. and lipase from *Rhizoma Oryzae* (RO)) and all other chemicals were purchased from Sigma–Aldrich, Deisenhofen, Germany.

Sample preparation

Implant manufacturing

Lipid tablets were used as lipid based model systems to mimic lipid implants. The tablets were prepared from either admixed lipid powder or from melted lipid mixtures.

Lipid powder mixtures

To simulate an accumulation of lauric acid in D112 matrices, mixtures of these two substances were prepared. The powdered components were ground together with liquid nitrogen in an agate mortar. Mixture ratios 1, 5, 10 and 20% lauric acid in D112 were prepared. These mixtures were analyzed using differential scanning calorimetry measurements. To investigate the influence of lipase incubation on the powder composition with Raman spectroscopy tablets were compressed from the obtained mixtures. Compressed tablets were prepared using a 5 ton hydraulic press. The components – trilaurate, trimyristate, tripalmitate or tristearate- were ground in an agate mortar. The resulting powder was compressed with a pressure of 2 tons for 30 seconds. Two sizes of tablets were produced using different compression tools. Big tablets consisted of 500 mg of lipid material compressed to a tablet exhibiting a diameter of 13 mm an average height of 3.7 mm.

Lipid mixtures prepared by melting

In order to obtain homogenous lipid material blends for analysis with Raman or FT-IR spectroscopy lipid mixtures were heated above the melting temperature of the pure components. The melt was then cooled down slowly and tempered at 30°C for 24 h to avoid polymorphic transformations. These mixtures were then compressed into small tablets using a hydraulic press resulting in implants with a diameter of 5 mm, an average weight of 50 mg and an average height of approximately 2.3 mm. The tablets were compressed for 30 seconds with a pressure of 2 tons.

Preparation of layered tablets

Lipid tablets consisting of two different lipid layers were prepared using the hydraulic press. Briefly, D118 powder was compressed for 30 s with a pressure of 2 tons resulting in a disc with a diameter of 13 mm and an average height of 3 mm. These discs were put back in the mould and layered with 50mg of D112 powder by compressing the disc for another additional 30 sec using 2 tons of pressure resulting in a tablet with a top layer of D112. The thickness of the applied D112 layer was determined using a calliper.

Characterisation methods**HPLC analysis**

To investigate the lipase induced degradation of different triglycerides chemical degradation studies were carried out. Briefly, the compressed tablets consisting of single components or mixtures of different triglycerides were incubated at 37°C in 2.0 ml of isotonic 0.01 M phosphate buffer pH 7.4 containing 100 U of lipoprotein lipase and RO-lipase. All tests were

run in triplicate. After 3 days the buffer media was completely removed and analyzed for free fatty acid contents. New buffer solution was added to the incubated samples. The samples were extracted using the modified Dole-extraction [7] method resulting in a free fatty acid (FFA) solution ready for derivatization. Phenacyl esters of fatty acids were prepared by the method described by Wood and Lee [8] followed by a RP-HPLC method for the separation and quantification of the different FFA. A Thermo Separation Products HPLC system (Thermo Fisher Scientific, Inc. Waltham, U.S.A.) equipped with a LiChrosphere RP C18 column (4.6 mm i.d. x 250 mm, 5 μ m) was used (Merck, Darmstadt, Germany). Mobile phase was a mixture of methanol-acetonitrile-water (80: 10: 10 (v/v)). Elution of the generated phenacyl esters was monitored by UV absorbance at 254 nm. The detection limit for stearic acid was about 5 μ gml⁻¹, i.e. approx. 20 nmol of fatty acid. The release of FFA in the buffer media (W_{FFA}) was used to quantify the percentage of degradation (D) as follows:

$$D = \frac{100}{W_0} \times W_{FFA} \quad (1)$$

Differential scanning calorimetry (DSC)

Samples of lipid drug delivery devices prior and after derivatization experiments were analyzed with a NETZSCH DSC 204 Phoenix® (Selb, Germany) instrument. To determine phase transitions of the various compositions samples were heated in the DSC at 10K min⁻¹. Samples were heated from -20°C to 100°C.

FT-IR spectroscopy

FT-IR-spectroscopy is a sensitive, quick and reproducible method for structural determination of lipids [3], and allows the analysis of changes to the triglycerides used in this study. A Bruker Tensor 27 FT-IR Spectrometer with a PIKE MIRacle™ sampling accessory equipped with a MIRacle™ micrometer clamp was used to analyse the samples. The diamond/ZnSe crystal plate had a surface area of 2.54 mm². Spectra were the average of 300 scans recorded from 4000 to 800 cm⁻¹ with a resolution of 4 cm⁻¹. In order to avoid interference with atmospheric humidity sample chamber was purged with dried nitrogen during the measurements. Spectra of D112, lauric acid and D118 powders were recorded and tablets of these materials were analysed after preparation and subsequent incubation as detailed in the Degradation section below.

Raman spectroscopy

Raman spectroscopy can be used to analyse solid state systems such as lipids [4, 5] in the presence of water and buffer substances. The technique was used to investigate the processes occurring on the lipid-water interface respectively on the surface of the lipid matrix during lipase incubation. Further on Raman-spectroscopy was used to detect changes in lipid composition as a result of the enzymatic degradation of lipid drug delivery devices used in this study. FT-Raman spectra were recorded from solid samples using a Bruker IFS-55 Equinox FT-interferometer bench (Bruker Optik GmbH, Ettlingen, Germany) equipped with a FRA-106 Raman accessory and a D418-T liquid nitrogen cooled Ge detector. A 1064 nm cw Nd:YAG laser (Coherent, Lübeck, Germany) was employed; the laser power was set to 490 mW. OPUS (version 5.5, Bruker Optik GmbH, Ettlingen, Germany) was used to record spectral data. Raman spectra were collected using a Bruker Optik SN 73 R361-S3 Raman probe coupled to a custom made flow through device.

Raman microscopic data was collected using a Senterra dispersive Raman microscope (Bruker Optics, Ettlingen, Germany). OPUS version 6.5 was used to control the microscope. An excitation wavelength of 785 nm was used, and a 1200 groove per millimetre grating. The resulting resolution was 3-5 cm^{-1} across the spectrum. Both the Sure_Cal[®] and Spectral shape correction options were implemented within OPUS to ensure wavenumber stability and transferability respectively. An Olympus 50x objective with a 50 μm confocal pinhole was used to collect the Raman signal. Each spectrum was collected from 60-1530 cm^{-1} . The laser power was set to 100mW. Spectra of D112, lauric acid and D118 were recorded and tablets of these materials were analysed after preparation and subsequent incubation as detailed in the Degradation section below.

Scanning Electron Microscopy

To investigate whether degradation of lipid drug delivery devices is visible SEM measurements were carried out. Samples were analyzed using a Field Emission Scanning Electron Microscope Joel JSM-6500F (Joel Inc., Peabody, USA). Therefore samples were attached on adhesive carbon tape (BAL-TEC AG, Balzers, Principality of Liechtenstein) to a custom made brass stub, carbon-sputtered and analyzed.

Digital microscopy

Changes in implant morphology were analyzed using a VHX-600 digital microscope (Keyence, Osaka, Japan).

Degradation studies

Chemical degradation

Spectroscopic analysis of the implants

The appearance of lauric acid in the D112 implants was directly measured using IR and Raman spectroscopy. Calibrations for the prediction of lauric acid within lipase-incubated D112 samples were formed on the basis of infrared and Raman spectral data collected from lipid powder mixtures prepared by melting. The calibration curve was constructed from binary mixtures of 0, 10, 20, 30 and 50% (w/w) lauric acid combined with D112. Each mixture was prepared in triplicate. Raman spectral data was collected using the Raman microscope. Both the infrared and Raman spectroscopic calibrations were partial least squares (PLS) based data (Unscrambler v. 9.8, CAMO Technologies, Inc, Norway), involved standard normal variate preprocessing and the use of a cross-validation procedure which removed one sample at a time (i.e. all three spectra per sample were removed at once). The Raman spectroscopic calibration used the 400-1530 cm^{-1} region, while the infrared spectroscopic calibration used the 900-1900 cm^{-1} region. The sample for which lauric acid concentration was predicted in the infrared study was a 500mg D112 implant which had been incubated for 8 h in 5 ml PBS containing 440 U of LPL. The implants were then washed 3 times with water in order to remove loosely attached degradation products. After drying of the implants using a vacuum chamber at reduced pressure (100mbar) at 25° C for 24 hours the implants were analyzed. The lipase-treated tablet was cut using a scalpel in order to analyse the core. The samples analysed in the Raman study were 50 mg D112 tablets incubated for 2.5h in 2ml PBS containing 100U of LPL and RO. After withdrawal the samples were blotted on absorbent paper in order to remove buffer media and loosely attached degradation products.

Erosion of implants

In situ Raman analysis

Since Raman spectra can be recorded from samples immersed in aqueous environments without any sample disturbance, a series of Raman spectra were collected *in situ* from tablets immersed in 25 mL PBS buffer containing 14U/ml Lipoprotein at a constant temperature of 37°C. The buffer medium was continuously stirred. In order to quantify lipid erosion tablets consisting of layered D112 over D118 were analyzed (preparation as described above). Each Raman spectrum was recorded over 8.5 min with 6 cm^{-1} resolution and across the 1010-1150 cm^{-1} region. Between each recorded Raman spectrum was a 5 second delay; the total series of Raman spectra took approximately 42 hours to collect.

The Raman spectra were analyzed using multivariate curve resolution (MCR) as implemented in the Unscrambler (version 9.8, CAMO Technologies Inc.). The spectra were SNV pretreated prior to MCR. Two spectra, pure D112 and pure D118, were input as initial spectral guesses. The non-negative concentrations constraint was applied. Ten spectra each of pure D112 and D118 were included within the data set analyzed to give a semi-quantitative indication of the presence of these two materials.

DSC analysis

Samples for DSC analysis were prepared as followed: D112 tablets (50mg) were incubated for 2.5 hours in 2 ml PBS pH 7.4 containing 100 U of LPL and RO lipase. After incubation implants were washed 3 times with water to remove loosely attached degradation products. After washing implants were blotted. A scalpel was used to cut the implant in half. The separated core material was collected and ground in an agate mortar. The resulting lipid mass was analyzed with DSC.

Physical analysis of D112 erosion and swelling behaviour

In order to analyze erosion and degradation processes simultaneously compressed D112 implants with a diameter of 13 mm and an average height of 3.7 mm were incubated in 5ml PBS containing 440 U lipoprotein lipase at 37 °C. All tests were run in triplicate. The average initial weight was 500 mg. After predetermined time points the implants were withdrawn from the medium washed three times in 20 ml water and blotted to remove excess water and then weighed (W1). The implants were then dried in a vacuum chamber at reduced pressure (100mbar at 25° C) for 24 hours. After the drying procedure implants were weighed (W2) using an analytical balance (model UMX2, Mettler–Toledo, Greifensee, Switzerland). Finally, the implants were visually characterized using a digital microscope (20X magnification).

The percentage increase in weight due to water uptake and swelling (S) of the lipid was determined at each time point from the following equation [9]:

$$S [\%] = \frac{W_1 - W_0}{W_0} \times 100 \quad (2)$$

The percentage of erosion processes (ES) was calculated from the following equation:

$$ES = \frac{100}{W_0} \times W_2 \quad (3)$$

The residual buffer media, containing main degradation products was extracted using the method described above and the derivatized FFA were analyzed using the RP-HPLC method. The quantified content of FFA released in the buffer media (W_{FFA}) accounted for the percentage of degradation (D) was calculated from equation (1):

$$D = \frac{100}{W_0} \times W_{FFA}$$

Results and discussion

Chemical analysis

HPLC analysis

A linear release of fatty acids due to the lipolytic activity of the lipase occurred during the degradation of the lipid implants prepared from single components. The degradation rate of glyceryltristearate, -tripalmitate and -trimyrystate was almost at the same level resulting in about 0.3% (w/w) degradation of the saponifiable lipid mass— revealing only slight differences in the degradation rate probably according to the chain length [10]. In contrast, glyceryltrilaurate (D112) implants exhibited a 15 fold higher degradation rate reaching up to 5 % percent degradation of the lipid mass after 30 days of incubation (Fig. 1a).

Interestingly, the morphology and structure of the D112 tablets changed dramatically during the incubation study. While tablets consisting of D118, D116 and D114 didn't change after 30 days of lipase incubation glyceryltrilaurate implants tended to melt during the incubation. Macroscopic investigation a few hours after start of the degradation study revealed a formation of a porous coat enclosing a dense core consisting of primordial D112. This porous coat was extending with increasing time of incubation. Eventually after a few hours the implants were melted. This phenomenon was surprising since the melting point of the pure component glyceryltrilaurate (46°C) is higher than the temperature of the incubation setup i.e., 37°C. Presumably this melting process and the resulting generation of lipid droplets enhanced the hydrolytic activity of the lipase probably due to an increase of the total surface area. As lipases are surface active enzymes there can be a correlation stated between the activity of the enzyme, i.e. the cleavage of substrate and the surface area available [11-13]. To investigate on the melting process of D112 DSC measurements were carried out.

Therefore, glyceryltrilaurate-lauric acid mixtures were analyzed to mimic processes probably occurring during incubation with lipase. Further on D112 implants drawn from the degradation experiments were analyzed with DSC in order to investigate on the physical changes induced by the lipase treatment. The incubation of lipid tablets consisting of D118 and D112 (mixture ratio 80:20) prepared from powder mixtures resulted in porous tablets. During the incubation suspended lipid particles could be noticed in the buffer media. FFA analysis revealed a high release of lauric acid generated during lipase incubation, whereas stearic acid was released much more slowly in accordance with the results of the experiments dealing with the pure components. Typically, when incubated for several days, these implants lost their structural integrity and disintegrated into numerous lipid particles. To analyze the effect of the observed preferential cleavage of D112 on the structure of the tablets consisting of the D118/D112 tablets were analyzed with DSC prior and after lipase incubation.

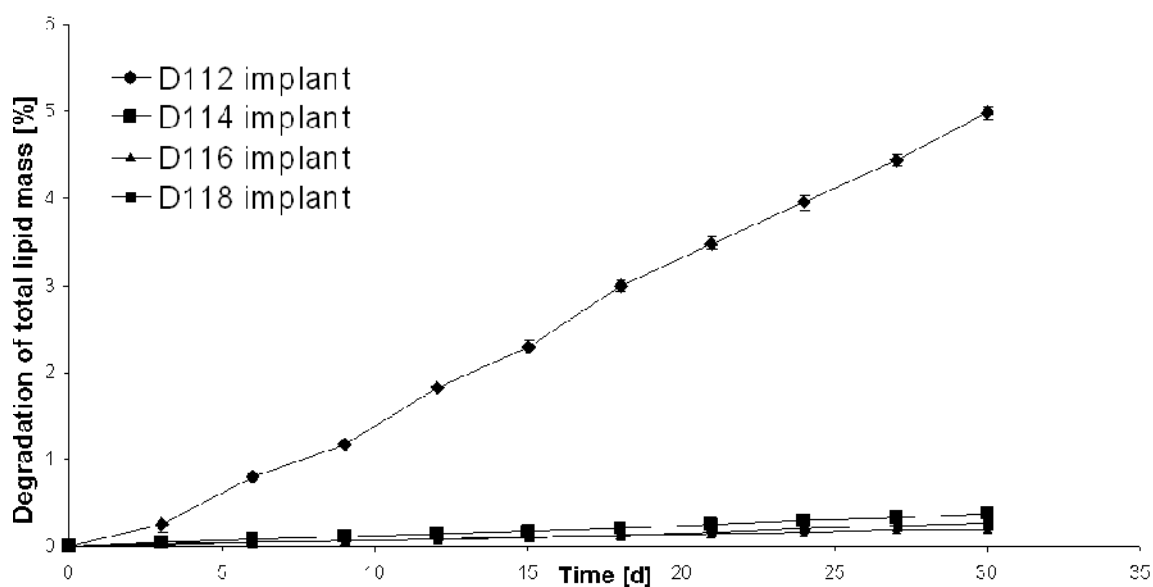


Figure 1: HPLC analysis of lipid degradation: degradation study of D112, D114, D116 and D118 compressed tablets over 30 days of incubation in 100 U lipoprotein lipase and 100 U lipase from *rhizoma oryzae* (average + S.D., n = 3).

Raman-spectroscopy of lipid implants during lipase incubation

The Raman and infrared spectra of D112 and lauric acid are shown in Figure 2.

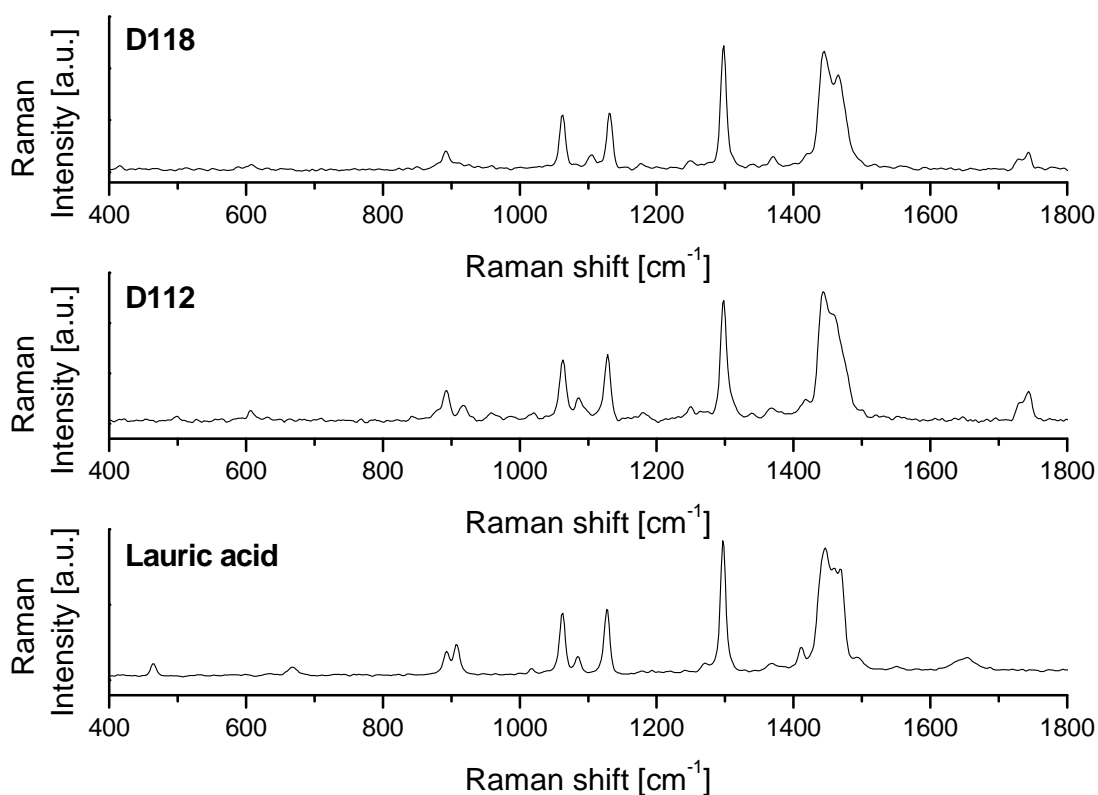


Figure 2: FT-Raman spectra of D118, D112 and lauric acid powders

Raman-analysis of implant surfaces after lipase incubation showed a distinct shift of the normal triglyceride Raman-spectra towards spectra indicating an accumulation of free fatty acids on the surface of the implants. This deposition of FFA on the surface of the implants after incubation with lipases isn't surprising as cleavage products of triglyceride hydrolysis are interfacial active substances thus tending to adsorb on hydrophobic surfaces [14]. After thoroughly washing the surfaces of the lipid implants with water the spectra shifted towards the normal triglyceride spectra. This finding indicates a reversible adsorption process of the fatty acids at the lipid water interface. The PLS models constructed from the IR spectra and Raman spectra of the D112 and lauric acid mixtures both involved two PLS factors. The model calibration and validation results are shown in Table 1. Based on these models, the incubated samples analysed by infrared spectroscopy contained a mean of $9.4 \% \pm 0.4 \%$ (w/w) lauric acid, while those analysed by Raman spectroscopy contained $14.8 \pm 0.8 \%$ (w/w) lauric acid. The incubation conditions and times were different for the samples analysed by the two techniques since both techniques require different amounts of sample and the procedure of analysis is different, and so the results should not be directly compared.

However, both results suggest that there is a significant amount of lauric acid production in the core of D112 tablets that are incubated in lipase solutions for several hours.

Table 1: PLS model calibration and validation results from infrared and Raman spectra

Model parameters		Infrared	Raman
Calibration	R ²	0.99	0.95
	RMSEC	2.02% (w/w)	3.96 % (w/w)
Cross-validation	R ²	0.91	0.83
	RMSECV	6.44% (w/w)	8.75 % (w/w)

Depth profiling of D118, D116 and D114 implants within a depth range of 10 to 100 μm below the surface revealed no changes in the spectra of the triglycerides (data not shown). Thus it can be stated that for D118, D116 and D114, according to literature [15] degradation is strictly happening on the lipid surface. However lipid cleavage through adsorbed lipase can lead to pores in the lipid matrix aggravating the diffusion of the cleavage products into the surrounding media.

Erosion analysis

In parallel to degradation, erosion of the D112 tablets during the incubation in lipase solution was also observed. The incubation time (8h) and lipase activity (440U/5ml) were adjusted to avoid complete melting of the lipid tablet. Soon after the incubation was started, suspended lipid particles were visible in the buffer media, indicating erosion. As the used analytical method is highly sensitive towards FFA and shows almost no reactivity towards triglycerides strict quantification of the degradation products could be ensured. Interestingly, both processes show linear behaviour for the period of analysis. As seen in Fig., 3 a after 8 hours a lipid degradation of only 2 % was reached. Erosion of the implant, i.e. the mass loss from the initial implant weight was about 12%. This imbalance of erosion and degradation processes can be explained as a bulk erosion process with degradation occurring not only at the lipid surface but also at lipid water interfaces within the lipid matrix. At the end of the experiment the implants showed a distinct swelling behaviour of 4% (Fig. 3b). This may be due to softening and melting of the lipid leading to an increased diffusivity of water into the matrices. This phenomenon is supported by the DSC described below. Water influx presumably is also supported by the generation of pores and the accumulation of cleavage products such as mono- or diglycerides in the inner part of the lipid tablet.

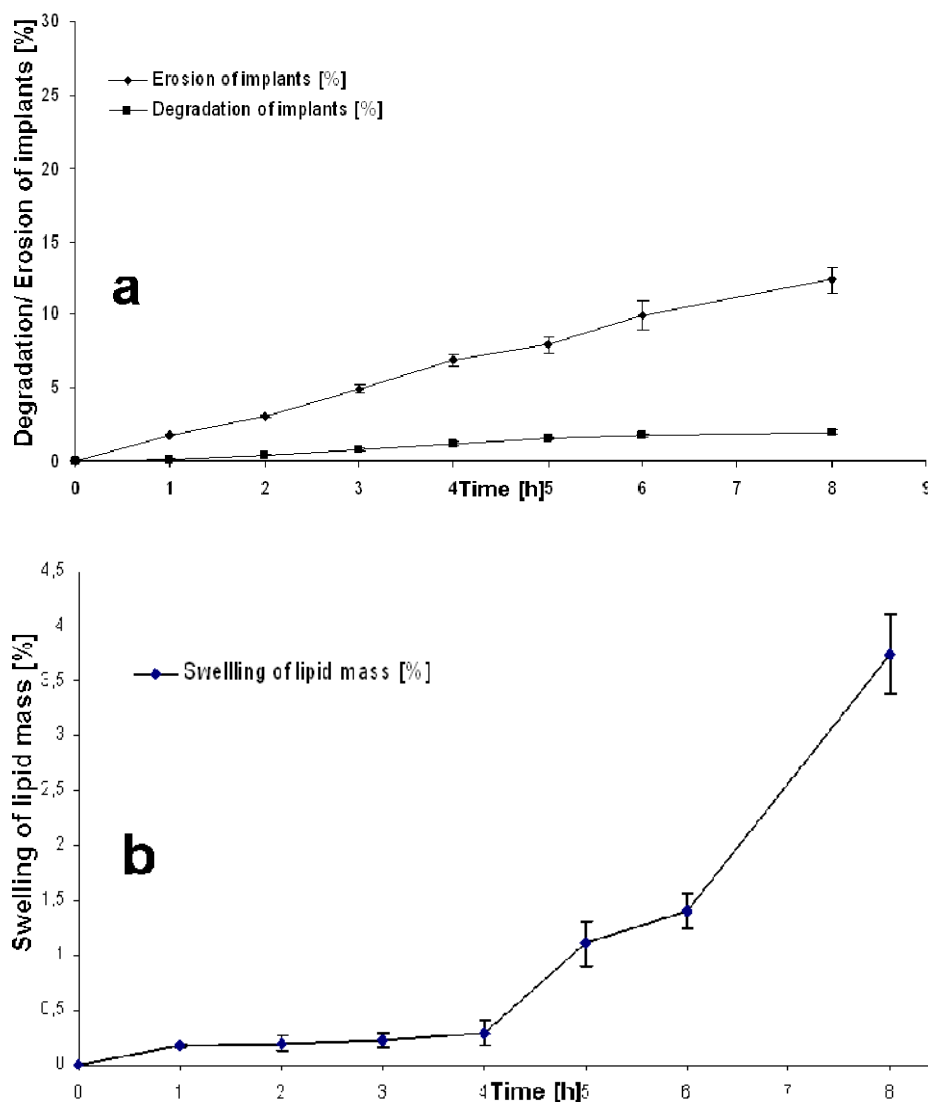


Figure 3: a) Erosion study of D112 tablets incubated for 8 h in 440 U lipoprotein lipase (Average + S.D., n = 3). b) Swelling behaviour of the incubated D112 tablets (Average + S.D., n = 3).

In situ Raman analysis

Raman spectra were recorded of the layered tablet with 300 μm D112 over D118 during stirring in flowing lipase solution. The MCR analysis provides a semi-quantitative analysis of the presence D112 and D118 within the tablet that was sampled by the Raman spectrometer. Within the same spectral region, the estimated spectra of D112 and D118 (Figure 4) are closely related to the spectra of the pure components (Figure 4). As the D112 was degraded over time due to the activity of the lipase, the layer thickness was constantly decreasing leading to a shift of the spectral bands towards the bands of the D118 tablet basis. According to the semi quantitative analysis, the sample is initially almost exclusively D112, and then the D112 content reduces with a simultaneous increase in D118 content. After approximately 800 min the sample is predominantly D118 and this remains unchanged during the remainder of the experiment. Since the D118 was initially underneath the D112, it appears that the D112

(together with lauric acid formed) eroded at a relatively steady rate to leave the D118 exposed.

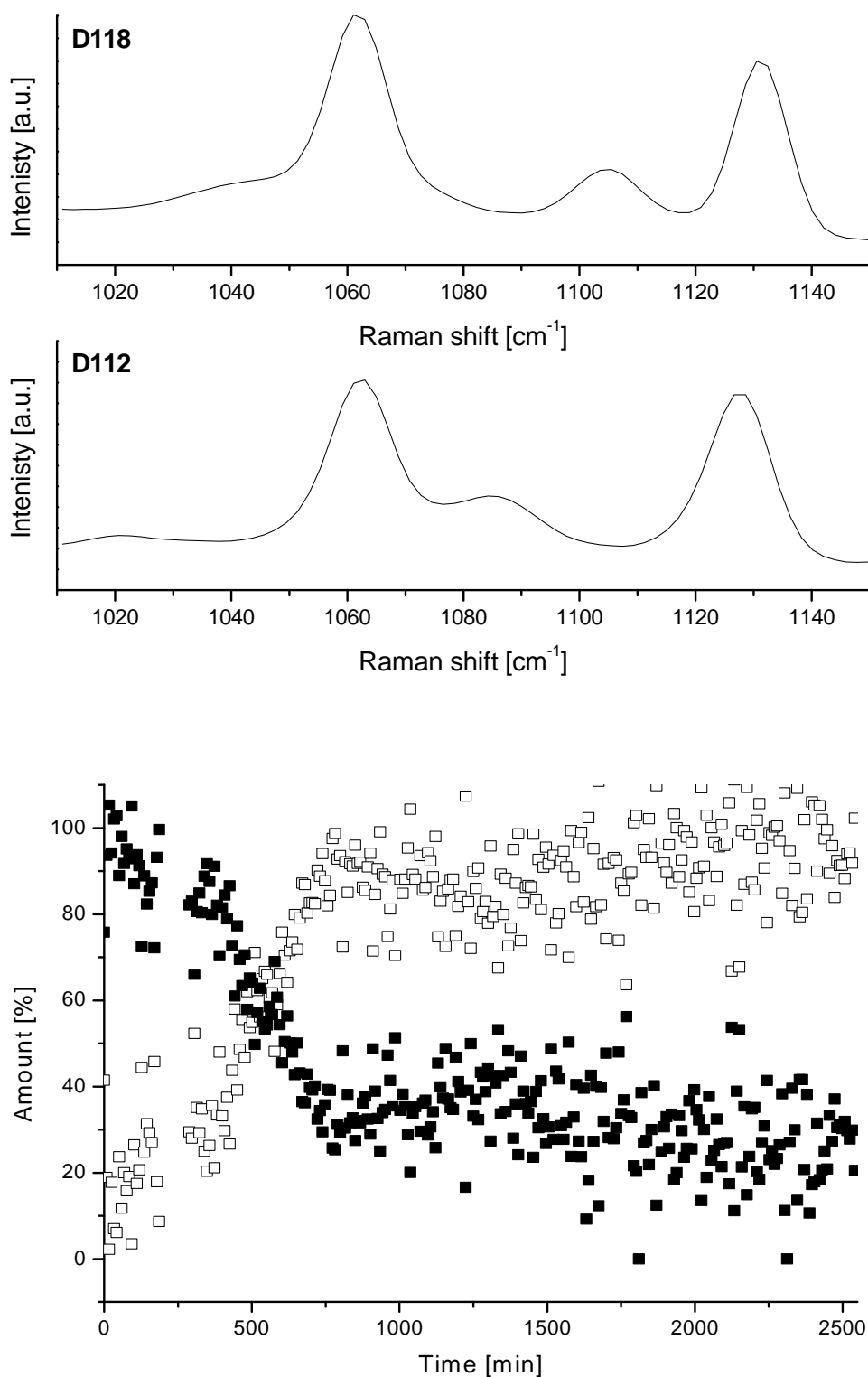


Figure 4: MCR analysis of tablet with D112 layer over D118 with estimated spectra of the two components (above) and predicted amount of D112 (black squares) and D118 (white squares) during immersion in lipase solution at 37 °C (below)

DSC Measurements

DSC measurements were conducted to measure changes in lipid composition before and after lipase incubation studies. Implants consisting of pure lipid components (D118, D116, and D114) showed no changes in the melting temperatures after lipase incubation (data not shown). As seen in Fig. 5 tablets prepared from powder mixtures of D118 and D112 (80:20) exhibited an almost complete loss of the D112 in the tablet after lipase incubation compared to the untreated tablet.

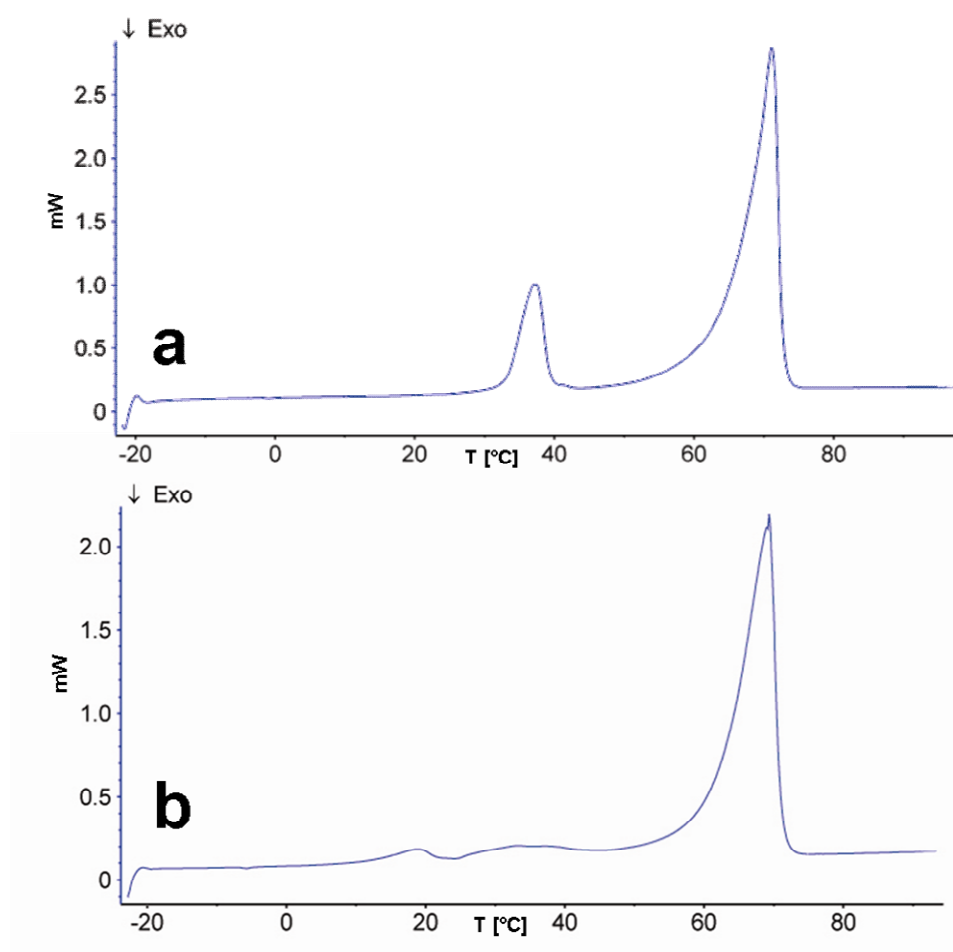


Figure 5: DSC thermograms of compressed lipid tablets prepared from powder (D118/D112 mixture ration 80:20) before (a) and after lipase incubation (b).

As already described above, lipase incubation lead to the formation of a porous coat enclosing a core consisting of the intact lipid material. While the core material did not exhibit changes in the melting temperature (Fig 6a), a distinctive shift in the melting temperature for the coating material revealed a melting process starting at approx, 20°C (Fig. 6b).

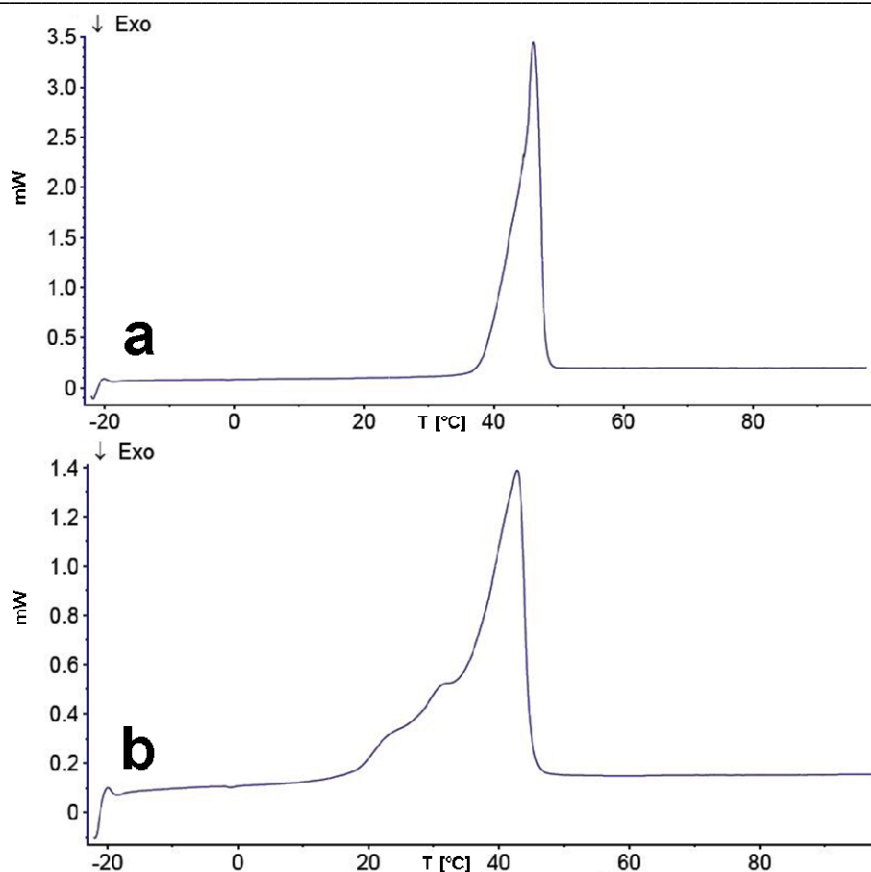


Figure 6: DSC thermograms of D112 tablet before (a) and after (b) incubation in lipase solution.

The thermograms indicate a shift of the D112 melting endotherm in combination with a decreasing melting enthalpy indicating the presence of less crystalline phases. Such behaviour has been described with lipid erosion processes [1]. The change in lipid crystallinity presumably can be explained by the accumulation of mixtures of triglyceride and corresponding degradation products in the porous coat material. This mixture of trilaurate, lauric acid and mono- or glyceryldilaurate-esters produced during the lipid cleavage probably exhibit a lower melting point compared to the pure triglyceride. To simulate the production of FFA and to elucidate their effect on the melting temperature of D112, mixtures of lauric acid and trilaurate were analyzed using DSC. The melting point decreased as the lauric acid content increased. As seen in Fig. 7, 1% lauric acid in D112 leads to a distinct shift of the melting point compared to the pure D112. However admixing 20% lauric acid in D112 seems to be sufficient to lower the melting temperature of this mixture beneath the level of the human body temperature.

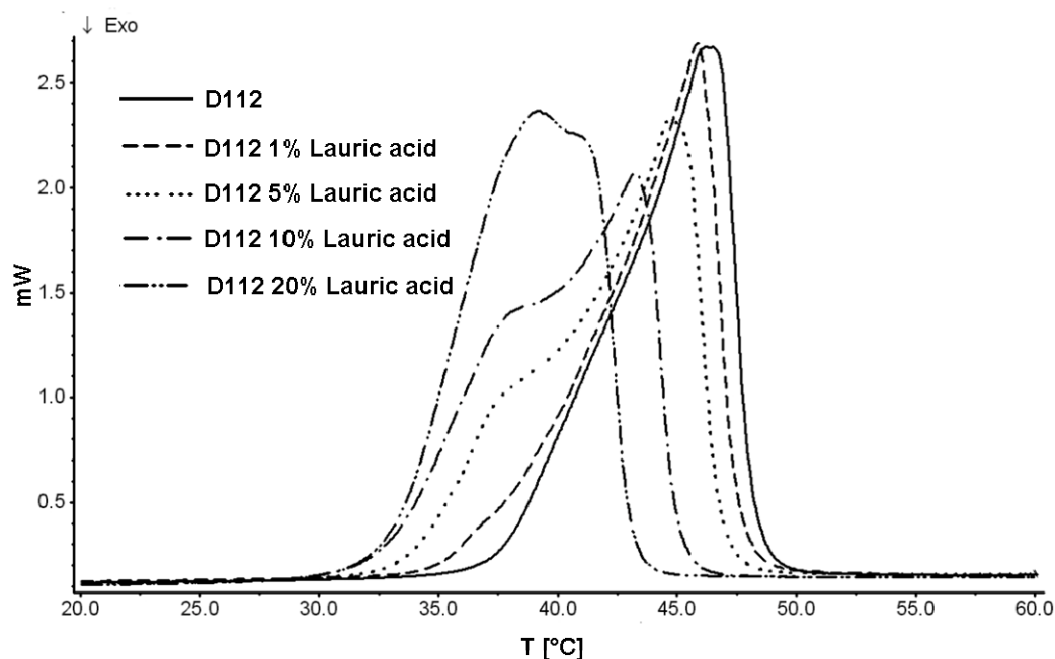


Figure 7: DSC thermograms of D112 and D112/lauric acid mixtures.

This finding may explain the high degradation velocity of the pure component D112 up to a certain point. As the presence of lauric acid within the lipid matrix leads to a shift in the melting temperature, eventually the whole implant melts although still consisting of triglycerides for the most part. This melting process leads to a generation of fatty droplets in the buffer media and therefore to a higher surface area.

Scanning electron microscopy analysis

SEM of tablets consisting of mixtures of D118 and D112 (80:20) convey the effect of rapid trilaurate degradation as observed in the above described degradation study. After incubating trilaurate, cleavage leads to a significant change in the structure of these systems. As seen in Fig. 8a microscopic pictures of the compressed lipid disc exhibit a smooth surface and no visible signs inhomogeneity. After incubation with 100 U of lipase for 2 h the implant morphology changed drastically. Pore formation was detected in the matrix of this tablet, probably due to the degradation of the entrapped D112. The resulting porous lipid matrix was crossed by numerous cracks, indicating a swelling of the D112 component upon erosion (Fig. 8b). Scanning electron microscopy of the D112 implants treated with lipase solution revealed noticeable changes in the implant surface morphology. As shown in Fig 8d the surface of the implants shows significant signs of degradation i.e. the formation of a rough and porous surface. When examining the cross section of incubated D112 tablets (Fig 8c) a clear distinction could be made between the porous coat and the dense core of the tablet.

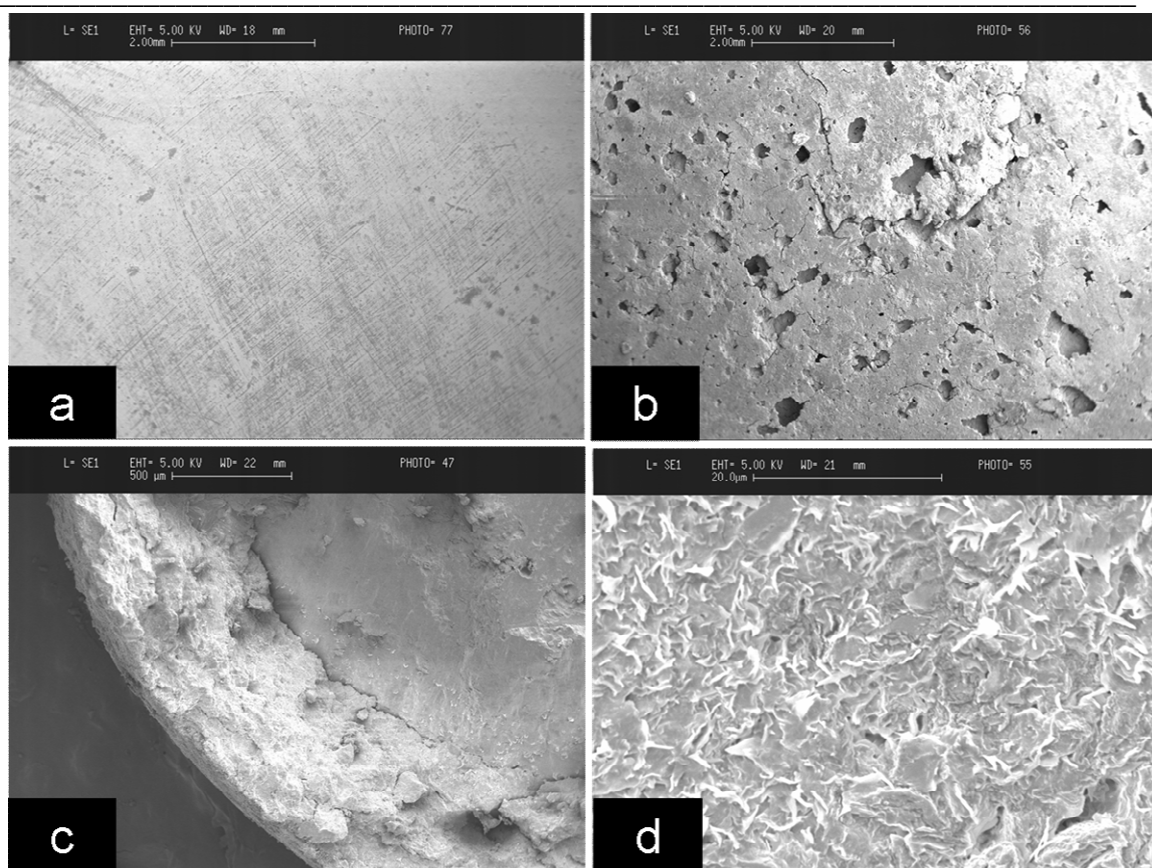


Figure 8: scanning electron microscopy: compressed lipid tablet prepared from powder (D118/D112 mixture ratio 80:20) before (a) lipase incubation (15X magnification). Tablet after lipase incubation (b) (15X magnification). (c) D112 implant after lipase incubation: cross section (15X magnification). (d) D112 implant after lipase incubation: porous implant surface (2000X magnification)

Digital microscopy

The lipid tablets incubated during the erosion and degradation study showed distinct changes in surface morphology after lipase treatment. As a result of the detected erosion processes pores and rough areas appeared on the formerly smooth tablet surface. The edges of the tablets lost their sharpness and eventually the tablet lost its biplane form and showed convex morphology. When analyzing the cross section of the tablets an increase in thickness of the porous layer was observed over time. After 8 hours a separation of the outer layer from the core was visible (Fig. 9). Probably the interface between the two lipid layers was filled with water and water pressure forced the layers apart.

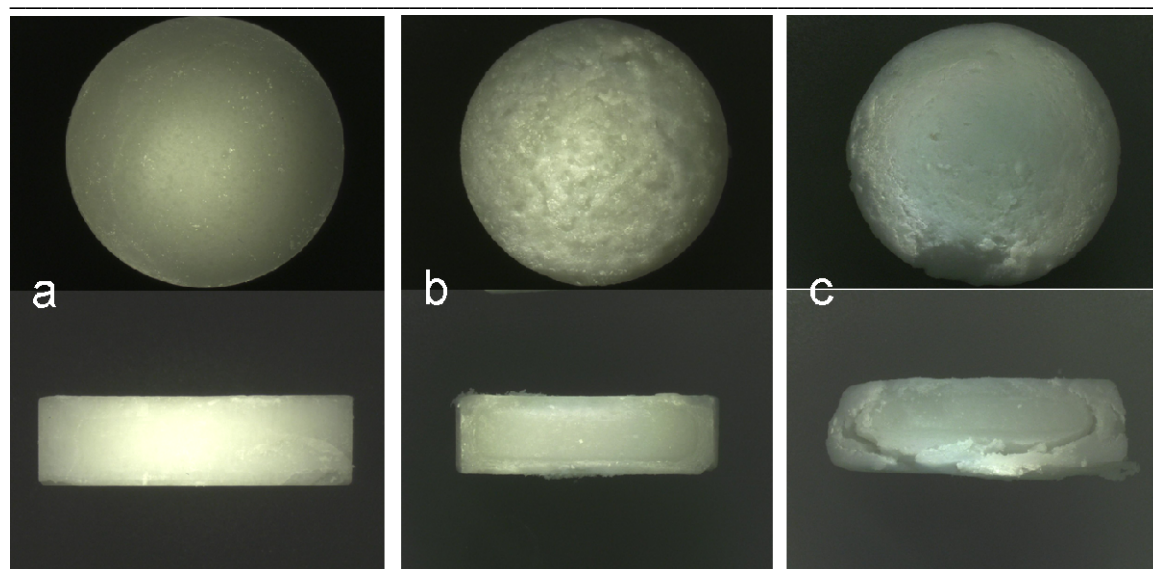


Figure 9: Digital microscopy: Overview and cross sections of D112 tablets (a) before lipase incubation, (b) after 3 hours of lipase incubation, (c) after 8 hours of incubation. All pictures with 20X magnification.

Conclusion

Glyceryltrilaurate (D112) was shown to possess degradation characteristics making it suitable for the preparation of biodegradable and bioerodible drug carrier systems. While other triglycerides like glyceryl tristearate – used for the preparation of lipid based drug delivery systems – didn't show detectable signs of degradation *in vivo*, D112 may fulfil all needs required to prepare fully biodegradable depot systems. In our *in vitro* degradation studies, glyceryltrilaurate showed an almost twenty-fold higher degradation rate than other comparable triglycerides. This high degradation rate could be explained by an increase in lipid surface due to the generation of lipid droplets as a direct consequence of a specific melting process. Glyceryltrilaurate starts to melt after incubation with lipase as degradation products and primordial trilaurate form mixtures with a melting point beneath the body temperature. During degradation, even more pronounced erosion processes occur, leading to distinct loss of lipid mass associated with the generation of small lipid particles before the total lipid mass has melted. It could be shown that the lipid matrix collapse we observed in earlier experiments is a direct consequence of the properties of glyceryltrilaurate used for the preparation of lipid based extruded implants. Upon erosion glyceryltrilaurate starts to swell due to an influx of water into the porous lipid matrix. This swelling process damages the structure of lipid mixtures consisting of glyceryltrilaurate and other triglycerides and the subsequent melting of the trilaurate leads to the generation of a porous network within such lipid matrices. Depending on the mixture ratio and the preparation technique systems these damaged systems disintegrate. Therefore we propose that the use of glyceryltrilaurate in mixture with other triglycerides may allow the custom made design of depot devices with predictable and controllable degradation and erosion properties.

References

1. Guse, C., et al., *Biocompatibility and erosion behavior of implants made of triglycerides and blends with cholesterol and phospholipids*. International Journal of Pharmaceutics, 2006. 314(2): p. 153-160.
2. Schwab, M., et al., *Correlation of in vivo and in vitro release data for rh-INF[alpha] lipid implants*. European Journal of Pharmaceutics and Biopharmaceutics, 2008. 70(2): p. 690-694.
3. Déléris, G. and C. Petibois, *Applications of FT-IR spectrometry to plasma contents analysis and monitoring*. Vibrational Spectroscopy, 2003. 32(1): p. 129-136.
4. Bresson, S., M.E. Marssi, and B. Khelifa, *Raman spectroscopy investigation of various saturated monoacid triglycerides*. Chemistry and Physics of Lipids, 2005. 134(2): p. 119-129.
5. Bresson, S., M. El Marssi, and B. Khelifa, *Conformational influences of the polymorphic forms on the CO and C-H stretching modes of five saturated monoacid triglycerides studied by Raman spectroscopy at various temperatures*. Vibrational Spectroscopy, 2006. 40(2): p. 263-269.
6. Kohler, K., et al., *Characterization of a Novel Class II bHLH Transcription Factor from the Black Widow Spider, Latrodectus hesperus, with Silk-Gland Restricted Patterns of Expression*. DNA and Cell Biology, 2005. 24(6): p. 371-380.
7. Dole, V.P.M., Hans., *Microdetermination of long-chain fatty acids in plasma and tissues*. . Journal of Biological Chemistry 1960. 235: p. 2595-2599.
8. Wood, R. and T. Lee, *High-performance liquid chromatography of fatty acids: quantitative analysis of saturated, monoenoic, polyenoic and geometrical isomers*. Journal of Chromatography A, 1983. 254: p. 237-246.
9. Sriamornsak, P., N. Thirawong, and K. Korkerd, *Swelling, erosion and release behavior of alginate-based matrix tablets*. European Journal of Pharmaceutics and Biopharmaceutics, 2007. 66(3): p. 435-450.
10. Olbrich, C., O. Kayser, and R.H. Müller, *Lipase degradation of Dynasan 114 and 116 solid lipid nanoparticles (SLN)--effect of surfactants, storage time and crystallinity*. International Journal of Pharmaceutics, 2002. 237(1-2): p. 119-128.
11. Birnbaum, M.J., *Lipolysis: more than just a lipase*. J. Cell Biol., 2003. 161(6): p. 1011-1012.

12. Brzozowski, A.M., et al., *A model for interfacial activation in lipases from the structure of a fungal lipase-inhibitor complex*. *Nature*, 1991. 351(6326): p. 491-494.
13. Maruyama, T., et al., *Oil-water interfacial activation of lipase for interesterification of triglyceride and fatty acid*. *Journal of the American Oil Chemists' Society*, 2000. 77(11): p. 1121-1127.
14. Reis, P., et al., *Competition between Lipases and Monoglycerides at Interfaces*. *Langmuir*, 2008. 24(14): p. 7400-7407.
15. Reis, P., et al., *Lipases at Interfaces: Unique Interfacial Properties as Globular Proteins*. *Langmuir*, 2008. 24(13): p. 6812-6819.

3.3. Discussion of the results of the degradation experiments

In the previous parts of this dissertation the effects of the enzymes on the lipid depot systems were always expected to be of chemical nature. It was expected that – due to their physico-chemical nature – the enzymes would attach on the lipid surface and slowly cleave the ester bonds of the outer lipid layer. It was therefore anticipated that degradation processes would occur in a classical surface eroding way. When starting with the work on these experiments the author didn't estimate the impact of the lipase incubation to be different from other surface-eroding systems described in literature except for the presence of the lipases. After examination of the first results the perception slowly arises that some other factors yet unregarded may play a greater part in the processes occurring at the lipid-lipase interface. The results of the experiments described in the first part of this chapter quickly lead to the realization that the influence of the chain length of the employed fatty acids has a big influence on the physical integrity of the lipid depot systems. This newly gained knowledge and the complete clarification of the underlying mechanism is one major milestone on the way of developing lipid depot systems with custom made degradation properties. Of course, at this point one should keep in mind that all the findings of the described experiment were produced in an artificial system which was strictly reduced to most necessary parameters. In that way it's self evident that it is impossible to predict if the prepared lipid depot systems would act similar in a natural environment, i.e. when incubated into a living organism. However, as already highlighted in the previous sections of this dissertation this discrepancy between the isolated in vitro system and the unpredictable and hardly reproducible surrounding of an in vivo experiment has always to be taken into account. Viewed from another point of view, this set of data gives the opportunity to compare the results from in vivo and in vitro experiments and to subsequently adjust and affect the prepared drug depot systems. Surely, the next step in the development and analysis of lipid drug depot systems will be to test the most promising formulations of the presented systems in vivo and compare and correlate the results gained from this animal experiment to the data produced so far in vitro. But before dealing with such issues the question whether the preparation method has a big influence on the degradation method is still open and therefore has to be dealt with. Currently, there are two main methods of preparing lipid drug depot systems: the discontinuous method of compressing the lipid mass via various compression tools and the continuous method of extrudating the lipid mass using a suitable thermo extruder. In the final section of this chapter both preparation techniques are compared with regards to their effect on the degradation properties.

3.4. Further studies on lipid drug depot degradation

In the first part of this chapter it was shown, that the rapid degradation of D112 in the presence of lipases is a consequence of the generation of fatty acid/triglyceride mixtures exhibiting a melting point beneath the human body temperature. Since the employed RP-HPLC described in the previous chapter is capable of separating and quantifying the FFA-components of all triglycerides used in the described experiments, characterization of the degradation behaviour of depot systems consisting of different triglycerides is possible. Therefore, in this section, the degradation of an extruded lipid implant is investigated with respect to the amount and the ratio of different FFA released over the time of lipase incubation. Scanning electron microscopy was used to characterize the changes in extrudate morphology occurring during the incubation. In addition to that, an experiment dealing with the comparison of the degradation behaviour of extruded implants and compressed implants with the same surface area is presented. As shown in the previous sections the surface area has a great influence on the degradation of lipid based depot systems, since the employed enzymes have to adsorb on the lipid surface in order to start lipid cleavage. As a consequence of their manufacturing process extruded implants exhibit a rod-shaped, cylindrical form, whereas compressed implants show a more tablet-like shape. It is understood that both systems are different concerning their surface area and thus these differences should be taken in account when comparing their degradation behaviour. Therefore, compressed implants with a similar surface area were prepared in order to compare the degradation of these two systems.

Materials and methods

Implant manufacturing

Implants were prepared by using a 5 ton hydraulic press (Maassen, Eningen, Germany). The implant components - tristearin powder 80% (D118) and H12 powder- were ground in an agate mortar after thoroughly cooling with liquid nitrogen. The resulting mixture was compressed with a pressure of 2 tons for 30 seconds. The obtained implants had a diameter of 5 mm and a height of 7 mm. The dimensions of the prepared implants were measured with a digital caliper. According to the dimensions of the implants the surface area was calculated to be 1.49 cm².

Extrudate preparation

The extrudated implants were prepared as described in chapter 2 using a Thermo Haake MiniLab microcompounder (Thermo Fisher Scientific, Inc. Waltham, U.S.A.). The prepared extrudates used for the study consisted of 80% D118 and 20% H12. The produced lipid extrudates had a diameter of 1.45 mm and were cut to a length of 32 mm in order to obtain the same surface area as the implants described above.

Scanning Electron Microscopy (SEM)

Samples were analyzed using a Field Emission Scanning Electron Microscope Joel JSM-6500F (Joel Inc., Peabody, USA). The samples were put on adhesive carbon tape (BAL-TEC AG, Balzers, Principality of Liechtenstein) and attached to a custom made brass stub, carbon-sputtered and analyzed.

HPLC analysis

The samples withdrawn from the various degradation experiments were treated and analyzed as explicitly described in chapter 2 and 3. Release of the different FFA was analyzed and the obtained FFA release was compared to the theoretical values.

Experimental setup

Implants and extrudates with the same surface area were incubated in 2ml PBS pH 7.4 containing 100U lipoprotein lipase from *pseudomonas sp.* After 3 days of incubation the buffer media was replenished. FFA were isolated from the drawn samples and, after derivatization, analyzed. Another set of extrudates was treated in the same manner after 1, 15 and 30 days samples were drawn and analyzed with SEM. All experiments were run in triplicate.

Results and discussion

Surface area

Analysis of the tested implants and extrudates exhibiting the same surface area revealed that both systems exhibit the same degree of degradation at least for the first days of incubation as seen in Fig. 1.

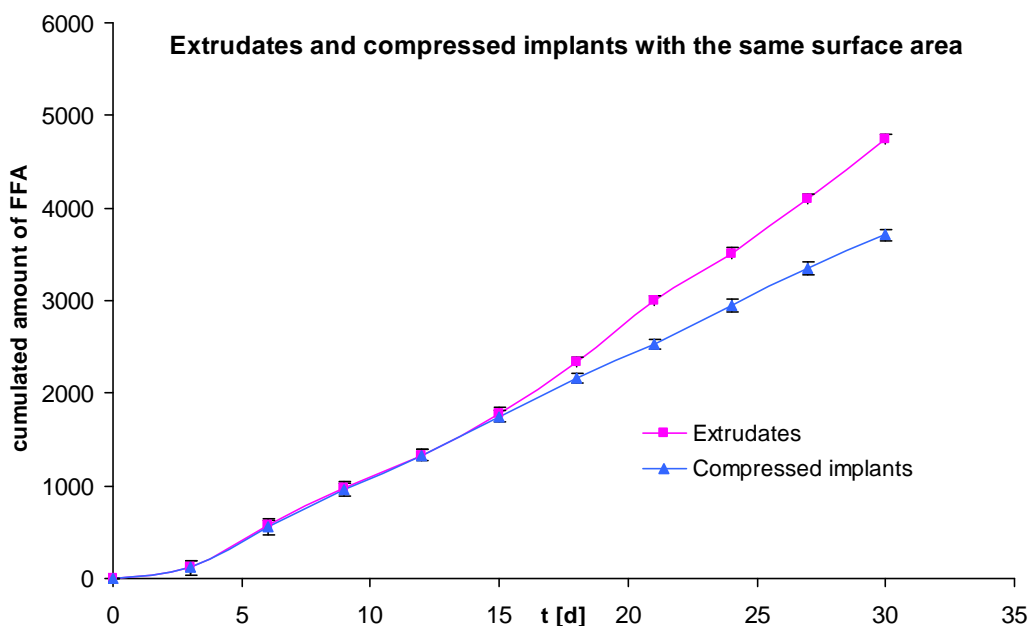


Figure 1: Implants and extrudates with a surface area of 1.49 cm^2 incubated in lipase containing buffer (Average + S.D., $n = 3$).

After day 15 the lipid structure of the extrudate collapsed resulting in different degradation behaviour (Fig.2). Presumably due to the preparation process and its dimensions the compressed implant maintained its structure and showed no signs of structural damage

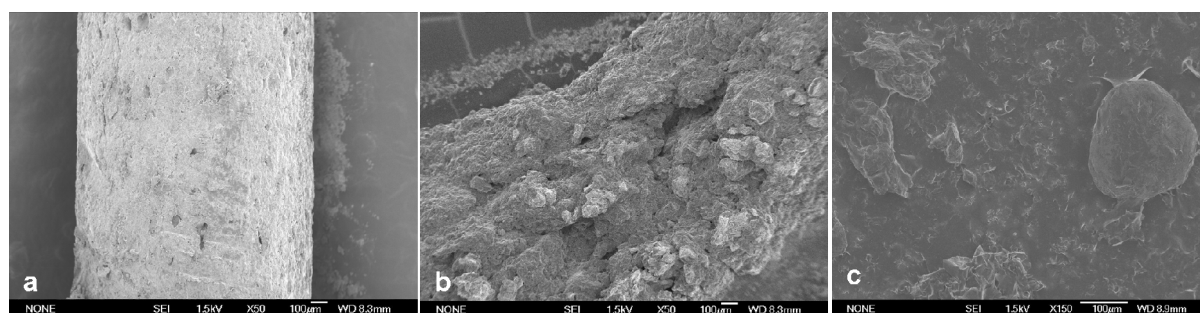


Figure 2: SEM pictures of an extruded lipid implant incubated for different periods of time in lipase solution. a) extruded lipid implant incubated for 1 day (50X magnification) b) lipid extrudate after 15 days of lipase incubation: loss of structural integrity (50X magnification) c) fragments derived from the lipid matrix collapse of the extruded implants, drawn after 30 days of incubation (50X magnification)

However after 30 days of incubation the surface of the compressed implant showed distinct signs of degradation in addition to that the diameter and length of the implant was significantly reduced. As seen in Fig.3 porous regions were visible when examining the implant with scanning electron microscopy. Presumably these porous regions are a consequence of the rapid degradation of the contained H12 component.

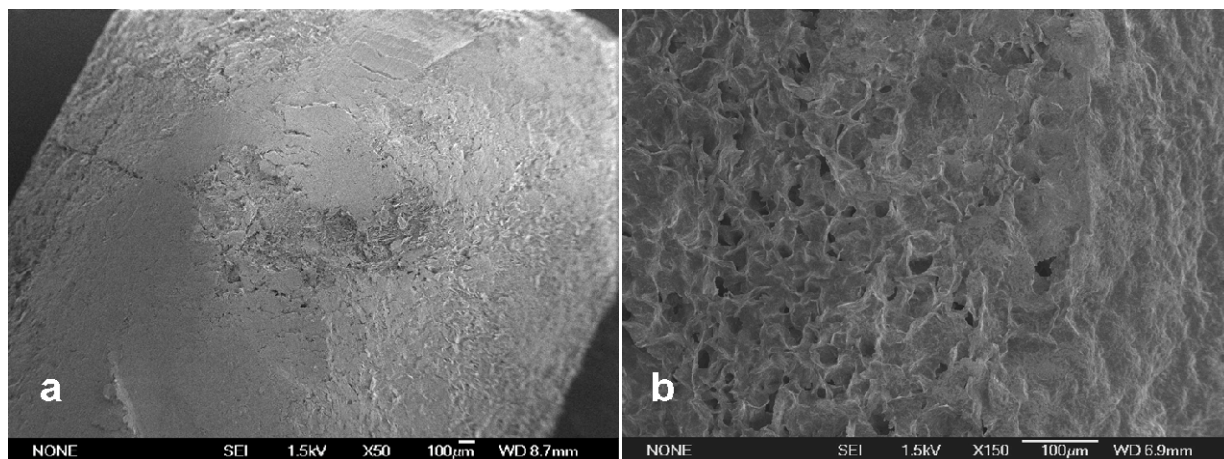


Figure 3: SEM photographs of the compressed implant incubated in lipase solution. a) Overview (50X magnification) b) porous area on the implant surface (150X magnification)

As a result it can be concluded that, concerning the first 15 days, manufacturing technique has no major influence on the degradation of lipid based drug delivery systems. Although a pressure of 2 tons was applied during the preparation of the compressed implants these systems showed no difference in the degradation rate compared to depot systems prepared by twin screw extrusion. Nevertheless the preparation technique especially the application of high pressure seems to stabilize the lipid matrix. As the detected lipid matrix collapse is highly desirable with regard to bioerosion processes the so far observed stability of the compressed lipid matrix would interfere with the requirement for bioerodible drug depot systems.

HPLC-Analysis of extrudate degradation

Free fatty acids (FFA) generated during the degradation of lipid extrudate formulation E1 (80:20 D118/H12) were separated and quantified with RP-HPLC as seen in Fig. 4.

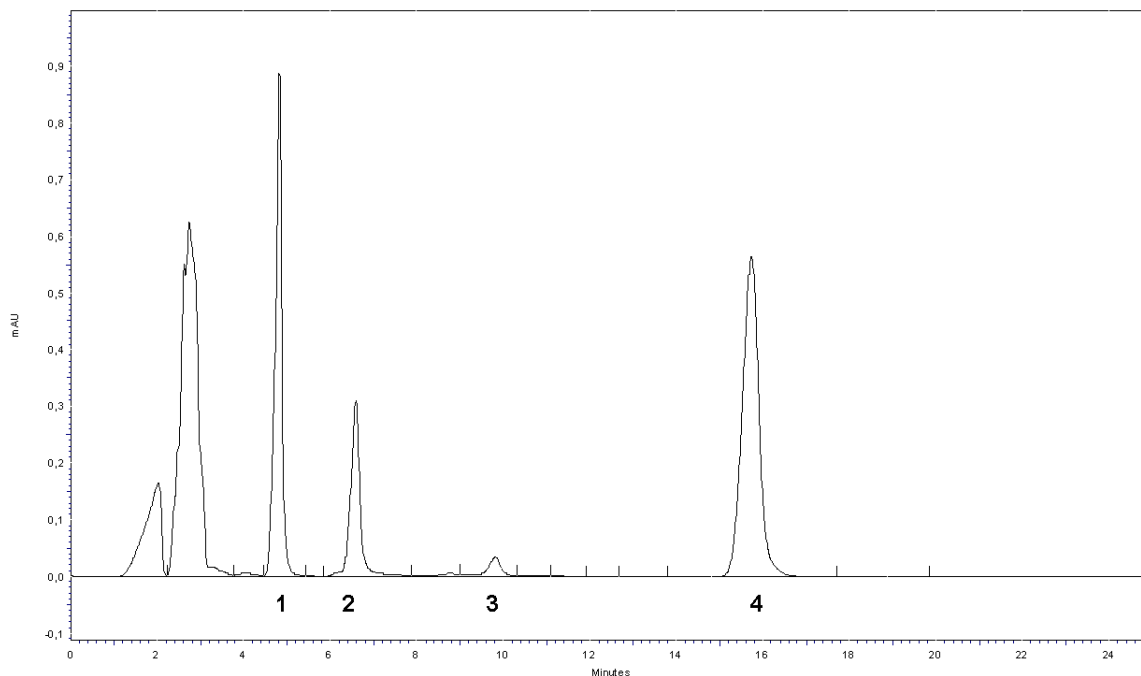


Figure 4: HPLC chromatogram of an extrudate degradation study. 1) lauric acid 2)myristic acid 3) palmitic acid 4) stearic acid.

After the first 3 days of incubation it was found that the release of lauric acid and myristic acid was almost 2 times higher than theoretically expected whereas the release of the stearic acid, i.e. the corresponding fatty acid of the main component, was significantly below the expected level (Fig. 5).

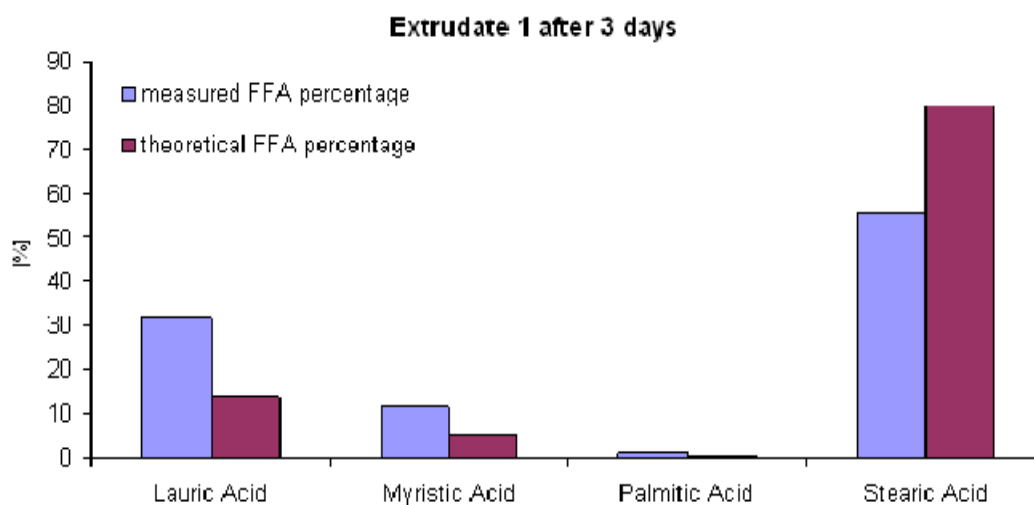


Figure 5: Theoretical and experimentally obtained FFA values after 3 days of lipase incubation

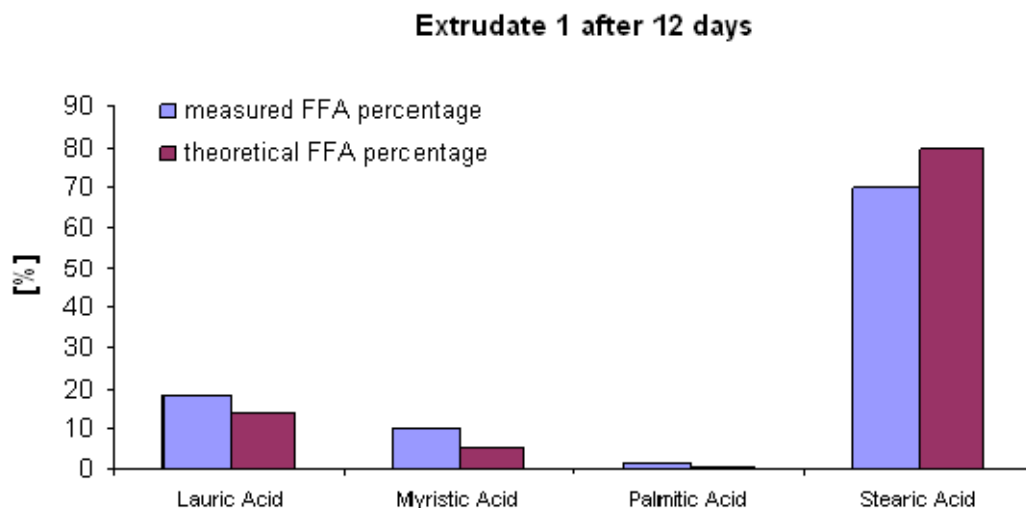


Figure 6: Theoretical and experimentally obtained FFA values after 12 days of lipase incubation

After 12 days of lipase incubation the amount of low melting fatty acids released from the extrudate was decreased, however it was still on a slightly higher level than theoretically expected (Fig. 6). According to this finding the release of stearic acid was increased and almost reaching the theoretical level. This decrease in low melting fatty acids indicates a depletion of H12 in the outer areas of the extrudate since the H12 erodes quickly as seen in the experiments described in the previous sections of this chapter. This decreasing trend for low melting fatty acids was continued regarding the FFA release data of day 30 (Fig. 7). Lauric acid release was decreased by two thirds of the theoretical level, whereas myristic acid release was still slightly increased. Concerning the release of stearic acid from the incubated extrudate the obtained values were almost identical to the theoretically expected values. Once again, these findings are in accordance to the results of 3.2 indicating a quick and preferential cleavage of the low melting component H12 -consisting mainly of triglycerides esterified with lauric acid – and a subsequent constant release of the main component stearic acid.

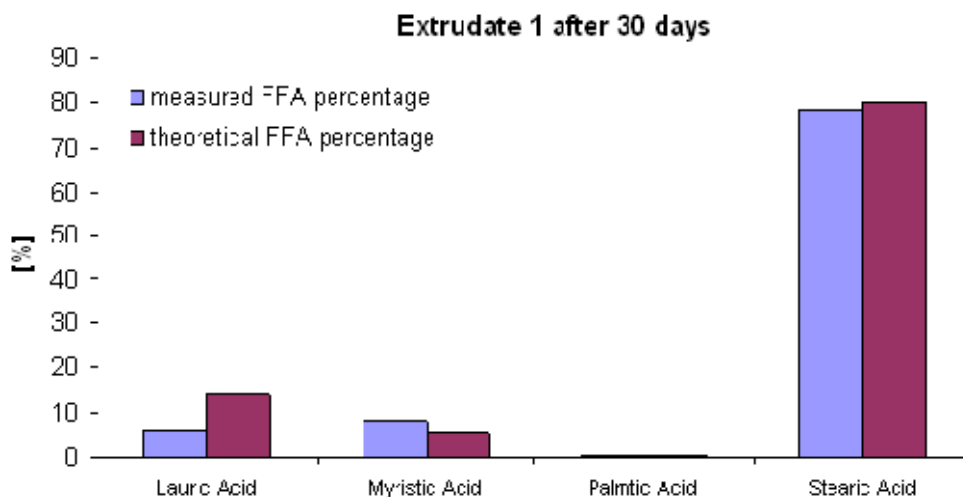


Figure 7: Theoretical and experimentally obtained FFA values after 30 days of lipase incubation

Conclusion

It was shown that the degradation of lipid based drug delivery systems isn't affected significantly by the preparation method of the lipid depot systems. In short, depot systems with a similar surface area exhibit similar degradation rates. However, as a consequence of the applied high pressure when using the hydraulic press as production method, compressed implants maintain their structure and show only minor changes in morphology upon degradation. Therefore since lipid matrix collapse is desirable extrusion methods should be chosen in order to obtain erodible drug depot systems. In addition to that the presented results of RP-HPLC analysis clearly show that the phenomenon of lipid matrix breakdown of certain extrudates – proposed in chapter 3- is a direct consequence of the heterogeneous FFA release during lipase incubation. Firstly, lauric acid release is high, leading to the formation of lauric acid/triglyceride mixtures which promote the erosion of the lipid matrix, then, after this initial phase, the lipid matrix is depleted on lauric acid and D118 degradation is mainly occurring.

4. Chapter Four: Investigations on spider silk proteins

4.1. Introduction

The following sections are dedicated to a material which is well-known to mankind since hundreds of years but relatively new to the science community and the scientific investigation of this material has only started some 10 years ago: spider silk proteins. Especially silk proteins from other organisms like the silk worm *bombyx mori* are used since centuries for clothing and many other purposes probably due to the fact that the silk worms can be easily bred and the harvest of the silk is relatively easy. In contrast to that, spider silk proteins have always been more precious since the cobweb exhibits only a very small amount of this flimsy material. Today the situation is somewhat similar. While silk worm silk is still easily available and cheap, spider silk still needs to be collected from the living spider which is a tricky undertaking as these animals show a distinct territorial behaviour and therefore must be held in solitary confinement. Normally such circumstances would influence the use and disposability of these materials in a way that, subsequently the interest on spider silk proteins and their use in science would fade away. However, since silk proteins from *bombyx mori* contain compounds which can lead to inflammation and immunogenic reactions, whereas spider silk doesn't exhibit such negative features, the interest on spider silk is still unquenched. With the rise of modern genetic engineering, finally the obstacle of harvesting the spider silk proteins from living spiders was overcome. Today it is possible to produce batch wise several hundred grams of this material in high quality and pureness. Eventually, the investigation on spider silk proteins for their use in pharmaceutical technology, i.e. their employment in the development of parenteral drug depot systems has started. The following sections detailedly describe the characterisation of this genetically engineered material, the preparation of spider silk proteins micro and nanospheres and finally the performance of these particles with regards to drug loading and drug release in in-vitro experiments. This fourth chapter is divided in two parts: the first part consists of a set of data already published and deals with the reproducible and controlled preparation of spider silk particles usable as parenteral drug carriers, the second part of this chapter is understood as a little discussion of the presented data and serves as transition to the next chapter which is dedicated different drug release experiments.

4.2. Processing conditions for the formation of spider silk microspheres

Andreas Lammel^{1*}, Martin Schwab^{2*}, Ute Slotta¹, Gerhard Winter² and Thomas Scheibel³

¹Lehrstuhl Biotechnologie, Lichtenbergstraße 4, Technische Universität München, D-85747 Garching, Germany

²Department of Pharmacy, Pharmaceutical Technology and Biopharmaceutics, Ludwig-Maximilians-Universität, D-81377 Munich, Germany

³Lehrstuhl Biomaterialien, Universitätsstraße 30, Universität Bayreuth, D-95440 Bayreuth, Germany

* These Authors contributed equally to that work

Published in: Journal of Chemistry and Sustainability, ChemSusChem, Vol. 1(5), May, 2008

Abstract

Spider silk is a material consisting of very large (>200 kDa) proteins and has a high potential for biomedical applications as a result of its biocompatibility and biodegradability. We report on the influence of physicochemical factors on structure formation of the engineered spider silk protein eADF4 (C16), which mimics the known sequence of the dragline protein ADF4 from the spider *Araneus diadematus*. Under certain experimental conditions, eADF4 (C16) forms stable microspheres that have been analyzed with respect to sphere size, size distribution, and surface inertness upon different preparation methods (dialysis, pipette and micromixing). As a result of their material strength, biocompatibility, and the possibility of functionalization, spider silk microspheres have a high potential for the development of targeted drug-delivery systems.

Key words: spider silk proteins, micro particles, biodegradation, preparation method

Introduction

Numerous biopolymers have been optimized over millions of years during evolution with respect to distinct applications. For instance spider silk exhibits a combination of extraordinary mechanical and chemical properties due to a high strength and resistance required for function as a trap for prey. Spider silk is a material consisting of very large proteins (> 200 kDa) with unique structural stability, mechanical toughness and elasticity which even exceeds the mechanical properties of Kevlar, one of the most stable and toughest synthetic fibers [1, 2]. Along with their biocompatibility and biodegradability, silk materials have a high potential for biomedical applications [3,4]. Especially in the area of new innovative and effective drug delivery systems spider silk proteins are very well suited because of their possible functionalization and coupling of active agents [5]. Spider silk proteins are very well suited to develop and create morphologies that can meet the demanding requirements of specificity and efficiency for the delivery of active ingredients such as drugs and pharmaceutical proteins [6, 7]. Conformational conversion of spider silk proteins can be triggered by potassium phosphate which is an important issue regarding the biocompatibility of the drug delivery device considering not only the material but also its processing [8-11]. Here we report on the influence of physicochemical factors on structure formation of engineered spider silk protein eADF4 (C16), mimicking the known sequence of the dragline compound ADF4 from the spider *Araneus diadematus* in addition to the biochemical analysis by Slotta et al (back-to-back contribution). Generally protein aggregation is driven by a shift of the thermodynamic equilibrium state caused by factors like temperature and ionic strength [12]. We detected, that under certain experimental conditions eADF4 C16) forms stable microspheres which were analyzed with respect to sphere size, size distribution and surface inertness for different preparation methods (dialysis, pipette and micro mixing). Based on our results the properties of spider silk microspheres can be controlled by varying parameters such as protein and potassium phosphate concentration as well as mixing intensity during the salting out process of spider silk protein.

Materials and methods

Materials

All materials used for protein dialysation, and sphere preparation were purchased from Sigma–Aldrich, Deisenhofen, Germany.

Preparation methods

Engineering of eADF4 (C16): The amino acid sequence of eADF4 (C16) was adapted from natural sequence of ADF4 from *Araneus diadematus*. The repetitive part of ADF4 is generally composed of a single conserved repeat unit displaying only slight variations. Repetitive elements in the sequence of ADF4 display a polyalanine-rich motif with high glycine content, which was named C. Our previously established engineering approach allowed the combination and multimerization of the single motifs, resulting in the eADF4 (C16) protein which comprises 16 repeats of the sequence GSSAAAAAAAAASGPGG YGPENQGPSGPGGYGPGGP resulting in a molecular mass of 48 kDa [9].

Protein dialysis: lyophilized protein eADF4 (C16) was dissolved in 6 M guanidinium thiocyanate. Dialysis was performed against 10 mM tris(hydroxymethyl)aminomethane(Tris)/HCl, pH 8, at 4°C using membranes with a molecular weight cut-off 6000-8000 Da (Spectrum Laboratories, Rancho Dominguez, USA).

Preparation of eADF4 (C16) microspheres: Four different preparation methods for inducing salting out were employed: 1) simple mixing (pipette) of 2M potassium phosphate (pH8) with eADF4 (C16) solution 2) mixing of 2M potassium phosphate (pH8) with eADF4 (C16) solution in a micromixing device under laminar flow conditions (2 ml/min, $Re = 85$). 3) mixing of 2M potassium phosphate (pH8) with eADF4 (C16) in a micro mixing device under turbulent flow conditions (50 ml/min, $Re = 2122$). 4) Dialysis of eADF4 (C16) solution against 1M potassium phosphate (pH8).

Micromixing Device: Constant volume flows of educt solutions (potassium phosphate (pH8) and eADF4 (C16) solution) were generated by two identical syringe pumps (Model 100DX, Teldyne Isco, Inc., USA). Pumps were operated by a digital controller (ISCO Series D, Teldyne Isco, Inc., USA). Mixing and precipitation was performed in a T-shaped mixing element with a circular mixing zone with a diameter of 500 μm (Peek Tee , P-728 Threads 10-32, Upchurch Scientific). The feed tubes were also 500 μm in diameter located opposite each other. In order to characterize the flow through the mixing element, a mixing Reynolds number is defined according to

$$Re = u \cdot d / \nu = 4 \cdot Q / (\pi \cdot d \cdot \nu)$$

where u is the average fluid velocity, d is the diameter of the mixing zone, ν is the dynamic viscosity of water and Q is the volumetric flow rate. In the discussed experiments mixing was conducted at flow rates of 2 ml/min and 50 ml/min which correspond to Reynolds numbers of $Re = 85$ and $Re = 2122$. The flow inside the mixing zone can be considered turbulent due to the impinging of the two solutions. The generated suspensions were collected in 1.5 ml Eppendorf tubes.

Analytical methods

Determination of protein concentration: The concentrations of obtained eADF4 (C16) solutions were determined by UV measurements at 20°C using Cary100 spectrophotometer (Varian Medical Systems, Palo Alto, USA). The molar extinction coefficient of eADF4 (C16) ($40974 \text{ M}^{-1}\text{cm}^{-1}$) at 276 nm and 20°C was employed.

Determination of sphere size: Particles sizes and their distributions were determined with Laser diffraction spectrometry (Horiba, Partica LA-950, Japan). Refractive indices of 1.33 for water and 1.60 for protein were taken for computation of particle sizes. In addition, a dry specimen of each preparation was analyzed by SEM to confirm sphere formation and sphere sizes.

Scanning electron microscopy (SEM): eADF4 (C16) microspheres were immobilized on Thermanox plastic cover slips (Nagle Nunc, USA), which had been coated with gold by sputtering under vacuum and analyzed by a JSM 5900 LV scanning electron microscope (JEOL Ltd., Japan at 20 kV).

Results

Salting out of eADF4 (C16) depends on ion concentration and temperature

eADF4 (C16) was incubated in Tris (10mM, pH 8) at 0.5 mg/ml or 1 mg/ml in presence of 500 mM or 1 M potassium phosphate (pH 8). It was determined that the required time for aggregation of 50% of eADF4 (C16) (t_{50}) was $t_{50} = 50 \text{ s}$ in the case of 500 mM potassium phosphate (pH 8) and $t_{50} = 30 \text{ s}$ in the case of 1 M potassium phosphate (pH 8) (Figure 1a). Independent of the starting protein concentration the limit of solubility is only dependent on potassium phosphate concentration and a constant amount of protein remained soluble in each sample: 333 μg calculated in case of incubation with 500 mM potassium phosphate and 250 μg calculated in case of incubation with 1 M potassium phosphate (Figure 1a and data not

shown). Further on, the influence of potassium phosphate concentration in combination with temperature was analyzed in greater detail. 50% of the protein was salted out with potassium phosphate after 1 hour of incubation at 381 ± 4.2 mM and 10°C , 205.5 ± 4.3 mM and 30°C and 85.2 ± 1.7 mM and 60°C respectively.

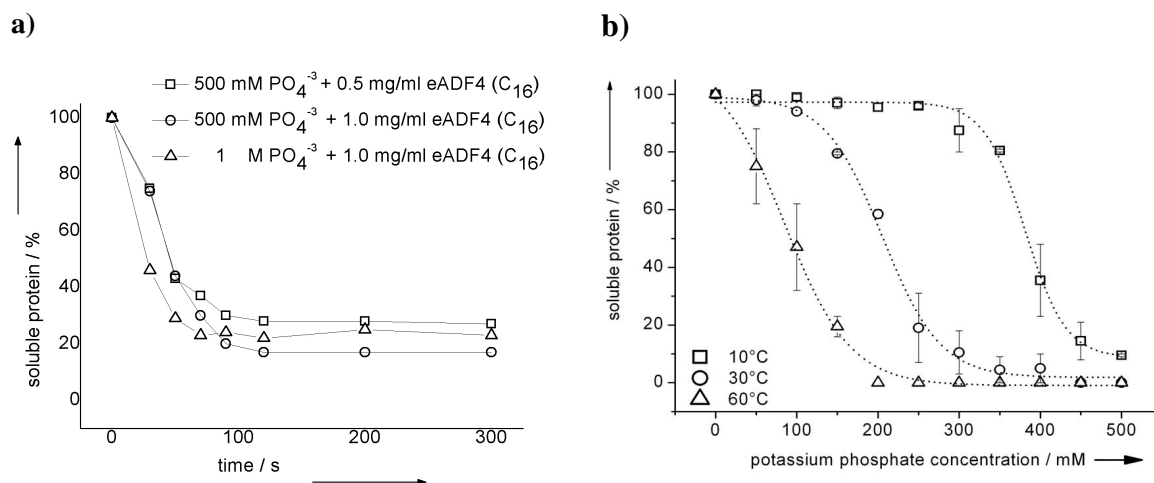


Figure 1: Aggregation assay of eADF4 (C16) protein. a) Aggregation behaviour of eADF4 (C16) as a function of time at 25°C at protein and potassium phosphate concentrations as indicated. b) eADF4 (C16) aggregation as a function of potassium phosphate concentration and temperature after 1 hour of incubation. At lower salt concentrations the aggregation is enhanced with increasing temperature. 50% of the protein is aggregated at 381 ± 4.2 mM and 10°C , at 205.5 ± 4.3 mM and 30°C and at 85.2 ± 1.7 mM and 60°C respectively.

Morphology of aggregates

Next the morphology of the aggregates was investigated. Above a potassium phosphate concentration of 500 mM the quantitative formation of microspheres could be detected (see also Slotta et al). Several different methods were employed for mixing eADF4 (C16) with potassium phosphate such as dialysis, simple mixing with pipette and micromixing within a T-mixing element. Upon mixing the samples were analyzed with laser diffraction spectrometry and scanning electron microscopy (SEM). Accordingly, different sphere characteristics with respect to sphere sizes, size distributions and formation of sphere clusters could be detected depending on the method of preparation. At 500 mM potassium phosphate (pH 8) silk spheres formed clusters at all examined preparation methods (dialysis, pipette, micromixing at 2 ml/min (Reynolds number: $\text{Re} = 85$, see Experimental Section) and 50 ml/min ($\text{Re} = 2122$)). Figure 2a shows a typical SEM picture of silk spheres produced by salting out with 500 mM potassium phosphate (pH 8). The picture illustrates that spheres with a diameter of approximately 500 nm build larger clusters of aggregates. In contrast, in salting out experiments performed with 1 M potassium phosphate (pH 8) mainly fully developed microspheres could be observed (Figure 2b). Micromixing with higher mixing intensities led to the formation of smaller spheres than salting out with dialysis or simple mixing with pipette. The SEM picture in Figure 2c depicts spheres produced by micromixing with 2

ml/min and Figure 2d spheres produced by mixing with a flow rate of 50 ml/min. Strikingly, sphere production by dialysis which reflects the slowest mixing conditions resulted in the largest spheres with diameters greater than 1 μm (Figure 2b).

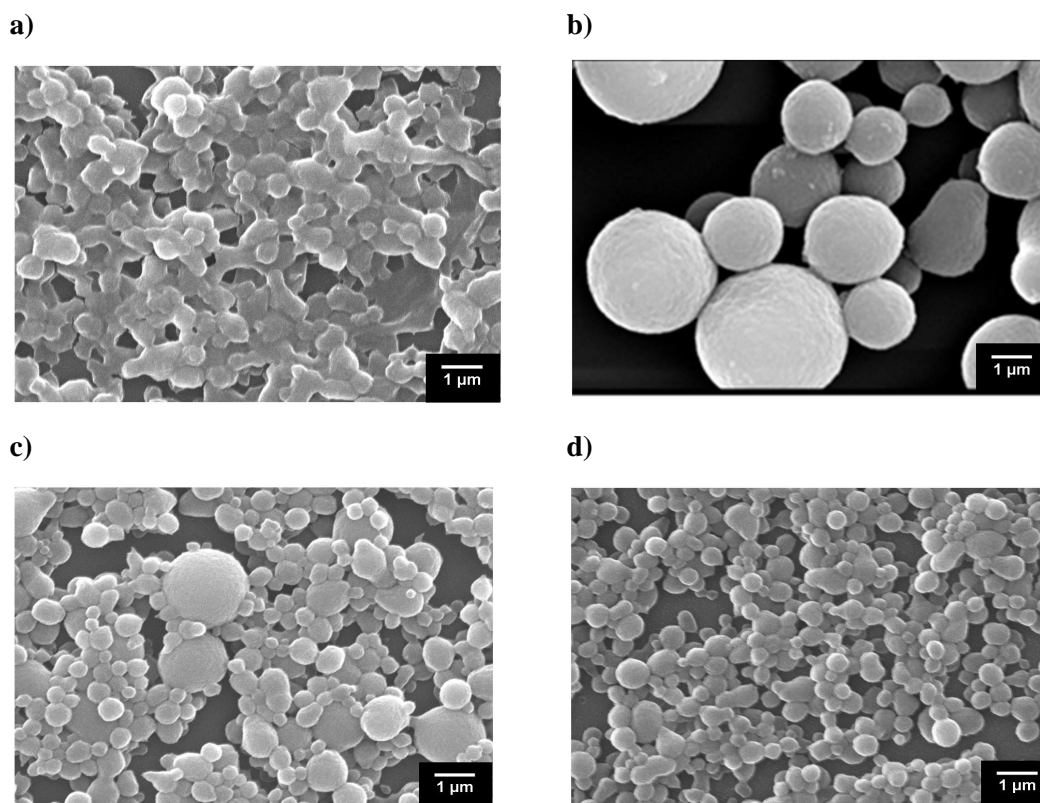


Figure 2: SEM images of microspheres produced by different methods. a) Micromixing of 500 mM potassium phosphate (pH8) with 0.5 mg/ml eADF4 (C16) solution with a flow rate of 50 ml/min. b) Dialysis of eADF4 (C16) solution with a protein concentration of 1 mg/ml against 1 M potassium phosphate (pH 8). c) Micromixing of 1M potassium phosphate (pH8) with 1 mg/ml eADF4 (C16) solution at a flow rate of 2ml/min. d) Micro mixing of 1M potassium phosphate (pH8) with 1 mg/ml eADF4 (C16) solution at a flow rate of 50 ml/min.

Size distribution of microspheres

For quantification of size distributions, as qualitatively observed by SEM, all samples without larger aggregates were analyzed by laser diffraction spectrometry. Thus, we analyzed all samples prepared by salting out with 1 M potassium phosphate (pH 8). Figure 3a shows the size distribution of spheres produced by mixing of 1 M potassium phosphate (pH 8) with 1 mg/ml eADF4 (C16) solutions with pipette as well as with micromixing at a rate of 2 ml/min and 50 ml/min. Figure 3b illustrates the size distribution of spheres salted out by dialysis of 0.5 mg/ml and 1 mg/ml eADF4 (C16) solution against 1 M potassium phosphate (pH 8). As seen by sharp peaks, controlled mixing with a micromixing device leads to a smaller size distribution compared to mixing with pipette or salting out by dialysis. Simple mixing with pipette at eADF4 (C16) concentrations of 0.5 mg/ml and 1 mg/ml led to stable micro spheres

with average diameters of 350 nm and 510 nm respectively (Figure 3c). By controlled mixing at a flow rate of 2 ml/min microspheres with an average size of 290 nm (0.5 mg/ml) and 370 nm (1 mg/ml) were formed, whereas at a flow rate of 50 ml/min smaller microspheres with an average diameter of 250 nm and 320 nm could be detected (Figure 3c). Dialysis yielded stable spheres with average sizes of 1.6 μm and 2.1 μm , respectively, with a rather broad size distribution (Figure 3c).

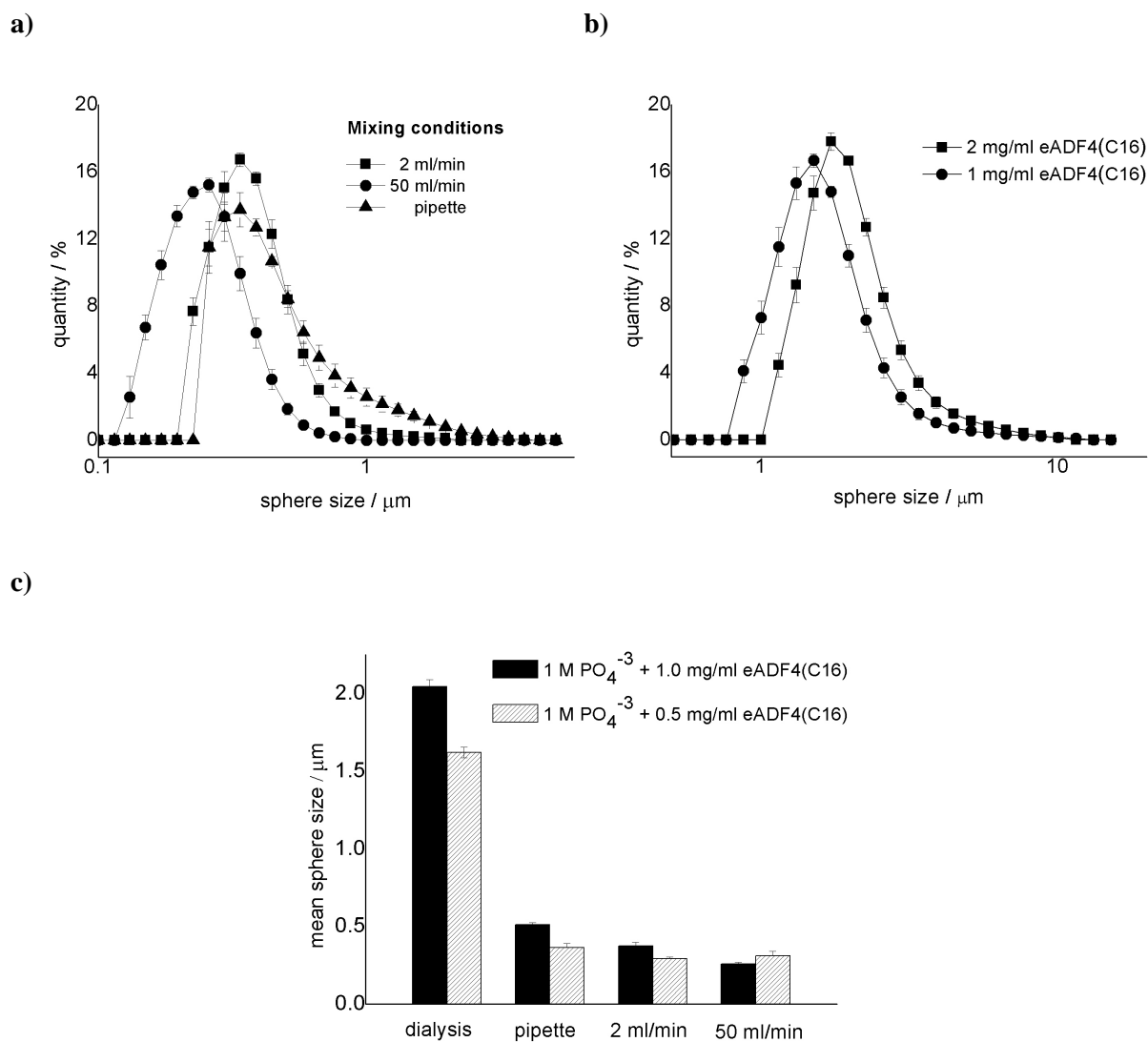


Figure 3: Size analysis of microspheres salted out with 1M potassium phosphate (pH 8). a) Size distribution of eADF4 (C₁₆) microspheres prepared by different methods: simple mixing with pipette and controlled mixing with a micromixing device at flow rates of 2 ml/min and 50 ml/min b) Size distribution of eADF4 (C₁₆) microspheres prepared by dialysis. c) Calculated mean sphere size of eADF4 (C₁₆) microspheres prepared by different methods as indicated.

Stability

To investigate the conformational stability of microspheres, sphere size distributions were measured with laser spectrometry over a time period of ten minutes with constant mixing to prevent sedimentation of microspheres. At low potassium phosphate concentration (500 mM, pH 8) aggregates were formed which could be separated by the induced shear stress provided by stirring (Figure 4). With 1M potassium phosphate (pH 8), stable microspheres could be produced independent of protein concentration or mixing condition (Figure 2c, Figure 2d, Figure 3c and Figure 4).

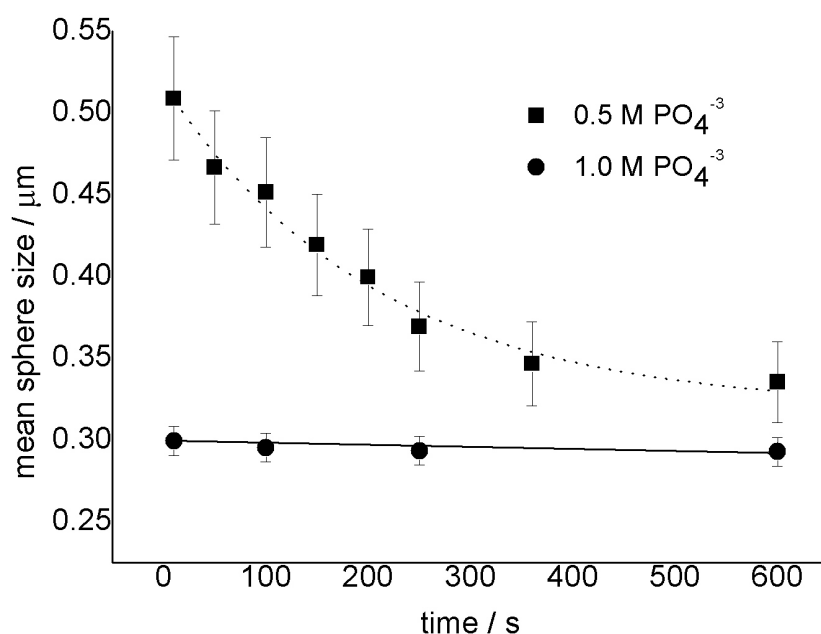


Figure 4: Conformational stability of microspheres produced by micromixing of 0.5 mg/ml eADF4 (C16) with potassium phosphate (pH 8) at a flow rate of 2 ml/min. Upon protein salting out with 1M potassium phosphate (pH 8) stable inert spheres are formed. After 10 min of stirring no decrease or increase in particle size could be detected. In the case of micromixing of 500 mM potassium phosphate (pH 8) with 0.5 mg/ml eADF4 (C16), particles were formed which decreased in size upon stirring.

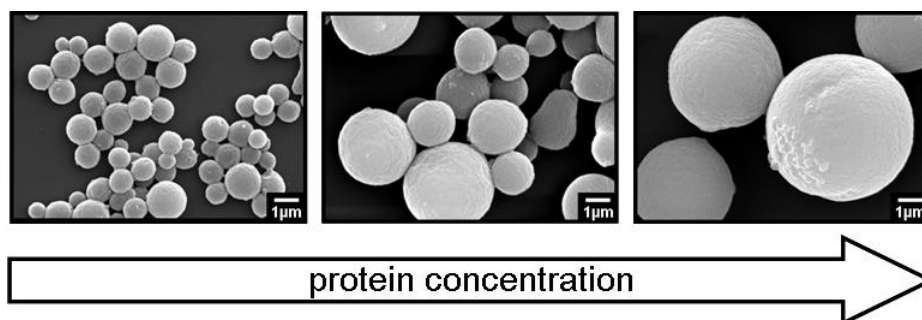


Figure 5: Influence of protein concentration on microspheres size produced dialysis of eADF4 (C16) solution against 1M potassium phosphate (pH 8). Employed eADF4 (C16) concentration from left to right: 0.1 mg/ml, 1 mg/ml and 10 mg/ml.

Conclusion

We conclude that for the production of spider silk microspheres by salting out a high concentration of potassium phosphate is required to obtain stable inert spheres. Generally, with increasing protein concentration sphere size is increased (Figure 5). The sphere size can be further adjusted by controlled micromixing inside a T-mixing element of eADF4 (C16) with 1M potassium phosphate (pH 8). The obtained microspheres represent a new class of biomimetic materials which are an alternative to microcapsules for incorporation of active ingredients such as therapeutic proteins. In contrast to spider silk microcapsules, the production of microspheres is much simpler since no formation of vesicles is required [6, 7] Incorporation of active ingredients into spider silk microspheres can be realized by adding a solution with the desired molecules before microspheres formation by addition of potassium phosphate. Presumably mechanical stability of the newly detected microspheres is much higher than that of the previously described microcapsules. In combination with material strength, biocompatibility and the possibility of functionalization, spider silk microspheres have a high potential for the development of targeted drug delivery devices.

References

1. F. Vollrath, *Reviews in Molecular Biotechnology* 2000, 74, 67-83
2. G. H. Altman, F. Diaz, C. Jakuba, T. Calabro, R. L. Horan, J. Chen, H. Lu, J. Richmond, D. L. Kaplan, *Biomaterials* 2003, 24, 401–416.
3. B. Panilaitis, G. H. Altman, J. Chen, H.-J. Jin, V. Karageorgiou, D. L. Kaplan, *Biomaterials* 2003, 24, 3079–3085.
4. R. L. Horan, K. Antle, A. L. Collette, Y. Wang, J. Huang, J. E. Moreau, V. Volloch, D.L. Kaplan, G. H. Altman, *Biomaterials* 2005, 26, 3385–3393.
5. D. Huemmerich, U. Slotta, T. Scheibel, *Appl. Phys. A* 2006, 82, 219 – 222;
6. K. D. Hermanson, D. Huemmerich, T. Scheibel, A. R. Bausch, *Adv. Mater.* 2007, 19, 1810–1815
7. K. D. Hermanson, M. B. Harasim, T. Scheibel., A. R. Bausch, *Phys Chem Chem Phys.* 2007, 9 (48), 6442-6446
8. T. Scheibel, *Microbial Cell Factories* 2004, 3,14
9. D. Huemmerich, C. W. Helsen, S. Quedzuweit, J. Oschmann, R. Rudolph, T. Scheibel, *Biochemistry* 2004, 43, 13604-13612.
10. U. Slotta, S. Hess, K. Spieß, T. Stromer, L. Serpell, T. Scheibel, *Macromol. Biosci.* 2007, 7, 183–188
11. J. H. Exler, D. Huemmerich, T. Scheibel, *Angew. Chem. Int. Ed.* 2007, 46, 1 – 5
12. V.N. Uversky, *Eur. J. Biochem.* 2002, 269, 2-12

4.3. Discussion of the presented data

In the above presented publication a production method for the preparation of micro sized spider silk particles is shown. The produced spider silk particles are formed by admixing spider silk protein solution with aqueous potassium phosphate solution. These two aqueous solutions are admixed via a micromixing device which allows the control of the mixing parameters. At a first glance the applied preparation technique is a simple precipitation method and therefore doesn't seem to stand out the mass of different techniques used for the preparation of polymer particles. However, the total absence of organic solvents in this preparation method and the use of physiological salts make this preparation technique special. Surveying literature one would find only few polymeric materials which allow the use of such harmless substances as potassium phosphate implemented in the preparation process and even less methods would allow such a high degree of controllability and reproducibility. Most often precipitation techniques of polymers such as PLGA involve the use of organic solvents. As already outlined detailedly in the introduction of this dissertation, the use of organic solvents is very often the driving force in drug especially therapeutic protein instability. But even if the drug intended to be encapsulated during the precipitation process shows up to be stable residual solvent content is a major issue to be dealt with when talking about application of such prepared systems into humans. It seems now that not only spider silk proteins seem to display a high degree of biocompatibility but also they uniquely feature the possibility of physio-compatible production methods. Considering the data so far the question arises whether the prepared spider silk protein particles are suitable for the controlled release of bioactive substance. Of course this question was the main impetus for the experiments described in 6.2 and normally one would assume that this question would have been dealt with within the first experiments conducted. However since the this produced material was relatively new to the research team there was so far no experience concerning the properties of this material with respect to controlled release. It was therefore our first aim to thoroughly characterize the production process and the resulting spheres before proceeding into another area of research. In addition to that we worked with very small amounts of this engineered material so that experiments which required higher quantities had to wait in line. Eventually the experience gained with these tentative experiments and the implementation of larger batch sizes lead to the start of the first drug release experiments. These experiments and their results are thoroughly highlighted in the next chapter dedicated to the application of this material in drug release.

5. Chapter Five: In vitro release studies of spider silk microparticles

5.1. Introduction

In the previous chapter we became acquainted with the preparation of genetically engineered spider silk protein spheres. A solvent free and easily controllable preparation method was shown and the resulting particles were analyzed with respect to their size, their surface morphology and their physical stability. Of course this set of data was understood as introduction in a very fascinating research area, essentially concentrating on the investigation of these semi-artificial spider proteins with special respect to their application as drug depot carrier. Apart from a preparation technique which allows their employment in physiological systems Chapter 4 so far didn't exhibit any hints that these proteins would feature special characteristics specially qualifying them for the preparation of controlled release systems. To close this gap, subsequently different experiments were conducted. After an early stage, when the first experiments lead to promising results the spectra of the analytical methods was expanded in order to examine the mechanism of drug loading and drug release from the prepared microspheres. The produced results – intended for publication – represent the main part of this chapter. The following manuscript therefore deals with the questions which need to be addressed when dealing with the implementation of a new drug depot system. After a little discussion about the presented manuscript additional data produced in subsequent experiments close this chapter and may serve as prospective view in the future research of this very fascinating material.

5.2. Spider silk particles for controlled drug delivery

Andreas Lammel^{1*}, Martin Schwab^{3*}, Gerhard Winter³, Thomas Scheibel²

¹Lehrstuhl Biotechnologie, Lichtenbergstraße 4, Technische Universität München, D-85747 Garching, Germany

²Lehrstuhl Biomaterialien, Universitätsstraße 30, Universität Bayreuth, D-95440 Bayreuth, Germany

³Department of Pharmacy, Pharmaceutical Technology and Biopharmaceutics, Ludwig-Maximilians-Universität, D-81377 Munich, Germany

* These Authors contributed equally to that work

Intended for publication in: Journal of Controlled Release

Abstract

We investigated the applicability of engineered spider silk protein eADF4 (C16) particles as drug delivery carriers. Spider silk particles have been produced by employing a precipitation method at ambient conditions with a particle formation yield above 99%. Particles morphology and sizes have been determined by Scanning Electron Microscopy (SEM) and Laser Diffraction Spectrometry (LDS) showing spherical shape and diameters in the range of 170 nm to 700 nm. We showed that eADF4 (C16) particles are colloidal stable in solution and thus are well suited as parenteral drug delivery devices. A detailed investigation of loading efficiencies of twelve small molecular model drugs with different chemical properties revealed that the obtainable loading efficiency correlates with the distribution coefficient (logD) of small molecules of alkaline nature. We could show that eADF4 (C16) particles can be uniformly loaded by diffusion of molecules into the spider silk protein matrix driven by electrostatic interactions. Release studies revealed that sustained pH sensitive release with constant release rates at physiological conditions can be realized for a period of two weeks. Enzymatic degradation studies of spider silk particles showed that they are fully degradable and undergo surface erosion.

Keywords: Biomimetics, biodegradation, controlled release, drug loading, proteins

Introduction

Since many drugs need to be administered regularly in order to achieve constant therapeutic relevant drug plasma levels drug depot systems have been developed to overcome drawbacks of multiple drug administration. Especially colloidal micro- and nanoparticulate carriers have extensively been investigated as a platform for targeted controlled drug delivery to realize a predictable systematic delivery of pharmaceutical agents [1-3]. The advantages of delivery systems compared to conventional administration forms are improved cellular uptake, increased bioavailability, a reduction of toxic side effects and improved patient compliance [4-7]. The employed material for controlled release should generally offer control of structure and function, while also exhibiting good mechanical stability, and be easily fabricated into desired morphologies [8]. Biodegradable and biocompatible polymers are preferred for such applications since they retain their properties for a limited period of time and then gradually degrade into soluble non-toxic products that can be excreted from the body. Many synthetic (aliphatic polyesters, PGA, PLA, PLGA etc.) and natural (polysaccharides, chitin, chitosan, proteins) polymers have been employed to produce degradable vehicles for encapsulation, incorporation or binding of active compounds [9-13]. While synthetic polymers have the advantage of sustaining the release of the encapsulated therapeutic agent over a period of days to several weeks they are in general limited by the use of organic solvents and relatively harsh formulation conditions [14]. Biocompatibility may be limited due to remaining toxic solvents. This has been tried to overcome by natural polymers which can be processed at ambient mild conditions. Most biopolymers investigated are hydrophilic which show relatively short duration of drug release. In spite of the possible advantages of natural polymers being biocompatible and processable at ambient conditions, most biopolymers present a main drawback of a rapid solubilization in aqueous environments, thus resulting in fast drug release profiles [15]. In order to overcome this problem, chemical cross-linking procedures (e.g. glutaraldehyde and formaldehyde treatment) have been considered [16-18]. Unfortunately, the presence of residual cross linking agents could lead to toxic side effects, in addition, unwanted reactions between the drug and cross-linker could result in the formation of toxic or inactivated derivatives [19, 20]. In contrast, a hydrophobic polymeric system has the capability of yielding sustained drug release [12]. Silk proteins as material unify all afore discussed properties necessary for its usage as a biomaterial in drug delivery systems [21, 22]. A special feature and advantage of silk proteins compared to other biopolymers is that the secondary structure of silk proteins can be triggered from a α -helical water soluble structure

into a β -sheet rich water insoluble structure by addition of lyotropic salts. Due to its unique properties and high potential as biomaterial, silk proteins especially bombyx mori fibroin but also silk proteins from spider species have been investigated for various biomedical applications including drug delivery [23, 24]. In the area of particulate drug carriers, silk fibroin microspheres with diameters of several microns using lipid vesicles as templates with microsphere yields of 55% and loading efficiencies of 21% have been reported [25]. Recently Wenk et al reported on the fabrication of fibroin spheres using a laminar jet break up technique by which they obtained encapsulation efficiencies close to 100% but with the trade off of sphere sizes from 100 to 440 μm in diameter. Nevertheless, the applied preparation techniques are quite sophisticated but exhibit a low up-scalability and sometimes involve organic solvents to stabilize the resulting silk fibroin preparations [23]. In our study we employed recombinantly produced engineered spider silk protein eADF4 (C16) mimicking the amino acid sequence from natural sequence of ADF4 from *Araneus diadematus* [26,29]. Detailed studies of the thermodynamic assembly process of eADF4 (C16) revealed that stable microspheres are formed by addition of high concentrations ($>400\text{mM}$) of lyotropic salts like potassium phosphate. Analysis of morphology and structure of obtained microspheres showed that they have a smooth surface and are solid with high β -sheet content ($>60\%$) and no apparent sub microstructure [27]. Further studies of the process parameters of eADF4 (C16) sphere formation showed that sphere size (250 nm to 3 μm) and size distribution can be controlled by mixing intensity and concentration of potassium phosphate and eADF4 (C16) solution [28]. The goal of the study was to investigate the applicability of engineered spider silk protein nanoparticles as drug carriers for parenteral applications. Spiders silk particles were fabricated by the above mentioned precipitation method under mild processing conditions suitable for the encapsulation of sensitive drugs. Several model drugs were applied and loading efficiencies were determined to elucidate the effect of drug molecule properties such as partition coefficient P and dissociation constant K_a on the loading efficiencies. In the following we report on the mechanism of drug loading, drug release behaviour and biodegradation of eADF4 (C16) particles.

Materials and methods

Materials

Engineering of recombinant spider silk protein eADF4 (C16): The amino acid sequence of eADF4 (C16) was adapted from the natural sequence of ADF4 from *Araneus diadematus*. The repetitive part of ADF4 is generally composed of a single conserved repeat unit displaying only slight variations. Repetitive elements in the sequence of ADF4 display a polyalanine-rich motif with high glycine content, which was named C. Our previously established engineering approach allowed the combination and multimerization of the single motifs, resulting in the eADF4 (C16) protein which comprises 16 repeats of the sequence GSSAAAAAAAASGPGGYGPENQGPSGPGGYGPGGP resulting in a molecular mass of 48 kDa [26,29]. The protein was purified as described previously to yield a purity of over 98% [29]. Due to its amino acid composition eADF4 (C16) features a theoretical isoelectric point at pH 3.48, which indicates that this protein is mainly negatively charged at a physiological pH of 7.4.

Small molecular model drugs: In order to investigate on the influence of different molecular parameters on the loading efficiency, 12 different small molecular drugs were used in this study. All drugs were dissolved in water with a drug molarity of 0.21 μmol . Drug substances and their featured properties are depicted in table 1. The main parameters focused on were the solubility in aqueous media expressed by the octanol/water partition coefficient (logP), the acid dissociation constant (pKa for protonated bases (BH⁺) or from acidic function (HA)) and the resulting charge in aqueous media (predominant or permanent charge). As molecular diffusivity is depending on molecular mass the molecular weight of each substance was taken into account.

Table 1: List of small molecular model drugs used for eADF4 (C16) nanosphere loading study. Values for molecular weight, dissociations constants (pKa) and partition coefficients (LogP) are taken from literature. The partition coefficient (logP) accounts for the unprotonated form of drug. The absorption wavelength λ_{Abs} was determined experimentally for each substance. All substances were purchased from Sigma-Aldrich (Deisenhofen, Germany).

Model drug	Molecular weight [Da]	λ_{Abs} [nm]	Dissociation constant of BH ⁺ (pKa)	Dissociation constant of HA (pKa)	Log P	Predominant charge at pH7	Permanently charged
Chlorthalidone	338	276	---	8,9	-0.03	uncharged	no
Nipagin	152	254	---	8.3	1.86	uncharged	no
Acetaminophen	151	272		8,0	0.38	uncharged	no
Phenol red	354	510	---	1.7; 7.7	3.0	negative	yes
Tetracaine*HCl	282	310	8.2	---	4.0	positive	no
Procaine*HCl	272	290	8.05	---	2.4	positive	no
Papaverine*HCl	376	248	8.07	---	3.5	positive	no
Ephedrine*HCl	165	256	9.6	---	1.30	positive	no
Propranolol *HCl	295	290	9.1	---	3.18	positive	no
Biperiden*HCl	347	210	9.6	---	3.5	positive	no
Ethacridine lactate	343	365	11	---	2.5	positive	no
Methyl violet	407	590	---	---	3.2	positive	yes
Thiamine chloride* HCl	337	240	4.8	4.8	-3.90	positive	no

Preparation of eADF4 (C16) particles

Lyophilized protein eADF4 (C16) was dissolved in 6M guanidiniumthiocyanate. Dialysis was performed against 10 mM tris(hydroxymethyl)aminomethane(Tris)/HCl, pH 8, at 4°C using membranes with a molecular weight cut-off at 6000-8000 Da (Spectrum Laboratories, Rancho Dominguez, USA). The concentration of eADF4 (C16) solution was determined by UV-Vis-spectrometry at 20°C using a Cary100 spectrophotometer (Varian Medical Systems, Palo Alto, USA). The molar extinction coefficient of eADF4 (C16) at 276 nm and 20°C was employed ($\epsilon = 46400 \text{ M}^{-1}\text{cm}^{-1}$). eADF4 (C16) particles were prepared using a phase separation procedure as described previously. Briefly, aqueous eADF4 (C16) ($c = 1.0 \text{ mg/ml}$) solution was admixed with potassium phosphate solution (2M, pH8) in volumetric ratio of 1:10 using a pipette. The resulting particles were centrifuged for 10 min at 10.000 g and washed three times with purified water. Obtained particles were redispersed in water and nanoparticle concentration was determined gravimetrically. A stock dispersion of known protein particle concentration was used for all experiments.

Drug loading of eADF4 (C16) particles

Drug loading of spider silk particles was conducted as followed: 100 μ l of spider silk particle suspension containing 1.0 mg silk protein were admixed with 1.0 ml of model drug solution. In order to obtain comparable results a molar ratio of eADF4 (C16) : model drug = 1:10 was realized for all model drugs employed. After 10 min of incubation at room temperature samples were centrifuged for 10 min with 10.000 g and the supernatant was analyzed for residual drug concentration with UV-Vis spectrometry. Standard calibration curves of model drugs by plotting the concentration versus absorbance were highly reproducible and used for drug quantification. A control group of samples containing only 100 μ l water admixed with 1.0 ml of model drug solution was prepared for each experiment. Drug concentrations from control and sample supernatant were used to calculate the amount of drug loaded on the spider silk particles. All experiments were performed in triplicate. Encapsulation efficiency and loading were determined by using equation (1) and (2), respectively:

$$\text{encapsulation efficiency (w/w \%)} = \frac{\text{amount of model drug in particles}}{\text{model drug initially added}} \quad (1)$$

$$\text{loading (w/w \%)} = \frac{\text{amount of model drug in particles}}{\text{amount of microspheres}} \quad (2)$$

In vitro release studies

Drug loaded eADF4 (C16) particles were washed with distilled water and suspended in 1 ml PBS (pH 7.4) and incubated at 37 °C while constant shaking. Each vial contained 2 mg of drug loaded spider silk protein particles. Medium from each sample was periodically removed and replaced with fresh PBS (pH 7.4). The model drug content in the medium was analyzed using UV-Vis- spectrometry at regular time intervals. The percentage of cumulative model drug release (% w/w) was investigated as a function of incubation time. Each experiment was performed in triplicate. To study the effect of different pH values on the release behaviour of drug loaded eADF4 (C16) particles we incubated ethacridine lactate loaded nanospheres (1 mg) in 1.0 ml PBS with 5 different pH values (2, 4, 6, 7.4 and 8.8) for 5 days. The incubation media was withdrawn daily and the particles were redispersed in fresh media. Supernatants of drawn samples were analyzed with UV-Vis spectrometry for drug content determination.

In vitro degradation of eADF4 (C16) particles

In order to simulate the degradation and cleavage of engineered spider silk protein eADF4 (C16) based drug depot systems we employed a mixture of two in the human body naturally occurring proteases namely elastase and trypsin. In our studies we incubated 1.0 mg of silk microspheres in 1.0 ml PBS containing 0.80 μg elastase and 12.5 μg trypsin. After 1, 2, 3, 4 and 5 days samples were centrifuged, the supernatant was carefully removed and analyzed with SDS-PAGE. The pellet containing the eADF4 (C16) particles was redispersed in distilled water and washed three times for further size and morphology analysis by laser diffraction spectrometry and scanning electron microscopy. Elastase and trypsin from hog pancreas were supplied by Sigma Aldrich (St. Louis, USA)

Characterization methods**Scanning electron microscopy**

The eADF4 (C16) particles were immobilized on Thermanox plastic cover slips (Nagle Nunc, USA), dried at room temperature and coated with gold by sputtering under vacuum, and analyzed with a JSM 5900 LV scanning electron microscope (JEOL Ltd., Japan, at 20 kV).

Laser diffraction spectrometry

Particles sizes and size distributions were determined with laser diffraction spectrometry (Horiba, Partica LA-950, Japan). Refractive indices of 1.33 for water and 1.60 for protein were taken for computation of particle sizes. In addition, a dry specimen of each preparation was analyzed by scanning electron microscopy (SEM) to confirm spherical shape and sphere sizes.

Fourier transform infrared spectroscopy (FTIR)

Fourier transform infrared (FTIR) spectra were collected using a Bruker Equinox 55 FTIR spectrometer. The samples were prepared by putting a drop of eADF4 (C16) particle suspension on CaF₂ disks and subsequent air-drying. Absorbance spectra of eADF4 (C16) particle ensemble were recorded in the spectral range between 400 and 4000 cm^{-1} with unpolarized light with a resolution of 4 cm^{-1} . An accumulation of 32 spectra ensured a high signal to noise ratio. The measurements were carried out at 25°C and 30% relative humidity. To analyze the secondary structure of eADF4 (C16) protein particles secondary structure we used the amide I band (1600–1700 cm^{-1}). Peaks at 1648-1660 cm^{-1} , 1625-1640 cm^{-1} and 1660-1668 cm^{-1} can be assigned to α -helical, β -sheet and β -turn structures respectively [30].

UV-Vis spectrometry

Ultraviolet–visible spectrometry using a Cary100 spectrophotometer (Varian Medical Systems, Palo Alto, USA) has been employed for determination of model drug content in supernatants for the calculation of loading efficiencies and release behaviour. Calibration curves for all model drugs investigated have been obtained by using five different concentrations of all stock solutions. The absorption wavelengths used for determination of drug concentration are summarized in Table 1.

Zetapotential Analysis

In order to elucidate and characterize the loading mechanism of eADF4 (C16) particles with model drugs, zeta potential measurements have been conducted as a function of added amount of model drug. The zeta potential was determined using a Nanoseries Malvern Zetasizer (Malvern, Worcestershire, UK). Automatic titration was conducted with a Malvern Multipurpose Titrator MPT-2. Experiments have been performed in distilled water (pH 7) at 25°C. Each measurement was performed in triplicate.

SDS gel electrophoresis

Sodium dodecylsulfate polyacrylamide gel electrophoresis (SDS-PAGE) as a sensitive method for protein species analysis was used for the determination of protein cleavage. Samples drawn from the degradation studies were diluted in SDS-running buffer, heated for 50 min at 95° C before loading on the gel. Gels were run with 40 mA for approximately 1.5 hours. Silver staining was used for visualization of separated protein bands. All materials were supplied by Invitrogen (Carlsbad, CA, USA).

Results and discussion

Spider silk protein eADF4 (C16) particle characterization

To characterize the morphology and quantify the sizes of obtained eADF4 (C16) particles the prepared stock dispersion used for further experiments was examined employing SEM and laser diffraction spectrometry. Figure 1a) shows that particles of spherical shape with diameters from 170 nm to 700 nm have been obtained. The determined average diameter of particles ensemble was $d_{avg} = 332 \pm 95$ nm with a polydispersity index of 0.72. The yield of nanoparticle formation by salting out was above 99% meaning that literally all protein initially in solution was transformed into particles. The colloidal stability of eADF4 (C16) particles in suspension was studied by adding 1.0 mg of particles to 1.0 ml of Na₂SO₄ solutions of varying concentration (0–2.0 M), and measuring the turbidity at a wavelength of 400 nm after 15 min. The onset of electrolyte induced flocculation in dilute dispersions can be

detected by a dramatic increase in turbidity of the dispersion at 400nm [31]. We found that eADF4 (C16) particles are colloidal stable within the complete studied concentration range from 0 to 2.0 M Na₂SO₄ (Figure 1b).

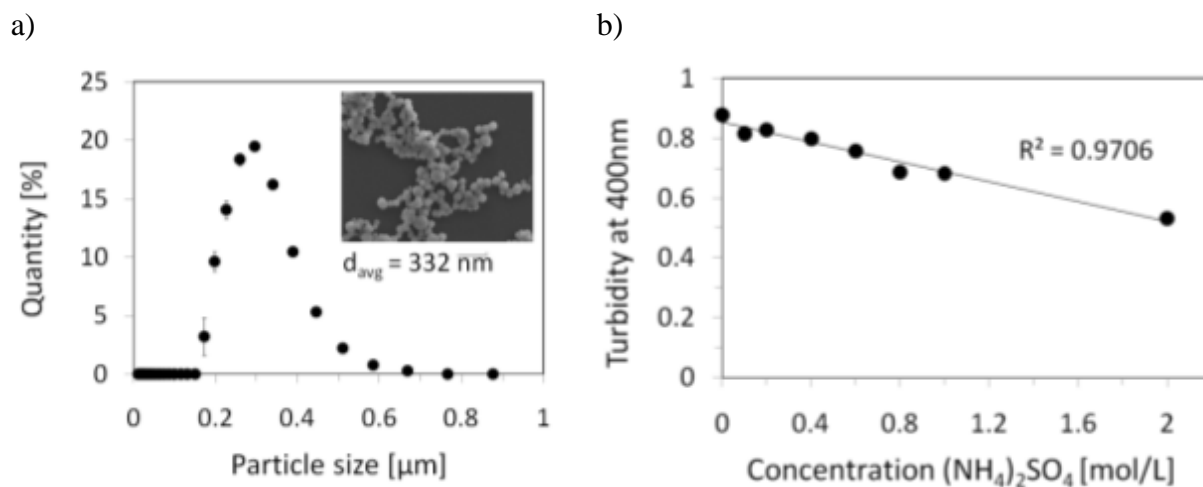


Figure 1: Spider silk protein eADF (C16) particle characterization: a) Size distribution of obtained eADF4 (C16) particles analyzed with laser diffraction spectrometry. The inset shows an scanning electron micrograph of corresponding eADF4 (C16) particles. b) Investigation of colloidal stability assessed by the turbidity method.

Loading efficiencies & loading mechanism

Due to its negative charge at pH 7 eADF4 (C16) has the potential to form complexes with positively charged molecules due to electrostatic interactions. Considering the tertiary structure of proteins, charged amino acid residues are mainly located on the surface of proteins whereas hydrophobic groups are buried in the closely packed interior [32]. Thus we concluded that loading and entrapment of drug molecules into eADF4 (C16) protein particles is mainly driven by the following three parameters. First, the charge of the drug molecule expressed by its proton dissociation constant K_a (accounted for BH^+ or HA). Secondly, the octanol water partition coefficient ($\log P_{o/w}$), as an indicator for the solubility of the model drug employed. And third, the molecular weight (MW) of model drugs which plays an important role in diffusion driven mass transport processes. Our aim was to correlate these dominating chemical parameters ($\text{p}K_a$, $\log P$ and MW) with experimentally obtained loading properties of eADF4 (C16) particles to understand the underlying mechanisms important for effective and successful loading. The distribution between a lipophilic and a hydrophilic phase of two different species of a specific drug, i.e. the native and the protonated form, can be described by its distribution coefficient ($\log D$). The distribution coefficient ($\log D$) for acids and bases was calculated with equation (3) and (4) respectively [33].

$$\text{for acids: } \log[D = \log P - \log(1 + 10^{pH - pK_a})] \quad (3)$$

$$\text{for bases: } \log[D = \log P - \log(1 + 10^{pK_a - pH})] \quad (4)$$

The $\log P$ and $\text{p}K_a$ values of individual species used for calculation of $\log D$ are listed in

Table 1. Table 2 summarizes the determined loading efficiencies, theoretical and actual amount of entrapped drug content as well as the calculated distribution coefficient (logD) for all model drugs investigated.

Table 2: List of model drugs investigated classified according to their chemical nature. The table provides an overview of theoretical and actual model drug content (expressed as percentage of wt drug/ wt spider silk protein particles), corresponding encapsulation efficiencies and calculated distribution coefficients (logD) for model drugs as listed.

Model drug	MW [Da]	Chemical nature	Theoretical drug content [w/w%]	Actual drug content [w/w%]	Encapsulation efficiency [%]	Log D
Ephedrin*HCl	165	base	3.38	0.7	20.7	-1.321
Procain*HCl	273	base	5.70	2.16	38.0	0.396
Biperiden*HCl	347	base	6.97	2.93	42	0.899
Propranolol*HCl	295	base	5.55	2.5	45.0	1.197
Papaverine*HCl	376	base	7.56	3.55	47	2.395
Tetracaine*HCL	282	base	5.67	3.01	53	2.773
Ethacridine lactat	343	strong base	7.33	7.2	98.2	2.899
Acetaminophen	151	weak acid	3.16	0.06	0.2	0.378
Chlortalidon	338	weak acid	7.22	0.7	9.7	-0.315
Nipagin	152	weak acid	3.47	0.6	17.3	0.544
Phenol red	354	strong acid	7.12	0.0	0.0	-
Methyl violet	407	---	8.72	8.7	98.1	-

All loading experiments were conducted at pH 7. We found that protonated weak organic bases could be loaded onto eADF4 (C16) particles with efficiencies ranging from 20.7 % up to 53.0 %. For this class of small molecular model drugs we found that the quotient of calculated logD divided by the molecular mass of individual molecule correlates linear with the obtained loading efficiencies (Figure 2). This linear relationship clearly indicates that the combination of charge and solubility (expressed by logD) and diffusion processes (expressed by the inverse proportionality of molecular weight) are the dominating factors responsible for effective loading of small molecular basic model drugs on eADF4 (C16) particles.

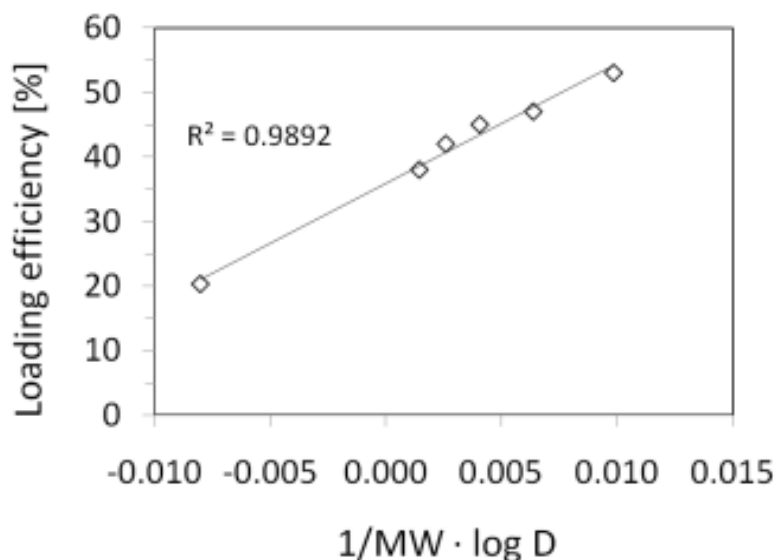


Figure 2: Loading efficiencies for model drug of basic nature plotted over $1/MW \cdot \log D$.

Strong basic molecules like ethacridine lactate showed a loading efficiency of even more than 98 %. By investigating molecules with permanent charge we found that positively charged molecules such as methyl violet were most successfully encapsulated whereas negatively charged molecules such as phenol red could not be encapsulated into spider silk protein particles at all. Model drugs exhibiting acidic nature exhibited relatively low loading efficiencies from 0.2 to 17.3 %. Despite the relatively high $\log D$ of acetaminophen (comparable to Nipagin) a loading efficiency of only 0.2 % has been determined which might be explained by its structure acting as weak phenolic base leading to the appearance of negatively charged acetaminophen species. We suspect that due to electrostatic repulsion of the negative charges these species cannot diffuse into the spider silk protein matrix. In order to proof the concept of drug permeation into the protein nanoparticle interior we used glass beads with a highly negative surface charge (-50mV) as control, assuming that permeation processes of drug molecules into the dense glass matrix cannot occur. Due to the high negative surface charge of glass beads the loading efficiency for glass beads should be higher than that for spider silk particles if no diffusion into the protein matrix would occur. For this experiment we employed methyl violet which was identified to have a loading efficiency above 98% for a molar ratio of methyl violet : eADF4 (C16) = 10:1. Figure 3a shows the obtained loading and loading efficiencies as a function of molar ratio. Up to a molar ratio of methyl violet : eADF4 (C16) = 10 the loading scales linear with the amount of methyl violet added. Above a molar ratio of 10 the loading efficiency decreases and the loading follows a saturation curve. Online zeta potential measurements during methyl violet loading revealed that zeta potential change upon sphere loading is a triphasic process (Figure 3b). First, the

potential changes gradually after addition of methyl violet solution to spider silk protein sphere suspension. After an initial constant slope, the zeta potential curve exhibits a plateau phase indicating no change of surface loading while increasing methyl violet concentration. Interestingly after reaching the concentration corresponding to the molar ratio of methyl violet : eADF4 (C16) = 10 a further increase of the zeta potential could be observed. We propose that the reduction of the zeta potential as seen in the titration curve is a direct consequence of the interaction with molecules of opposite charge. The initial lowering of surface charge can be explained by the charge compensation due to the addition of opposite charged methyl violet molecules. The plateau region indicates an equilibrium state of drug adsorbed at the solid-liquid particle interface and a diffusion of molecules into the hydrophobic core of the protein sphere. After the core matrix is saturated the influx of methyl violet molecules is reduced and eventually terminated, at that point the zeta potential starts to decrease again as can be seen by the second slope in Figure 3b.

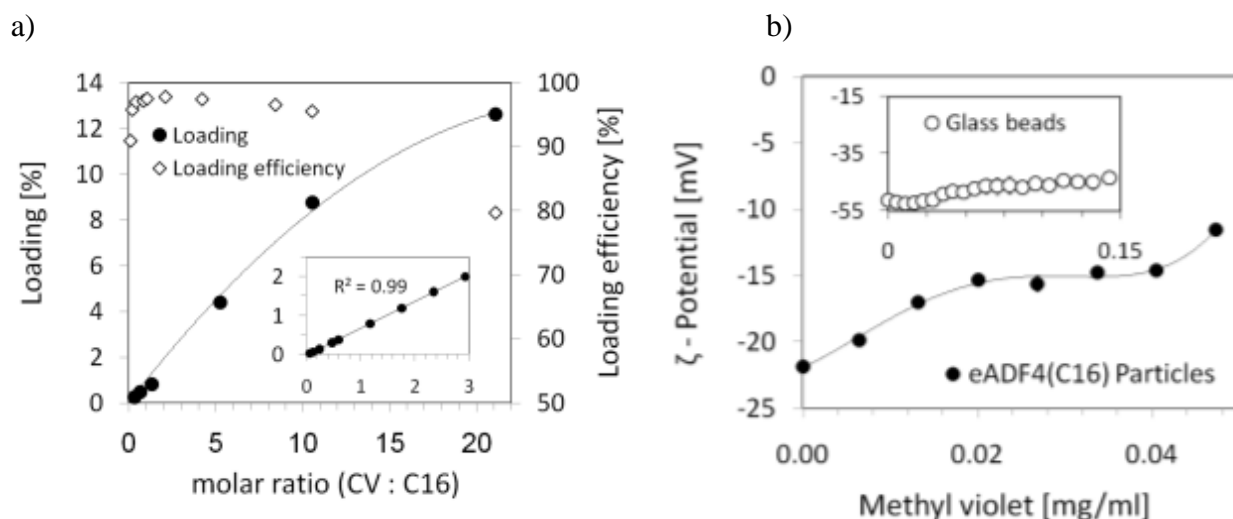


Figure 3: Characterization of loading mechanism: a) Loading and loading efficiency of methyl violet on eADF4 (C16) particles as a function of molar ratio. b) Zeta-Potential of eADF4 (C16) particles as a function of added methyl violet. For comparison the inset shows the Zeta-potential of glass beads with methyl violet.

In contrast to loading experiments conducted with glass microparticles showed distinctive differences. The zeta potential curve during methyl violet addition showed no distinctive change. The only observation which can be stated is that the zeta potential of glass beads increased slightly and constantly during titration upon addition of methyl violet. The initial assumption that methyl violet cannot permeate into the glass particle matrix was confirmed by UV-Vis analysis of supernatant after completed titration. While the surface charge of glass particles is approximately two times higher compared to silk particles the determined loading efficiency was only 0.03%. Furthermore the loading of methyl violet could be easily washed off the surface by three washing steps with purified water.

According to our results we propose that distribution coefficient $\log D$ can be used to estimate the obtainable loading efficiency for weak organic bases without permanent charge. Molecules with permanent charge cannot be included in this model as it is not possibility to calculate the corresponding $\log D$ value. Furthermore we propose that for an effective loading of spider silk protein particles, drug molecules ideally should feature a positive charge combined with a certain degree of lipophilicity and a molecular weight enabling it to diffuse freely into the spider silk protein matrix.

In vitro release studies

Encapsulated drugs (methyl violet and ethacridine lactate) were released in a constant manner for more than 30 days. Most interestingly loaded particles showed no signs of drug burst, i.e. an initial high drug release within the first 24 hours of incubation. The release of ethacridine lactate and methyl violet within the first 24 hours was 11% of the total amount encapsulated. Subsequently eADF4 (C16) particles released approx. 5% of the entrapped molecules per day within the first week (Figure 4a,b). To characterize the release behaviour the semi empirical power law equation introduced by Siepmann and Peppas [34] was used

$$\frac{M_t}{M_\infty} = kt^n \quad (5)$$

where M_t/M_∞ is the fractional amount of the drug released at time t , k is a characteristic constant of the system, and exponent n is related to the geometrical shape of the formulation and describes the kinetics and release mechanism. Thus, for spherical systems n is equal to 0.43 and 0.85, when pure Fickian diffusion or pure Case II transport is operating, respectively. Case II transport reflects the influence of polymer relaxation on molecules' movement in the matrix. When n is in the interval between $n = 0.43$ and $n = 0.85$ a superposition of both transport processes occurs which is known as anomalous transport. In order to obtain a linear fit for the drug release data, equation (5) was modified by taking the logarithm as shown in equation (6)

$$\log\left(\frac{M_t}{M_\infty}\right) = \log(k) + n \log(t) \quad (6)$$

where n can be obtained from the slope of the log-log plot of release M_t/M_∞ versus time t by linear fitting (Figure 4d). We identified three time intervals with different dominating release mechanisms. To distinguish between different time intervals we used the criterion that the coefficient r^2 had to be above 0.99 for the individual linear fits. The values of release exponent (n), correlation coefficient (r^2), and characteristic constants (k) obtained are

summarized in Table 3. For validation of the determined release parameters we compared the experimental release data with the semi-empirical power law and found very good agreement from post-initial burst stage (>24 hours) stage up to 100% release (Figure 4a).

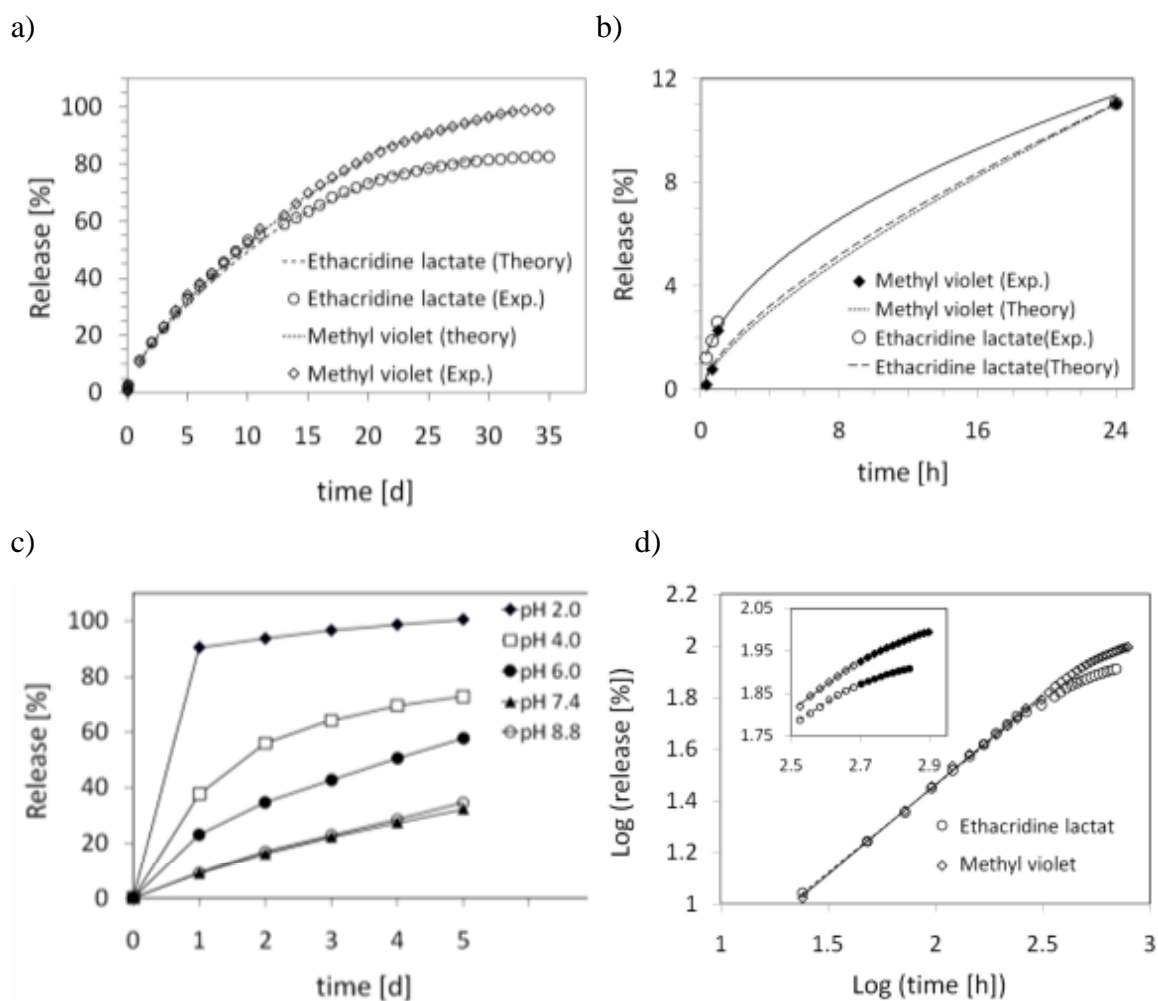


Figure 4: Release studies of ethacridine lactate and methyl violet: a) Experimental and theoretical release kinetics of model drugs as indicated over a period of 35 days. b) Experimental and theoretical release kinetics in the initial burst region (release < 11%). c) Release of ethacridine lactate as a function of pH as indicated d) Experimental release data of ethacridine lactate and methyl violet based on the power law model. A linear fit with a correlation parameter (r^2) above 0.99 was determined for three distinct time intervals. The linear fit for the interval from day 1 to day 13 is depicted in the main plot, whereas the inset shows the data and linear fits for the time intervals from day 14 to day 20 (no filling) and day 21 to day 35 (black filling) respectively.

Table 3: Drug release parameters (n : release exponent; r^2 : correlation coefficient; k : characteristic constant) for methyl violet and ethacridine lactate for defined release intervals as indicated.

Model drug	time [d]	Release [%]	N	R2	k
Methyl violet	0-13	≤ 60	0.692	0.998	1.17
	14-20	60 - 82	0.6079	0.994	1.92
	>20	≥ 82	0.3537	0.993	9.20
Ethacridine lactate	0-13	≤ 60	0.6754	0.998	1.25
	14-20	60 - 73	0.5083	0.994	3.18
	>20	≥ 73	0.2641	0.992	14.4

Within the first two weeks of release both exponents n for ethacridine lactate and methyl violet are almost identical and clearly above 0.43 ($n_{el} = 0.6754$, $n_{mv} = 0.692$) indicating an anomalous diffusional release. In the second identified time interval from day 14 to day 20 we found that release profiles diverge from each other where the release exponent of ethacridine lactate drops to 0.51 and that of methyl violet decreases less to a value of 0.61. This shows that for ethacridine lactate Fickian transport begins to dominate. After 20 days release exponent n values for methyl violet and ethacridine lactate fall below the limiting value of 0.43 indicating a Fickian release behavior. Release experiments with ethacridine lactate loaded eADF4 (C16) nanoparticles incubated in PBS at 37°C and different pH values showed a strong pH influence on the release rates (Figure 4c). We observed that an acidic environment accelerates the drug release. Almost 80% of the loaded drug was released after 24 hours from silk nanospheres incubated in pH 2 buffer media. For silk particles incubated at pH 4 an initial release rate of almost 40% was obtained after the first day of incubation. Particles incubated in pH 6 buffer showed an accelerated but similar release to pH 7.4 and 8.8. No significant difference between the release of nanospheres incubated in pH 7.4 and pH 8.8 was observed. The observed results confirm the predicted importance of electrostatic interactions between eADF4 (C16) and drug molecules. Presumably an influx of protons into the biopolymer leads to a displacement of drug molecules from the matrix. In addition to that the decreased pH influences the distribution of charged drug species by shifting the equilibrium towards the charged species. As these species are driven towards the negatively charged surface of the protein they can easily be washed away by the surrounding media.

In vitro degradation

Degradation of drug depot systems is highly desirable as non degradable drug depot systems carry the risk of inflammation and intoxication and therefore need to be removed surgically [35,36]. As many natural occurring polymers feature the ability of enzymatic degradation [37] thus we conducted degradation studies using proteases [38, 39] naturally occurring in the human body to simulate the degradation of our eADF4 (C16) drug carriers. Results from the degradation study revealed that eADF4 (C16) microspheres undergo degradation in the presence of proteases. Soluble degradation products were verified with SDS-PAGE (Figure 6a). Interestingly, the molecular weight of eADF4 (C16) degradation products decreases over time. The phenomenon can be explained by the protease activity at different sites of the eADF4 (C16) peptide chain. Elastase and trypsin, i.e. serine proteases can cleave peptide bonds on the carboxy side of small, hydrophobic amino acids such as glycine, alanine, and valine [40]. Due to the relative high content of glycine and alanine in eADF4 (C16) (~ 50

percent of the total amino acid composition) such proteases may cleave peptide bonds at several sites in the amino acid backbone of eADF4 (C16). The resulting fragments of eADF4 (C16) exhibit a molecular weight of about 18 kD. When soluble eADF4 (C16) was incubated with proteases, degradation products with a molecular weight of 6 kD were generated (Figure 6a, lane 3). We presume that the degradation of spider silk particles would continue upon incubation for a longer period of time resulting in soluble fragments comparable to those observed in the degradation experiment with eADF4 (C16) solution. Size analysis of particles drawn from the degradation experiments at specific time points showed a continuous decrease of 50 nm in mean particle diameter within five days (Figure 5 a, b). As enzymatic degradation is a process controlled by the interfacial activation of the enzymes and considering the decrease in particles size one can assume the silk nanospheres undergo surface erosion. Results obtained by scanning electron microscopy show a distinct reduction in particle size; however particle morphology appears to be conserved (Figure 5 c, d). The incubated particles still exhibit a smooth surface. If spider silk protein particles would undergo bulk erosion particle morphology would be altered and particle size presumably would increase as bulk erosion is accompanied with polymer swelling.

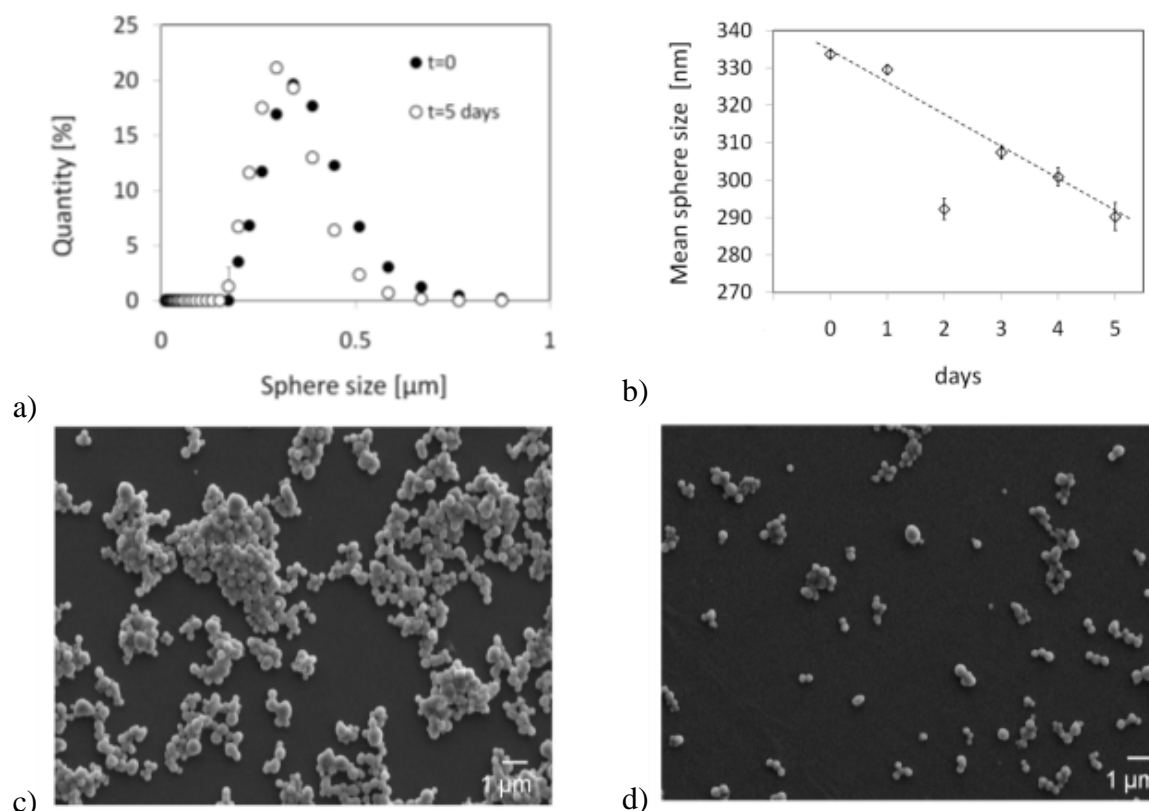
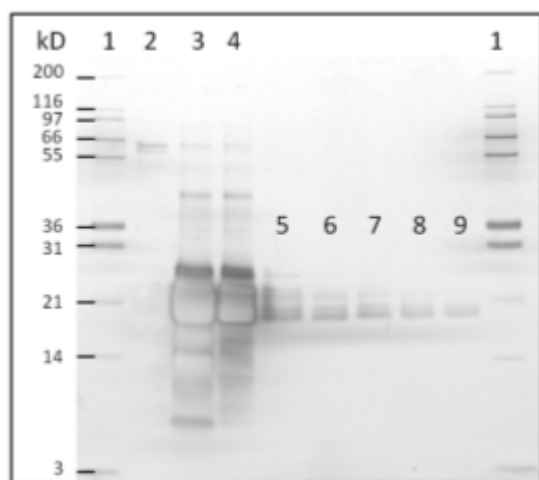


Figure 5: Characterization of eADF4 (C16) particles upon enzymatic degradation: a) Size distribution of nanoparticles upon degradation at timepoints as indicated b) Mean diameter of eADF4 (C16) spheres upon degradation over time. c) SEM image of eADF4 (C16) nanospheres before degradation d) SEM image of eADF4 (C16) nanospheres after degradation with elastase ($c = 4 \mu\text{g/ml}$) and trypsin ($c = 50 \mu\text{g/ml}$) for 5 days.

FTIR analysis of eADF4 (C16) particles upon enzymatic degradation revealed that the percental β -sheet content increases whereas the α -helical content decreases. This can be most effectively seen by changes of the second derivative of FTIR spectra at the wavenumbers 1648-1660 cm^{-1} and 1625-1640 cm^{-1} assigned α -helical and β -sheet structures respectively (Figure 6b). The result that α -helical structures are degraded faster than β -sheet structures is advantageous for the long term stability and release behaviour of eADF4 (C16) particles at physiological conditions. β -sheet-structures are not soluble in aqueous environments and thus a hydrophobic core of the particles is maintained important for desired surface erosion.

a)



b)

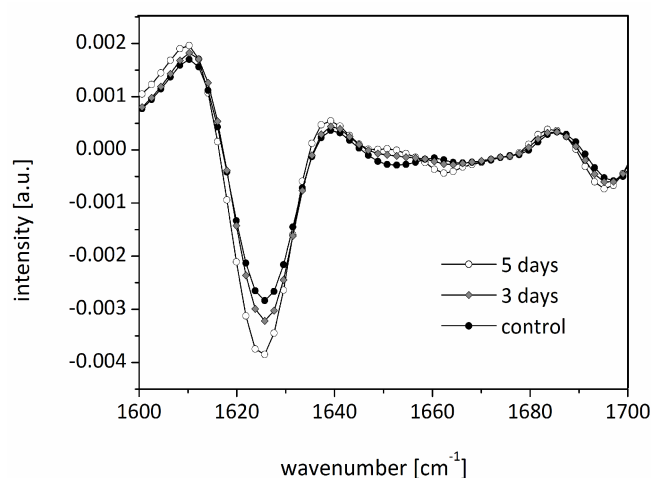


Figure 6: Degradation analysis of eADF4 (C16) particles: a) SDS Page of degradation products of eADF4 (C16) particles. 1: Marker (Mark 12, Invitrogen); 2: eADF4 (C16) solution ($c = 0.05 \text{ mg/ml}$) used for nanosphere preparation; 3: Degradation of eADF4 (C16) solution ($c = 0.05 \text{ mg/ml}$) with elastase ($c = 150 \text{ }\mu\text{g/ml}$) and trypsin ($c = 600 \text{ }\mu\text{g/ml}$) for 1 h at 25°C ; 4: elastase ($c = 150 \text{ }\mu\text{g/ml}$) and trypsin ($c = 600 \text{ }\mu\text{g/ml}$) without any substrate; 5-9: Degradation of 1 mg eADF4 (C16) nanospheres with elastase ($c = 4 \text{ }\mu\text{g/ml}$) and trypsin ($c = 50 \text{ }\mu\text{g/ml}$) 5: after 1 day, 6: after 2 days, 7: after 3 days, 8: after 4 days, 9: after 5 days. b) Second derivative of FTIR spectra of eADF4 (C16) particles upon degradation at time points as indicated.

Conclusion

Our results show the potential utility of engineered spider silk protein eADF4 (C16) particles for sustained controlled drug delivery. Our detailed investigation of the loading procedure including the parameters like the octanol/water partition coefficient (logP) and dissociation constants (pKa) of twelve different investigated model drugs showed that the presented encapsulation procedure can efficiently applied for weak organic bases which represent the majority of drug molecules available today. Additionally, using an online zeta potential measurement during particle loading allows monitoring of the loading processes and facilitates determination of loading endpoint. Especially for high potential drugs used in cytostatics therapy such as Doxorubicin*HCl this particulate carrier system may be ideal due to its ease of preparation. Furthermore as shown eADF4 (C16) particles can be produced and loaded within an all-aqueous process under ambient conditions which is a major advantage considering encapsulation of labile compounds and the biocompatibility of the product. Due to its size eADF4 (C16) particles are applicable for drug targeting, since the diameter of the microspheres is appropriate for phagocytosis by macrophages or cellular uptake by carcinoma cells [41,42]. For biomedical application especially engineered spider silk proteins seem to be ideal. Due to the biotechnological production process no degumming process as for bombyx mori silk is required to get rid of the sericin which was identified as a source of immunogenic reactions in vivo [43]. Our results show that eADF4 (C16) particles undergo surface erosion which can be explained by the fact that the interior of the particles is hydrophobic enough to keep water from penetrating and degrading the interior of the materials faster than the surface layer erodes. The property of surface erodible eADF4 (C16) particles supports the applicability as drug delivery systems since bulk erosion processes lead to a massive interference with the drug release mechanism resulting in accelerated and uncontrolled release. We conclude that engineered spider silk particles have the potential for diverse applications where controlled release from biocompatible, mechanically tough, and slowly biodegradable carriers is desirable.

References

1. Allen TM, Cullis PR. Drug Delivery Systems: Entering the Mainstream. *Science* 2004;303:1818-1822.
2. Edlund U, Albertson AC, Degradable Polymer Microspheres for controlled drug delivery. *Advances in Polymer Science* 2002;157:67-112.
3. Arshady R. Biodegradable Microcapsular Drug Delivery Systems: Manufacturing Methodology, Release Control and Targeting Prospects. *Journal of Bioactive and Compatible Polymers* 1990;5:315-342.
4. Panyam J, Labhasetwar V. Biodegradable particles for drug and gene delivery to cells and tissue. *Advanced Drug Delivery Reviews* 2003;55:329-347.
5. Vasir JK, Tambwekar K, Garg S. Bioadhesive microspheres as a controlled drug delivery system. *International Journal of Pharmaceutics* 2003;255:13–32.
6. Roser M, Fischer D, Kissel T. Surface-modified biodegradable albumin nano- and microspheres. II: effect of surface charges on in vitro phagocytosis and biodistribution in rats. *European Journal of Pharmaceutics and Biopharmaceutics* 1998;46:255–263.
7. Uhrich KE, Cannizzaro SM, Langer RS, Shakesheff KM. Polymeric Systems for Controlled Drug Release. *Chem. Rev.* 1999;99:3181-3198.
8. Altman GH, Diaz F, Jakuba C, Calabro T, Horan RL, Chen J, Lu H, Richmond J, Kaplan DL. Silk-based biomaterials. *Biomaterials* 2003;24:401–416.
9. Freiberg S, Zhu X-X. Polymer microspheres for controlled drug release. *International Journal of Pharmaceutics* 2004;282:1–18.
10. Langer R, Peppas NA. Advances in Biomaterials, Drug Delivery, and Bionanotechnology. *AIChE Journal* 2003;49(12):2990-3006.
11. George M, Abraham TE. Polyionic hydrocolloids for the intestinal delivery of protein drugs: alginate and chitosan. *Journal of Controlled Release* 2006;114:1–14.
12. Liu X, Sun Q, Wang H, Zhang L, Wang J-Y. Microspheres of corn protein, zein, for an ivermectin drug delivery system. *Biomaterials* 2005;26:109–115.
13. Won Y-W, Kim Y-H. Recombinant human gelatin particles as a protein drug carrier. *Journal of Controlled Release* 2008;127:154–161.
14. Morlock M, Koll H, Winter G, Kissel T. Microencapsulation of rh-erythropoietin, using biodegradable poly(D,L,-lactide-co-glycolide): protein stability and the effects of stabilizing excipients. *European Journal of Pharmaceutics and Biopharmaceutics*, 1997;43(1): 29-36.

15. Soppimatha KS, Aminabhavia TM, Kulkarnia AR, Rudzinski WE. Biodegradable polymeric particles as drug delivery devices. *Journal of Controlled Release* 2001;70:1–20.
16. Vandelli MA, Rivasi F, Guerra P, Forni F, Arletti R. Gelatin microspheres crosslinked with d,l-glyceraldehyde as a potential drug delivery system: preparation, characterization, in vitro and in vivo studies. *Int J Pharm* 2001;215(1-2):175–84.
17. Sahin S, Selek H, Ponchel G, Ercan MT, Sargon M, Hincal AA, Kas HS. Preparation, characterization and in vivo distribution of terbutaline sulfate loaded albumin microspheres. *Journal of Controlled Release* 2002;82:345–58.
18. Latha MS, Rathinam K, Mohanan PV, Jayakrishnan A. Bioavailability of theophylline from glutaraldehyde cross-linked casein microspheres in rabbits following oral administration. *Journal of Controlled Release* 1995;34:1–7.
19. Speer DP, Chvapil M, Eskelson CD, Ulrich J. Biological effects of residual glutaraldehyde in glutaraldehyde-tanned collagen biomaterials. *J Biomed Mater Res* 1980;14:753–64.
20. Digenis GA, Thomas BG, Shah VP. Cross-linking of gelatin capsules and its relevance to their in vitro–in vivo performance. *J Pharm Sci* 1994;83:915–21.
21. Vollrath F, Barth P, Basedow A, Engström W, List H. Local tolerance to spider silks and protein polymers in vivo. *In Vivo* 2002;16(4):229-34.
22. Allmeling C, Jokuszies A, Reimers K, Kall S, Choi CY, Brandes G, Kasper C, Scheper T, Guggenheim M., Vogt PM. Spider silk fibres in artificial nerve constructs promote peripheral nerve regeneration. *Cell Proliferation* 2008;41(3):408-20.
23. Wenk E, Wandrey AJ, Merkle HP, Meinel L. Silk fibroin spheres as a platform for controlled drug delivery. *Journal of Controlled Release* 2008;132(1):26-34.
24. Liebmann B, Hümmerich D, Scheibel T, Fehr M. Formulation of poorly water-soluble substances using self- assembling spider silk protein. *Colloids and Surfaces A: Physicochem. Eng. Aspects* 2008; 331(1-2):126-32.
25. Wang X, Wenk E, Matsumoto A, Meinel L, Li C, Kaplan DL. Silk microspheres for encapsulation and controlled release, *Journal of Controlled Release* 2007;117:360-70.
26. Scheibel T. Spider silks: recombinant synthesis, assembly, spinning, and engineering of synthetic proteins. *Microbial Cell Factories* 2004;3(1):14.
27. Slotta UK, Rammensee S, Gorb S, Scheibel T. An Engineered Spider Silk Protein Forms Microspheres. *Angew. Chem. Int. Ed.* 2008;47:4592-94.

-
28. Lammel A, Schwab M, Slotta UK, Winter G, Scheibel T. Processing conditions for spider silk microsphere formation. *ChemSusChem* 2008;1(5):413-416.
 29. Hueimmerich D, Helsen CW, Quedzuweit S, Oschmann J, Rudolph R, Scheibel T, Primary structure elements of spider dragline silks and their contribution to protein solubility. *Biochemistry* 2004;43:13604-12.
 30. Tamm LK, Tatulian SA. Infrared spectroscopy of proteins and peptides in lipid bilayers. *Q Rev. Biophys.* 1997;4:365-429.
 31. Riley T, Govender T, Stolnik S, Xiong CD, Garnett MC, Illum L, Davis SS. Colloidal stability and drug incorporation aspects of micellar-like PLA-PEG particles. *Colloids and Surfaces B: Biointerfaces* 1999;16:147-159.
 32. Banga AK. *Therapeutic Peptides and Proteins: Formulation, Processing, and Delivery Systems*. Taylor and Francis 2006 (2nd Edition).
 33. Dossou U. Vorhersage intestinaler Absorption auf der Basis von physikalisch-chemischen Parametern und Verbesserung von Absorptionseigenschaften potenzieller Arzneistoffe. Dissertation 2005. Universität Saarbrücken, Naturwissenschaftlich-Technische Fakultät III.
 34. Siepmann J, Peppas NA. Modeling of drug release from delivery systems based on hydroxypropyl methylcellulose (HPMC). *Advanced Drug Delivery Reviews* 2001;48:139-157.
 35. Shard AG, Tomlins PE. Biocompatibility and the efficacy of medical implants. *Regenerative Medicine* 2006;1(6):789-800.
 36. Schlosser M, Wilhelm L, Urban G, Ziegler B, Ziegler M, Zippler R. Immunogenicity of polymeric implants: Long-term antibody response against polyester (Dacron) following the implantation of vascular prostheses into LEW.1A rats. *Journal of Biomedical Materials Research* 2002;61(3):450-57.
 37. Nair LS, Laurencin CT. Biodegradable polymers as biomaterials. *Progress in Polymer Science* 2007;32(8-9):762-798.
 38. Shimizu T, Yamashiro Y, Igarashi J, Fujita H, Ishimoto K. Increased serum trypsin and elastase-1 levels in patients undergoing L-asparaginase therapy. *European Journal of Pediatrics* 1998;157(7): 561-63.
 39. Del Favero G, Fabris C, Plebani M, Panucci A, Piccoli A, Perobelli L, Burlina A, Naccarato R. Serum elastase 1 in chronic pancreatic disease. *Journal of Molecular Medicine* 1985;63(13):603-06.

40. Page MJ, Di Cera E. Serine Protease and Serine Protease Inhibitors. Wiley Encyclopedia of Chemical Biology 2008, John Wiley & Sons.
41. Bartlett DW, Su H, Hildebrandt IJ, Weber WA, Davis ME. Impact of tumor-specific targeting on the biodistribution and efficacy of siRNA particles measured by multimodality in vivo imaging. PNAS, 2007;104(39):15549-54.
42. Chavanpatil MD, Khdair A, Panyam J. Particles for Cellular Drug Delivery: Mechanisms and Factors Influencing Delivery. Journal of Nanoscience and Nanotechnology 2006;6:2651-63.
43. Panilaitis B, Altman GH, Chen J, Jin H-J, Karageorgiou V, Kaplan DL. Macrophage responses to silk. Biomaterials 2003;24(18):3079-85.

5.3. Discussion of the presented data

In the previous section it was shown that spider silk protein particles are very suitable for the employment as drug release carriers. Since they carry a permanent negative charge in aqueous media of pH 7 they can interact with conversely loaded drug molecules thus determining the observed highly efficient loading phenomenon and the well defined drug release rates. Additionally, the observed surface erosion process and the expected high biocompatibility is another promotional argument for the application of the genetically engineered material in pharmaceutical technology. However, when talking about the well defined release and the release period exceeding one month, one should keep in its mind that due to the small size of these particles the entrapped drug molecules have to diffuse only short distances. It is therefore appropriate to question whether the observed diffusion controlled release mechanism would be transferable to release systems featuring larger dimension, i.e. implants which exhibit unlike longer distances to be traversed by the entrapped drug molecules. Another question which needs to be answered deals with the preparation techniques of such larger release systems consisting of spider silk proteins. It has been previously shown that the employed spider silk proteins can be successfully transferred into films either by casting from organic solvents or from aqueous solution. However, preliminary experiments - as reported previously in the general introduction of this dissertation - showed that the casting process from aqueous solution isn't capable of producing films larger than a few square millimetres and exhibiting a thickness of only a few micrometers. This incapability is presumably a consequence of the transition of α -helical protein structure into β -sheet rich structure occurring inhomogeneously during water evaporation. Therefore, in order to prepare larger films and implants organic solvents have to be introduced in the preparation process. Unfortunately the spectrum of solvents capable of dissolving spider silk proteins is not very broad. Apart from concentrated formic acid - a component which is not suitable for the preparation of drug depot systems due to its extreme pH - only hexafluoroisopropanol (HFIP) is capable of dissolving the engineered proteins in a reasonable amount of time. According to what we already learned about organic solvents such as HFIP- a polar solvent, miscible with water - we would now assume that this component jeopardizes the stability of the encapsulated proteins by inactivating them via water- HFIP interfaces. Eventually, the final part of this chapter highlights experiments dealing with the questions of spider silk film preparation and protein stability issues associated with the applied preparation techniques.

5.4. Characterization of eADF4 (C₁₆)-films for their application in drug release systems

Introduction

As seen in the previous part of this chapter recombinant produced spider silk protein eADF4 (C₁₆) enables diffusion controlled release from nanoparticulate systems. The featured Higuchi kinetic of the release profiles is consistent with the proposed structure of the genetically engineered silk material as a hydrophobic densely packed protein matrix.

Concerning the known properties of this unique material, the question arises, if C16 is applicable as release controlling layer, i.e. as coating material for various biomedical applications like stents or drug releasing implants. For silk fibroin we know of successful application as coating material for stents continuously releasing smooth muscle cell inhibitors such as clopidogrel and paclitaxel [1]. Theophyllin release from tablets was significantly reduced when coating the tablets with silk fibroin resulting in protein layers with an average thickness of about 50µm [2]. When preparing drug loaded silk fibroin films a biphasic release pattern was achieved by Hofmann et al. An initial release phase without burst effect was followed by a lag phase and continuous drug release between day 3 and 11[3]. The results of this experiment confirm that films and matrices consisting of high molecular fibroin – exhibiting a molecular of about 60 kD[4] – are suitable as a release modifying material due to the diffusion of the drug molecule through the matrix. Therefore it was the aim of the presented experiments to characterize films prepared from recombinant spider silk protein eADF4 (C₁₆) for their application as drug release controlling matrix material.

Films were characterized using FT-IR spectroscopy (FT-IR), Scanning Electron Microscopy (SEM), Differential scanning Calorimetry (DSC) and tested for their permeability of various drugs.

Materials and methods

Materials

Rh-interferon α -2a-(rh-IFN α , Roche Diagnostics, Penzberg, Germany; protein conc. 1.7 mg/ml in a 25 mM acetate buffer of pH 5.0, 120 mM sodium chloride) was lyophilized in a 1:3 ratio with hydroxypropyl- β -cyclodextrin (HP- β -CD, Merck, Darmstadt, Germany).

GCSF (Stada AG, Bad Vilbel, Germany; protein concentration 4.04mg/ml in a 20mM acetate buffer of pH 4) was lyophilized in 1:4 ratio with trehalose and 0.01% Tween 20.

Lyophilized bovine serum albumin (BSA) and all other chemicals and solvents used in the presented experiments were purchased from Sigma-Aldrich, Steinheim, Germany.

Methods

Preparation of silk films

Spider silk films were prepared using a casting method.

Solutions of recombinant spider silk protein eADF4 (C16) were cast on a custom made PTFE plate with drilled moulds with an average diameter of 26mm and an average depth of 4mm (Fig. 1). Films made of aqueous or hexafluoroisopropanol (HFIP) eADF4 (C16)- solutions were post-cast treated with methanol or potassium phosphate solution to stabilize the film, i.e. to make them water insoluble. Films cast from formic acid solutions were already water insoluble after solvent evaporation.

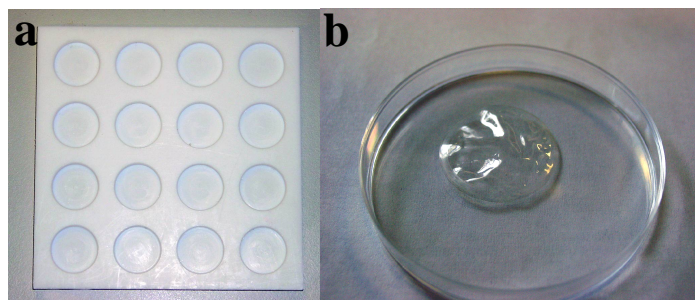


Figure 1: a) Custom made Teflon moulds b) cast film after solvent evaporation and removed from mould.

Silk films for examination with differential scanning Calorimetry

To determine the effect of different solvents on the properties of spider silk protein films were prepared from HFIP, formic acid and water. The silk content of the different solutions is listed in Table 1.

Solvent	Silk content in solvent [%]
HFIP	10
Formic acid	10
Water	2

Table 1: Solvents and silk concentrations in solutions for film casting

Spider silk protein eADF4 (C16) fibrils form spontaneously in aqueous solution, formation is concentration dependent. Silk concentration in aqueous solution was therefore limited to 2% since protein concentration is increasing when water is evaporating. As films from eADF4 (C16) are very sensitive towards changes in atmospheric humidity especially towards drying out, resulting in brittleness and fragility, the effect of plasticizer was analyzed with DSC. Triacetin was used as plasticizer and applied in a concentration of 10% in HFIP solutions.

Silk film preparation for permeability experiments

Solutions prepared for film casting were dilutions of stock solutions.

For casting procedure 330µl of stock solution (silk content 150mg/ml) were admixed in the casting mould with 250µl of pure solvent to allow the solution to bedew the surface of the mould. This final silk solution had a silk content of 5%. Cast solutions were stored over night in order to evaporate the solvent. After solvent evaporation the dried films were carefully removed from the mould and stored in a refrigerator for later use.

Film thickness determination

Thickness of the prepared films was determined with light microscopy (data were collected through a Leica DFC 320 camera (Leica Microsystems, Wetzlar, Germany) mounted on an Orthoplan microscope (Leica, Wetzlar, Germany). and by using a digital calliper.

For microscopic thickness determination films were cut in slices of approximately 1 mm width by using a scalpel. These slices were mounted on microscopic glass slides using Scotch Tape. Thickness of the fixed slice was calculated with calibrated computer software (LUCIA Screen Measurement Version 3.52a)

Karl-Fischer measurements

The residual moisture of spider silk films and lyophilized powder was analyzed using a Karl-Fischer titrator AQUA 40.00 with headspace module. Samples of freshly prepared films and freshly lyophilized spider silk protein were sealed in vials with rubber stoppers. These vials were then used for water determination.

Scanning Electron Microscopy

To investigate surface structure and morphology, films cast from HFIP, water and formic acid were analyzed using a Field Emission Scanning Electron Microscope Joel JSM-6500F (Joel Inc., Peabody, USA). Films were fixed with adhesive carbon tape (BAL-TEC AG, Balzers, Principality of Liechtenstein) to a custom made brass stub, carbon-sputtered and analyzed.

FT-IR spectroscopy

In order to investigate on the structural changes prior and after the treatment of films cast from water and HFIP a Bruker Tensor 27 FT-IR Spectrometer with a PIKE MIRacle™ sampling accessory equipped with a MIRacle™ micrometer clamp was used to analyse the samples. The diamond/ZnSe crystal plate had a surface area of 2.54 mm². Samples were spread on the crystal surface and compressed with the attached micrometer clamp in order to optimize the spectral quality. Spectra were recorded from 4000 to 800 cm⁻¹ with a resolution of 4 cm⁻¹

Differential scanning Calorimetry

Samples of eADF4 (C16) films cast from different solvents with or without plasticizer were analyzed with a NETZSCH DSC 204 Phoenix® instrument. Films derived from HFIP or aqueous solution were methanol treated in order to initiate structural conversion. To determine the glass transition temperature and the decomposition temperature samples were heated in the DSC at 10K min⁻¹. Starting temperature was -20°C; end temperature was 200°C.

SDS-PAGE

To investigate whether HFIP has detrimental effects on therapeutic proteins, HFIP and mixtures of HFIP and water were prepared and lyophilized therapeutic proteins (rh-INF, GCSF) were suspended respectively dissolved in the prepared mixtures. In order to mimic long term contact, i.e. residual solvents in spider silk matrices and solvent evaporation over a longer period of time, samples of the prepared protein-solvent mixtures were stored for one week and analyzed thereafter. Samples drawn from the stored and from freshly prepared solutions were diluted in SDS-running buffer, heated for 50min at 95° C before loaded on the

gel. Gels were run with 40mA for approx. 1.5 h. Silver staining was used to visualize the protein bands, a mark 12TM protein standard was run in duplicate in order to determine the size of the analyzed samples. All materials were supplied by Invitrogen (Carlsbad, CA, USA).

SEC-HPLC

Protein stability of the samples was examined with a SEC-HPLC method. rh-INF α samples were analyzed using a Thermo Separation Products HPLC system equipped with a Tosoh TSK-Gel G3000 SWxl column. 120 mM disodium hydrogen phosphate dehydrate, 20 mM sodium dihydrogen phosphates and 4 g/L sodium chloride, adjusted with hydrochloric acid to a pH of 5 was used as mobile phase. The flow rate was set to 0.6 mL/min, UV detection was performed at 210 nm wavelength. GCSF was analyzed with the same instrument and column, as mobile phase a mixture of acetonitrile water (60:40) with an addition of 1ml trifluoro acetic acid per liter was used. Flow rate was adjusted to 1ml and the detection wavelength was 225nm. In order to quantify protein concentration of the samples calibration curves with known protein concentrations were generated.

Permeation experiments

Physical properties of the model drugs used are listed in Table 2. The permeability coefficients of these drugs were determined using diaphragm diffusion cells made of two custom made Plexiglas compartments (donor and acceptor) divided by the silk film to be investigated serving as diaphragm. The area of the orifice was 2.21 cm² and the capacity of both cells was approximately 1.2 ml each thus the solution in the two compartments was constantly exchanged by fresh media to maintain the diffusion pressure due to concentration differences on both sides of the diaphragm. The overall volume of the donor and the acceptor media was 50.0 ml. The measurement of permeability was performed in 10mM phosphate buffer at a pH of 7.4. Prior to an experiment, the hydrated membrane mounted between the two diffusion cells was swollen in the buffer solutions without diffusion solutes for about 2 h.

Model drug	Isoelectric point	Dominant charge at pH 7.4	Permanently charged	Molecular weight [Da]	λ_{max}
Nipagin	-----	uncharged	no	152	254
Phenol Red	-----	negative	yes	354	510
Methyl violet	-----	positive	yes	407	590
rh-INF	6	positive	no	19.23k	280
BSA	4.8	negative	no	66.3K	210

Table 2: List of model drugs and their physical properties.

The permeability coefficients of the model drugs then can be calculated by the following

$$\text{equation [5, 6]: } \ln\left(1 - \frac{2C_t}{C_0}\right) = 2 \frac{A}{V} * P_t \quad (1)$$

Whereas, C_t is the drug concentration in the receiving cell at time t , C_0 the initial drug concentration in the source cell, V the solution volume in the two cells and A is the effective area of permeation. By plotting $-(V/2A) \times \ln(1 - 2C_t/C_0)$ versus time t , the permeability coefficient can be calculated from the slope. All experiments were run in triplicate.

UV Vis-Spectroscopy

Ultraviolet-visible spectrometry using a Cary100 spectrophotometer (Varian Medical Systems, Palo Alto, USA) and for BSA determination a CS-930-1PC plate reader (Shimadzu, Kyoto, Japan). was employed for determination of model drug content in the donor and the acceptor compartment for the calculation of the permeability coefficient. Calibration curves for all model drugs investigated have been obtained by using 5 different concentrations of a stock solution. The wavelengths used for drug concentration are listed in Table2.

Drug concentration in donor media was as followed for the different drugs:

Nipagin (1mg/ml), Methyl violet (0,03mg/ml), Phenol red (0,6 mg/ml), rhINF(1mg/ml) and BSA (0,4mg/ml).

Results and discussion

Karl-Fischer

Although using analytical grade solvents, i.e. 99-100% purity, films cast from Formic acid and from HFIP featured water contents comparable to the residual water content of films cast from aqueous solution. Probably these solutions were hygroscopic and adsorbed atmospheric water. The water contents of the films and the lyophilized C₁₆ powder are listed in Table3.

Sample	Residual water content [%]
Film cast from HFIP	4.56
Film cast from Formic acid	6.73
Film cast from Water	7.21
Lyophilized eADF4 (C16)	3.42

Table 3: Residual water content in eADF4 (C16) films and powder

Film thickness

Examination of the prepared film slices could confirm a uniform thickness of about 20 μ m of all cast films. Microscopic surface analysis revealed a glassy translucent film surface with few imprints probably derived from the casting mould. The cross section of the films didn't differ significant from the analyzed surface morphology

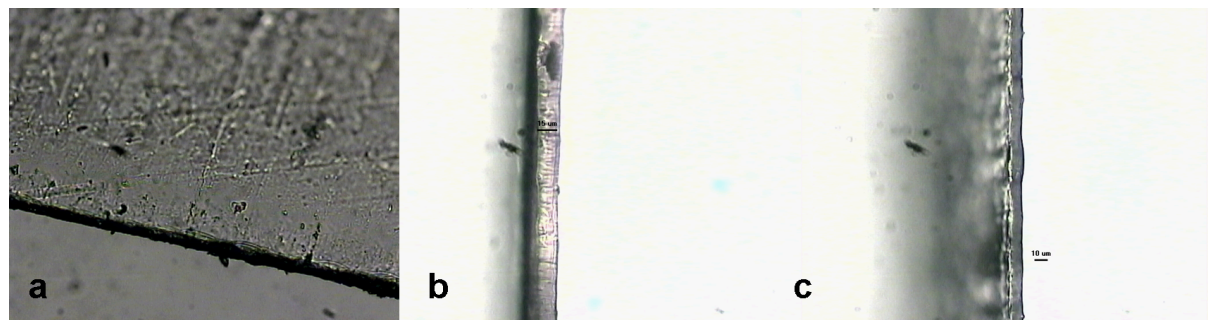


Figure 2: Light microscopy; a) film surface with mould imprints (50*magnification) b) cross section of a film prepared from HFIP solution (100x magnification) c) Formic acid derived film (100x magnification)

Scanning electron microscopy

SEM analysis of all prepared films revealed no significant difference in surface morphology and detectable microstructure. All films showed a pore free surface, cracks or other abnormalities in the morphology couldn't be detected. Although the applied SEM technique requires water free samples no detrimental effect of the drying within the evacuated SEM observation chamber was detected. Analysis of cross sections of the films could confirm the pore less structure of the film matrix. Films prepared from aqueous solutions (Fig. 2) exhibited a slightly rougher surface than films prepared from HFIP (Fig. 3), or Formic acid (Fig. 4).

This phenomenon can be explained by the concentration effect of the solution due to water evaporation. Upon water evaporation the resulting higher concentrated eADF4 (C16) triggers the conversion of the random coil conformation to β -sheet rich fibrils which are insoluble and therefore precipitate before water evaporation was complete. Nevertheless the cross section of this film shows no negative side effect of this phenomenon, i.e. no brittle and porous structure due to high fibril content.

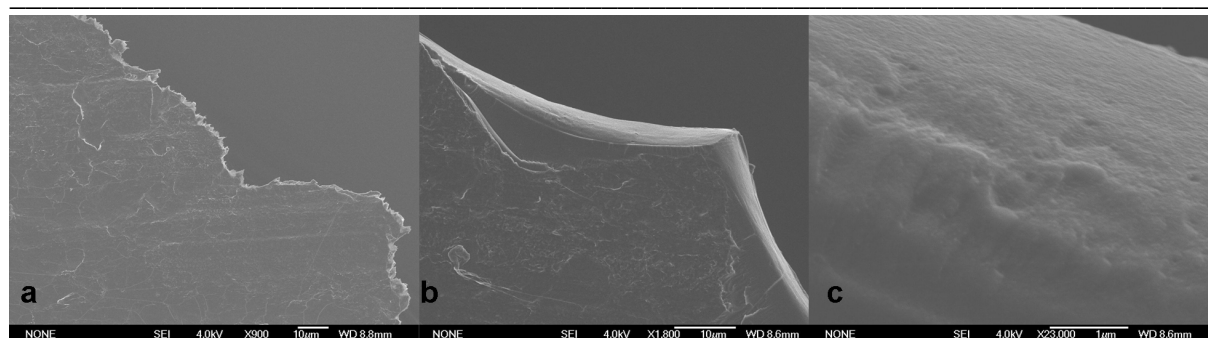


Figure 3: SEM photographs of eADF4 (C16) cast from aqueous solution. A) On the left side of the picture: film surface revealing the fibrous surface structure (900X magnification) b)cutting edge of the same film with smooth microstructure (1800X magnification) c)Fine structured cross section of aqueous eADF4 (C16) film (23000X magnification)

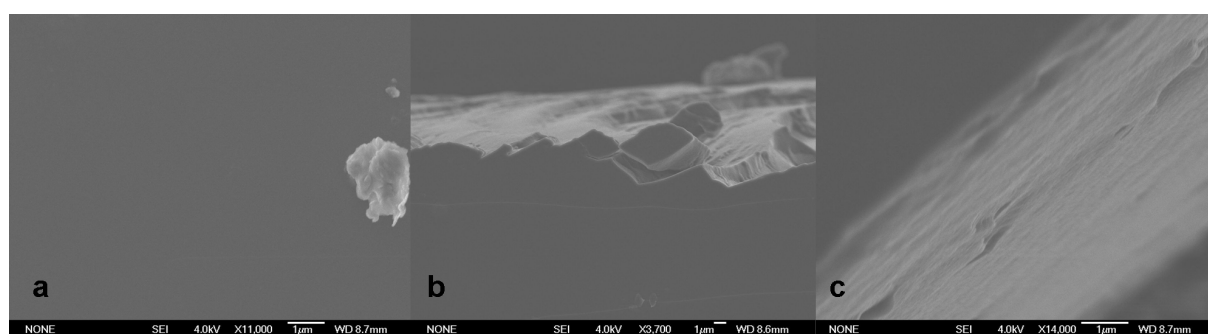


Figure 4: SEM photographs of eADF4 (C16) cast from HFIP solution. a):Smooth film surface with dust particle (11000X magnification) b)cutting edge of the same film (3700X magnification) c)Close up of the cutting site (14000X magnification)

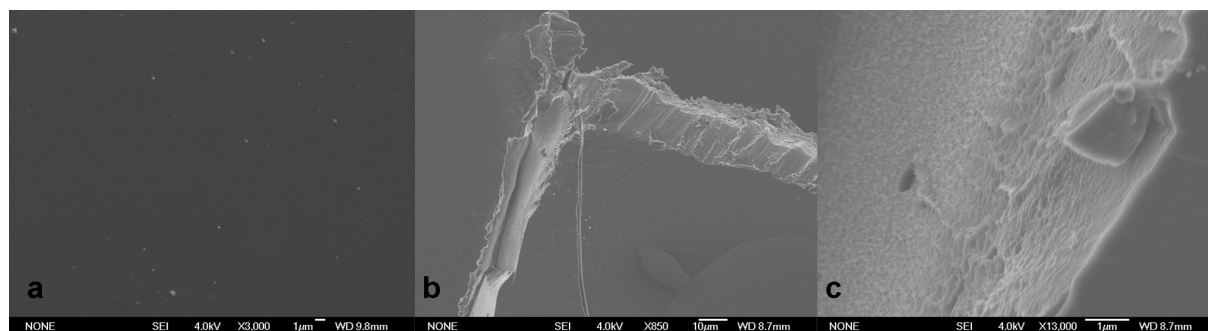


Figure 5: eADF4 (C16) films cast from formic acid solution. a) film surface (3000X magnification) b) cutting edge of the same film (850X magnification) c) Close up of the cutting site (13000X magnification)

DSC measurements

Similar to conventional polymers such as PLGA spider silk protein films exhibited a second order phase transition and a corresponding relaxation peak at temperatures between 40 and 55°C (Fig. 6). Presumably this phase transition can be explained as protein unfolding, i.e. a conversion of residual α -helical structure into β -sheet. As seen in Fig. 6a the addition of triacetin as plasticizer decreases this phase transition temperature presumably unfolding is facilitated when the amount of water in the protein film is increased. Overall there is no major difference in this phase transition temperature for all films except for films prepared from aqueous solutions. These films showed no distinct phase transition, probably due to the

arrangement of proteins upon water evaporation and the formation of insoluble fibrils within the aqueous solution. When increasing the temperature of the oven all samples showed an endothermic event at about 130°C.

This phenomenon indicates an irreversible folding process and the start of protein decomposition.

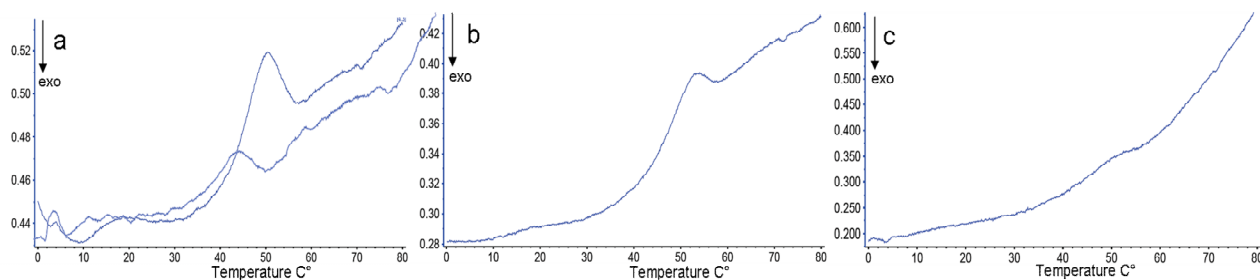


Figure 6: Phase transition of protein films derived from a) HFIP with a decrease of phase transition temperature for films with 10% triacetin content (lower Thermogram) b) Formic acid c) and films prepared from aqueous solution c).

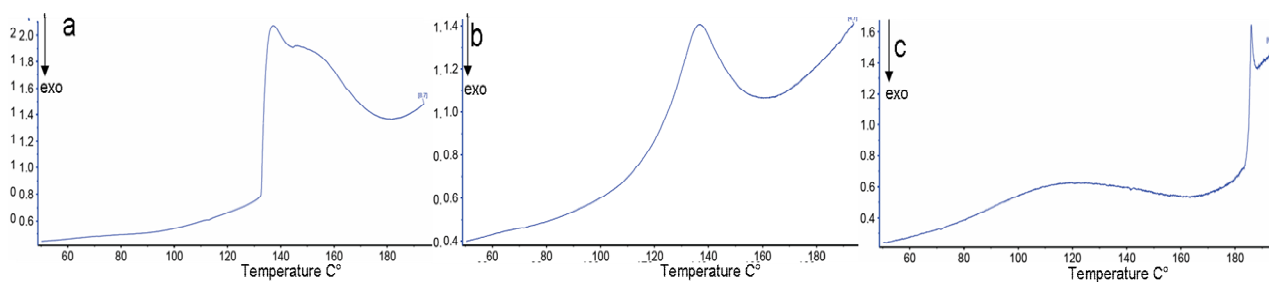


Figure 7: Protein decomposition for films prepared from a) HFIP b) Formic acid c) water.

FT-IR measurements

FT-IR measurements were conducted with films before and after methanol treatment in order to analyze the structural changes and to determine the content of α -helical, respectively β -sheet structure. In contrary to untreated films which exhibited only α -helical structure (Fig. 8 blue line), treated films (Fig. 8 red line) still exhibit significant amounts of α -helical structured domains as seen in the second derivative of the spectral range from 1580 cm^{-1} and 1720 cm^{-1} . These domains can undergo structural conversion into β -sheet when treated with heat as seen in the thermograms depicted in Fig. 7. In addition to that there was no significant change in β -sheet or α -helical structure concerning films treated either with methanol or with potassium phosphate (Data not shown).

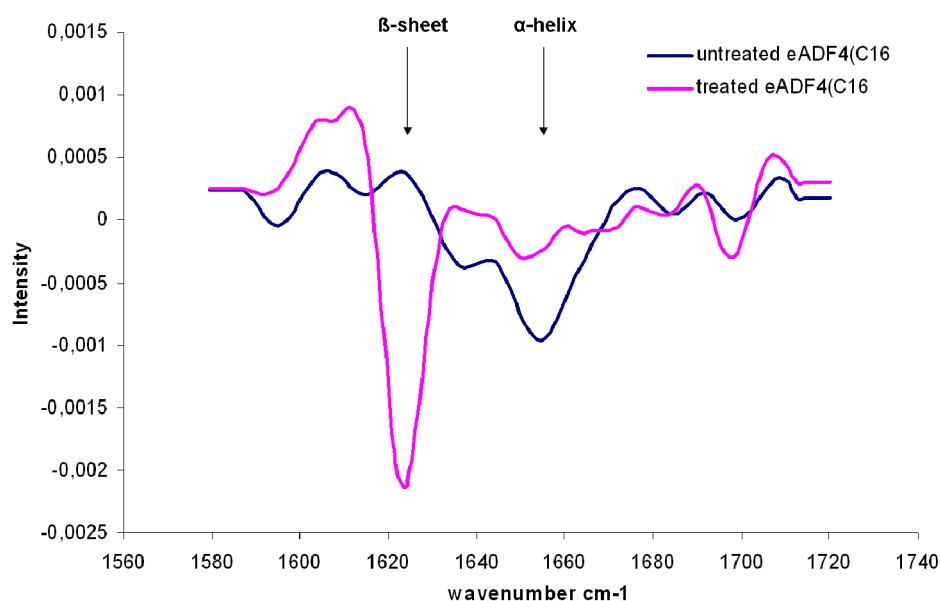


Figure 8: 2nd derivative of FT-IR spectra of native and methanol treated films.

Permeation studies of eADF4 (C16) films

Except for the negatively charged Phenol red, all tested drugs permeated through the spider silk protein films. Experiments with Methyl violet lead to a dark dyed spider silk film and a quick permeation through the films, thus confirming the electrostatic interaction of both molecules. According to equation (1) permeation coefficients were calculated from the linear part of the slope since transport parameters can be recovered more accurately in this region (Fig. 9). All obtained permeation coefficients were normalized for a membrane thickness of 1 μm . The permeation coefficients are listed in Table.4. As expected rh-INF α permeation was triggered by its isoelectric point and the resulting positive charge at the employed pH milieu of 7.4. Compared to that the measured permeation coefficient for the small molecule Nipagin was on a similar level and only slightly higher, presumably permeation of this uncharged molecule was unaltered due to the loss of electrostatic interaction with C₁₆. The 66 kD molecule BSA featured the lowest permeation coefficient presumably as a result of both, its high molecular weight and its negative charge at pH 7.4. This finding is in accordance to experiments conducted with silk microcapsules tested for their permeability for FITC-dextran with different molecular weights. While the membrane was easily permeable for small molecules it was found that capsules showed no permeation of 60 kD FITC-dextran after incubation for 12h at room temperature [7].

Model drug	P (cm·s-1/μm).
Nipagin	$1,63 \cdot 10^{-3}$
Phenol Red	impermeable
Methyl violet	$1,9 \cdot 10^{-2}$
rh-INF α	$1,1 \cdot 10^{-3}$
BSA	$2,56 \cdot 10^{-5}$

Table 4: Permeation coefficients P of different model drugs

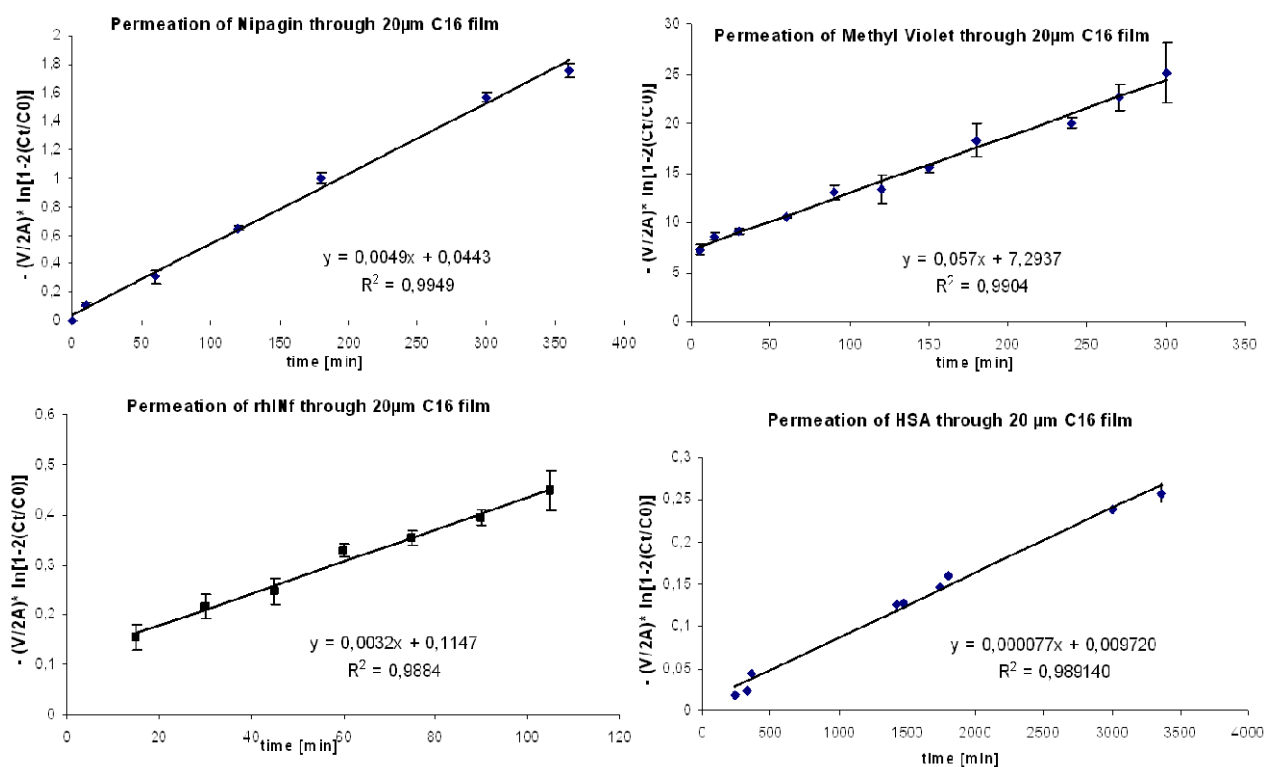


Figure 9: Permeability studies of model drugs: Determination of permeation coefficient P.

SDS-PAGE

As HFIP and Formic acid are the only known solvents to dissolve β -sheet structured eADF4 (C16) their effect on the stability of drugs during the preparation of drug loaded depot systems has to be investigated thoroughly. Investigation was mainly concentrating on HFIP since Formic acid is known to have detrimental effects on various drugs due to its extreme pH level of 1.2 resulting in drug hydrolysis and protein denaturation.

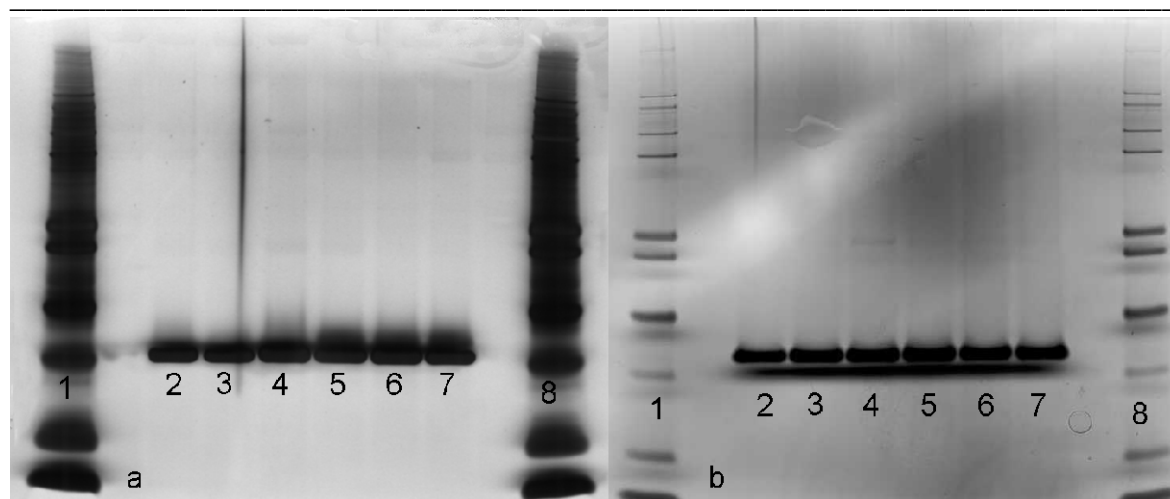


Figure 10: SDS-PAGE of rh-INF (a) and GCSF (b)

a) lane 1&8 marker, lane 2 rh-INF α standard, lane 3 rh-INF α dispersed in HFIP for 2 hours, lane 4 rh-INF α stored in HFIP:water (1:1) for 2 hours, lane 5 rh-INF α in aqueous solution stored at 5°C for 14 days, lane 6 rh-INF α dispersed in HFIP and stored for 14 days at 5°C, lane 7 rh-INF α stored in HFIP:water (1:1) for 14 days at 5°C. **b)** lane 1&8 marker, lane 2 GCSF standard, lane 3 GCSF dispersed in HFIP for 14 days at 5°C, lane 4 GCSF stored in HFIP:water (1:1) for 14 days at 5°C, lane 5 GCSF in aqueous solution stored at 5°C for 14 days, lane 6 GCSF dispersed in HFIP stored for 2 hours, lane 7 GCSF stored in HFIP:water (1:1) for 2 hours.

As seen in Figure 10 gel-electrophoresis did not show strong destabilizing effects on protein stability for samples either suspended in HFIP or dissolved water, even after storage for 14 days. However, HFIP/water mixtures seem to have negative effect on protein stability as proteins stored in this solution exhibited traceable aggregates, i.e. dimers. Additional experiments with HFIP/water mixtures could show that these mixtures featured an acidic pH of about 3. Presumably this low pH levels in the prepared HFIP/water mixtures initiated protein aggregation.

SEC-HPLC

Results from chromatographic analysis of the protein samples prepared for SDS-PAGE analysis confirm the negative effect of HFIP/water mixtures on the protein stability. Whereas rh-INF and GCSF incubated in pure water or pure HFIP maintained their stability, analysis of samples incubated in HFIP/water mixtures for 14 days clearly revealed the presence of dimers. For rh-INF α samples a dimer content of 4.3% was quantified for the samples incubated for 14 days in HFIP/water solutions. GCSF samples stored for the same amount of time in HFIP/water mixtures exhibited 4.7% Dimers (Figure 11b). This finding is in accordance with literature stating that traces of water in organic solvents have tremendous effect on protein stability and activity [8, 9].

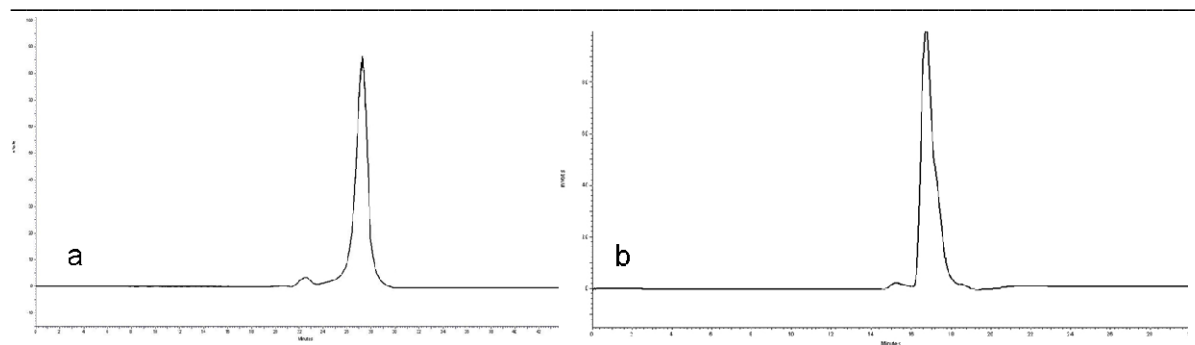


Figure 11: Chromatograms of rhINF α (a) and GCSF (b) with dimer peaks.

So far SEC-HPLC analysis is consistent with the results of SDS-PAGE experiments. Surprisingly a negative effect on protein stability of pure HFIP cannot be stated, especially for proteins applied as lyophilized powder. This material wasn't soluble in the organic solvent, thus protein solvent interactions as described in literature couldn't occur [10].

Conclusion

Results of the presented experiments attest the high potential of genetically engineered spider silk protein eADF4 (C16) for the application in pharmaceutical technology. Especially for the preparation of drug depot systems such as drug releasing films or coated implants, microparticles and biomedical devices like stents. Due to the permeability properties membrane diffusion controlled systems for small drug molecules are achievable. For larger drugs or proteins with a molecular weight higher than 60kD the application as diffusion controlling membrane might be possible by rendering the membrane permeability properties by means of pore formation upon film preparation. eADF4 (C16) films can be easily prepared using simple casting techniques. Plasticizers can be added in order to achieve a higher flexibility of the films. It was shown that films prepared from aqueous solutions exhibit a fibrous surface and thermo analytical measurements of these films revealed changes in phase inversion properties. Usually these films were brittle and fragile. To obtain thicker films prepared from aqueous solutions subsequent casting and stabilization steps have to be applied resulting in sandwich structured film. However, the employment of HFIP as good solvent for eADF4 allows the quick and reproducible preparation of stable films without pores. Results of our stability studies showed that it is possible to integrate proteins as lyophilized powder in HFIP-based silk solution without any detrimental effects on protein stability. However, contamination of HFIP- eADF4 (C16)-drug solution with traces of water or an accumulation of water from atmospheric humidity has to be prevented, as small amounts of water endanger drug stability in these solutions.

References

1. Wang, X., et al., *Controlled release from multilayer silk biomaterial coatings to modulate vascular cell responses*. *Biomaterials*, 2008. 29(7): p. 894-903.
2. Bayraktar, O., et al., *Silk fibroin as a novel coating material for controlled release of theophylline*. *European Journal of Pharmaceutics and Biopharmaceutics*, 2005. 60(3): p. 373-381.
3. Hofmann, S., et al., *Silk fibroin as an organic polymer for controlled drug delivery*. *Journal of Controlled Release*, 2006. 111(1-2): p. 219-227.
4. Yeo, J.-H., et al., *Simple preparation and characteristics of silk fibroin microsphere*. *European Polymer Journal*, 2003. 39(6): p. 1195-1199.
5. He, H., X. Cao, and L.J. Lee, *Design of a novel hydrogel-based intelligent system for controlled drug release*. *Journal of Controlled Release*, 2004. 95(3): p. 391-402.
6. Liang, S., L. Zhang, and J. Xu, *Morphology and permeability of cellulose/chitin blend membranes*. *Journal of Membrane Science*, 2007. 287(1): p. 19-28.
7. K. D. Hermanson, M.B.H., Thomas Scheibel and Andreas R. Bausch, *Permeability of silk microcapsules made by the interfacial adsorption of protein*. *Phys. Chem. Chem. Phys.*, 2007. 9: p. 6442-6446.
8. Mattos, C. and D. Ringe, *Proteins in organic solvents*. *Current Opinion in Structural Biology*, 2001. 11(6): p. 761-764.
9. Ru, M.T., et al., *Salt-Induced Activation of Enzymes in Organic Solvents*, in *Enzymes in Nonaqueous Solvents*. 2001. p. 3-11.
10. Griebenow, K. and A.M. Klibanov, *On Protein Denaturation in Aqueous-Organic Mixtures but Not in Pure Organic Solvents*. *Journal of the American Chemical Society*, 1996. 118(47): p. 11695-11700

III. FINAL SUMMARY & CONCLUSION

The presented thesis deals with 2 main objectives treated in five chapters of this publication. Firstly, this work focuses on lipid based drug delivery systems for the long term delivery of bioactive substances e.g. therapeutic proteins and, in particular the degradation and erosion behaviour of these systems. In the introduction the current state of the art concerning the preparation of these systems was highlighted. Despite the long period of experience – starting already in the 70ies of the last century – until today data dealing with those systems in respect of their degradation behaviour in vivo is still insufficient. In order to learn more about the fate of lipid drug depot systems an animal experiment with rh-INF-releasing Tristearin implants was conducted which is the main topic of **chapter 1**. This animal experiment proved the high applicability of compressed implants consisting of Tristearin since the release mechanism in vivo wasn't affected by tissue reactions and immune response of the animal organism. A high causal correlation between the observed in vivo release data and in vitro release data could be stated for the employed implants. No fever or other signs of inflammation and foreign tissue reaction were observed during the animal experiment. After sacrifice of the animals the implants were surgically removed. First examinations revealed no significant degree of bioerosion; the implants maintained their physical structure. At the first glance this result was somewhat disappointing since it was nearly expected that the employed implants would undergo biodegradation. However scanning electron microscopy analysis gives evidence that the lipid structure of the implants wasn't unaffected by the onslaught of the immune cells occurring always when foreign material comes in contact with living tissue. A change in lipid matrix crystallinity and structure was detectable. Anyway the question whether these detected changes would have resulted in significant lipid implant erosion could not be answered in the scope of the presented data. To be more independent of animal experiments and to fully characterize degradation and erosion processes presumably happening during bio-incubation an in vitro model for the simulation of biodegradation processes was developed. The developed model and the employed analytical methods allowed for the first time a qualitative and quantitative analysis of the lipid degradation process upon incubation with lipases. In **chapter 2** these experiments dealing with different types of lipids and different particulate or monolithic systems derived thereof are presented. It could be shown that certain triglycerides can be hydrolyzed easily by natural enzymes and depot systems consisting of these triglycerides materials degrade fast, eventually collapsing into small and innocuous lipid particles which are even more susceptible to lipid hydrolysis. It was also shown that, when using small lipid microparticles instead of large compressed implants the degradation velocity was substantially accelerated. This was previously observed in animal experiments when

FINAL SUMMARY & CONCLUSION

injecting a lipid microparticle suspension. To learn more about these interesting phenomena and to investigate on the underlying mechanism of rapid lipid degradation and implant erosion, additional experiments were conducted. This time, the analytical spectrum was extended and so far untouched aspects, i.e. especially the lipid erosion was covered. The results of these experiments are described in the scope of **chapter 3**. Here it could be clearly shown that certain physical properties of the employed materials such as the melting point, the miscibility with degradation products and the crystallinity are main factors determining the degradation behaviour. It was found that the water uptake of lipid matrices which is very low for pure triglycerides is enhanced after treatment with lipases. This finding is not unexpected, since the hydrolyzed molecules feature one or more hydroxyl functions capable of interacting with water molecules. Furthermore this effect was found to substantially enhance the lipid erosion. The water penetrating into the lipid matrix presumably interferes with the lipid crystal lattice. The generated pores serve as gateway for lipase molecules which presumably can diffuse into the weakened matrix. The produced degradation products of the triglycerides - mainly fatty acids and mono- and diglycerides - subsequently promote the erosion process. These substances accumulate within the pore network inside the lipid matrix. This accumulation of substances featuring a lower melting point can eventually lead to the generation of an eutectic mixture exhibiting a melting point beneath the melting temperature of the single substances involved in this system. The subsequent melting process of the lipid structure destroys the physical stability of the compressed implant or extrudate. It can therefore be stated that the observed processes leading to lipid implant disintegration are of both, chemical and physical nature and both pathways are synergistically amplifying each other. As already mentioned, this statement is only valid for triglyceride substances featuring a low melting point slightly above the body temperature of the human body such as glyceryltrilaurate. This may explain why the applied tristearate implants didn't show significant signs of degradation neither in the animal experiments nor in the first in vitro lipase incubation studies. Since glyceryltristearate exhibits a melting point significantly higher than the human body temperature it was not susceptible to the observed erosion process and only minor degradation was detected with the applied analytical methods. After presenting this set of data the author would like summarize that the **chapters 1- 3** emblaze the applicability of these fascinating natural and ubiquitous materials for the production of highly biocompatible drug depot systems. Based on the presented data it should be possible to design, prepare and characterize triglyceride based depot systems with predefined degradation and erosion properties. These systems could be used for example for a long term delivery of bioactives e.g. for a period of several months to a few years depending on the employed lipid composition and on the system prepared. For instance when preparing lipid microparticles a

FINAL SUMMARY & CONCLUSION

short shelf life in living animals can be assumed due to the observed size effects which boost the degradation velocity. When applying larger monolithic implants it can be assumed that total degradation doesn't take place before the delivery phase has run. However it will be possible to design the implant in a way that the lipid system eventually fully degrades within the scope of several months.

The second part of the presented dissertation concentrates on the application of genetically engineered spider silk in the field of pharmaceutical technology and drug delivery. A comprehensive aggregation of this interesting research theme is included in the general introduction of this work. Since the research concentrating on proteins derived from spiders or silk worms is a relative new chapter in the book of biotechnology science there are only few data available dealing with the application of spider for the preparation of drug delivery systems. However, it is generally understood that these proteins exhibit properties which make them ideal for the preparation of tissue scaffold and drug delivery systems. Especially the high degree of biocompatibility is a major factor promoting their application in bioscience. Furthermore, experiments have shown that spider silk proteins promote healing processes and seem even capable of supporting the regeneration of nerve cells. Due to cooperation with the University of Bayreuth, especially with the research team of the department of biomaterial science it was possible to conduct research on newly prepared semi synthetic spider silk proteins. In contrast to other natural proteins which very often exhibit an irregular composition of amino acids these genetically engineered spider silk proteins were available in qualities of high purity. Since these proteins were so far not examined for their application in the area of pharmaceutical technology their basic properties with respect to the preparation of drug depot systems were analyzed. In **chapter 4** for the first time the preparation and characterization of semi synthetic spider silk microspheres and methods to control the particle size of the resulting particles are presented. It was found that these proteins can be processed easily into stable microparticles with a narrow particle size distribution. The preparation process is based on a precipitation mechanism involving the transition of water soluble α -helical rich proteins into β -sheet rich, water insoluble proteins. This transition is achieved upon the addition of lyotropic salts such as potassium phosphate. In summary, a solvent free easily up scalable method was presented. The conducted method additionally features an almost 100% yield of protein spheres, an important issue for high price material. It is obvious that described preparation method is ideal in terms of biocompatible production of drug depot systems since all applied materials and solvents are absolutely physiologically uncritical. Subsequently the generated spider silk particles were analyzed and investigated for their use as particulate drug carrier.

FINAL SUMMARY & CONCLUSION

Chapter 5 is dedicated to the analysis of these particles with regards to the loading mechanism and the resulting drug release for small molecules. Drug loading efficiencies of up to 98% were achieved for positively charged drug molecules. Surprisingly it is not necessary to include the drug loading process into the process of particle preparation. In fact it is possible to prepare the particles, subsequently concentrate them by centrifugation and eventually subject them to the drug loading step. As the semi synthetic spider silk particles are negatively charged at neutral pH-levels due to the isoelectric point of their amino acid composition they can attract positively charged drug molecules. It was further on shown using on-line analysis methods during drug loading processes that the attracted positively charged drug molecules enter the interior of the protein particles and accumulate within. When investigating more than 10 different drug molecules with respect to their loading performance it was found that it is possible to correlate molecular parameters such as drug charge (calculated from the acid dissociation constant pK_a) and the distribution coefficient D with the achieved loading efficiency. Interestingly the high hydrophobicity within the interior of the spider silk particles allows as well a high degree of drug loading for uncharged water soluble drugs, whereas negatively charged drugs are almost impossible to encapsulate into the spider protein particles. In terms of the release of the entrapped drug molecules from the spider silk particles release periods exceeding one month were achieved. The observed release kinetics was characterized. Drug release from these systems is characterized as anomalous diffusional release within the first weeks. After that period Fickian release behaviour is predominant. In another set of experiments the biodegradation of this silk molecule was investigated. These experiments could clearly show that the spider silk particles are erodible in the presence of physiological proteases such as Elastase. As expected when incubating the particles in enzyme-containing buffer media surface erosion processes were observed via SEM and particles size analysis. Additional data highlighting the applicability of spider silk macro layers and films usable for the release of drugs or the modulation of drug release from implants is presented in the additional data closing **chapter 5**. In summary genetically engineered spider silk proteins especially the employed eADF4 are of very high potential for the application in pharmaceutical technology due to their unique properties regarding applicable preparation techniques, drug loading, and drug release and due to their expected biodegradation in physiological surroundings.

ACKNOWLEDGEMENTS

Acknowledgements

This thesis has been prepared between May 2005 and February 2009 at the Department of Pharmacy, Pharmaceutical Technology and Biopharmaceutics, Ludwig-Maximilians-University Munich under the supervision of Prof. Dr. Gerhard Winter.

Foremost, I want to express my honest gratitude to my supervisor Prof. Winter for giving me the opportunity to be a member of his research group and to prepare this thesis. I am very grateful for his highly professional guidance and for the numerous inspiring discussions. In particular, I am extremely grateful for his encouragement which allowed me to conduct an internship as visiting researcher at the School of Pharmacy in Dunedin.

Consequently, I am exceptionally grateful to Prof. Dr. Thomas Rades for giving me the opportunity to work for three months in his labs at the School of Pharmacy, Dunedin, New Zealand. I really enjoyed the time in and outside the lab and the numerous discussions we had.

Moreover, I would like to thank Prof. Dr. Keith Gordon for his guidance and his support during my work in his labs at the Chemical Department of the University of Otago, New Zealand. In this context I also would like to express my deepest gratitude to Cushla McGoverin and Clare Strachan for their support and the great efforts they made to facilitate my research work and for the many discussions concerning our research project.

I especially want to thank Alex and Kristina for the great times we had in and outside the lab and during our countless cooking sessions. I will keep them always in my mind!

My very special appreciation goes out to my cooperation partners, who were essential for the success of this work

- Prof. Dr. Eckhardt Wolf and his research team, especially Dr. Barbara Kessler at the Institute of Molecular Animal Breeding and Biotechnology in Oberschleißheim, for our successful animal experiment and the many efforts she made in the numerous hours of this project.
- Gregor Jordan, from Roche Pharma Research R&D Protein Analytics in Penzberg, for the great job he did when dealing with IVIVC-correlation.

ACKNOWLEDGEMENTS

- Prof. Dr. Thomas Scheibel and his team at the Department of Biomaterial Research at the University of Bayreuth, for giving me the unique opportunity to work with these new materials which made me thinking out of the box with regards to the applied preparation and characterization methods. Thanks to Ute Slotta for introducing me to this new research theme. Many thanks and my highest acknowledgement go to Andreas “Andy” Lammel for the numerous discussions we had about our joint research project. Andy, we kinda had a stringy start together and we had to learn that we had to change the way of our communication, but eventually it was just cool. I always appreciated it to work with you, as I always could learn so much from you. Thank you very much!

Thanks are extended to Dr. Sandra Schulze and Gerhard Sax, who made it possible that I could travel to New Zealand with hundreds of samples in my suitcase and even more ideas in my head. In this context, I also want to thank Sandra for our time we had together during student teaching.

Consequently, I want to express my thanks to Sebastian “Fuchsi” Fuchs. We had so much fun together “torturing” students in the oral examinations. Sebastian, I always appreciated working with you, especially the time we had during our Barcelona tour.

Many thanks go to the team of the bubble lab. Steliyan, Stefan and Klaus, it was always fun to witness your special working atmosphere and the many crazy ideas you had in your minds. Special thanks go to Klaus; I believe everybody should learn from your steady and calm but cheerful attitude.

Overall, I want to thank all present and former members of our research groups for the brilliant atmosphere and the good time we had.

At this point, I want to express my deepest appreciation to Alice Hirschmann, who had to cope with my – sometimes - special and noisy manner. Alice, I truly believe that I’ve found a real friend in you after all that years.

Finally, I want to thank my parents and my siblings, my families in Ettenheim and Munich and especially Lisa for their love and support.

Publications and presentations associated with this work

ORIGINAL PAPERS

M. Schwab, B. Kessler, E. Wolf, G. Jordan , S. Mohl, G. Winter

Correlation of in vivo and in vitro release data for rh-INF α lipid implants.

European Journal of Pharmaceutics and Biopharmaceutics. Volume 70, Issue 2, October 2008

A. Lammel , M. Schwab , U. Slotta , G. Winter, T. Scheibel

Processing Conditions for the Formation of Spider Silk Microspheres

Chem Sus Chem, Vol. 1(5), May, 2008

M. Schwab, G. Sax, S. Schulze, G. Winter

Studies on the lipase induced degradation of lipid based drug delivery systems

Accepted for publication in: Journal of Controlled Release

M. Schwab, C. McGoverin, C. Strachan, K. Gordon, T. Rades, G. Winter

Studies on the lipase induced degradation of lipid based drug delivery systems. Part II –

Investigations on the mechanisms leading to collapse of the lipid structure

Submitted to: Journal of Controlled Release

A. Lammel, M. Schwab, G. Winter, T. Scheibel

Spider silk particles for controlled drug delivery

Prepared for publication in: Journal of Controlled Release

POSTER PRESENTATIONS

M. Schwab, B. Kessler, E. Wolf, G. Jordan , S. Mohl, G. Winter

Correlation of in vivo and in vitro release data for rh-INF α lipid implants, AAPS Annual Meeting and Exposition, San Diego, CA, November 11 – 15, 2007

M. Schwab, G. Winter

Investigations on the biodegradability of lipid implants, microparticles and extrudates

6th World Meeting on Pharmaceutics, Biopharmaceutics and Pharmaceutical Technology,

Barcelona, Spain, April, 6th-10th 2008

M. Schwab, A. Lammel, U. Slotta, T. Scheibel, G. Winter

Characterization of spider silk protein films for application in pharmaceutical technology

6th World Meeting on Pharmaceutics, Biopharmaceutics and Pharmaceutical Technology,

Barcelona, Spain, April, 6th-10th 2008

CURRICULUM VITAE

Curriculum Vitae

Martin Schwab

Date of birth January 29, 1977

Place of birth Ettenheim

Nationality German

Work experience and academic training

Since 03/2009 Transfer manager, Technical Services
Intervet International GmbH, Unterschleißheim, Germany

05/2005-02/2009 PhD studies at the Department of Pharmacy
Pharmaceutical Technology and Biopharmaceutics of the
Ludwig-Maximilians-University Munich, Germany
Supervisor: Prof. Dr. Gerhard Winter

07/2008-10/2008 Research stay at the School of Pharmacy of the University of
Otago, Dunedin, New Zealand

01/2004-04/2005 Supervisor: Prof. Dr. T. Rades
Pharmacist, Munich, Germany

Education

05/2003-10/2003 Practical education in pharmacy (industry), department of
galenics and development, Hexal Ag, Holzkirchen, Germany

11/2002-04/2002 Practical education in pharmacy, Rohan-Apotheke, Ettenheim,
Germany

05/1998-09/2002 Study of pharmacy, Ludwig-Maximilians-University Munich,
Germany

01/1997-02/1998 Civilian Service: care assistant, Kreiskrankenhaus Ettenheim,
Germany

1987-1996 High School, Städtisches Gymnasium Ettenheim, Graduation
with Abitur.